Investigating the biosynthesis and mode of action of the formicamycin antibiotics

Hannah Patricia McDonald

A thesis submitted in fulfilment of the requirements for the degree of Doctor of Philosophy at the University of East Anglia

University of East Anglia

School of Biological Sciences

December 2022

Abstract

One of the most pressing issues of our time is antimicrobial resistance to currently used antibiotics. Therefore, new antibiotics are needed to ensure that we can continue to treat and prevent infections. Actinomycetes, such as *Streptomyces*, have predominately been at the forefront of antibiotic discovery for more than half a century and continue to provide new potential antibiotics. *Streptomyces formicae* is a new species which was isolated from the bodies and habitats of the fungus farming ants, *Tetraponera penzigi,* that has previously been found to produce a new class of antibiotics, the formicamycins. During this work, the biological activities, target(s) and mode of action of the formicamycins and their biosynthetic intermediates, fasamycins are investigated. We determined that both molecules are potent against Gram-positive organisms such as methicillin-resistant *Staphylococcus aureus* (MRSA) and vancomycin-resistant Enterococci (VRE). Chemical analysis of *S. formicae* strains containing mutants within the formicamycin gene cluster allowed us to generate high yielding formicamycin strains and through heterologous expression of the *for* BGC we have identified several new glycosylated fasamycin congeners. Attempts to generate fasamycin of formicamycin resistant bacterial strains were unsuccessful, even after 40 days of sub-MIC exposure, we therefore determined that these compounds display a high barrier to resistance. Due to this high barrier to resistance and several lines of other *in vitro* evidence, we hypothesised that both fasamycin and formicamycin have multiple cellular targets. Previous work had identified the fasamycins as inhibitors of bacterial type II fatty acid synthesis (FAS-II), specifically FabF inhibitors, an essential elongation condensation enzyme within the FAS-II pathway. This work however reveals a second target of fasamycin and the first reported target of formicamycin, type II bacterial and archaeal topoisomerases. Overall, this work demonstrates that novel antibiotics can be found by exploring actinomycetes in under-explored environments.

Publications arising from this work

Devine, R., **H. P. McDonald**, Z. Qin, C. J. Arnold, K. Noble, G. Chandra, B. Wilkinson and M. I. Hutchings (2021). "Re-wiring the regulation of the formicamycin biosynthetic gene cluster to enable the development of promising antibacterial compounds." Published in Cell Chemical Biology. DOI 10.1016/j.chembiol.2020.12.011

H. P. McDonald,‡ A. Alford,‡ R. Devine, E. S. Hems, S. A. Nepogodiev, C. J. Arnold, M. Rejzek, N. A. Holmes, M. I. Hutchings and B. Wilkinson. "Heterologous expression of the formicamycin biosynthetic gene cluster unveils new glycosylated fasamycin congeners" Awaiting submission to Journal of Natural Products

List of Abbreviations

ACC - acetyl-CoA carboxylase

ACP - Acyl carrier protein

AMR - Antimicrobial resistance

AT - Acyltransferase

BGC - Biosynthetic gene cluster

CFX - Ciprofloxacin

CoA - Coenzyme A

DEBS - 6-deoxyerythronolide B

DH - Dehydratase

ds -Double stranded

ER - Enoylreductase

FAS-II - Type II fatty acid synthesis

for - Formicamycin

KR - Ketoreductase

KS – Ketosynthase

MIC – Minimum inhibitory concentration

MRSA - Methicillin resistant Staphylococcus aureus

MSSA - Methicillin sensitive Staphylococcus aureus

NPs - Natural products

PKS - Polyketide synthase

SD8 - Simocyclinone D8

SPR - Surface plasmon resonance

TE - Thioesterase

Topo IV - Topoisomerase IV

VRE - Vancomycin resistant Enterococci

Contents

Acknowledgements

Firstly, I would like to thank my supervisors, Professor Barrie Wilkinson and Professor Matt Hutchings who have helped me become the scientist I am today through their guidance and supervision, I will never be able to thank you both enough. Thank you for trusting me, encouraging me, and always pointing me in the right direction. To Professor Tony Maxwell and Dr Dmitry Ghilarov, thank you for letting me spend the last 6 months of my PhD in your labs, what could have been an incredibly stressful time was instead an absolute honour. To all of my supervisors, I especially thank you for helping me feel like I am finally ready to become an independent scientist, something I never thought would happen when I first walked through the doors of the JIC. This project could not have been possible without extensive collaboration from Dr Rebecca Devine, Dr Zhiwei Qin, Dr Edward Hems and Dr Corinne Arnold, thank you for everything.

I would like to thank all the members of the Wilkinson, Hutchings, Maxwell and Ghilarov groups, both past and present. Working with all of you made me look forward to coming to work every day and for this, a mere thank you will never be enough. To the department of Molecular Microbiology, thank you for making me feel so much at home, this department truly is more like a family than a workplace.

Special thanks go to Kathryn Stratton, Dr Catriona Thompson, Dr Claudio Greco, Dr Rebecca Devine, (soon to be Dr) Jonathon Liston, (soon to be Dr) Ben Scott, Dr Sibyl Batey, Dr Matthew Bush, Dr Joe Sallmen, Dr Tom McLean, Katie Noble, Myfanwy Adams, Dr Dmitry Ghilarov and Dr Tung Le – Thank you for listening to and believing in me especially when I did not.

 Colleen Sprigg lets end this how we started it – together. I don't know what I did to deserve a friend like you. The hardest part of writing this thesis is trying to get down in words what your friendship has meant to me over the past 9 years, for once I am almost at a loss for words - all I can say is you are home.

To my partner Ben, I will never be able to thank you enough for your love and support during my 4 years of PhD. You have been my constant cheerleader and my supplier of dog videos to cheer me up. I am so looking forward to everything that life holds in store for us both.

Lastly, I would like to thank all of my family for their love and support during my PhD, even when you didn't understand what I have actually been doing for all of these years (I still don't work on ants!!!)! Special thanks go to my Dad, Alex McDonald, thank you for raising me to never quit and for loving me unconditionally, I am so proud to be your daughter.

I dedicate this thesis to my Gran, Patricia McDonald. Gone but never forgotten and always in my heart, you are my inspiration every single day and I'm honoured to share your name, now, let's put Dr in front of it, solidify my title as 'The chosen one' and Let's Go Fly A Kite.

1.0 Introduction

1.1   Antibiotics

One of the scientific communities' greatest achievements was the advent of antimicrobials which first began in the 1900s with the synthesis of salvarsan by Paul Ehrlich and the discovery of penicillin from a *Penicillium* fungus by Alexander Fleming (Fleming 1944, Bosch and Rosich 2008, Gelpi, Gilbertson et al. 2015, Gaynes 2017). Antibiotics are molecules or compounds that have an adverse effect on bacteria, some of which can be used to treat or prevent the spread of bacterial infections. Although we attribute antibiotic discovery to Ehrlich and Fleming, the use of microbes and environmental samples, such as soil, to cure and prevent diseases stretches back millennia with documents such as the Eber's papyrus, showing that people 2000 years ago were using mouldy bread and soil to treat open wounds (Haas 1999). The discovery of modern antibiotics has not only been revolutionary to the treatment of diseases caused by bacteria such as cholera and tuberculosis but has also paved the way for all types of surgery and organ donations to take place with reduced risk from bacterial infections. It is estimated that the introduction of antibiotics throughout the clinic has increased the life-expectancy of the human population by upwards of 23 years and therefore the importance of these compounds cannot be overstated (Hutchings, Truman et al. 2019).

The most successful clinical antibiotics, also referred to as drugs, have selectivity towards bacterial cells over human cells which limits toxicity to the user whilst inhibiting an essential biological process in the bacterial cell. Targets of antibiotics include protein synthesis (e.g., tetracycline), cell wall biosynthesis (e.g., β-lactams) maintenance of DNA and RNA (e.g., ciprofloxacin and rifampicin), inhibition of essential metabolic pathways (e.g., fatty acid synthesis inhibitors such as isoniazid) or disruption of the cell membrane (e.g., polymyxins) (Reygaert 2018). Multiple antibiotics can inhibit the same bacterial target but do so in different ways, for example both ciprofloxacin and novobiocin inhibit DNA gyrase, an enzyme required for the maintenance of DNA, but ciprofloxacin does so by binding to the enzyme and physically stopping it from carrying out its function, whereas novobiocin stops the enzyme from getting the energy it needs to carry out its functions (Khan, Sankhe et al. 2018). The biochemical interactions through which an

antibiotic produces its inhibitory effect is referred to as the mechanism of action. Although there are a large range of antibiotics, each categorised by their chemical structures and their mechanism of action, they can be classed into two broad categories, bactericidal and bacteriostatic, depending on how they inhibit bacterial cells. Bactericidal antibiotics are able to kill bacterial cells (e.g., via lysis of cells) whereas bacteriostatic antibiotics stop the bacteria from being able to replicate and halt them in a stationary phase (Pankey and Sabath 2004).

Many of the classes of clinically used antibiotics today were discovered between 1940 and 1960 in a time referred to as the 'golden age' of antibiotic discovery (**Figure 1.1**), (Davies 2006, Katz and Baltz 2016, Lewis 2020) during which the vast majority were derived from the specialised metabolites of microorganisms, also referred to as natural products (NPs) (Katz and Baltz 2016). The analysis of a microbe's ability to produce antibiotics was led by Selman Waksman who undertook a systematic study of antibiotic production from actinomycetes, a group of filamentous bacteria. This study led to the discovery of the first antibiotic of clinical importance, Streptomycin, named after its discovery from the bacteria *Streptomyces griseus*, which became the first antibiotic used for the treatment of tuberculosis (Waksman, Schatz et al. 1946). Waksman was the first to realise the clinical importance of actinomycetes, such as *Streptomyces*, as prolific antibiotic producers, and many of the antibiotics used today are derived from actinomycete bacteria. After these findings, a large discovery effort isolated and characterised many different classes of antibacterial compounds from microorganisms including *Streptomyces* bacteria. A large proportion of the antibiotics discovered during this time are still used in the clinic today such as chloramphenicol, the cephalosporins (β-lactams), and kanamycin. Following these advances, synthetic derivatives of these classes of antibiotics shortly followed and deaths from common bacterial infections reduced dramatically (Zaffiri, Gardner et al. 2012).
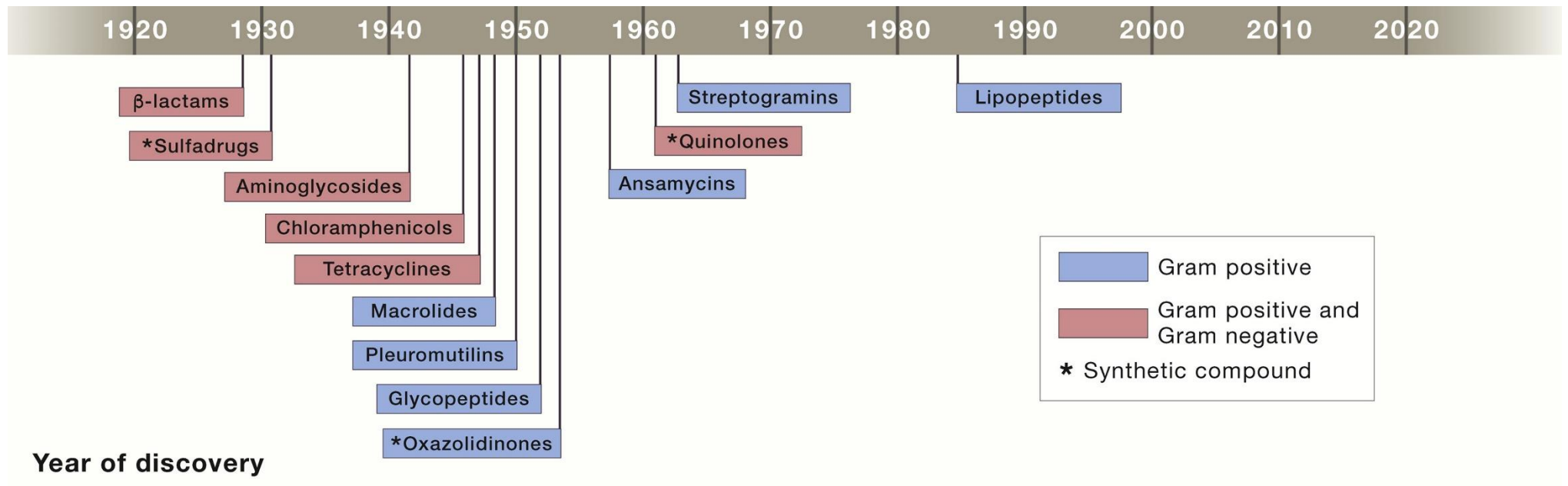
Figure 1.1 Timeline of the 'golden age' of antibiotic discovery, showing classes of antibiotics that inhibit just Gram-positive and both Gram-positive and Gram-negative bacteria. Most classes of compounds were discovered between the 1940s and 1970s. Adapted from Lewis (2020).

Unfortunately, the 'golden age' of antibiotic discovery rapidly declined in the 1970s due to a lack of new classes of antibiotics being discovered and the rediscovery of previously characterised antibiotics. This caused the antibiotic pipeline to diminish, resulting in a lack of new antibiotics being discovered between 1970 to 2020 (**Figure 1.1**). Furthermore, pharmaceutical interest and investment in antibiotic discovery has fallen due to the limited profits that could be made from antibiotics which are only prescribed to individual patients for for short periods of time, causing many of the pharmaceutical and agrochemical companies to shut down their antibiotic discovery programmes in favour of discovery of long-term clinical compounds such as anti-cancer agents (Katz and Baltz 2016). Efforts to develop new antibiotics have focused instead on the use of high throughput screens for new synthetic antibiotics but unfortunately, the majority of these screens were unsuccessful and still to this day the majority of synthetic antimicrobials derive from microbially produced classes of antibiotics discovered in this time.

1.2   Antimicrobial Resistance (AMR)

The rapid discovery and characterisation of new antibiotics during a short period of time led to excessive usage of these compounds to treat all manner of illnesses, including those that could not be cured by antibiotics such as viral infections, which influenced the natural process of antimicrobial resistance (AMR). AMR occurs when bacteria (or other microbes) evolve mechanisms which allow them to tolerate or completely resist inhibition by antibiotics, rendering the antibiotic ineffective and allowing for the bacteria's survival (Ventola 2015). Growing cases of antibiotic resistant bacteria are especially detrimental in clinical settings with major increases in resistance seen in clinically relevant pathogens, in particular, multidrug resistant *Mycobacterium tuberculosis*, methicillin resistant *Staphylococcus aureus* (MRSA) and vancomycin resistant *Enterococcus* (VRE) bacterial species, all of which can cause severe disease in humans with resistant isolates increasing the chance of mortality in patients (Davies and Davies 2010, Ventola 2015). Some human pathogens have developed multiple resistances to antibiotics and are therefore almost untreatable such as some extremely resistant *M. tuberculosis* which have evolved resistance to isoniazid and rifampin, fluoroquinolones and at least one of three second-line drugs such as amikacin,

kanamycin, or capreomycin (Calfee 2012). Increased prevalence of infections from multidrug resistant bacteria not only cause a burden on the health care system, but the treatment of them can be incredibly expensive; reports in the United States alone indicate that infections with drug resistant bacteria incurs increased costs per patient in comparison to drug sensitive infections and it has been estimated that the total economic burden placed on the U.S. economy by antibiotic-resistant infections is as high as $20 billion per year (Ventola 2015). The effects of AMR can be seen in every country across the globe and it is estimated that at least 700,000 people die per year from drug-resistant infections (Clardy, Fischbach et al. 2009, O'Neill 2016). As such the World Health Organisation has named antimicrobial resistance as one of the key threats to global health.

Antibiotic resistance can develop due to bacteria encoding genes that provide a greater fitness in the presence of antibiotics or, exposure to antibiotics can lead to accelerated evolution of bacteria to develop mechanisms to resist antibiotic effects. There are many contributing factors toward antibiotic resistance and although genes encoding for the resistance of antibiotics in bacteria pre-date the usage of antibiotics in the clinic (D'Costa, King et al. 2011, Perry, Waglechner et al. 2016), the main driver of this resistance is the overuse and improper stewardship of antibiotics as indicated by the tight correlation between increased antibiotic usage and increased incidences of bacterial resistance (Meyer, Gastmeier et al. 2013, Wushouer, Zhang et al. 2018). Furthermore, antibiotic usage in agriculture, in the prophylactic treatment of livestock, has contributed to the increased prevalence of resistant bacterial isolates in the environment (Witte 1998, Solomon, Van Houten et al. 2001). To complicate matters further, bacteria are particularly efficient at acquiring DNA from other bacterial species and microorganisms which means that antibiotic resistance encoding genes can be obtained at an alarming rate, once resistance has been identified (Hawkey 1998). There are two origins of resistance, natural and acquired, in bacteria. Natural resistance refers to mechanisms or traits that are shared universally within a bacterial species and are independent of previous antibiotic exposure; in comparison, acquired resistance refers to mechanisms of resistance that can be attributed to the acquisition of foreign DNA, encoding for antibiotic resistance, by transformation, transduction as well as

conjugation, or genetic mutations which arise due to stress or antibiotic exposure (Reygaert 2018).

There are four main mechanisms that bacteria employ to mitigate the action of antibiotics, all of which can be of natural or acquired origin (**Figure 1.2**): (**1**) limiting the uptake of antibiotics; (**2**) modifying the antibiotic target; (**3**) inactivating the antibiotic; (**4**) increasing antibiotic efflux (Reygaert 2018). These mechanisms are widespread across all bacteria, but some mechanisms are more prevalent in either Gram-negative or Gram-positive bacteria.
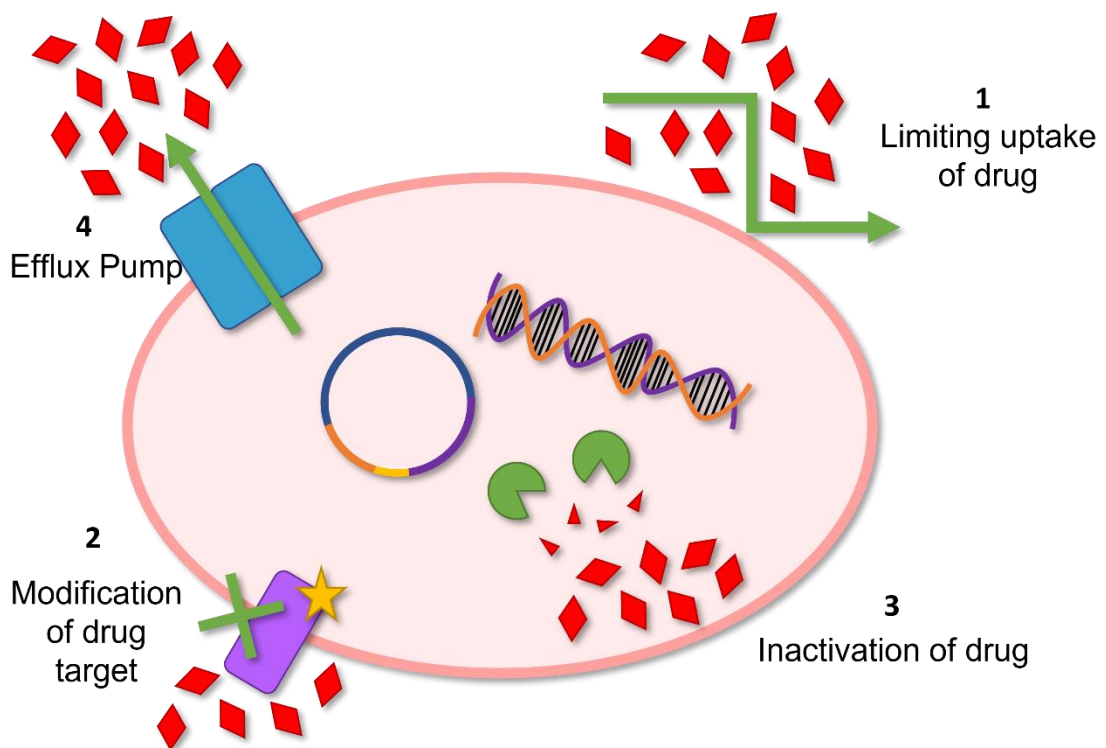
Figure 1.2 Diagrammatic representation of the 4 main mechanisms of antibiotic resistance.

Limiting uptake

Limiting the uptake of antibiotics is a mechanism of resistance which stops antibiotic compounds from entering bacterial cells. Gram-negative bacteria, such as the clinically relevant human pathogen *Pseudomonas aeruginosa,* are intrinsically adept at limiting the uptake of antibiotics due to their lipopolysaccharide rich outer membranes and reducing the amount of porins they have which can impede the ability of antibiotics to enter the Gram-negative cell, stopping them from acting upon their cellular target

(Breijyeh, Jubeh et al. 2020). These mechanisms alone make Gram-negative bacterial infections extremely hard to treat. Although limiting uptake of antibiotics as a mechanism of resistance is mainly employed by Gram-negative bacteria, there are examples of Gram-positive organisms that also use this mechanism, such as *M. tuberculosis* which has a lipid rich outer membrane, an unusual feature for Gram-positives, which limits the ability of hydrophilic antibiotics to penetrate and gain access to the cell (Gygli, Borrell et al. 2017). Furthermore, there have been several cases of *S. aureus* strains showing increased tolerance to vancomycin, a cell wall targeting antibiotic, in the absence of defined vancomycin resistance genes (*vanABCDE*). This increased tolerance is hypothesised to be attributed to an increase in cell wall turn over causing thickened cell walls preventing vancomycin from entering the cell(Sieradzki and Tomasz 1999, Weinstein and Fridkin 2001).

<u>Target modification</u>

Bacteria have developed ways of circumventing antibiotic exposure by physically altering the cellular target of specific antibiotics. This can be achieved by either modifying the structure of the target in some way i.e., mutating the binding site of an antibiotic, or increasing the production of the target to limit inhibition. One of the most well studied examples of target modification as a mechanism of resistance is that of β-lactam resistance. β-lactams interrupt bacterial cell wall formation by covalently binding to essential penicillin-binding proteins (PBPs) which are transpeptidase enzymes crucial in the crosslinking step of peptidoglycan formation. To circumvent the action of β-lactam antibiotics, many Gram-positive bacteria have developed ways to alter the structure or number of PBP proteins they encode. As an example, *S. aureus* which have acquired the *mecA* gene are able to encode an altered PBP (PBP2a) that β-lactams are unable to bind to and therefore cannot exert their inhibitory activity (Fishovitz, Hermoso et al. 2014). The modification of drug targets can also be due genetic mutations within the target itself; for example resistance to the DNA gyrase inhibiting antibiotics such as ciprofloxacin is due to mutations within the genes that encode the two subunits of DNA gyrase (*gyrA* and *gyrB*). These mutations encode for alterations in the structure of the DNA gyrase subunits and eliminate the ability of the fluroquinolones to bind and inhibit, rendering bacteria with these mutations resistant to the fluroquinolone antibiotics (Hooper and Jacoby 2015). Similarly, resistance to rifampicin, an antibiotic that

interferes with bacterial RNA synthesis, can be conferred by mutations within the gene (*rpoB)* which encodes the β subunit of bacterial RNA polymerase, and these mutations lead to structural changes in the encoded protein which causes decreased affinity of rifampicin for the ribosome (Xu, Zhou et al. 2005).

Antibiotic inactivation

Bacteria have also developed ways to inactivate the antibiotic itself, whereby the antibiotic is able to enter the cell but is inactivated before it can act upon its cellular target. Inactivation is either achieved through the degradation of the antibiotic itself or by the addition of a chemical group onto the antibiotic, rendering it inactive. The inactivation of β-lactams by β-lactamases, such as archetypal plasmid-encoded TEM, is a well-studied phenomenon. β-lactamases are a group of enzymes that can inactivate β-lactam antibiotics, such as methicillin, by hydrolysing the β-lactam ring to give a ring open β-amino acid which is unable to bind PBP and therefore cannot inhibit the bacteria (Bradford 2001). Similarly, the effects of the protein synthesis inhibiting antibiotic tetracycline, can be halted in bacteria which encode or have acquired a flavin-dependant monooxygenase, TetX, which hydroxylates the compounds, rendering it inactive (Yang, Moore et al. 2004). Alternatively, bacteria have been able to utilise transferases which are able to transfer a chemical group onto the antibiotic, such as acetyl and adenyl groups. One of the main causes of resistance to the protein synthesis inhibiting antibiotic chloramphenicol is chloramphenicol acetyltransferase, an enzyme which catalyses the acetylation of chloramphenicol at the 3-hydroxyl group. This acetylated product is then unable to bind bacterial ribosomes (Shaw 1983).

Efflux pumps

One of the most widespread mechanisms of antibiotic resistance, since most bacteria chromosomally encode them, is the use of drug efflux pumps which are primarily used to transport toxic substances from the bacterial. These pumps can be constitutively expressed or induced by environmental stimuli. Bacteria encode five classes of efflux pump families, most of which are single-component pumps which aid in the transport of substances across the cytoplasmic membrane (Blanco, Hernando-Amado et al. 2016). The five classes are the ATP binding cassette (ABC) family; small multidrug resistance (SMR) family; the major facilitator superfamily (MFS); resistance nodulation cell division

family (RND); multidrug and toxic compound extrusion (MATE) family (Reygaert 2018). Gram-positive bacteria generally chromosomally encode for members of the MFS and MATE families whereas all five of the efflux pump families have been observed in Gram-negative bacteria, including the most clinically significant efflux pump family, RND. This family are multi-component efflux pumps and can efflux compounds across the entire cell envelope. The most studied RND pump is the dual-binding pocket AcrAB-TolC pump from *Escherichia coli* that has the ability to efflux and therefore confer resistance to a multitude of compounds including tetracyclines, fluroquinolones and penicillin antibiotics (Du, Wang et al. 2014).

Many scientists and clinicians thought we had won the war against bacterial infections during the golden age of antibiotic discovery, however increased incidences of AMR and the lack of new antibiotics in the drug discovery pipeline has shifted this arms race in favour of the bacteria. Worryingly, a review on the prevalence of antibiotic resistance indicated that if incidences of AMR continue at the current rate then by 2050, approximately 10 million people will die per year from infections that are currently treatable (O'Neill 2016). In this report, several key interventions have been proposed to aid in combatting AMR such as, providing better incentives for pharmaceutical companies to investment in new antibiotic development, a global awareness campaign about the dangers of AMR and a global innovation fund for early stage and non-commercial research and development of new antibiotics (O'Neill 2016). To avoid the prospects of a post-antibiotic era, research efforts should return to the discovery and characterisation of novel antimicrobials and as there has been a relative lack of success with bringing synthetic antibiotics into the clinic, the way forward appears to be to head back to nature to search for novel classes of natural products.

1.3 Natural products

Natural products (NPs) or synthetic derivatives of natural products are the leading source of compounds used in the clinic to date, many of which were discovered during the 1940s to 1960s. The term NPs is given to compounds isolated from natural organisms such as bacteria, fungi and plants produced from the organism's secondary metabolism (hence the alternative term, secondary metabolites), which is defined as products not required for growth, development, or reproduction of the organism (Katz and Baltz

2016). Many of these NPs have been utilised by humans as (for example) antibiotics, immunosuppressants, anti-cancer agents and antivirals (Newman and Cragg 2016, Huang, Lu et al. 2021). Although many organisms biosynthesise bioactive NPs (**Figure 1.3**), it is estimated that approximately 70 % of NPs that have been used as or developed into clinically useful antibiotics have been isolated from the bacterial order Actinomycetales, which are a group of generally Gram-positive, filamentous bacteria that are referred to as actinomycetes (Hutchings, Truman et al. 2019). One of the most important members of this order are the *Streptomyces* bacteria which are responsible for the production of two thirds of the currently used antibiotics.
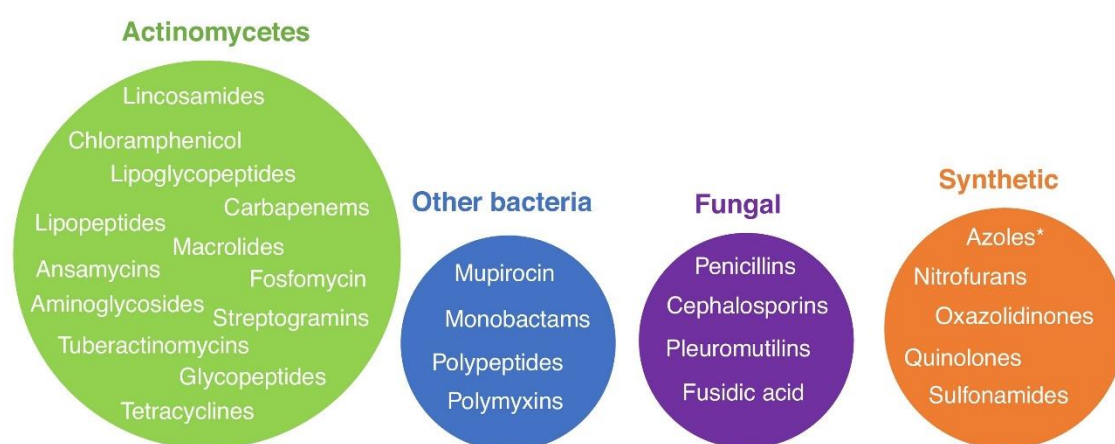
Figure 1.3 Classes of clinically used antibiotics and where they have derived from. * Denotes synthetic derivatives based on natural product discoveries. Adapted from Hutchings et al (2019) (Hutchings, Truman et al. 2019)

NPs have been suggested to be the best candidates for antibiotic development because they have been optimised by evolution to be stable and freely diffusible. It is proposed that the production of secondary metabolites is to give the producing organism a selective advantage in the environment through functions such as direct competition with other bacterial species and the regulation of endogenous defence mechanisms. Therefore, as these compounds are produced from microorganisms themselves, they are generally better at entering bacterial cells and interacting with bacterial specific targets, than synthetic antibiotic compounds (Atanasov, Zotchev et al. 2021).

The genes encoding for these NPs are generally clustered together in the producer's genome in what we refer to as a biosynthetic gene cluster (BGC), which can be up to 100 kilobases (kb) in size (Bibb 2005). These BGCs contain all the genes required for the

biosynthesis of a particular compound, with all genes encoding for core enzymes, accessory enzymes, regulators and transporters all being adjacent to each other on the genome. NPs are generally characterised by their scaffold diversity and structural complexity which is a product of the core and accessory proteins encoded by these gene clusters (Atanasov, Zotchev et al. 2021). There are several classes of NPs including the terpenoids, alkaloids, ribosomally synthesised and post-translationally modified peptides (RiPPs), non-ribosomal peptides (NRPS) and the polyketides. The work in this thesis is focussed upon a family of polyketide antibiotics and thus only a discussion of polyketide NPs is given below.

1.3.1 Polyketides

Polyketides are a remarkable class of compounds owing to their impressive range of functional and structural diversity which has led to many of them being medicinally important compounds. Polyketides are characterised by the decarboxylative Claisen condensation of multiple extender units such as methylmalonyl coenzyme A (CoA) and malonyl-CoA, generating an elongated carbon chain which is then extensively modified to produce the large plethora of polyketide compounds (Staunton and Weissman 2001, Rutledge and Challis 2015). Polyketides are synthesised from polyketide synthetases (PKSs) which consist of either multi-domain enzymes or enzyme complexes which encode all of the required enzymes to perform condensation of the multiple starter units as well as enzymes involved in the modification of the polyketide (Wang, Zhang et al. 2020). Although all PKSs use a similar synthetic process, they can be separated into three main types, type I PKSs, type II PKSs and type III PKSs.

Type I PKS

Type I PKSs are multi-functional enzymes which are organised into modules containing different catalytic domains and therefore are often referred to as modular PKSs. These modules contain ketosynthase (KS), acyltransferase (AT) and acyl-carrier protein (ACP) domains that are required for the catalysis of one cycle of chain extension, as well as encoding any domains within a module that are required for the modification of the β-keto intermediate. The AT of the loading module loads a single starter unit onto the ACP, and subsequent modules elongate the β-keto intermediate by 2 carbons through the action of the KS which catalyses the formation of the carbon-carbon bond formation

between the extender unit and the growing product (Dutta, Whicher et al. 2014). Modification of the growing β-keto intermediate can then take place depending on which enzymes are present in the module; modification of the β-keto group to a hydroxyl group can be undertaken by ketoreductases (KR), formation of a double carbon bond can be catalysed by dehydratases (DH) whilst single carbon bond formation can be performed by enoylreductases (ER). Once the chain has been extended to the correct length, which is generally determined by the number of modules present in the type I PKS, the ACP transfers the polyketide product to the thioesterase (TE) unit where the polyketide is released by hydrolysis. Any post-PKS modification steps can then be undertaken by accessory enzymes to finalise the biosynthesis of the desired product (Staunton and Weissman 2001).

An exemplar of modular type I PKS biosynthesis is that of erythromycin A, a NP used in the clinic to treat chest, ear and sexually transmitted infections, which is produced from *Saccharopolyspora erythraea.* Erythromycin A biosynthesis utilises a product, 6-deoxyerythronolide B (DEBS), of a type I PKS, in its biosynthesis which is then acted upon by tailoring enzymes to produce erythromycin A. The DEBS PKS is comprised of a loading module, 6 extending modules and the end module (**Figure 1.4**). The loading module contains an AT which loads the starter unit (propionyl-CoA) onto the ACP. Each of the 6 extending modules increases the length of the polyketide by the addition of 2 carbons through the cooperation of the AT and KS of each of the modules, which add a single propionyl-CoA into the growing chain. All of the six extender modules, except for module 3, encode a KR domain which modifies β-keto groups to hydroxyl groups. Module 4 also contains DH and ER domains which orchestrate the addition of double and single carbon bonds respectively. After each module has performed its modifications to the poly-β-keto intermediate DEBS, it is released from the ACP through the activities of TE which finalises the PKS steps of erythromycin A biosynthesis. Further post-PKS steps, including glycosylation, hydroxylation and methylation, are then performed to convert 6-deoxyerythronolide B into erythromycin A (Cummings, Breitling et al. 2014). Further examples of NPs derived from type I PKSs are the antiparasitic agent avermectin and the antifungal nystatin (Staunton and Weissman 2001).
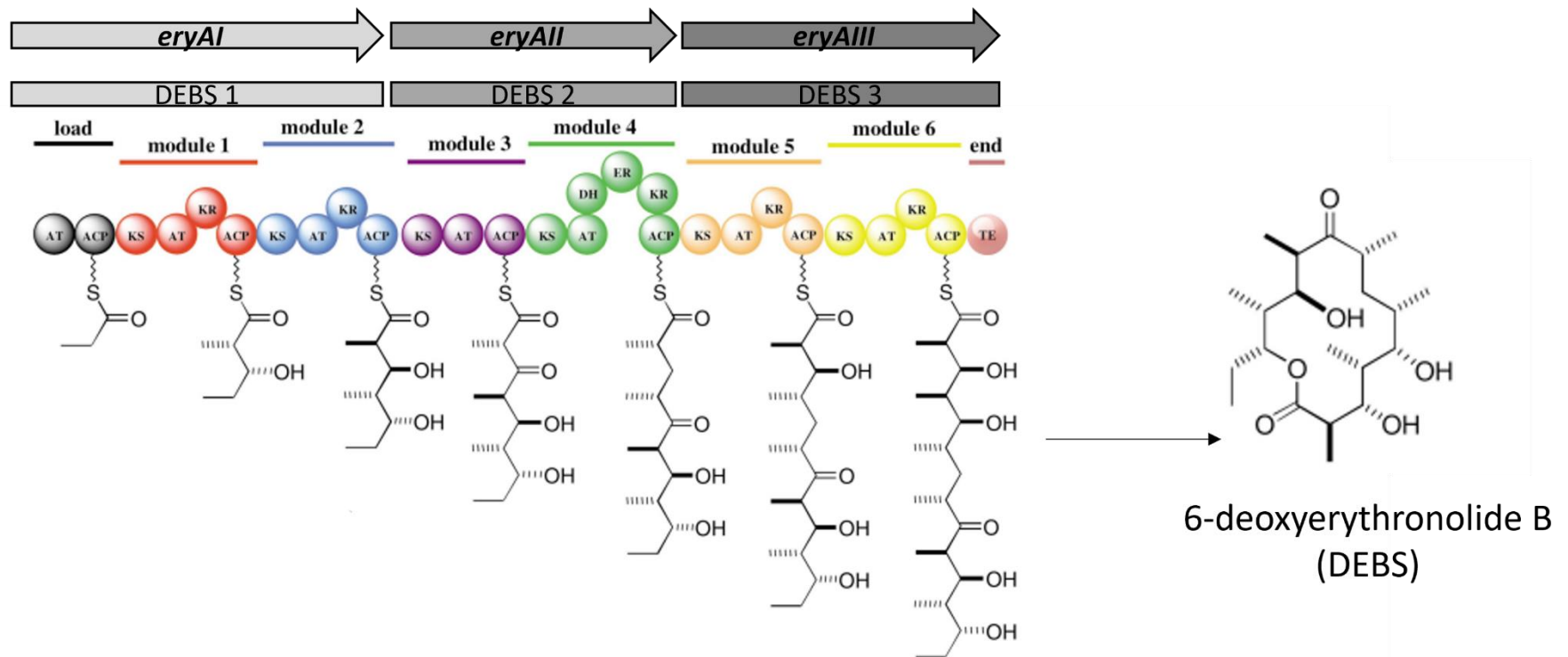
Figure 1.4 Biosynthesis of DEBS for the production of erythromycin A from the DEBS type I polyketide synthase. Arrows represent the three genes, *ery* AI, *ery* AII and *ery* AIII, which encode the proteins of the type I PKS. Boxes represent the proteins that make up the DEBS type I PKS. Individual modules are colour coded and circles represent distinct domains: **AT**; acyltransferase, **ACP**; acyl-carrier protein, **KS**; ketosynthase, **KR**; ketoreductase, **DH**; dehydratase, **ER**; enolreductase, **TE**; thioesterase. Adapted from (Staunton and Weissman 2001).

<u>Type II PKS</u>

Metabolites produced by type II PKSs are generally aromatic polyketides such as anthracyclines, angucyclines, tetracyclines, and pentangular polyphenols (Hertweck, Luzhetskyy et al. 2007, Wang, Zhang et al. 2020) (**Figure 1.5**) and, unlike the multifunctional enzymes of type I PKSs, type II PKSs are comprised of several individual enzymes which are each expressed from a distinct gene. A hallmark for the biosynthesis of type II polyketides, such as the blue-pigmented actinorhodin antibiotic produced by *Streptomyces coelicolor* A3(2) (Hopwood 1997)(**Figure 1.5**), is the presence of a minimal set of iteratively used enzymes, KS_{α}, KS_{β} and ACP. The KS enzymes are responsible for the catalysis of the Claisen condensation to produce carbon-carbon bonds from activated acyl as well as malonyl building blocks (KS_{α}) and the determination of the carbon chain length (KS_{β}), alongside the ACP which serves as an anchor to the growing polyketide chain (Das and Khosla 2009). Over several iterations of decarboxylative condensation of malonyl-CoA via the actions of the minimal PKS, a carbon chain of correct length is generated which for aromatic polyketides is usually either 16 (octaketides), 20 (decaketides), 24 (dodecaketides) or in some rarer cases 13 (tridecaketide) carbons in length. After the carbon chain has reached the determined length, KRs can introduce hydroxyl groups to the β-keto groups, before cyclases and aromatases then act upon the resulting poly-β-keto intermediate to generate polyphenol compounds which can be further modified by BGC encoded tailoring enzymes such as oxygenases, halogenases, methyltransferases, and glycosyltransferases to provide the structural diversity displayed by this class of compounds. An example of type II PKS biosynthesis is given in section **1.7**. Many of the compounds produced or derived from type II polyketides are used clinically as antibiotics (i.e., tetracyclines) or as anticancer agents (i.e., doxorubicin).
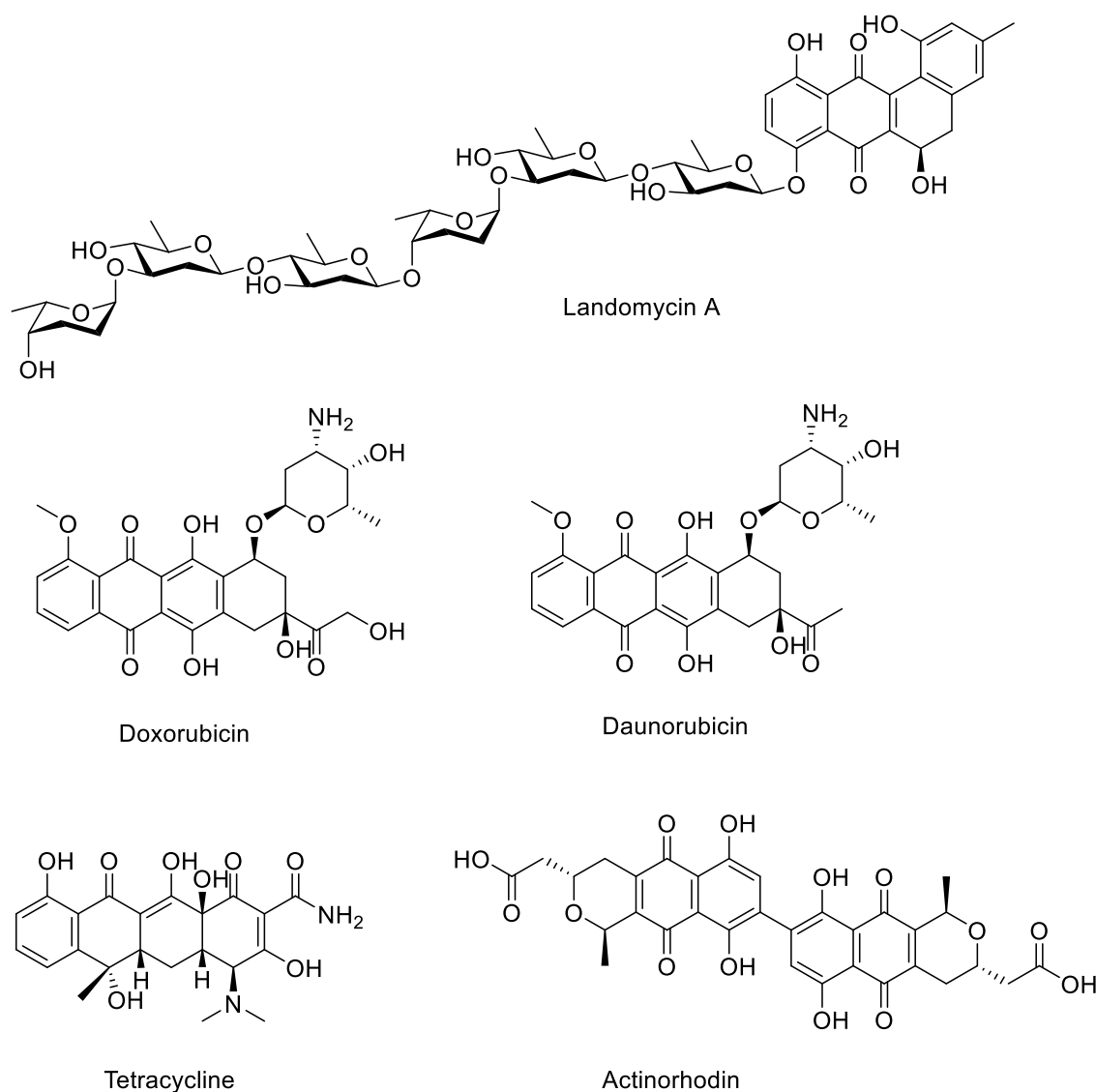
Figure 1.5 Structures of several type II polyketide NPs.

In comparison, type III PKS are made up of homodimers of small proteins that embody all of the activities of the essential type I and type II domains with the main difference being that they do not utilise ACPs and instead act upon free CoA-linked thioester substrates (Katsuyama and Ohnishi 2012).

The essential enzyme machineries that are required for the biosynthesis of these different classes of NPs, encoded by BGCs, are generally well conserved and, because they are encoded to contain all the essential proteins and tailoring enzymes, we can generally predict what molecules they produce. This information coupled with the

advent of genome sequencing means many techniques have been developed that can use genome sequencing data to predict the different kinds of BGCs organisms can encode, which we call genome mining (Albarano, Esposito et al. 2020). Several bioinformatic platforms have been established to highlight potential genes that are likely to govern the biosynthesis of NP scaffold structures and therefore aid in the identification of potential BGCs. One of these predictive bioinformatic tools is antiSMASH which can be used to mine the genomes of bacteria, plants and fungi, this tool can further be used to determine if organisms produce previously identified bioactive NPs which can aid in limiting time wasted on the rediscovery of compounds, one of the major challenges of modern NP discovery (Medema, Blin et al. 2011, Blin, Shaw et al. 2021). Furthermore, genome mining tools have been incredibly useful for discovering silent BGCs which do not normally produce their NPs in normal lab settings. This has allowed us to grasp the full potential of NP producers and may aid in the discovery of novel chemistry (Liang, Liu et al. 2022).

1.4 Streptomyces

Streptomyces are spore forming, filamentous, Gram-positive actinomycete bacteria and are the largest genus of the order Actinomycetales. These aerobic bacteria are widespread in almost all environments including marine and desert environments but are most commonly found in the soil where they undertake a saprophytic lifestyle converting cellulose and chitin into useable sugars by the secretion of enzymes that are able to degrade these insoluble organic polymers. *Streptomyces* are abundant in soil and have even been found to be partly responsible for the characteristic earthy smell of soil, which has been attributed to the production of a conserved secondary metabolite in *Streptomyces* species called geosmin (Gerber and Lechevalier 1965). To date, there are approximately 600 validated and named *Streptomyces* species which have been heavily studied due to their complex lifestyle and their ability to encode and produce a large variety of secondary metabolites including medicinally useful NPs.

However, *Streptomyces* species are not just found as free-living soil bacteria, and they have also evolved to live in symbiosis with plants, fungi and invertebrates (Seipke, Kaltenpoth et al. 2012). There are however, several examples of parasitic *Streptomyces* such as *Streptomyces scabies* which causes a scab disease in several crop species such

as potato plants. Furthermore, although rare, two species have been identified to cause pathogenesis in humans. Both *Streptomyces sudanensis* and *Streptomyces somaliensis* have been reported to cause actinomycosis infections and bacteriemia in humans after entering the skin via cutaneous wounds (Borelli and Middelveen 1986, Quintana, Wierzbicka et al. 2008). Overall parasitic *Streptomyces* are rare, and in many cases, organisms recruit these actinobacteria to promote growth of the host organism or to provide a protective function. Symbioses between *Streptomyces* and plants have been found to be common which may be in part due to their filamentous and spore forming lifestyle which allows for this genus of bacteria to colonise roots of plants and ultimately gain entry into the host plant leading to endophytic symbioses. The *Streptomyces* symbiont usually confers benefits to the plant species, for example, by producing auxin which promotes growth of the plant, or they can also provide a protective effect towards the plant through the production of bioactive secondary metabolites to protect the plant from disease, in exchange for access to the organic substrates *Streptomyces* can utilise for growth (Seipke, Kaltenpoth et al. 2012).

Over the past few years, it has become apparent that *Streptomyces* are also very well adapted to live in symbioses with invertebrates, as well as plants, where they are assumed to confer a protective effect towards these invertebrates for example by protecting invertebrates' foods sources from parasites (Flórez, Biedermann et al. 2015). Symbioses between actinobacteria and several invertebrate species have been documented including in marine environments such as with sea snails and marine sponges (Quezada, Licona-Cassani et al. 2017, Guerrero-Garzón, Zehl et al. 2020). One of the most well studied examples of these symbioses is with attine fungus-growing ants such as ants from the *Acromyrmex* genus. These ants farm a coevolved fungus, *Leucoagaricus gongylophorus*, which produces specialized hyphae, which serve as the sole food source for the ant colony. These ants have been found to also live in association with several actinobacteria including *Streptomyces* species which have been shown to produce antifungal compounds, such as the polyene antifungal candicidin and antimycin, that can contribute to the protection of this fungal garden against the pathogenic microfungus, *Escovopsis*, which can completely destroy the ants only food source in a single infection (Currie, Scott et al. 1999, Haeder, Wirth et al. 2009, Seipke, Barke et al. 2011). *Streptomyces* have therefore been able to adapt and colonize many

different niches, due to their beneficial roles including protection from disease them an incredibly successful genus.

1.4.1 *Streptomyces* biology and antibiotic production

The ability of these bacteria to take advantage of so many ecological niches is due in part to their complex life cycle; *Streptomyces* bacteria can be found in two distinct forms of multicellular mycelium or as unicellular spores. Their life cycle revolves around the ability to interconvert between these multiple modes of existence. A diagrammatic representation of the *Streptomyces* life cycle is shown in **Figure 1.6** and is explained below. Upon encountering favourable conditions spores of *Streptomyces* swell and start to germinate to produce hyphae which grow by tip extension (**1**), these hyphae branch out deeply into the substrate, such as soil, that they are growing in and thus gives rise to a vegetative colony (**2**). Vegetative mycelial growth can then begin to differentiate to begin the production of reproductive mycelium whereby they begin to grow upwards, out of the aqueous environment of the vegetative colony and grow up into the air (**3**). To date the exact cause of this life stage switch is poorly understood but it is hypothesised to be influenced by a multitude of factors such as environmental conditions, the availability of nutrients, iron availability and extracellular signalling such as quorum sensing. Once the production of aerial hyphae has been initiated genetically programmed morphological differentiation takes place which leads to the formation of multiple septum to make sporogenic aerial hyphae (Bush, Tschowri et al. 2015). During this septation, each aerial hypha differentiates into a chain of pre-spore compartments which each house a copy of the chromosome (**4**). The pre-spores containing a single copy of the chromosome then further mature and differentiate to become thick-walled spores (**5**). These spores are then dispersed, and the life cycle re-starts when the spores encounter favourable conditions and begin to germinate (**6**).
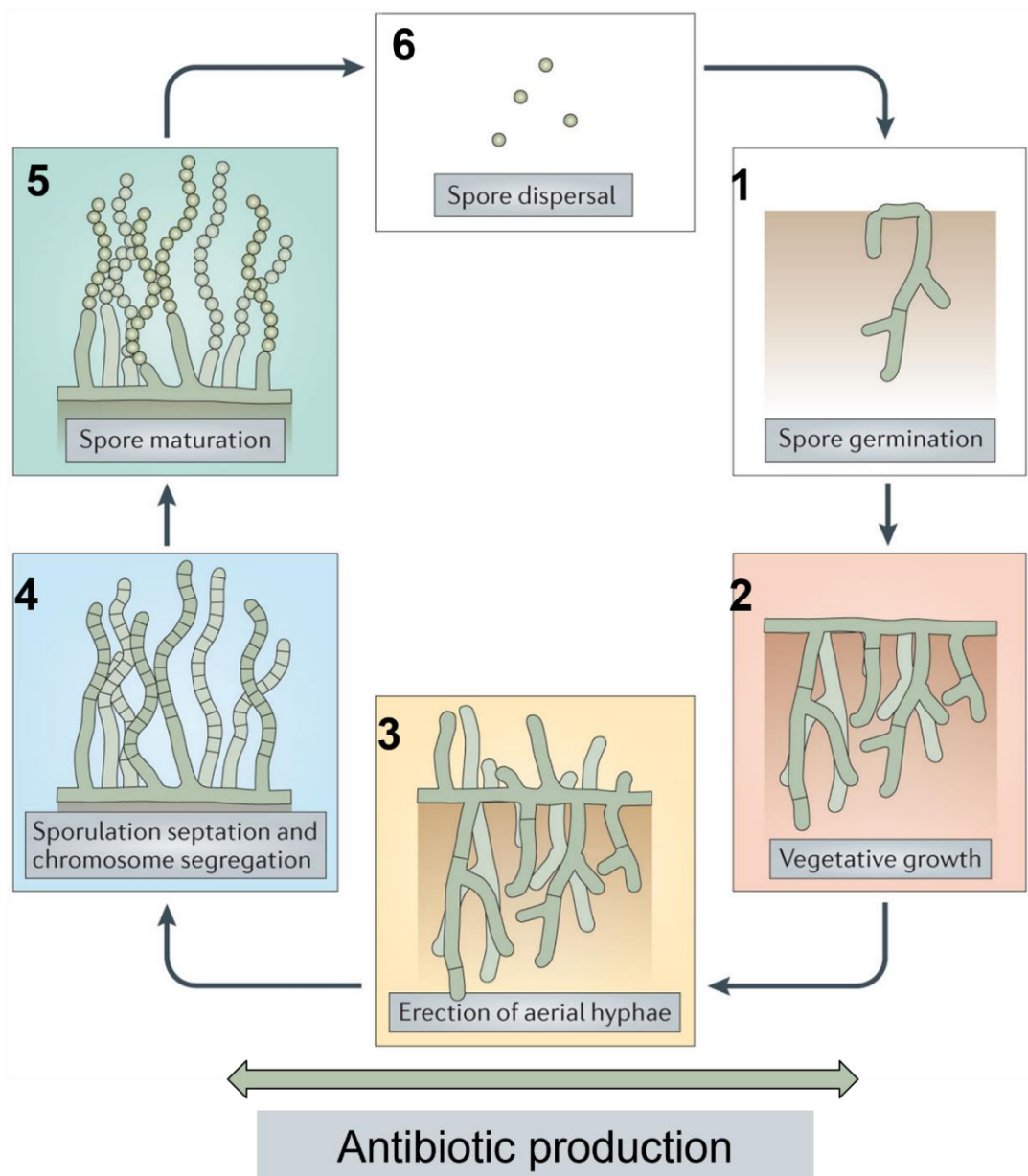
Figure 1.6 Diagrammatic representation of the Streptomyces life cycle. Double arrow corresponds to the stage of the life cycle that antibiotics are produced Adapted from Bush et al (2015).

Secondary metabolites, such as antimicrobials, are produced during the transition from vegetative growth to sporulation, and many of the molecules produced by *Streptomyces* have been or still are used in the clinic as antibiotics (**Table 1.1**) (Bibb 2005). Although it is not fully understood why *Streptomyces* encode and produce so many bioactive secondary metabolites, several hypotheses have been put forward; the most likely explanation is that these bacteria encode these secondary metabolites for a

multitude of reasons such as defensive and offensive chemical weapons, signalling molecules for the interaction with other microbes and to mediate interactions with non-bacterial organisms such as eukaryotic hosts (i.e., plants and attine hosts) (Chater, Biró et al. 2010, Seipke, Kaltenpoth et al. 2012, Klassen 2014).

Table 1.1 Clinically used antibiotics isolated from *Streptomyces* species.

Class of antibiotic	Example compound	Producing organism	Molecular target
Aminoglycosides	**Kanamycin A**	*Streptomyces kanamyceticus*	Protein synthesis (30s ribosome subunit)
Tetracyclines	**Tetracycline**	*Streptomyces aureofaciens*	Protein synthesis (30s ribosome subunit)
Amphenicols	**Chloramphenicol**	*Streptomyces venezuelae*	Protein synthesis (50s ribosome subunit)
Tuberactinomycins	**Viomycin**	*Streptomyces puniceus*	Protein synthesis (30s and 50s ribosome subunit)
Cycloserines	**Seromycin**	*Streptomyces orchidaceus*	Cell wall synthesis
Streptogramins	**Pristinamycin**	*Streptomyces pristinaespiralis*	Protein synthesis (50s ribosome subunit)
Phosphonates	**Fosfomycin**	*Streptomyces fradiae*	Cell wall synthesis
Lipopeptides	**Daptomycin**	*Streptomyces roseosporus*	Cell membrane disruption

Although research efforts during the 1940s to the 1960s initiated by Waksman and colleagues had already identified *Streptomyces* as prolific antibiotic producers, the advent of genome sequencing revealed that they had the capability to produce many more secondary metabolites than we had first realised (Waksman, Schatz et al. 1946). Genome sequencing has allowed for us to determine that all *Streptomyces* species encode between 20 and 60 BGCs for secondary metabolite production including a diverse range of polyketides, NRPSs and RiPPs (Doroghazi and Metcalf 2013). Furthermore, only a fraction of these metabolites are produced under standard laboratory conditions, with the rest of these encoded BGCs being referred to as cryptic

BGCs. The discovery of cryptic BGCs further indicates that the majority of bioactive secondary metabolite production is triggered by environmental cues that are often missing in standard laboratory culture conditions (Doroghazi and Metcalf 2013). With this knowledge in hand, *Streptomyces* bacteria have been brought back into the limelight of antibiotic discovery and, alongside the advent of genome mining techniques, scientists have begun to try and decipher the products of these encoded cryptic BGCs in search of new antimicrobials by trying to induce the expression of these cryptic BGCs.

Analysis of the frequently isolated *Streptomyces* species has led to the rediscovery of previously identified bioactive NPs. As we know that many of these *Streptomyces* species can cultivate many ecological niches, research efforts have recently been focusing on uncovering new *Streptomyces* species, from under sampled environments such as the deep sea, the desert and invertebrate symbioses in the search for novel natural products (Dharmaraj 2010, Sivakala, Gutiérrez-García et al. 2021).

1.5 *Streptomyces formicae* KY5

Research published in 2013 documented the analysis of the bacterial communities associated with two ant-plant symbiosis in the hopes of uncovering new species of antibiotic producing actinomycetes (Seipke, Barke et al. 2013). One of the ant-plant symbioses sampled was that of the Kenyan plant ant *Tetraponera penzigi* which lives in an obligate symbiosis with the thorny acacia plant (*Acacia drepanolobium*), a common plant found within the Kenyan Laikipia District (Young, Stubblefield et al. 1996). *T. penzigi* are one of four species of ant that have been employed by the acacia plant to provide protection against medium and large-sized herbivores, alongside the use of long hollow thorns. The *T. penzigi* ants reside within large hollow swellings called domatia on the acacia plant (**Figure 1.7**), where they farm a fungal cultivar from the *Chaetomium* genus which they are hypothesised to use as a food source (Baker, Martins et al. 2017). It was within this symbiotic community that researchers discovered a new actinobacterial species, *Streptomyces formicae* KY5 (*S. formicae*), the name being derived from *formicae* meaning 'ant' in Latin, which residies on the bodies and habitats of the *T. penzigi* ants. It is not currently known if *S. formicae* confers any benefits to the ants themselves. The whole genome of *S. formicae* was sequenced in 2018 using sequencing platforms PacBio, 454 and Illumina (Holmes, Devine et al. 2018) and was

found to be comprised of a 9.6 Mbps linear chromosome with a high GC content (~71 %) characteristic of actinobacteria which contains 8162 protein coding sequences. As *Streptomyces* are known to encode a large amount of BGCs, the genome was analysed by predictive analysis software (antiSMASH) and was predicted to encode at least 45 BGCs for potential NPs including several RiPP, NRPS and polyketide synthase clusters (Holmes, Devine et al. 2018).

Figure 1.7 *Tetraponera penzigi* ants on the thorny acacia plant. The large swelling is called a domatia and is where the ants reside and farm a fungal species. Image taken by Dr Dino Martins.

1.6 Novel antimicrobials from *S. formicae*

In preliminary bioassays *S. formicae* was found to produce compounds that were inhibitory towards *B. subtilis*, *C. albicans* and *L. prolificans* indicating compounds of an antibacterial and antifungal nature. Further analysis of this bacterial activity using antibacterial guided fractionation revealed the presence of several novel compounds which were isolated and characterised by structural elucidation (Qin, Munnoch et al. 2017). The compounds responsible, in part, for this antibacterial bioactivity were determined to be a new class of compounds called the formicamycins and a previously identified class of related compounds, the fasamycins (originally identified by Feng et al,

2012). 10 formicamycins (A-J) and 3 novel fasamycins (C-E) were originally isolated from *S. formicae* and a further 3 formicamycins (K-M) containing bromine atoms were identified after growth of *S. formicae* on media supplemented with sodium bromide (**Figure 1.8**). All these compounds displayed bioactivity against methicillin resistant *S. aureus* and vancomycin resistant *E. faecalis*, both of which are clinically relevant pathogens. Furthermore, recent work by Devine et al (2021), isolated 6 new fasamycin congeners (L-Q) and 2 new formicamycins (R and S) from genetically modified *S. formicae* strains (**Figure 1.8**), which also were found to exhibit potent bioactivity against Gram-positive bacteria (Devine, McDonald et al. 2021). Alongside the discovery of the formicamycins from *S. formicae*, several congeners of formicamycin (N-Q), have been isolated from a rhizospheric soil-derived *Streptomyces* sp. KIB-1414 (Yuan, Wang et al. 2020). Furthermore, new congeners of fasamycins have been identified under the names accramycins, streptovertimycins and napthacemycins, from several different actinomycete strains (Maglangit, Zhang et al. 2020, Yang, Li et al. 2020, Yuan, Wang et al. 2020). A characteristic of both classes of compounds is that they all exhibit bioactivity against clinically relevant Gram-positive bacteria making them interesting candidates for further investigations.

Fasamycin C R$_1$ = H, R$_2$ = H, R$_3$ = H, R$_4$ = H, R$_5$ = H, R$_6$ = CH$_3$, R$_7$ = H, R$_8$= H
Fasamycin D R$_1$ = H, R$_2$ = Cl, R$_3$ = H, R$_4$ = H, R$_5$ = H, R$_6$ = CH$_3$, R$_7$ = H, R$_8$ = H
Fasamycin E R$_1$ = Cl, R$_2$ = Cl, R$_3$ = H, R$_4$ = H, R$_5$ = H, R$_6$ = CH$_3$, R$_7$ = H, R$_8$ = H
Fasamycin F R$_1$ = H, R$_2$ = H, R$_3$ = H, R$_4$ = H, R$_5$ = H, R$_6$ = CH$_3$, R$_7$ = H R$_8$= COOH
Fasamycin L R$_1$ = Cl, R$_2$ = Cl, R$_3$ = H, R$_4$ = Cl, R$_5$ = H, R$_6$ = CH$_3$, R$_7$ = H, R$_8$ = H
Fasamycin M R$_1$ = Cl, R$_2$ = Cl, R$_3$ = H, R$_4$ = H, R$_5$ = CH$_3$, R$_6$ = H R$_7$ = Cl, R$_8$= H
Fasamycin N R$_1$ = Cl, R$_2$ = Cl, R$_3$ = Cl, R$_4$ = H, R$_5$ = H, R$_6$ = CH$_3$, R$_7$ = H, R$_8$ = H
Fasamycin O R$_1$ = Cl, R$_2$ = Cl, R$_3$ = H, R$_4$ = Cl, R$_5$ = CH$_3$, R$_6$ = CH$_3$, R$_7$ = H, R$_8$ = H
Fasamycin P R$_1$ = Cl, R$_2$ = Cl, R$_3$ = Cl, R$_4$ = H, R$_5$ = CH$_3$, R$_6$ = OH R$_7$= Cl, R$_8$ = H
Fasamycin Q R$_1$ = Cl, R$_2$ = Cl, R$_3$ = Cl, R$_4$ = Cl, R$_5$ = H, R$_6$ = CH$_3$, R$_7$ = H, R$_8$ = H

Formicamycin A R$_1$ = H, R$_2$ = Cl, R$_3$ = H, R$_4$ = H, R$_5$ = CH$_3$,R$_6$= H
Formicamycin B R$_1$ = Cl, R$_2$ = Cl, R$_3$ = H, R$_4$ = H, R$_5$ = H,R$_6$= H
Formicamycin C R$_1$ = H, R$_2$ = Cl, R$_3$ = Cl, R$_4$ = H, R$_5$ = CH$_3$,R$_6$= H
Formicamycin D R$_1$ = Cl, R$_2$ = Cl, R$_3$ = Cl, R$_4$ = H, R$_5$ = H,R$_6$= H
Formicamycin E R$_1$ = Cl, R$_2$ = Cl, R$_3$ = Cl, R$_4$ = H, R$_5$ = CH$_3$,R$_6$= H
Formicamycin F R$_1$ = Cl, R$_2$ = Cl, R$_3$ = H, R$_4$ = Cl, R$_5$ = CH$_3$,R$_6$= H
Formicamycin G R$_1$ = H, R$_2$ = Cl, R$_3$ = Cl, R$_4$ = Cl, R$_5$ = CH$_3$,R$_6$= H
Formicamycin H R$_1$ = Cl, R$_2$ = H, R$_3$ = Cl, R$_4$ = Cl, R$_5$ = CH$_3$,R$_6$= H
Formicamycin I R$_1$ = Cl, R$_2$ = Cl, R$_3$ = Cl, R$_4$ = Cl, R$_5$ = H,R$_6$= H
Formicamycin J R$_1$ = Cl, R$_2$ = Cl, R$_3$ = Cl, R$_4$ = Cl, R$_5$ = CH$_3$,R$_6$= H
Formicamycin R R$_1$ = Cl, R$_2$ = Cl, R$_3$ = Cl, R$_4$ = Cl, R$_5$ = H, R$_6$= Cl
Formicamycin S R$_1$ = Cl, R$_2$ = Cl, R$_3$ = Cl, R$_4$ = Cl, R$_5$ = CH$_3$, R$_6$= Cl
Formicamycin T R$_1$ = H, R$_2$ = Cl, R$_3$ = H, R$_4$ = Cl, R$_5$ = CH$_3$,R$_6$= H
Formicamycin U R$_1$ = Cl, R$_2$ = H, R$_3$ = Cl, R$_4$ = H, R$_5$ = CH$_3$,R$_6$= H
Formicamycin V R$_1$ = Cl, R$_2$ = H, R$_3$ = Cl, R$_4$ = H, R$_5$ = CH$_3$,R$_6$= H
Formicamycin W R$_1$ = H, R$_2$ = Cl, R$_3$ = Cl, R$_4$ = Cl, R$_5$ = CH$_3$,R$_6$= H
Formicamycin X R$_1$ = H, R$_2$ = Cl, R$_3$ = Cl, R$_4$ = Cl, R$_5$ = OH,R$_6$= H
Formicamycin Y R$_1$ = H, R$_2$ = H, R$_3$ = Cl, R$_4$ = Cl, R$_5$ = OH,R$_6$= H

Figure 1.8 Structures of fasamycin and formicamycin compounds isolated from wild-type and genetically modified *S. formicae.*

1.7 Biosynthesis of formicamycin

The formicamycins isolated from *S. formicae* are biosynthesised from the formicamycin (*for*) BGC which is comprised of 24 genes expressed on 9 transcripts which encode a type II polyketide synthase and required tailoring enzymes, the expression of which, is regulated by two MarR regulators, ForJ and ForZ, as well as a two-component system consisting of the sessor kinase ForG and the response regulator ForF (**Figure 1.9**). Details of formicamycin regulation are discussed in Chapter 6 of this thesis (Devine, McDonald et al. 2021).

Gene	Annotation
forN	Acyl hydrolase
forM	Methyltransferase
forL	PKS cyclase
forK	Na$^+$/H$^+$ exchanger
forJ	MarR family transcriptional regulator
forI	ACC biotin carboxylase
forH	ACC carboxyl transferase
forG	Sensor histidine kinase
forF	LuxR family response regulator
forE	ACC biotin carboxy carrier protein
forD	PKS cyclase/dehydratase
forC	PKS ACP
forB	KS$_\beta$
forA	KS$_\alpha$
forR	Putative PKS cyclase/chaperone
forS	PKS chaperone
forT	Methyltransferase
forU	Putative PKS cyclase/chaperone
forV	Halogenase
forW	Methyltransferase
forX	Monooxygenase
forY	Oxidoreductase
forZ	MarR family transcriptional regulator
forAA	Multidrug resistance protein

Figure 1.9 Diagrammatic representation of the formicamycin BGC and details of all the genes encoded by the *for* BGC. Arrows represent the individual genes of the *for* BGC and which genes are expressed on each transcript. Adapted from Devine et al 2021.

Using isotope feeding experiments, mutational analysis of the *for* BGC and comparative bioinformatics, a biosynthetic pathway of the formicamycins has been
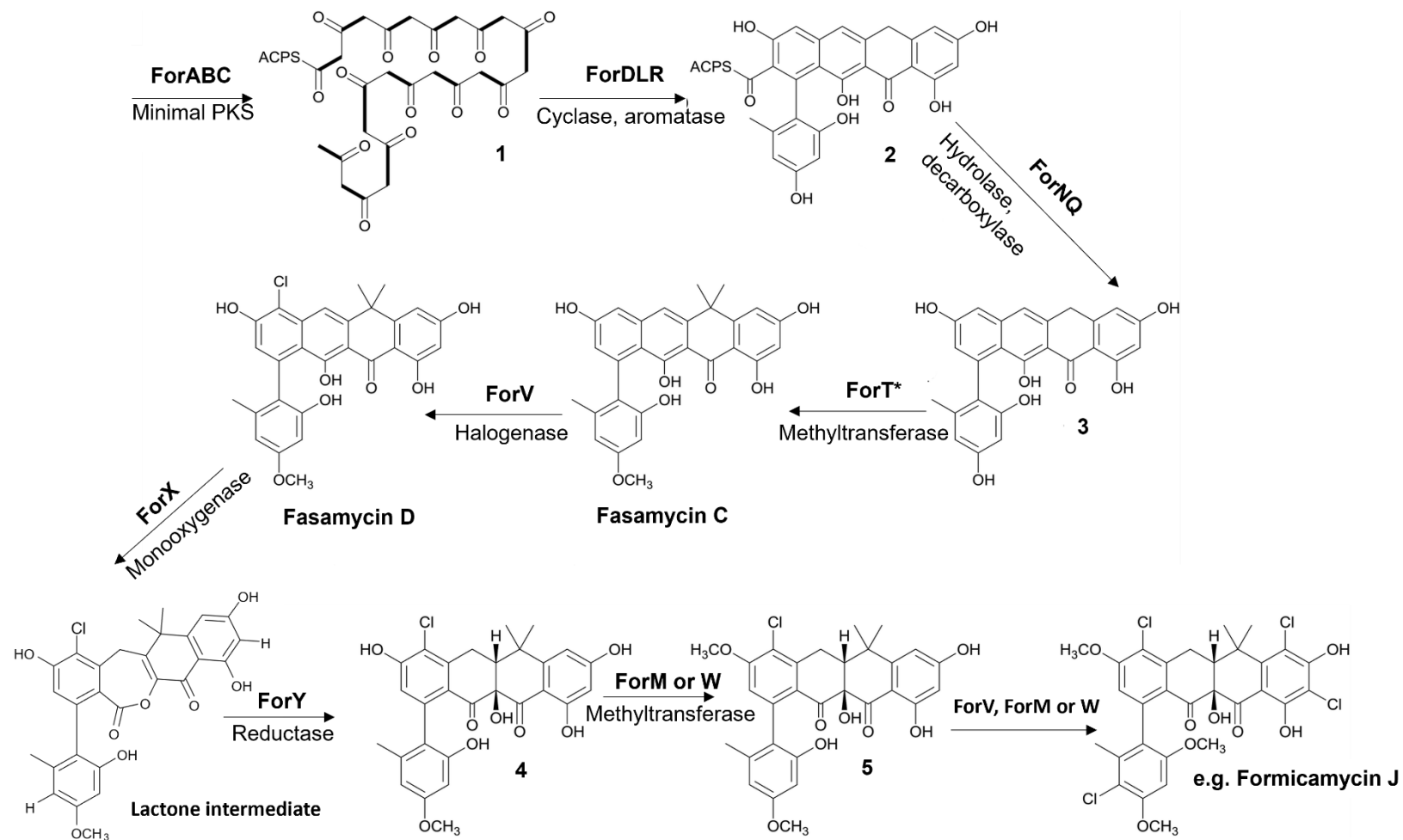
Figure 1.10 Proposed biosynthetic pathway of the formicamycin compounds. * Refers to the proposed methyltransferase in this step in the biosynthetic pathway.

proposed. An explanation of the biosynthetic pathway is described below and in **Figure 1.10**.

ForABC are the minimal PKS of the *for* BGC, comprising of the heterodimeric β-ketosynthase (KS) proteins KS$_\alpha$/KS$_\beta$ (ForAB) and an acyl carrier protein (ForC) all of which are fundamental in determining the length of the polyketide chain and the overall topology of the ring system. It is hypothesised that ForABC produce a tridecaketide intermediate **1** which is then converted into **2** through the action of cyclases and dehydratases ForD, ForL and ForR. The hydrolase, ForN, and a decarboxylase, ForQ, then convert intermediate **2** into intermediate **3**. The first post-PKS modification is proposed to be the addition of the *gem*-dimethyl group at C18 as every fasamycin and formicamycin compound contain these two methyl groups. Qin et al (2017) propose that the methyltransferase responsible for this *gem*-dimethyl group is ForT due to the fact that it shares high sequence identity with the methyltransferase from the benastatin gene cluster (BenF) which catalyse the *gem*-dimethyl group in benastatin biosynthesis (Feng, Kallifidas et al. 2011). One of the other methyltransferases of the pathway, either ForM or ForW are then hypothesised to be responsible for the *O*-methylation of C3 and therefore, through the combined action of ForT, ForM and ForW the intermediate **3** is converted to the non-halogenated **fasamycin C**. Chlorination of the fasamycin intermediates is essential for the conversion of fasamycin to formicamycin and therefore inferred to be the next step of the pathway whereby the halogenase, ForV, catalyses the addition of one or more chlorine atoms onto the fasamycin backbone yielding, in this example, the mono-chlorinated **fasamycin D**. After chlorination of the fasamycin backbone, biosynthesis of formicamycins then progresses through the introduction of a tertiary hydroxyl group at C10 and subsequent modification of ring-C through the action of the Baeyer–Villiger monooxygenase ForX and the flavin-dependant reductase ForY which leads to the production of **4**. The modification of ring-C has been confirmed to be through the action of a two-step ring-expansion ring-contraction mechanism whereby ForX catalyses the oxidation of a chlorinated fasamycin intermediate causing the production of a Baeyer-Villiger lactone intermediate. Several of these lactone intermediates, henceforth referred to as formicalactones (A-E), were purified from a *S. formicae* Δ*forY* strain as documented in Qin et al (2020). ForY reduces this lactone intermediate to allow for the progression to formicamycin compounds. A second *O*-methylation at C23, which is observed on all formicamycin compounds, is

proposed to take place on intermediate **4** to give **5** through the action of either of the methyltransferases ForM and ForW. The last proposed step is orchestrated through the combined actions of ForV, which acts as a promiscuous halogenase, and the methyltransferases ForM and ForW which decorate the formicamycin structure, giving rise to different formicamycin congeners in this example, **formicamycin J**.

Analysis of the lowest energy conformers of both fasamycin and formicamycin molecules indicted that, although fasamycins are intermediates in formicamycin biosynthesis, the compounds themselves exhibit extremely different three-dimensional (3D) structures. Fasamycin compounds exhibit a planar structure along rings B, C, D and E whereas the formicamycin compounds appear to have a bend in the tetracyclic backbone that makes them have a different 3D structure in comparison to the fasamycin compounds (**Figure 1.11**) (Qin, Munnoch et al. 2017).

Fasamycin   Formicamycin
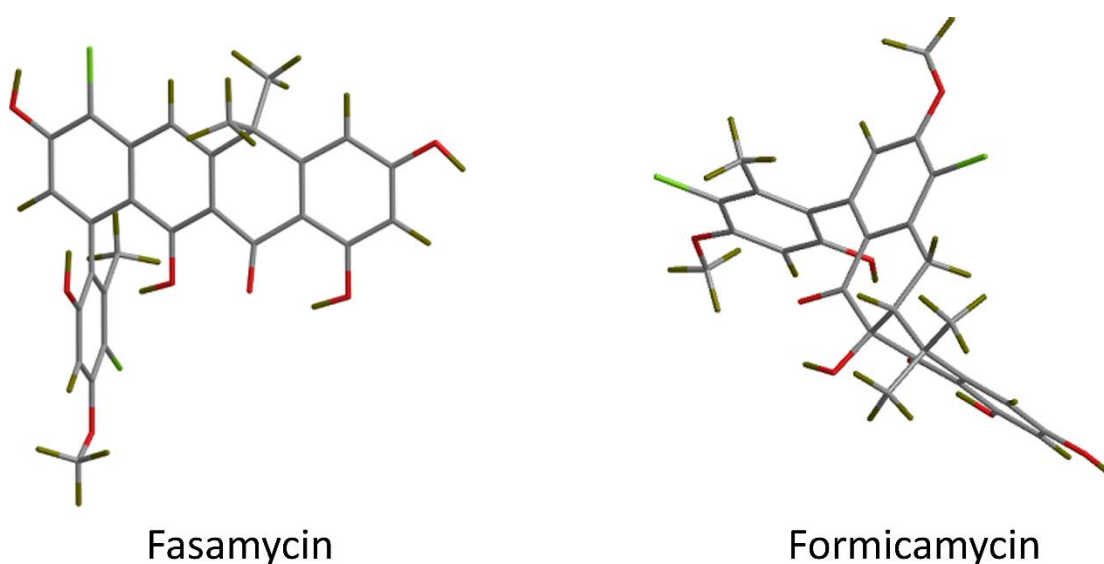
Figure 1.11 Lowest energy conformations of both fasamycin and formicamycin compounds. Fasamycin and formicamycin take up different 3-dimensional space. Adapted from Qin et al (2017).

1.8 Biological target of fasamycin

Fasamycin compounds had been identified prior to the isolation of fasamycins (C-E) of *S. formicae*, through the expression of soil derived cosmid DNA containing a type II PKS using *Streptomyces albus* as a heterologous host which led to the isolation and characterisation of fasamycin A and B (Feng, Kallifidas et al. 2011, Feng, Chakraborty et

al. 2012). The bioactivity of these compounds was assessed, and both were found to exhibit potent bioactivity against clinically relevant Gram-positive bacteria such as *Enterococcus faecalis* and methicillin resistant *Staphylococcus aureus.* Alongside their discovery and characterisation, research by Feng *et al* (2012) generated spontaneous resistant mutants in *Enterococcus faecalis* OG1RF to fasamycin A by exposure to high concentrations of fasamycin A. Upon genome sequencing analysis several genomic changes were identified and all nine mutant colonies were found to have alterations, including a 118 bp deletion, several single base pair deletions and a base pair insertion within the *fabT* gene, which is a MarR transcriptional regulator responsible for the regulation of the fatty acid synthase II gene cluster (Lu and Rock 2006, Feng, Chakraborty et al. 2012).
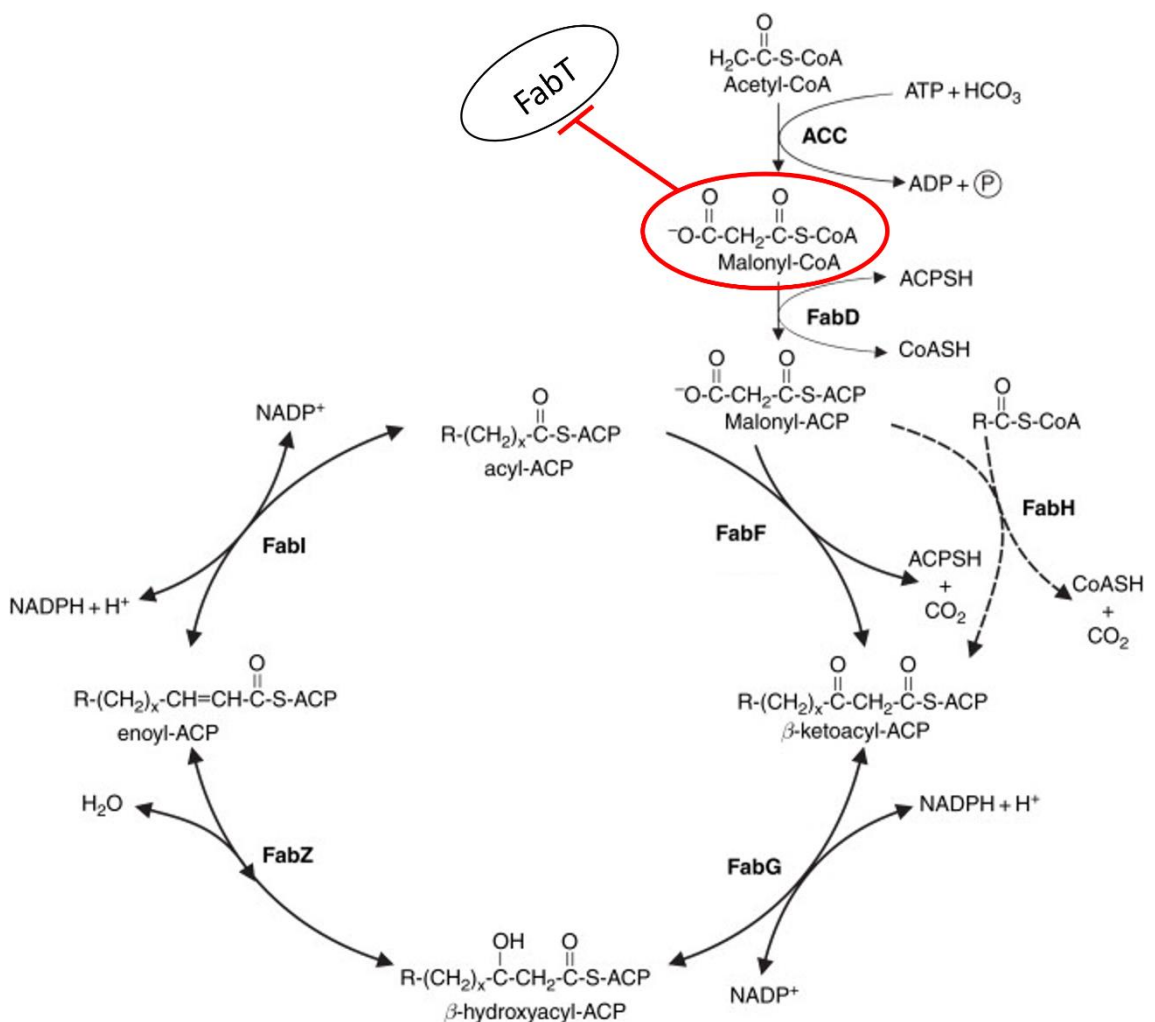
Figure 1.12 Diagrammatic representation of fatty acid biosynthesis in bacteria. Red circle denotes malonyl-CoA which is the ligand of FabT. Adapted from de Mendoza and Schujman (2009).

Type II fatty acid synthesis (FAS-II) is an essential process used by bacteria to generate the fatty acid components of membrane phospholipids which is achieved by the action of several highly conserved proteins in bacteria, each of which is responsible for individual steps in the pathway. Each of the proteins of the pathway are located in the cytosol, and reaction intermediates are covalently attached to acyl carrier protein (ACP). There are several discrete differences in protein naming and proteins utilised in FAS-II between different bacteria, but an overview of FAS-II biosynthesis is given below and in **Figure 1.12**. FAS-II biosynthesis begins with the carboxylation of acetyl-CoA by acetyl-CoA carboxylase (ACC) to form malonyl-CoA (de Mendoza and Schujman 2009). The malonyl transacylase, FabD, then aids in the attachment of malonyl-CoA onto the ACP to form malonyl-ACP to allow for chain elongation to begin. The fatty acid chain is elongated by the condensation of acyl groups, derived from either acyl-ACP or acyl-CoA, with malonyl-ACP by two classes of condensing enzymes (FabH and FabF). FabH is responsible for the initiation of elongation whereas FabF is responsible for subsequent rounds of elongation, both of which condense malonyl-ACP with acyl-ACP to extend the acyl chain by two carbons to form β-ketoacyl-ACP. FabG then reduces β-ketoacyl-ACP to β-hydroxyacyl-ACP. The next step in the cycle is the dehydration of β-hydroxyacyl-ACP to *trans*-2-enoyl-ACP by FabZ. The last step in the elongation cycle is performed by FabI, which reduces the double bond of *trans*-2-enoyl-ACP to a saturated acyl-ACP which results in the production of straight chain fatty acids. However, some Gram-positive bacteria such as *Bacillus subtilis*, produce branched chain fatty acids which are formed through the actions of a branched-chain α-ketoacid dehydrogenase complex. These branched branched-chain acyl-CoAs are then incorporated into the pathway by FabH (de Mendoza and Schujman 2009). FabT acts as a global regulator of the FAS-II pathway, upon binding of malonyl-CoA, the repression is lifted, and the genes of the pathway are expressed.

As FabT is the repressive regulator of the FAS-II pathway, it was proposed that disruption of *fabT* would cause an increase in expression of all the individual FAS-II genes in the cluster (Lu and Rock 2006, Feng, Chakraborty et al. 2012). Therefore, it was hypothesised that fasamycin A inhibits one of the essential enzymes of fatty acid biosynthesis. Fasamycin anti-FAS-II activity was analysed *in vitro* via fatty acid elongation assays using FAS enzymes purified from *S. aureus* and it was determined that

both fasamycin A and B inhibited fatty acid elongation with IC_{50} values of 50 and 80 µg/ml, respectively. Fasamycin A FAS-II elongation assays were further examined using urea polyacrylamide gel electrophoresis to differentiate between malonyl-ACP and longer chain acyl-ACPs. Fasamycin A did not affect the formation of malonyl-ACP but did inhibit the production of long-chain fatty acids indicating that fasamycin A inhibits FabF, the initial condensation enzyme in the production of long chain fatty acids. To confirm this hypothesis a further investigation using candidate gene overexpression was undertaken whereby each of the FAS-II genes was individually overexpressed in *E. faecalis* and assayed for the ability to confer fasamycin A resistance. It was observed that the only overexpression strain that conferred an increased minimum inhibitory concentration (MIC) to fasamycin A was overexpression of FabF, confirming the results of the elongation assay experiments (Feng, Chakraborty et al. 2012). Therefore, fasamycins A and B were determined to be FAS-II inhibitors through the inhibition of fatty acid chain elongation orchestrated by FabF. To gain further understanding of fasamycin inhibition of FabF, computational docking studies were undertaken whereby fasamycin A was docked into a model of FabF. From these investigations, it was hypothesised that fasamycin compounds bind into the active site of FabF, similarly to other FabF inhibitors such as platensimycin, and therefore stop the ability of this enzyme to perform condensation reactions (Feng, Chakraborty et al. 2012). Currently, there have been no reports in the literature of investigations into the cellular target or mode of action of the formicamycin compounds. As the formicamycins have shown potent activity against clinically relevant pathogens, it would be of interest to understand the target and mechanism of action of these compounds.

1.9 Aims and objectives of this thesis

The aim of this thesis was to investigate the target and mode of action of the formicamycins and their intermediates fasamycins. Using a combination of microbiology and biochemistry techniques two potential *in vivo* targets of both fasamycin and formicamycin were identified during this work, alongside an extensive characterisation of one of these cell targets. Furthermore, during the work presented, the consequences of targeted mutation within the formicamycin biosynthetic gene cluster on formicamycin production were also characterised alongside an analysis of the resistance profile and biological activity of both classes of compound. Work in this thesis also

discovered and isolated several new glycosylated fasamycin compounds. has All of this work contributes to a preliminary understanding of the mechanism of action of the novel formicamycin compounds, which is the first investigation of its kind.

This thesis is presented in two halves with the first half discussing the main body of work during this PhD project which was investigations into the target and mode of action of the fasamycin and formicamycin compounds. However, whilst undertaking the characterisation of the target and mode of action of these compounds, several skills had to be acquired including isolation and structural determination of compounds, as well as quantitative metabolomics analysis. Therefore, some aspects of work in the first half of this thesis, such as compound congeners, derive from these findings, but for continuity and emphasis on the main body of the work, they will be discussed during the second half of this thesis.

2.0 Materials and methods

2.1 Chemicals and reagents

Chemicals and reagents were purchased from Merck, formerly Sigma Aldrich (UK), or Thermo Fischer Scientific (UK) unless otherwise stated. Unless otherwise stated all topoisomerases and DNA substrates were purchased from Inspiralis (UK).

2.2 Bacterial strains and media

Table 2.2 Strains used in this thesis

Strain	Description/Genotype	Plasmid	Resistance	Reference
Escherichia coli TOP10	F− mcrA Δ(mrr-hsdRMSmcrBC) Φ80lacZΔM15 ΔlacX74 recA1 araD139 Δ(ara leu) 7697 galU galK rpsL (StrR) endA1 nupG			Invitrogen™
Escherichia coli DH10B	str. K-12 F⁻ Δ(*ara-leu*)*7697*[Δ(*rapA'-cra'*)] Δ(*lac*)*X74*[Δ('*yahH-mhpE*)], duplication(514341-627601)[*nmpC-gltI*] *galK16 galE15* e14⁻(*icd*ᵂᵀ *mcrA*) φ80d*lacZΔM15 recA1 relA1 endA1* Tn *10.10 nupG rpsL150*(StrᴿR) *rph⁺ spoT1* Δ(*mrr-hsdRMS-mcrBC*) λ⁻ Missense(*dnaA glmS glyQ l pxK mreC murA*) Nonsense(*chiA gatZ fhuA? yigA ygcG*) Frameshift(*flhC mglA fruB*)			Invitrogen™
Escherichia coli BW25113	λ- , Δ(araD-araB)567, ΔlacZ4787(::rrnB-4), lacIp4000(lacIQ), rpoS369(Am), rph-1, Δ(rhaD-rhaB)568, hsdR514	pIJ790	Cml	(Datsenko and Wanner 2000)
Escherichia coli ET12567	*E. coli* ET12567 is a methylation deficient (*Δdcm Δdam*) strain containing driver plasmid pUZ8002	pUZ8002	Cml/Kan	(MacNeil, Gewain et al. 1992)
Escherichia coli BL21(DE3) Star	F⁻ompT hsdSᵦ (rᵦ⁻, mᵦ⁻) galdcmrne131 (DE3)			Thermo Life Technologies
Escherichia coli	ATCC 25922			ATCC
Methicillin sensitive *Staphylococcus aureus*	ATCC 6538P			ATCC

Methicillin resistant *Staphylococcus aureus*	ATCC BAA-1717		Methicillin	ATCC
Escherichia.coli NR698	MC4100 *lptD4213*			(Ruiz, Falcone et al. 2005)
Enterococcus faecalis O1GRF	ATCC 47077			ATCC™
Bacillus subtilis 168	*trpC2*			(Burkholder and Giles Jr 1947)
Staphylococcus aureus clinical isolate			Methicillin	Kindly gifted from Dr Justin O'Grady (UEA Medical School)
Streptomyces formicae				(Holmes, Devine et al. 2018)
Streptomyces coelicolor M1146	Host strain [Δact Δred Δcpk Δcda]			(Gomez-Escribano and Bibb 2011)
Streptomyces coelicolor M1146 215G	M1146 + *for* BGC	pESAC-13 215-G		This work
Streptomyces coelicolor M1146_215G *ΔforJ*	M1146 + *for* BGC *ΔforJ* (de-repressed)	pESAC-13 215-G *ΔforJ*		This work
Saccharopolyspora erythraea Δery	*Δery*			Isomerase Therapeutics™ (Cambridge, UK)
*Saccharopolyspora erythraea Δery_* 215G	+ *for* BGC	pESAC-13 215-G		This work
Saccharopolyspora erythraea Δery_215G ΔforJ	+ *for* BGC *ΔforJ* (de-repressed)	pESAC-13 215-G *ΔforJ*		This work
Sacchromyces cerevisiae	ATCC 200060			ATCC™

Table 2.3 Media recipes used in this thesis

Media	Recipe (per liter)	pH	Notes
Soya flour mannitol SFM	20 g soy flour 20 g mannitol 20 g agar	N/A	Streptomyces growth medium
Luria-Bertani LB	10 g tryptone 5 g yeast extract 10 g NaCl 20 g agar – omitted if liquid media	7.5	General *E.coli* and bacterial strain media
Tryptone soy broth TSB	17 g tryptone 3 g soya peptone 5 g NaCl 2.5 g dipotassium phosphate 2.5 g glucose 20 g agar – omitted if liquid media	7.3	*S. aureus* and *S. formicae* growth medium
2xYT	16 g tryptone 10 g yeast extract 5 g NaCl	7.0	Protein purification media
Soft nutrient agar SNA	4g Difco Nutrient Broth Powder 5g Agar	N/A	Spot on lawn bioassay media
Brain Heart Infusion Media BHI	beef heart 5 g calf brains 12.5 g disodium hydrogen phosphate, 2.5 g D(+)-glucose, 2 g peptone, 10 g sodium chloride, 5 g 20 g agar – omitted if liquid media (Merck)	N/A	Culturing *Enterococcus faecalis*
MaConkey agar	peptone 17.0 g	6.9 - 7.3	Analysis of *E.coli* mutants

	proteose Peptone 3.0 g lactose 10.0 g bile Salts 1.5 g sodium Chloride 5.0 g neutral Red 0.03 g crystal Violet 0.001 g agar 13.5 g (Merck)		

2.3 Glycerol stocks of bacterial strains used in this thesis

All glycerol stocks were prepared by mixing overnight bacterial cultures and glycerol (50 %) in a 1:1 concentration. All stocks were stored at –80°C.

2.4 Bacterial growth conditions

All strains except *Streptomyces* and *Saccharopolyspora* strains were streaked out onto LB,TSB or BHI agar for single colonies prior to inoculation. A single colony was used to inoculate either LB, TSB, BHI or 2 x YT liquid medium. Cultures were grown at 37°C and shaken at 250 RPM overnight. *Streptomyces* and *Sacchropolyspora* strains, unless stated, were streaked for single colonies on SFM agar, and after 10 days a single colony was used to inoculate TSB liquid media (10 ml). Subsequent cultures were grown for 2 days at 30°C and shaken at 250 rpm; the resulting seed cultures were then used to inoculate SFM agar plates or SFM liquid media.

2.5 PCR reaction mixes and conditions

Amplification of DNA fragments for cloning was performed using Q5 High-Fidelity DNA polymerase. GoTaq polymerase (Promega, UK) was used in colony PCR reactions. PCRs were conducted using an Applied Biosystems SimpliAmp PCR machine.

Table 2.4 General conditions used for Q5 DNA and Taq polymerase PCR reactions

Number of cycles	Temperature (°C)	Time
1	95	2 minutes
	95	30 seconds
30-35	52-62	30 seconds

	72	30 seconds per kb
1	72	10 minutes
1	4	∞

2.5.1 Q5 polymerase PCR

Table 2.5 Standard reaction mixture for a Q5 PCR reaction

Reagent	50 µl reaction (µl)
5X Q5 Reaction Buffer	10
5X GC Enhancer	10
Forward primer (10 µM)	2.5
Reverse primer (10 µM)	2.5
10 mM dNTPs	1
DNA template	1
dH$_2$O	22.5
Q5 High-Fidelity Polymerase	0.5

2.5.2 GoTaq colony PCR

Table 2.6 Standard reaction mixture for a GoTaq colony PCR reaction

Reagent	25 µl reaction (µl)
GoTaq Green Master Mix (2X)	12.5
Forward primer	2.5
Reverse primer	2.5
DNA template	1
dH$_2$O	6.5

2.6 Gel electrophoresis

DNA gels were made using 1% agarose in TAE buffer and supplemented with 2 µg/ml ethidium bromide. DNA samples were loaded alongside a 1 kb plus DNA ladder. Gels were run at 120 V for 40-60 minutes. Visualization of DNA by UV-light was done using a Gel-Doc (BIORAD) system.

2.7 Gel Extraction of DNA

DNA was extracted from agarose gels by cutting out relevant bands using a razorblade. DNA was obtained from subsequent gel slices by using a QiaQuick Gel Extraction Kit (Qiagen) as per the manufacturer's instructions. DNA was eluted in sterile dH_2O (25-50 µl).

2.8 Cloning of DNA fragments using Gibson Assembly

pET28b vector was linearized by PCR amplification. DNA fragments were assembled into pET28b backbone (PCR purified) using overlapping regions of DNA from the pET28b plasmid. DNA fragments and plasmid were incubated with Gibson Assembly master mix (NEB) in a ratio of 1:3 of plasmid:insert at 50°C for 1 hour.

2.9 Transformation of chemically competent *E. coli* cells

Commercially bought *E. coli* BL21 DE3 Star cells (50 µl) thawed on ice and then incubated with 1 µl of the Gibson reaction mixture and incubated on ice for 30 min. Cells were heat shocked at 42 °C for 30 sec and then further incubated on ice for 5 minutes. Cells were then resuspended in 950 µl SOC and recovered for 1 hour at 37 °C and shaking at 250 rpm. Resulting cell cultures were plated on LB agar containing kanamycin (50 µg / ml) and incubated overnight at 37 °C.

2.10 Colony PCRs

Single colonies of *E.coli* BL21 DE3 Star containing potential conctructs were picked with sterile toothpicks and resuspended in 30 µl sterile dH_2O. 1 µl of resuspended cells was used as DNA template in a GoTaq PCR reaction as described above. Subsequent PCR reactions were run on an agarose gel and analyzed by UV-light. For positive colonies 20 µl of resuspended cells were used to inoculate overnight cultures (LB + kanamycin for plasmid amplification and subsequent purification.

2.11 Sequencing of assembled plasmid inserts

Inserts of assembled plasmids were confirmed by Sanger sequencing using the Genewiz overnight sequencing service. Manufacturer's instructions were followed to give correct concentrations of DNA template and primers.

2.12 Metabolite analysis

Solid culture: All strains (n= 3) were grown on soya flour mannitol (SFM) agar at 30°C for 10 days. Extraction methods for solid and liquid experiments were as described in Devine et al (2021) and clarified here. Agar plugs (1 cm^3) were taken, in triplicate, from each plate, and shaken with ethyl acetate (1 ml) for 1 hour before being centrifuged for 5 minutes at 13,000 rpm. The ethyl acetate solution was transferred to a clean tube and the solvent was removed under reduced pressure. The resulting extract was dissolved in 300 µl methanol (HPLC grade) before being analysed by HPLC (Agilent 1290 UHPLC). To confirm peak identity a representative set of samples were analysed by LCMS (Shimadzu IT-ToF LCMS platform). Chromatography was undertaken for both HPLC and LCMS analysis using the following method: Phenomenex Gemini NX C18 column (150 × 4.6 mm); mobile phase A: water + 0.1% formic acid; mobile phase B: methanol. Elution gradient: 0–2min, 50% B; 2–16 min, 50–100% B; 16–18 min, 100% B; 18–18.1 min, 100–50% B; 18.1–20 min, 50% B; flow rate 1 ml min−1; injection volume 10 µl.

Liquid culture: Strains (n = 3) were grown in liquid TSB (10 ml) at 30°C and 250 rpm. After 2 days, 100 µl the culture was used to inoculate 10 ml of SFM liquid media in sterile 50 mL falcon tubes with sterile bungs in triplicate and incubated at 30°C and 250 rpm. After 10 days, 3 x 1ml aliquots were removed from each individual culture and shaken with ethyl acetate (1 ml) for 1 hour, and then centrifuged at 13000 rpm for 5 minutes. The resulting ethyl acetate fraction (300 µl) was transferred to a clean tube and the solvent removed under reduced pressure. The resulting residue was dissolved in methanol (200 µl) before being analysed by HPLC and LCMS as described above (Devine, McDonald et al. 2021).

Titre determination: Titres of fasamycin and formicamycins were determined by comparing peak areas from the above HPLC analysis to those of standard calibration curves and correcting for the concentration change that occurred during the extraction process. Calibration curves were determined using standard solutions of fasamycin E (10, 20, 50, 80 and 200 µM) and formicamycin I (10, 20, 50, 100, 200 and 400 µM) dissolved in methanol (**SI Figures 12-13** and **SI Tables 2-3**). The content of fasamycin E and formicamycin I was determined by UV absorption at 418 nm and 285 nm respectively. Each standard solution was measured three times (Devine, McDonald et al. 2021).

2.13 Computational analysis

All graphs including box plots, IC_{50} curves and violin plots were generated using GraphPad Prism.

2.14 Purification of fasamycin and formicamycin congeners

The fermentation and isolation of fasamycin and formicamycin congeners was undertaken jointly by Hannah McDonald, Corinne Arnold, and Edward Hems.

For the purification of fasamycin and formicamycin compounds, a single colony of either *S. formicae ΔforJ*, for the production of formicamycin compounds, or *S. formicae ΔforJX* for the production of fasamycin compounds, was grown in TSB liquid (10 ml) for two days at 30°C and shaking at 250 rpm. Resulting culture was used to inoculate either SFM agar plates (6 L) or TSB liquid medium (6 L). Plates were incubated statically at 30°C for 10 days and liquid cultures were incubated at 30°C and shaking at 200 rpm for 7 days. After incubation, agar was chopped up into small pieces and washed twice in ethyl acetate (6 L), or liquid cultures were washed twice in ethyl acetate (6 L). Ethyl acetate extracts were dried down using a rotor vap and extracts were fractionated on a Biotage Isolerea monitoring at 250 and 418 nm (fasamycins) or 250 and 285 nm (formicamycins). Peaks containing absorbance at 285 nm were pooled and dried using a rotor vap. Resulting extracts were resuspended in acetonitrile (100% HPLC grade) and a diluted sample was subjected to LCMS analysis to confirm the presence of formicamycin compounds (described in **2.12**).

Further purification for both the isolation of fasamycin and formicamycin compounds was then performed on an Agilent 1260 preparative HPLC system, with a Kinetex XB-C18 100Å column (250 × 21.2 mm, 5.0 μm particle size) and UV absorbance monitoring at 418 nm (fasamycins) and 285 nm (formicamycins). Flow rate 20 ml/min, solvent A water + 0.1% formic acid, solvent B acetonitrile + 0.1% formic acid; Gradient: 0 min, 50% B; 4 min, 50% B; 16 min, 98% B; 18.3 min, 98% B; 18.3-19 min 2% B, 19-20 min 2% B. Fractions were analysed for purity by HPLC/ LCMS analysis and either confirmed to be of sufficient purity or subjected to further rounds of preparative HPLC, as described. Extracts containing formicamycins T-Y were further purified by normal phase preparative HPLC to separate out individual formicamycin congeners Normal phase preparative HPLC was performed on a Dionex Ultimate 3000 HPLC system, with a Luna

5 µm Silica (2) column (250 × 21.2 mm, 5.0 µm particle size) and UV absorbance monitoring at 418 nm or 285 nm. Flow rate 20 ml/min; solvent A hexane, solvent B ethyl acetate. Gradient: 0 min, 1% B;-1 min, 1%B; 3 min, 30%B; 20 min, 45% B; 22 min, 80% B; 24 min, 80% B; 25 min, 1% B; 26 min, 1% B. Fractions were analysed for purity by HPLC/ LCMS analysis, purified congeners were then subjected to NMR analysis and compared to previously characterised NMR spectra or, for new congeners, NMR analysis to solve the structures were undertaken by Dr Edward Hems.

2.15 Spot on lawn assays for minimum inhibitory concentration determination

Stocks of compounds (fasamycin, formicamycin and glycosylated fasamycin derivitives) were made up in 100% MeOH and further diluted in MeoH to 2-fold serial dilutions. Single colonies of *Escherichia coli* 25922*, Escherichia coli* NR698, Methicillin sensitive *Staphylococcus aureus* ATCC 6538P, Methicillin resistant *Staphylococcus aureus* BAA 1717 and Vancomycin sensitive *Enterococcus faecalis* OG1RF were grown in LB (*E. coli)*, tryptic soy broth (*S. aureus*) and brain heart infusion (*E. faecalis*) liquid medium and incubated overnight at 37°C and with shaking (at 250 rpm). The resulting cultures were sub cultured into fresh liquid medium and grown to exponential phase (OD$_{600}$ 0.4-0.6). Cultures were used to inoculate soft nutrient agar and 10 µl compounds of interest were spotted onto each agar plate. Plates were incubated at 37°C overnight after which they were examined for clearance zones due to growth inhibition by eye.

2.16 Resazurin assays for minimum inhibitory concentration determination

Resazurin assays were performed to determine minimum inhibitory concentrations of fasamycin, formicamycin and formicalactone compounds. A 20 X stock solution of compound was prepared in DMSO and further diluted to obtain a 2-fold serial dilution range in DMSO before 5 µl of stock was added to LB, TSB, YPD or BHI media to give a selected concentration range of the material to be tested, and a final concentration of 5% DMSO. In addition to the test material a series of controls were run: Positive control (PC) for preparations in LB, BHI and TSB was apramycin at 50 µg/ml. Negative control (NC) and media control (MC) contained media (LB, BHI, YPD or TSB) and DMSO at 5%, no bacteria was added to NC. Methods were followed as detailed in Heine et al (Heine et al., 2018). All experiments were conducted in biological triplicate. Cultures of bacterial strains to be tested (*E. coli, E.coli* Nr698, *B. subtilis 168*, MRSA, MSSA, VRE, VSE and *S. cerevisiae*) were grown to confluence overnight by incubating at 37˚C or 30˚C for *S.*

cerevisiae and 250 rpm. Resulting overnight cultures were then diluted 1/100 in fresh media and further incubated until they reached an OD_{600} of 0.4. These were then diluted to match a 0.5 McFarlands standard prepared by the addition 0.5 ml of a 1.175% (w/v) barium chloride dihydrate solution to 99.5 mL of 1% (v/v) sulfuric acid, and further diluted 1/100 in fresh media. 5 µl of diluted culture was then aliquoted into each well of the 96 well plate excluding the NC well. The resulting plates were incubated at 37°C and shaking at 250 rpm overnight after which with 5 µl of resazurin dye (6.75 mg / ml, Sigma Aldrich) in water was added to each well. Colorimetric outcomes were recorded 4 hours after addition of the resazurin solution. Wells exhibiting a blue colour were determined to contain non-viable (dead) cells and wells exhibiting a pink colour were determined to contain viable cells.

2.17 *B. subtilis* reporter strains for antibacterial target determination

A panel of *B. subtilis* reporter strains containing promoter fusions to genes sensitive to antibiotic exposure were kindly gifted to us from Professor Jeffery Errington. Strains used were: *B. subtillus* PL39 *gyrA::pMUTIN4* ermC gyrA'lacZ PspacgyrA+ (PL39 - DNA gyrase inhibition reporter), *B. subtillus* ypuA*::pMUTIN4* ermC ypuA'-lacZ (ypuA -cell wall damage reporter) ,*B. subtillus* fabHA*::pMUTIN4* ermC gyrA'-lacZ Pspac-gyrA+ (FabHA - fatty acid synthesis inhibition reporter), *B. subtillus* o105 (o105 -lacZ fusion to a late promoter in a o105 prophage DNA damage reporter), *B. subtillus* helD::pMUTIN4B helD-lacZ ermC (HelD -RNA polymerase inhibition reporter) and *B. subtillus* lial::pMUTIN4 lial-lacZ ermC (Lial -cell envelope reporter) (Kepplinger, Morton-Laing et al. 2018).

All strains were grown in LB media (10 ml) supplemented with erythromycin (1 µg/ ml) except for *B. subtillus* o105 which was supplemented with chloramphenicol (5 µg/ ml) at 37°C and shaking at 250 rpm overnight. Overnight cultures were sub-cultured 1:100 and further incubated until they reached an OD_{600} of 0.4. 2 ml of the resulting culture was used to inoculate 200 ml of molten SNA (at 50°C) containing 100 µg / ml X-gal (5-bromo-4-chloro-3-indolyl-beta-D-galacto-pyranoside), agar containing reporter strains (30 ml) was poured into round petri dishes. Once plates had dried, all antibiotics to be tested were spotted onto resulting agar plates at the same time and in the same volume: 5 µl of 100 µg fasamycin E or formicamycin I in 100 % methanol, positive control, negative control and solvent control (100 % methanol) were spotted onto agar plates and left to dry. Plates were incubated at 37°C. The negative control used for all strains

was spectinomycin (50 µg/ml) for all strains except the o105 strain where chloramphenicol (25 µg/ml) was used. Positive controls for each strain are as follows: FabHA = 150 µg/ ml triclosan in 100% Ethanol, ypuA = 125 µg / ml cefotaxime in water, PL39 = 10 µg/ ml novobiocin in water, O105 = 10 µg/ ml doxorubicin in DMSO, helD = 10 µg/ ml rifampicin in methanol and lial = 500 µg/ ml bacitracin in water.

2.18 Investigation of inhibitory activity of fasamycin and formicamycin against two archaeal strains

Experiments were conducted by Timothy Klein (UEA). AOA strains 'Ca. *Nitrosocosmicus franklandus* C13' and *Nitrososphaera viennensis* EN76 were routinely maintained in liquid fresh-water medium (FWM) as previously described (Tourna et al. 2011: Lehtovirta-Morley et al. 2016). The pH indicator, phenol red, was added to the medium of both neutrophilic AOA strains at a final concentration of 1.4µM. All cultures were incubated at 37˚C in the dark under static conditions. 500 ml of an exponentially growing culture (700 - 1000µM NO2-) was harvested in a vacuum manifold onto a 0.02µM filter (PES, Millipore). Cells were washed once with 35 ml sterile FWM and resuspended in 10ml of FWM (1x salt solution only). Cell suspension was diluted (1:10) and 10 ml of FWM was aliquoted into 30 ml plastic universal vials before each vial was inoculated with 80 µl of the diluted cell suspension. Growth of AOA cultures was monitored by measuring nitrite accumulation. Nitrite concentration in the culture medium was measured using the Greiss colorimetric assay with sulphanilamideand N-(1-naphthyl) ethylenediamide in a 96-well plate format as previously described (Lehtovirta-Morley et al. 2016). Absorbance was measured at 540 nm using a VersaMax™ plate reader (Molecular Devices).

2.19 Assessing the barrier to resistance of fasamycin and formicamycin compounds against *S. aureus*

Methicillin resistant *Staphylococcus aureus* (MRSA) and Methicillin sensitive *Staphylococcus aureus* (MSSA) were streaked out for single colonies on TSA and grown in a static incubator overnight at 37˚C. Three single colonies of each strain were grown in TSB liquid medium (5 ml) inoculated with either 0.5 µg/ml fasamycin E, fasamycin L, formicamycin I, formicamycin J resuspended in DMSO or DMSO (inhibitor vehicle control). Resulting cultures were grown overnight at 37˚C and shaking at 250 rpm. Every

day overnight cultures from the previous day were used to inoculate fresh TSB + compound or DMSO only. Procedures were repeated every day for 40 days. Every 10 days a resazurin assay (described in **2.16**) was performed to determine MIC in liquid and to establish if any strains had generated resistance. Unfortunately, due the Covid19 pandemic, the experiment had to be halted at day 39 whereby *S. aureus* strains were stored in 25% glycerol (w/v) and stored at -80˚C. Upon resuming lab work, strains were grown back up in TSB supplemented with either fasamycin (E and L), formicamycin (I and J) or DMSO overnight. Resulting cultures were then assayed by resazurin assay to determine MIC for day 40. Resistance was determined as anything above 4 X MIC.

2.20 Generation of spontaneous resistant mutants

Overnight cultures of sensitive bacterial strains (MRSA, MSSA, *B. subtilis* and *E. coli* NR698) were plated onto varying concentrations (1, 2 and 6 X MIC) of fasamycin or formicamycin congeners which were supplemented into LB or TSB agar from compound stocks made up in DMSO. Plates were incubated at 37°C overnight and checked for colonies. Any colonies formed were struck onto agar containing the same and higher concentrations of compound as used in the isolation plates. Colonies that were able to grow on above 1 X MIC concentrations of fasamycin and formicamycin compounds were subjected to MIC testing using the resazurin assay method (described in **2.16**).

2.21 Assaying simocylinone resistant mutants for resistance against fasamycin and formicamycin

Simocylinone resistant mutants *E. coli* NR698 *gyrA* V44G (**SP 8.1**), *gyrA* H45Y (**SP 8.6**), *gyrA* H45Q (**SP 6.6**), *gyrA* G81S (**SP5**), *gyrA* D87Y (**SP 1**) and NR698 (**SP 6.3**) were used to inoculate LB media (10 ml) and incubated grown overnight at 37˚C with shaking at 250 RPM. The resulting cultures were subjected to resazurin assays, as described in **2.16**, against fasamycin L (256-1 µg/ml), formicamycin J (256-1 µg/ml) and simocylinone D8 (32-0.12 µg/ml) to determine MICs.

2.22 Preparing electrocompetent *S. aureus* strains and electroporation protocol

Two competent *S. aureus* strains, *S. aureus* ATCC BAA-1717 and *S. aureus* RN4220 were used in this work. To generate competent cells, overnight cultures of both *S. aureus* strains were set up in 10 ml TSB liquid medium and grown at 37˚C and shaking at 250

RPM. Resulting overnight cultures were diluted to OD_{600} of 0.5 in 50 ml prewarmed TSB medium. Cultures were incubated for a further 30 minutes at 37˚C and shaking at 250 RPM until reaching an OD_{600} of 0.8. Cultures were then incubated on ice for 10 minutes. Cells were harvested at 4˚C in a swinging bucket at 39,00 xg for 10 minutes. Supernatant was discarded from pellets and pellets were washed with 50 mL of ice cold sterile dH_2O, cells were subjected to centrifugation as before and sterile dH_2O was discarded. this was repeated twice more. After washing, pellets were resuspended in 10 ml sterile ice cold 10% glycerol (w/v) in dH_2O. Cells were centrifuged as above, and supernatant was discarded. The pellet was then resuspended in 2 ml sterile ice cold 10% glycerol (w/v) in dH_2O and centrifuged again. Supernatant was discarded and pellets were made up to 250 μl in sterile ice cold 10% glycerol (w/v) in dH_2O. Cells were aliquoted and frozen at -70˚C.

For electroporation of plasmids into competent *S. aureus* (ATCC BAA-1717 or RN4220), competent cell aliquots were thawed on ice for 5 minutes before being left at room temperature for a further 5 minutes. Cells were centrifuged at 5000 xg for 1 minute. Supernatant was discarded and cells were resuspended in 50 μl of 10% glycerol (w/v), 500 mM sucrose in dH_2O. 1 μl of plasmid DNA was added to each 50 μl aliquot of cells and cells were mixed by gentle flicking. Cells and plasmid were added to a 1mm electroporation cuvette. Cuvettes were then placed into the electroporator and pulsed at 21 kV/cm (2.1 V), 100 Ω, 25 μf. Immediately after electroporation, 1 ml of TSB + 5mM sucrose and cells were transferred to a 1.5 mL Eppendorf. Cells were recovered for 1 hour at 37˚C and shaking at 250 RPM before being plated onto BHI agar plates supplemented with 10 μg/ml chloramphenicol. Plates were incubated overnight at 37˚C.

2.23 Fatty acid synthase enzyme over- expression bioassays

S. aureus (MRSA) fatty acid gene over-expression strains were generated by Dr Corinne Arnold (JIC). Strains were created by cloning DNA sequences encoding for individual fatty acid synthase genes into the over-expression plasmid pRAB11. pRAB11 is a chloramphenicol and carbenicillin resistant plasmid as well as being inducible by the addition of tetracycline (Helle, Kull et al. 2011).

Table 2.7 Fatty acid synthase gene overexpression primers. Yellow highlighted DNA sequences correspond to ribosome binding sites that have been added to primers to ensure expression. Green highlighted sequence refers to BglII restriction site. Blue highlighted sequence refers to EcoRI restriction site. Red highlight corresponds to SacI restriction site.

Primer name	Sequence (5'-3')
FabD forward	GATCAGATCTTATATAGGGAAAGGTGGTGAACTACTATGAGTAAAACAGCAATTA
FabD reverse	ATATGAATTCTTAGTCATTTTCATTCCATC
FabF forward	GATCAGATCTTATATAGGGAAAGGTGGTGAACTACTATGAGTCAAAATAAAAGAGTAG
FabF reverse	ATATGAATTCTTATGCTTCAAATTTCTTGAATAC
FabG forward	GATCAGATCTTATATAGGGAAAGGTGGTGAACTACTATGACTAAGAGTGCTTTAG
FabG reverse	ATATGAATTCTTACATGTACATTCCACC
FabH forward	GATCAGATCTTATATAGGGAAAGGTGGTGAACTACTATGAACGTGGGTATTAAAGG
FabH reverse	ATATGAATTCCTATTTTCCCCATTTTATTG
FabI forward	GATCAGATCTTATATAGGGAAAGGTGGTGAACTACTATGTTAAATCTTGAAAAC
FabI reverse	ATATGAGCTCTTATTTAATTGCGTGGAATC
FabZ forward	GATCAGATCTTATATAGGGAAAGGTGGTGAACTACTATGGAAACAATTTTTGATTATAAC
FabZ reverse	ATATGAATTCTTATTTTACATCTTGAATTG

DNA sequences for each of the fatty acid synthase genes, *fabD, fabF, fabG, fabH, fabI* and *fabZ* were PCR amplified from *S. aureus* ATCC BAA-1717, primer details can be found in Table X. PCR fragments were ligated into pRAB11 which had previously been digested with BglII and EcoRI (or SacI for FabI) . Each plasmid was transformed into *E.coli* DH5α and plated on LB agar supplemented with 50 µg/ml carbenicillin and grown overnight at 37˚C, resulting colonies were checked by colony PCR using sequencing primers (forward: 5'- TGATAGAGTATGATGGTACCGTT -3', reverse: 5'- GTTGTAAAACGACGGCCAGT -3'). Colonies that gave bands of a determined length for each gene of interest were grown overnight in 10 mL LB liquid medium supplemented with 50 µg/ml carbenicillin at 37˚C and shaking at 250 RPM. Resulting overnight cultures were used to extract plasmids using a Qiagen miniprep kit. Plasmids were sent for overnight sequencing. After conformation by sequencing, plasmids were electroporated into the cloning

intermediate host strain, *S. aureus* RN4220 which contains a mutation within the *sau1 hsdR* gene, making it restriction deficient. Transformations were plated onto BHI agar supplemented with 10 µg/ml chloramphenicol and grown overnight at 37 ˚C. Resulting colonies were used to set up overnight cultures in 10 mL TSB supplemented with 10 µg/ml chloramphenicol and incubated overnight at 37˚C and shaking at 250 RPM. Resulting overnight cultures were used to extract plasmids using a Qiagen miniprep kit. Plasmids were then electroporated into electrocompetent *S. aureus* ATCC BAA-1717 and plated onto BHI agar supplemented with 10 µg/ml chloramphenicol and grown overnight at 37˚C.

S. aureus ATCC BAA-1717 strains encoding for over-expression of FabD, FabF, FabG, FabH, FabI, FabZ and empty vector control were grown overnight on BHI agar supplemented with 10 µg/ml chloramphenicol at 37˚C . Resulting single colonies of over-expression strains were grown in TSB liquid medium supplemented with 10 µg/ml chloramphenicol overnight, resulting overnight cultures were used to inoculate fresh medium and grown until they reached an OD_{600} of 0.5. These cultures were used to inoculate SNA medium supplemented with 10 µg/ml chloramphenicol and 4 µM anhydrotetracycline. Molten agar supplemented with bacterial strains was poured into round petri dishes and were allowed to set. Once plates had dried the test antibiotics at a range of concentrations (listed below; dissolved in acetonitrile) were spotted onto the agar. The negative control was 100% acetonitrile and positive control was apramycin (1.4 µg/ml) in acetonitrile. Plates were incubated overnight at 37°C and MIC determination was determined by eye. Inhibitory concentrations were determined as concentrations which gave a clear zone of inhibition.

All antibiotics were spotted in a serial dilution range with each subsequent concentration being half that of the previous. Concentration ranges were as follows: formicamycin J and fasamycin G, 256 –2 µg/ml; triclosan, 8-0.0625 µg/ml; BABX, 128-1 µg/ml; and platensimycin, 32-1 µg/ml.

2.24 ParC and ParE overexpression construct creation

pET28b containing *E.coli* gyrase subunit A and pET28b containing *E.coli* gyrase subunit B DNA gifted from Dr Dmitry Ghilarov, were used as template to PCR amplify the plasmid backbone, excluding the gyrase genes. Topoisomerase IV genes ParC and ParE were PCR

amplified from *E.coli* K12 MG1655 (**Table 6**). Plasmid backbone and Topo IV subunits (ParC and ParE) were assembled together using Gibson assembly. pET28b plasmids containing ParC (pET286_ParC) and ParE (pET286_ParE) were transformed into BL21(DE3) Star (Thermo Life Technologies) following the manufacturers protocol. Plasmid DNA was extracted from overnight cultures in LB media (5-10 ml) using a Qiagenprep Spin Miniprep kit (Qiagen) as per the manufacturer's instructions. DNA was eluted in sterile dH$_2$O (30-50 μl).

Table 2.8 Primers used in ParC and ParE over-expression vector construction

Primer	Sequence
ParC forward	ACCATGAAAACCTGTACTTCCAATCCATGAGCGATATGGCAGAGCG
ParC Reverse	CGGACCCTGAAACAGAACTTCCAGCTCTTCGCTATCACCGCTGCTGG
ParE forward	GTTCTGTTCCAGGGGCCCATGACGCAAACTTATAACGCTGATGCCATTG
ParE reverse	GACCAGGATTGGAAGTACAGGTTTTCAACCTCAATCTCCGCCATGTCGC
pET28b A F	CTGGAAGTTCTGTTTCAGGGTC
pET28b A R	GGATTGGAAGTACAGGTTTTCATGG
pET28b B F	GAAAACCTGTACTTCCAATCCTGGTCA
pET28b B R	GGGCCCCTGGAACAGAAC

2.25 Expression and purification of topo IV subunits ParC and ParE

E. coli BL21(DE3) Star cells were transformed with pET286_ParC and ParE pET286_ParE and single colonies used to generate overnight cultures in 2xYT media. These were used to inoculate (1:100) 6L of 2xYT media supplemented with 30 μg/ml kanamycin. These cultures were incubated at 37°C with shaking at 250 rpm until they reached an OD$_{600}$ of 0.6, at which point the cultures were induced with IPTG (0.5 mM final concentration) and incubated overnight at 20°C with shaking at 250 rpm.

The resulting cells were collected by centrifugation at 6,500 xg for 15 minutes at 4°C. The cell pellets were resuspended in 100 ml HisTrap lysis buffer (50 mM Tris.HCl pH 7.5, 300 mM NaCl, 10% glycerol, 20 mM imidazole) into which one cOmplete™ EDTA-free Protease Inhibitor Cocktail tablet (Roche) had been dissolved. The cells were disrupted by passing through an Avestin ImulsiFlex C3 disruptor at 4°C, with the resulting lysate was passed through twice in total, and then centrifuged at 50,000 xg for 30 minutes at

4°C. The supernatant was then loaded onto a 5 ml HisTrap™ Cytiva column, after which it was washed with 3 column volumes (CV) of HisTrap lysis buffer. Proteins were eluted using HisTrap elution buffer (50 mM Tris.HCl pH 7.5, 300 mM NaCl, 10% glycerol, 250 mM imidazole). Eluted fraction with absorbance at 280 nm were pooled and loaded onto a pre-equilibrated 5 ml StrepTrap™ High Performance (Cytiva) column and washed with 3 CV StrepTrap binding buffer (20 mM Tris.HCl pH 8, 200 mM NaCl, 10% glycerol, 1 mM EDTA pH 8, 1 mM DTT). Bound proteins were isocratically eluted in StrepTrap elution buffer (20 mM Tris.HCl pH 8, 200 mM NaCl, 10% glycerol, 1 mM EDTA pH 8, 1 mM DTT, 3 mM desthiobiotin). Resulting fractions that showed absorbance at 280 nm were diluted in StepTrap binding buffer, containing no NaCl, until the NaCl concentration was 150 mM. The diluted fraction was loaded onto a 5 ml HiTrap Q High Performance (Cytiva) column before being washed with 3 CV TGED buffer (50 mM Tris.HCl pH 8, 10% glycerol, 1 mM EDTA pH 8, 2 mM DTT, 150 mM NaCl), protein was eluted over a NaCl gradient using TGED + 1M NaCl. Protein concentration was calculated using a nanodrop. Histidine and streptavadin tags were cleaved overnight using both TEV and 3C proteases in a 1:50 ratio to protein. The final protein sample were run on 12% SDS PAGE gels (BIO-RAD) to ensure subunit purity and to ensure tags had been cleaved.

ParC and ParE subunits were mixed together in equal concentrations and incubated at room temperature for 30 minutes to reconstitute the A_2B_2 heterotetramer. Reconstituted topo IV was loaded onto a Superdex 200 sepharose (10/ 300 GL) column which was pre-equilibrated with buffer A and the holoenzyme was eluted in the same buffer (50 mM Tris-HCl (pH 7.5 at 4°C), 5 mM DTT, 1 mM EDTA, 10% (v/v) glycerol, 200 mM NaCl) (Peng and Marians 1999). Resulting topo IV complex was used in biochemical assays and mechanism of action studies.

2.26 Protein analysis by SDS-PAGE

Protein gels were purchased from BIO-RAD. 10 µl of protein loading dye (NuPAGE) was added to each 20 µl protein sample to be analysed and boiled at 100°C for 5 minutes before being loaded onto the gel. Gels were electrophoresed (180V, 45 minutes) in 1 X MES buffer (BIO-RAD). Gels were stained with InstantBlue Protein Stain (Abcam) by gentle agitation at room temperature for 1 hour. Gels were de-stained in dH_2O for 1 hour and the gel was imaged using a scanner.

2.27 Quantification of protein

Protein samples of unknown concentration were analysed on a Nanodrop (DeNovix) at A_{280}. Using the molecular weight and extinction coefficient of the protein.

2.28 Topoisomerase IV DNA relaxation and cleavage assays

Topoisomerase IV catalysed DNA relaxation assays were conducted using the *E.coli* Topo IV relaxation assay kit from Inspiralis but using topo IV purified as described above. Assays were performed at least in duplicate.

Assays were conducted as per manufacturers protocols as described below. Assays were performed by incubating 12.5 nM topo IV in assay buffer (40 mM HEPES.KOH (pH 7.6), 100 mM potassium glutamate, 10 mM magnesium acetate, 10 mM DTT, 1 mM ATP, and 50 µg/ml albumin) with 0.5 ug/ ml supercoiled pBR322 DNA, in the presence of a concentration range of either fasamycin (C,E or L), formicamycin (A, I or J) congeners, ciprofloxacin or 1.6 % DMSO (inhibitor vehicle control). Fasamycin and formicamycin compounds were dissolved in DMSO and DMSO concentration was kept to 1.6 % in all assays. Reactions were incubated for 30 minutes at 37°C. The reaction was stopped by the addition of 30 µl chloroform/isoamyl alcohol (v:v, 24:1) and 30 µl STEB (40 % (w/v) sucrose, 100 mM Tris-HCl pH8, 10 mM EDTA, 0.5 mg/ml Bromophenol Blue). Samples were vortexed for 1 min and centrifuged at 17,00xg for 5 min,15 µl of the resulting aqueous phase was loaded onto a 1% TAE agarose gel and ran at 15 V overnight. Gels were stained in ethidium bromide (1ug /ml) in TAE for 15 minutes, and de-stained in TAE for 10 minutes before being visualised using a SYNGENE G:box gel doc.

DNA cleavage assays were performed using the protocol above with the following amendments: assays were incubated for 1 hour at 37°C before 3 µl of 2% (w/v) sodium dodecyl sulphate (SDS) in water and 1.5 µl proteinase K (10 mg/ ml in water) was added to each sample. Assays were incubated for a further 30 minutes, after which 30 µl of chloroform/isoamyl alcohol (v:v, 24:1) and 30 uL STEB was added to each reaction and samples were vortexed for 1 min and centrifuged at 17,000 xg for 5 min before 15 µl of the resulting aqueous phase was loaded onto a 1% TAE agarose gel containing 1 ug /ml ethidium bromide and ran at 100 V for 1 hour. Gels were stained in ethidium bromide (1ug /ml) in TAE for 15 minutes, and de-stained in TAE for 10 minutes before being visualised using an a SYNGENE G:box gel doc.

2.29 *Staphylococcus aureus* DNA gyrase supercoiling assays

Staphylococcus aureus DNA gyrase supercoiling assays were performed using the same protocols as described in **2.28** with the following amendments. *S. aureus* gyrase was supplied by Inspiralis, *S. aureus* supercoiling assay buffer (40 mM HEPES. KOH (pH 7.6), 10 mM magnesium acetate, 10 mM DTT, 2 mM ATP, 500 mM potassium glutamate, 0.05 mg/ml albumin) was instead of assay buffer, and the DNA substrate was relaxed pBR322 (0.5 µg/µl). The reaction was worked up and visualised as described in **2.28**

2.30 Human topoisomerase relaxation assays

Human topoisomerase IIα and IIβ relaxation assays were performed using the same protocols as described in **2.28** with the following amendments. Both Human topoisomerase IIα and IIβ enzymes were purchased from Inspiralis (UK) which were diluted in dilution buffer (50 mM Tris.HCl (pH 7.5), 100 mM NaCl, 1 mM DTT, 0.5 mM EDTA, 50 % (v/v) glycerol, and 50 µg/ml albumin). Assay were conducted in Human Topo II assay buffer (50 mM Tris.HCl (pH 7.5), 125 mM NaCl, 10mM MgCl2, 5 mM DTT, 1 mM ATP and 100 µg/ml albumin). The DNA substrate was supercoiled pBR322 (0.5 µg/µl). The reaction was worked up and visualised as described in **2.28.**

2.31 IC_{50} determination of DNA gyrase and topoisomerase IV inhibition by fasamycin and formicamycin

Gels from all relaxation and supercoiling assays, described in **2.28-2.30** were analysed using Fiji Omero image J. Bands of nicked, relaxed and supercoiled DNA were quantified and relaxed/ supercoiled DNA were determined as a percentage of total DNA per well. IC_{50} curves were created using GraphPad Prism.

2.32 DNA intercalation assays

Intercalation assays were performed by Inspiralis by incubating Wheatgerm topoisomerase I in assay buffer (50 mM Tris.HCl (pH 7.9), 1 mM EDTA, 1 mM DTT, 20 % (v/v) glycerol, 50 mM NaCl) and supercoiled pBR322 plasmid DNA (0.5 µg/µl) with m-AMSA (positive control) or fasamycin C, fasamycin E, formicamycin A and formicamycin J. Reactions were run at 1, 10 and 100 µM substrate concentrations for 30 minutes at 37°C. The assay was stopped by the addition of 30 µL chloroform/isoamyl alcohol (v:v, 24:1) and 30 µl STEB (40 % (w/v) sucrose, 100 mM Tris-HCl pH8, 10 mM EDTA, 0.5 mg/ml

Bromophenol Blue). Samples were centrifuged for 5 min at 17,000 xg and 20 µl of aqueous phase was loaded onto a 1% TAE agarose gel and ran at 80 V for 2 hours. Gels were stained in ethidium bromide (1ug /ml) in TAE for 15 minutes, and de-stained in TAE for 10 minutes before being visualised using a SYNGENE G:box gel doc.

2.33 Surface plasma resonance (SPR) of topo IV DNA binding ability in the presence of fasamycin and formicamycin

SPR experiments using the ReDCaT method were designed to analyse if fasamycin and formicamycin compounds were able to inhibit the ability of topo IV to bind DNA. A streptavidin chip (Cytiva) was prepared by annealing a single-stranded biotinylated linker DNA sequence (GCAGGAGGACGTAGGGTAGG) (prepared by Dr Clare Stevenson). This chip was used in a Biocore 8K+ SPR system with HBS-EP+ buffer (150 mM NaCl, 3 mM EDTA, 0.05% (v/v) surfactant P20, 10 mM HEPES (pH 7.4); GE Healthcare), water and 1 M NaCl/ 50 mM NaOH reagent. Double stranded DNA oligos were prepared by annealing complementary single stranded oligos (ACCAAGGTCATGAATGACTATGCACGTAAAACA) with the complementary linker sequence to the linker (CCTACCCTACGTCCTCCTGC) on the reverse oligo. The oligos were resuspended in water (100 µM) and annealed at equal molarity by heating to 90°C and cooling to 4°C by ramping at 0.1°C per second increments in a thermocycler. The annealed oligos were diluted to 1000 nM in HBS-EP+ buffer (150 mM NaCl, 3 mM EDTA, 0.05% (v/v) surfactant P20, 10 mM HEPES (pH 7.4); GE Healthcare). The annealed oligos were captured on the chip by flowing them over the surface for 60 seconds at 10 µl/min. A concentration gradient of topo IV (0, 1, 25, 50 and 100 nM) was then flowed over the chip at 50 µl/min for 60 seconds allowing protein to bind, followed by another 60 seconds of buffer alone to allow the interaction to stabilise. The binding response was recorded at both early and late time-points. Finally, a regeneration step was performed using the 1 M NaCl/ 50 mM NaOH reagent (60 seconds at 10 ul/min) to removed protein and DNA from the chip before the next cycle. The level of protein binding to the immobilised DNA was measured in response units and then expressed as a percentage of the theoretical maximum response, R_{max}, where 100% represents the response from a single topo IV enzyme binding to one immobilized ds DNA oligomer.

2.34 Analysis of fasamycin E binding to topo IV– protein binding experiments

Experiments were conducted to investigate if we could visualise fasamycin compounds binding to topo IV holoenzyme and individual ParC and ParE subunits by monitoring characteristic wavelengths after protein elution from a size exclusion column. The aim of this experiment was to determine which of the two subunits that make up topo IV (ParC and ParE), fasamycin compounds interact with. Holoenzyme topo IV at a concentration of 400 nM was incubated in buffer A (50 mM Tris-HCl (pH 7.5 at 4°C), 5 mM DTT, 1 mM EDTA, 10% (v/v) glycerol, 200 mM NaCl) + 150 mM NaCl + 4 mM MgCl at room temperature in the presence of 200 nM annealed double stranded DNA (5'-3' ACC AAG GTC ATG AAT GAC TAT GCA CGT AAA ACA G. after 30 minutes 1 mM ADPNP was added to the sample and incubated together for a further 30 minutes. Fasamycin E (25 µM) was added and left for an additional 15 minutes. Samples were injected onto a Superdex 200 (5/150 GL) Sepharose column and eluted with buffer A + 150 mM NaCl + 4 mM MgCl monitoring at 260, 280 and 418 nm. Fasamycin E binding experiments with ParC and ParE proteins were conducted using the same methods as documented above but with the amendment that both ParC and ParE were incubated in the absence of DNA or ADPNP.

2.35 Generation of heterologous expression strains

Heterologous host strains were generated by Dr Rebecca Devine (JIC) and Dr Abigail Alford.

<u>Generating phage-derived artificial chromosome (PAC) 215GΔ*forJ*</u>

E. coli ReDirect PCR targeting was used to replace the *forJ* coding region in pESAC-13_215G with an apramycin resistance gene in *E. coli* using Lambda RED (Gust, Chandra et al. 2004). The apramycin resistance gene was PCR amplified from pIJ773 with flanks complementary to the 3' and 5' ends of the *forJ* coding region, (forward: CGG TCT CGA AGC ACG TCA CAG CAG AGG TGA GCG AAC ATG GCT CAC GGT AAC TGA TGC CG; reverse: GCG GAC CGT GCC TAG GCC CCG CCG GGA ACG ACC GCG TCA TGT AGG CTG GAG CTG CTT C) and purified using the Qiaquick PCR purification kit. The resulting PCR fragment was electroporated into *E. coli* BW25113/pIJ790 containing pESAC-13_215G. The expression of Lambda *red* genes was induced by addition of L-arabinose (10 mM) to the LB growth medium (10 g/L tryptone, 5 g/L yeast extract, 10 g/L NaCl) to induce

recombination between the introduced PCR fragment and pESAC-13_215G. The edited PAC was isolated by resuspending the cell pellet from 1 ml overnight culture of *E. coli* BW25113 + pESAC-13_215GΔ*forJ* in 100 µl of solution 1 (50 mM Tris/HCl, pH8; 10 mM EDTA), adding 200 µl of solution 2 (200 mM NaOH; 1% SDS) followed by 150 µl of solution 3 (3 M potassium acetate, pH 5.5) and mixed by inverting. After centrifuging at 20,784 ×g for 5 minutes, the supernatant was extracted in 400 µl of 1:1 phenol/chloroform, vortexed for 2 minutes and centrifuged again. The upper phase was transferred to a tube containing 600 µl 2-propanol and left on ice for 10 minutes to precipitate the DNA, before being centrifuged again. The pellet was then washed in 200 µl 70% ethanol, left to dry for 5 minutes at room temperature and then resuspended in sterile dH$_2$O. The edited PAC was electroporated into *E.coli* Top10 and isolated by the same method as above. The desired edit was confirmed using restriction digest with *Xho*I.

The target PACs (pESAC-13_215G and the edited version pESAC-13_215GΔ*forJ*) were moved into the conjugation strain *E. coli* ET12567 by tri-parental mating. 20 µl of each cell type (*E.coli* DH10B pESAC13_215G or *E. coli* Top10 pESAC-13_215-G Δ*forJ*, *E. coli* TOP10 + pR9604 and *E. coli* ET12567 for conjugation) was spotted on top of each other in the centre of an LB agar plates and incubated overnight at 37°C. The resulting cell spot was streaked for single colonies on LB agar plates containing appropriate antibiotics to select for *E. coli* ET12567 strains containing both the cosmid and the transfer plasmid pR9604. The resulting strains (*E. coli* ET12567/pR9604/215G and *E. coli* ET12567/pR9604/215GΔ*forJ*) were grown in liquid culture overnight for conjugation into *S. coelicolor* M1146 and *S. erythraea* Δ*ery* using previously described methods previously (Gust, Chandra et al. 2004).

2.36 Scale up fermentation of *S. erythraea* Δ*ery*/215G_Δ*forJ*

Spores of *S. erythraea* Δ*ery*/215G_Δ*forJ* were spread onto 30 ml SFM agar plates (6 L) and grown at 30°C for 10 days. Agar was sliced into small pieces and soaked in ethyl acetate (6 L) twice over two concurrent nights. The agar was removed by filtration and the ethyl acetate fractions combined and solvent removed under reduced pressure to give a crude extract. A 1 µl sample of the resulting extract was resuspended in 1 ml methanol before being diluted a further 1/ 100 in methanol and analyzed by LCMS using the metabolite analysis HPLC method (section **2.12**) to confirm the expected compounds

were present and their approximate titres. For both fermentations the crude extract was fractionated using a Biotage Isolera™ system fitted with a SNAP Ultra 25 g silica cartridge using gradient elution and UV monitoring at 280 nm and 418 nm. Mobile phase A: chloroform; mobile phase B: methanol; flow rate 75 ml/min; elution started from 0% B for 1 column volumes (CV), then gradient to 10% B over 12 CV, then gradient to 30% B over 1.2 CV, then holding at 30% B for 3.1 CV which was performed with the help of Dr Edward Hems (JIC). Fractions that gave absorbance at 418 nm were pooled and subjected to preparative HPLC purification.

2.37 Preparative HPLC method for isolation of fractions 1-8

Fractions from biotage purification were purified using a Thermo Scientific Dionex Ultimate 3000 HPLC system fitted with a Phenomenex Gemini-NX reversed-phase column (C18, 110 Å, 150 × 21.2 mm).   The following conditions were applied: mobile phase A: water with 0.1% formic acid; mobile phase B: methanol; flowrate 20 mL/min; injection volume 500 µl; gradient: 0 min, 5% B; 2 min, 5% B; 2.5 min, 20% B; 17 min, 70% B; 19.5 min, 95% B; 21.5 min, 95% B; 23.5 min, 5% B. Absorbance was monitored at 418 nm by UV detector and peaks were manually collected

2.38 LC-MS and LC-MS/MS analysis of fractions 1-6

LCMS/MS analysis was performed with the assistance of Dr Lionel Hill (JIC) by using a Thermo QExactive LCMS instrument on a Kinetex C18 column (50 x 2.1 mm, 1.7 µm). LC-MS/MS method Mobile phase A: water with 0.1% formic acid; mobile phase B: acetonitrile with 0.1% formic acid; flowrate 0.7 ml/min; injection volume 10 µl; gradient from 0 min, 30% B, 6 min, 95% B,, 7.7 min, 95% B,,8 min, 30% B, 11.1 min, 30% B.The sample was analysed in positive mode over the range of 200-2000 m/z with a resolution of 35,000. The spray voltage was set to 3000 V and the capillary temperature 350 °C. The sheaf gas was set to 35 and the auxiliary gas to 10. Data dependent MS^2 with 17,500 resolution and an isolation window of 4.0 m/z and an isolation offset of 1.0 m/z was employed with normalized collision energies of 10%, 30% and 50%. Instrument was calibrated according to manufacturer's instructions, and the LC-MS/MS data was analysed using Thermo Scientific FreeStyleTM 1.7 software.

2.39 Direct injection HRMS analysis of fractions 7 and 8

For HRMS, the samples were diluted into 50% methanol/0.1% formic acid and infused into a Synapt G2-Si mass spectrometer (Waters, Manchester, UK) at 10 µl min^{-1} using a Harvard Apparatus syringe pump. The mass spectrometer was controlled by Masslynx 4.1 software (Waters). It was operated in resolution and positive ion mode and calibrated using sodium iodide. The sample was analysed for 1 min with 1 s MS scan time over the m/z range 50-1200 with 2.0 kV capillary voltage, 40 V cone voltage, 120°C cone temperature. Leu-enkephalin peptide (1 ng.µl^{-1}, Waters) was infused at 10 µl min^{-1} as a lock mass (m/z 556.2766) and measured every 10 s. Spectra were generated in Masslynx 4.1 by combining a number of scans, and peaks were centered using automatic peak detection with lock mass correction.

2.40 Carbohydrate HPAEC-PAD analysis

Carbohydrate analysis was undertaken by Dr Edward Hems (JIC). Samples were sealed in a tube containing trifluoroacetic acid (TFA; 1.0 M, 1 ml) and heated to 105 °C overnight. The resulting sample was diluted with water (20 ml) and freeze dried to remove all TFA. The residue was then dissolved in water/methanol (95:5, 1 ml) and passed through a C18 solid phase extraction cartridge (Waters, Sep-Pak® Plus Short 360 mg). The cartridge was washed with water/methanol (95:5, 2 ml) and the eluted solvent was combined and solvents under reduced pressure to yield the carbohydrate residues which were dissolved into water (150 µl) for HPAEC-PAD analysis. For samples 1-6 the cartridge was further washed with water/methanol (5:95, 3 ml) to elute the retained fasamycin aglycones which were used for aglycone analysis. Carbohydrate analysis was performed by high-performance anion-exchange chromatography with pulsed amperometric detection (HPAEC-PAD) on a Dionex ICS-5000 system using a CarboPacTM PA20 (3 × 150 mm) analytical column coupled to a CarboPacTM PA20 (3 × 30 mm) guard column. For HPAEC-PAD analyses the following conditions were used: flow rate 0.25 mL/min; injection volume was 5 µl; mobile phase A: 7.8 mM NaOH; mobile phase B: 156 mM NaOH with 100 mM AcONa; elution started with 0% B for 30 min, then gradient to 100% B over 3 minutes, hold 100% B for 20 min, gradient to 0% B over 3 min, hold 0% B for 14 min. Peaks were identified by comparison with authentic standards for the hexoses glucose, galactose and mannose; and for the pentoses arabinose, ribose and

xylose; and for the uronic acids glucuronic acid and galacturonic acid. Co-injections with standards were also performed for verification.

2.41 NMR Analysis

NMR analysis was undertaken by Dr Zhiwei Qin (JIC) and Dr Sergey Nepogodiev (JIC) 1D and 2D NMR spectra were recorded in CD_3OD at 298 K on a Bruker Neo 600 MHz spectrometer equipped with 5 mm TCI CryoProbe. 2D ^1H-^1H-COSY, ^1H-^{13}C-HSQCed, HMBC and ROESY experiments were performed using standard pulse sequences from the Bruker Topspin library. Data were processed using Topspin 4.1.4 and MestReNova 14.2.3 software and spectra were calibrated to the residual solvent signals ($\delta_{H/C}$ 3.31/49.00 ppm).

Part I: Investigating the target and mechanism of action of formicamycins and their biosynthetic intermediates, fasamycins.

3.0 Sensitivity testing and structural activity relationship of fasamycin and formicamycin

3.1 Introduction

The formicamycin compounds and their biosynthetic precursors, the fasamycins, were previously shown by our lab to inhibit the growth of clinically relevant Gram-positive organisms such as methicillin resistant *Staphylococcus aureus* (MRSA) and vancomycin resistant *Enterococci* (Qin, Munnoch et al. 2017). When the products of the *for* BGC were identified, 10 formicamycin (A-J) and 3 fasamycin (C-E) congeners were isolated (Qin, Munnoch et al. 2017). Additionally, several literature reports have described further formicamycin (N-Q), fasamycin (A-B and G-K) and fasamycin-like compounds under the names accramycins, streptovertimycins and naphthacemycins that have been identified from other *Streptomyces* spp. (Feng, Chakraborty et al. 2012, Fukumoto, Kim et al. 2017, Yang, Li et al. 2020, Yuan, Wang et al. 2020). As discussed later in this thesis (Chapter 6), deletion mutants of regulatory genes within the *for* BGC led to the isolation of several new fasamycin (L-Q) and formicamycin congeners (R and S). These congeners differed from our previously identified fasamycins (C-E) and formicamycins (A-J) in the number and position of chlorine atoms and *O*-methylation (Devine, McDonald et al. 2021). Furthermore, lactone intermediates, called formicalactones, were isolated from knockout mutants produced after identifying the genes responsible for the conversion of fasamycins into formicamycins. This conversion from fasamycin to formicamycin occurs via a two-step ring expansion-ring contraction pathway and is mediated by two gene products of the *for* BGC, ForX and ForY (**Figure 3.1**). ForX is a Baeyer-Villiger monooxygenase which is able to dearomatize ring C of fasamycin intermediates by ring expansion, leading to the production of formicalactones. The formicalactone intermediate is then converted to formicamycin through a reductive ring contraction catalysed by ForY, a flavin-dependent oxidoreductase (Qin, Devine et al. 2020). Deletion of *forY* was found to lead to the accumulation of these lactone containing intermediates and the structures of

five formicalactones (A-E) were determined by NMR and mass spectrometry.
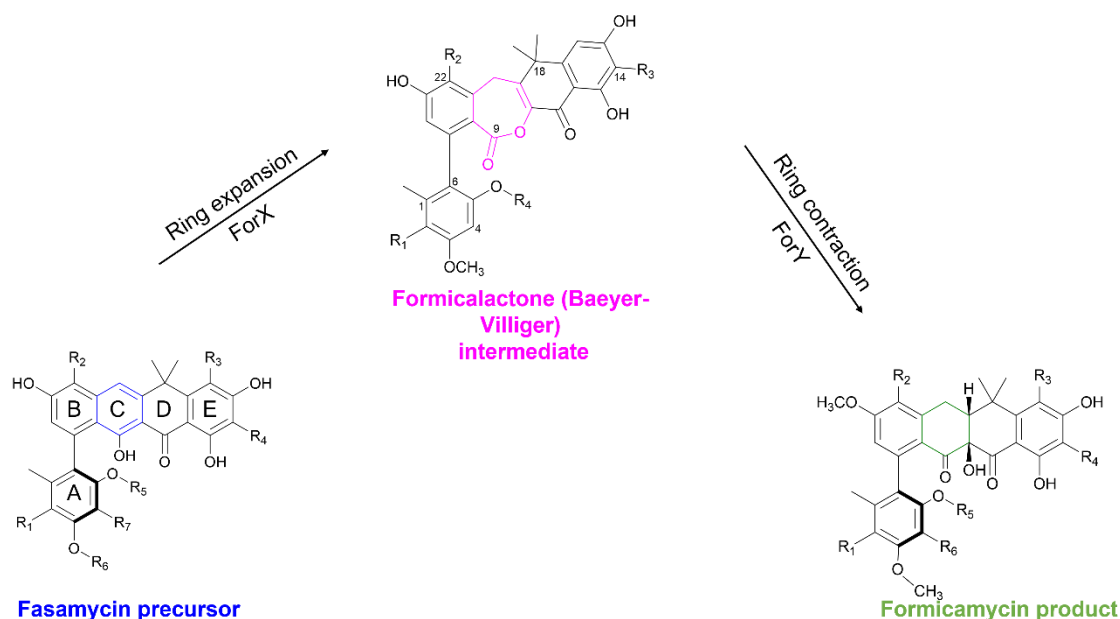
Figure 3.2 Formicamycins are formed from a two-step ring-expansion ring-contraction pathway involving two *for* encoded gene products ForX and ForY.

On the basis of these investigations we now have a diverse repertoire of fasamycins, formicamycins and formicalactones isolated from wild-type and mutant *S. formicae* strains. In this chapter an analysis of the antibacterial activity of these compounds was undertaken against a panel of bioassay indicator strains and the resulting bioassay data allows for us to draw some conclusions about a structural activity relationship. This provides some insight into which part of the compound may make up the pharmacophore which is important for interaction with the target of these compounds.

3.2 Results

3.2.1 Sensitivity testing of compounds isolated from *S. formicae* and structural activity relationship

To investigate the biological activity of the repertoire of isolated compounds that we we needed to determine their minimum inhibitory concentration (MIC), which is an *in vitro* characterisation of the potency of an antibacterial molecule, against a panel of bioassay strains (Kowalska-Krochmal and Dudek-Wicher 2021). A MIC is defined as the lowest concentration of a compound that completely inhibits the growth of a selected organism (i.e., bacterial strain) and is usually represented in µg/ml or mg/l. MIC analysis can be undertaken by different methods including determination of MIC on solid or liquid

medium. The European Committee on Antimicrobial Susceptibility Testing recommends determining MICs in liquid medium using the broth microdilution method and therefore we decided to utilise an adapted version of the microdilution method called a resazurin assay to determine the inhibitory nature of our compounds (Kowalska-Krochmal and Dudek-Wicher 2021). The resazurin assay utilises the non-toxic resazurin dye which is reduced to resorufin by respiration of viable metabolically active cells causing the dye colour to change irreversibly from blue to pink (**Figure 3.2A**). We therefore define any cultures that do not reduce resazurin to resorufin, and therefore stay blue, as non-viable, and cultures that become pink are classed as viable (Travnickova, Mikula et al. 2019) .

The bioassay panel consists of several Gram-positive bacterial strains: methicillin resistant and sensitive isolates of *Staphylococcus aureus* (MRSA and MSSA respectively), *Bacillus subtilis,* and vancomycin resistant and sensitive isolates of *Enterococcus faecalis* (VRE and VSE). It also includes the Gram-negative *Escherichia coli* and a mutated version *E. coli* NR698, which is a membrane permeabilised *E. coli* strain that may be thought to simulate a Gram-negative "without" its outer membrane (Ruiz, Falcone et al. 2005). We included the yeast strain *Saccharomyces cerevisiae* as a eukaryotic indicator strain. Of the 10 fasamycins, 18 formicamycins and 7 formicalactones that have been identified from *S. formicae* (published and unpublished work) availability of compounds meant we could only test 9 fasamycins, 14 formicamycins and 6 formicalactones against these bioindicator panel.

Single colonies of bioassay indicator strains were used to prepare overnight cultures in liquid medium (LB, TSB or BHI) and the resulting cultures were used to subculture fresh liquid medium. The cells were grown to exponential phase (OD_{600} 0.4) before being diluted to match a 0.5 McFarlands standard, a solution used to standardise bacteria to a specific optical density (OD_{600} 0.08), and then further diluted 1/100. Compounds were made up in DMSO to a concentration of 5.12 mg/ ml, a concentration is 20 times (20 X) that of the highest concentration to be tested in these assays (256 µg/ml) to ensure that when compounds were added into liquid medium, DMSO concentration was kept at 5 % to limit toxicity to the bacterial strains tested. A 2-fold dilution range of the relevant compounds were made up by diluting into DMSO. 5 µl of the 20 X stock of compounds

were then added to 95 µl liquid medium (TSB, LB or BHI) in a 96-well plate alongside wells containing liquid media supplemented with a positive control of apramycin (50 µg/ml) and two wells containing only DMSO (5% v/v in liquid media, inhibitor vehicle control), serving as a media control, to ensure the bacteria can grow in these media conditions, and a negative control. The diluted bacterial culture is used to inoculate all the wells except the negative DMSO control well, which allows us to ensure there is no contaminant growing in the medium. The 96-well plates were incubated at 37 ˚C with shaking overnight after which time the resazurin dye was added to each well before being incubated at 37 ˚C for four hours. Colorimetric results were determined by eye and we defined MIC as the lowest concentration of compound that gives a blue colour with the resazurin dye. Resazurin assays were performed in triplicate and were undertaken by myself and Dr Corinne Arnold (JIC). The assay set up is shown in **Figure 3.2B**. MIC values for all compounds and strains are documented in **Table 3.1**.
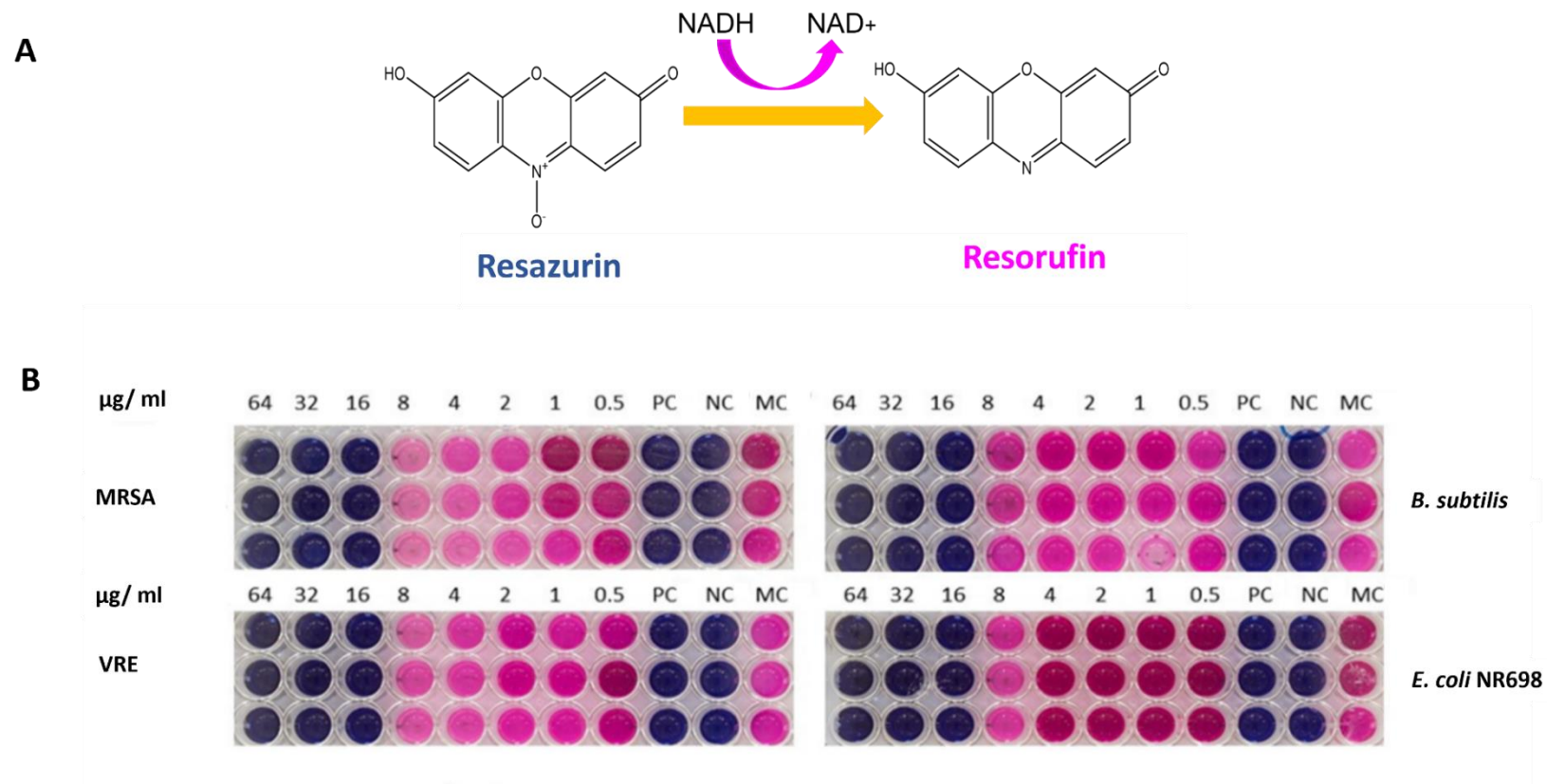
Figure 3.3 A -The reduction of resazurin to resorufin. **B**- An example of a resazurin assay set up. Indicator strains are grown in liquid media containing a serial dilution of the compound of interest (here, fasamycin C). PC – positive control (apramycin 50 µg/ml), NC – negative control (no inoculation of bacteria) and MC – Media control (indicator strain grown in the media containing 5% DMSO to ensure the strain can grow). Resazurin assays were undertaken by Hannah McDonald and Dr Corinne Arnold.

Table 3.1 Minimum inhibitory concentrations (µg/mL) of isolated compounds against a panel of bioassay strains as determined by the microdilution resazurin assay. N. D - Not determined. Strain details in order of table appearance: *E. coli* ATCC 25922, *E. coli* NR698, *S. aureus* ATCC BAA-1717, *S. aureus* ATCC 6538P, *B. subtilis* 168, *E. faecalis* O1GRF, *E. faecalis* clinical isolate and *S. cerevisiae* ATCC 200060.

Strain	Minimum inhibitory concentration (MIC) (µg/ml)							
	E. coli	*E. coli* NR698	MRSA	MSSA	*B. subtilis*	VSE	VRE	*S. cerevisiae*
Fasamycin C	>256	16	16	16	16	8	8	>256
Fasamycin E	>256	8	2	2	4	4	4	>256
Fasamycin F	>256	>256	>256	128	128	N. D	N. D	N. D
Fasamycin L	>256	8	2	2	8	8	8	>256
Fasamycin M	>256	8	4	4	8	16	8	>256
Fasamycin N	>256	2	4	2	4	4	4	>256
Fasamycin O	>256	16	4	2	8	16	16	>256
Fasamycin P	>256	8	2	4	8	16	8	>256
Fasamycin Q	>256	16	4	4	6	N. D	N. D	N. D
Formicamycin A	>256	>256	16	8	4	16	16	>256
Formicamycin B	>256	32	8	8	4	16	8	>256
Formicamycin C	>256	>256	8	8	4	16	16	>256
Formicamycin D	>256	16	8	4	4	16	16	>256
Formicamycin E	>256	32	4	4	4	8	8	>256
Formicamycin G	>256	8	4	4	2	16	16	>256
Formicamycin H	>256	4	4	4	2	8	8	>256
Formicamycin I	>256	8	4	2	4	4	8	>256
Formicamycin J	>256	4	2	2	2	8	8	>256
Formicamycin R	>256	8	2	2	2	4	16	>256
Formicamycin S	>256	4	2	2	<1	2	4	>256
Formicamycin T	>256	32	16	16	8	32	32	>256
Formicamycin W	>256	16	8	8	8	32	16	>256
Formicamycin Y	>256	16	8	16	16	32	32	>256
Formicalactone A	>256	32	32	32	64	N. D	N. D	N. D
Formicalactone B	>256	64	32	64	32	N. D	N. D	N. D
Formicalactone D	>256	8	16	8	16	N. D	N. D	N. D
Formicalactone E	>256	4	8	16	16	N. D	N. D	N. D
Formicalactone F	>256	8	16	16	16	N. D	N. D	N. D
Formicalactone G	>256	4	8	8	8	N. D	N. D	N. D

The nine fasamycin compounds are pentacyclic compounds with 4 aromatic rings. The fasamycin scaffold can be decorated with different combinations of chlorine atoms, *O*-methyl groups and, in one case, a carboxylic group to form different congeners. The variety of isolated fasamycins are shown in **Figure 3.3**. MIC assays showed that none of the fasamycin congeners tested in this study exhibited any bioactivity against the Gram-negative *E. coli* strain. However, all the fasamycins, except the carboxylic acid containing fasamycin F, a shunt metabolite whereby decarboxylation has failed to occur, showed inhibitory activity against the permeabilised gram-negative strain, *E. coli* NR698, albeit with increased MICs when compared to Gram-positive strains. This is most likely due to the inability of the compounds to access the target as they cannot cross the characteristic outer membrane of Gram-negative bacteria. The fasamycins exhibited bioactivity against all the Gram-positive bacteria tested (*S. aureus, B. subtills* and *E. faecalis*) and of all the strains tested in this study, *S. aureus* strains (MSSA and MRSA) were the most sensitive to the fasamycin congeners with MICs ranging from 2-16 µg/mL. The inhibitory activity of fasamycins against Gram-positive bacteria, but lack of inhibition of Gram-negative organisms, is consistent with other fasamycin-like compounds documented in the literature (Feng, Chakraborty et al. 2012, Fukumoto, Kim et al. 2017, Yang, Li et al. 2020).

Analysis of the biological activities of the fasamycins toward the bacterial strains allowed for some assumptions to be drawn about the effect of compound structure on biological activity. Firstly, the addition of a carboxylic acid group on the B ring of fasamycin F essentially abolishes bioactivity against all bacterial strains tested, and fasamycin F was found to be the least active of all the fasamycin congeners. The addition of a carboxylic acid group may impede the ability of the fasamycin compound to penetrate the cell membrane, or, as this is the only congener to demonstrate substitution at C24, it alters binding to the target. Furthermore, chlorination of the fasamycin backbone is not essential for bioactivity as the non-chlorinated fasamycin C shows inhibitory activity, albeit reduced, against the bacterial strains however, chlorination of the fasamycin backbone increases bioactivity by approximately 4-fold as determined by the high MICs seen for the non-chlorinated fasamycin C in comparison to all other congeners which are decorated with between 2-4 chlorine atoms. Although chlorinated fasamycins show

increased bioactivity in comparison to non-chlorinated congeners, there appeared to be no obvious relationship between the absolute number of chlorine atoms and observed bioactivity. Furthermore, as all the fasamycin compounds tested here, except fasamycin C and F, have chlorine atoms at positions C2 and C22 it is hard to determine whether the regiochemistry of the chlorination events have particular roles in increased bioactivity. These finding contradicts those for the first fasamycins reported, fasamycins A and B, which indicated that the mono-chlorinated fasamycin A exhibited increased bioactivity against *E. faecalis* and *S. aureus* in comparison to the di-chlorinated fasamycin B (Feng, Chakraborty et al. 2012). The tri-chlorinated streptovertimycin G was found to be the most biologically active against *S. aureus* and *E. faecalis* whereas the most chlorinated streptovertimycin H (4 chlorines) was found to exhibit the least biological activity against indicator strains. Furthermore, accramycin J, another fasamycin like analogue, which has 4 chlorine atoms and contains the most chlorine atoms of all of the accramycins identified , was found to be the most potent even in comparison to mono and di-chlorinated congeners (**Figure 3.4**), this may suggest that the positioning of the chlorine atoms on the fasamycin backbone, instead of the absolute number, has importance in terms of bioactivity (Maglangit, Zhang et al. 2020, Yang, Li et al. 2020). All of the fasamycin compounds tested in our work contain at least one *O*-methyl group at either position C3 or C5 on ring A of the fasamycin scaffold, however, there does not appear to be any significant effect on bioactivity related to where on ring A these *O*-methyl groups are. The first identified fasamycins, fasamycin A and B as well as fasamycin J, isolated by Yuan and colleagues, contain no *O*-methyl groups and still show potent activity toward both *S. aureus* (fasamycin A, B and J) and *E. faecalis* (fasamycin A and B) strains and therefore *O*-methylation cannot be an essential factor for bioactivity against these Gram-positive strains (Feng, Chakraborty et al. 2012, Yuan, Wang et al. 2020). Upon analysis of other fasamycin like molecules reported in the literature it was found that fasamycins G,H and I as well as all of the isolated accramycins (A-K), have at least one *O*-methyl group on rings B, C and E, all of which exhibit bioactivity against Gram-positive organisms. Multiple *O*-methyl groups on the fasamycin backbone does not appear to impede or enhance bioactivity (Maglangit, Fang et al. 2019, Maglangit, Zhang et al. 2020, Yuan, Wang et al. 2020). Our results indicate that the ability of the fasamycin compounds to exhibit bioactivity may be due to subtle differences in positionings of both chlorination and *O*-methyl groups in combination, rather than being

due to absolute number or positionings of these groups alone. In our work, we found that Fasamycin E and L were the most potent of all the congeners against the *S. aureus* strains and that none of the fasamycin congeners exhibited any bioactivity toward the eukaryotic yeast species, *S. cerevisiae*.

Formicamycins possess a different chemical structure to that of their intermediates fasamycins, with a loss of aromaticity at ring C which results in tetrahedral bridgehead positions at C10 and C19. Moreover, C10 is quaternary and both C10 and C19 are chiral centres (Qin, Munnoch et al. 2017, Qin, Devine et al. 2020). This change means the 3D structure of the formicamycins is very different to than that of the fasamycins, adopting a twisted chair-like confirmation (Qin, Munnoch et al. 2017). However, the structures at each 'end' of the molecule remain similar, suggesting that one of these regions is key for interaction with the cellular target. As with the fasamycin congeners, the formicamycin backbone can be decorated with chlorine atoms and *O*-methyl groups at specific positions (R groups) to form the different congeners (**Figure 3.3**).

All 14 formicamycin congeners tested in this experiment showed inhibitory activity towards the Gram-positive strains but no activity towards the Gram-negative *E. coli* strain. All but two of the congeners (A and C) were able to inhibit the growth of the permeabilised *E. coli* NR698 strain thus indicating that the outer membrane of *E. coli* also likely impedes formicamycin penetration. Overall, the formicamycins displayed the most potent activity against the *B. subtilis* and *S. aureus* strains tested in this study exhibiting MICs of <1-16 µg/ml. Analysis of MICs toward *S. aureus* strains indicates that chlorination of the formicamycin backbone appears to increase inhibitory activity of the formicamycins as indicated by the fact that the mono-chlorinated congener, formicamycin A, has the highest MICs of all the formicamycins tested (16 µg/ml). Formicamycin congeners with subsequently more chlorine atoms displayed reduced MICs, and therefore increased potency. For example, the di-chlorinated formicamycin B has increased activity against *S. aureus* in comparison to formicamycin A (8 vs 16 µg/ml) and the tri-chlorinated formicamycins E-H show increased activity in comparison to formicamycin B (4 vs 8 µg/ml). Formicamycin congeners containing 4 or 5 chlorine atoms show the most potent activity with MICs of 2 µg/ml but there is no obvious difference in activity between congeners with 4 or 5 chlorine atoms. In terms of regiochemistry, formicamycins which contain a chlorine atom at C14 on ring E, generally appear to show
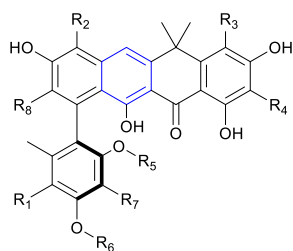
enhanced bioactivity in comparison to those that do not (formicamycin A-E), which may indicate that chlorination at this position on the formicamycin scaffold may enhance interactions with the bacterial cell target but is not essential for bioactivity. All the formicamycins tested in this work contain a *O*-methyl group at C3 of ring A and C25 on ring B on the formicamycin scaffold, several congeners also contain a second *O*-methyl group on ring A at C5, the presence or absence of this second *O*-methyl group does not appear to confer significant effects on bioactivity. There is only one example in the literature of a formicamycin compound which does not contain any *O*-methyl groups, formicamycin P, which exhibits moderate inhibitory activity (12.5 μg/ml) against *S. aureus* but shows poor activity (50 μg/ ml) against *B. subtilis* indicating that differences in positionings of chemical groups may lead to differences in antibacterial activity between bacterial species. Formicamycin J and S showed the most potent inhibitory activities to the strains tested. As with the fasamycins, no inhibitory activity was observed against *S. cerevisiae.*

Due to limited compound availability, the formicalactone compounds were tested against a limited panel of strains. Interestingly, these biosynthetic intermediates did exhibit bioactivity against several of the indicator strains. The formicalactones displayed reduced bioactivity (4-64 μg/ml) across all the strains in comparison to the fasamycin and formicamycin compounds overall which indicates that the lactone ring impedes potency in some way, maybe by reducing the affinity of the compounds to their target. Interestingly, these lactone intermediates do still display bioactivity, especially in the case of formicalactone E and G which indicates that even though there is a significant change in 3D structure in comparison to fasamycin and formicamycin, this set of compounds are still able to exert inhibitory effects meaning that the pharmacophore of the compounds is likely at either ends of the molecule, for example at either ring B or E.

Formicalactone E and G exhibited increased activity against *E. coli* NR698 strain in comparison to the Gram-positive strains whereas the majority of fasamycin and formicamycin congeners exhibit more potent activity towards the Gram-positive strains. The least biologically active congeners were formicalactone A and B, whilst formicalactone G was found to be the most biologically active. Unlike the formicamycins, increased chlorination did not appear to have a direct correlation with increased

bioactivity. As with fasamycin and formicamycin, there was no activity observed against the *E. coli* strain.

Other than fasamycin F, all the compounds isolated from wild-type and *for* BGC mutant *S. formicae* strains and tested here display bioactivity against all of the Gram-positive strains tested, in addition to the permeabilised *E. coli* strain NR698, but not toward the *E. coli* strain. We hypothesise that the outer-membrane of Gram-negative strains inhibits activity by limiting access to the bacterial cell target. None of the fasamycin or formicamycin congeners displayed any toxicity toward the eukaryotic indicator strain *S. cerevisiae* which may indicate that they cannot penetrate eukaryotic cells or that the target of both fasamycins and formicamycins are unique to bacterial cells, at least within the range of concentrations tested.

Fasamycin C $R_1 = H$, $R_2 = H$, $R_3 = H$, $R_4 = H$, $R_5 = H$, $R_6 = CH_3$, $R_7 = H$, $R_8 = H$
Fasamycin D $R_1 = H$, $R_2 = Cl$, $R_3 = H$, $R_4 = H$, $R_5 = H$, $R_6 = CH_3$, $R_7 = H$, $R_8 = H$
Fasamycin E $R_1 = Cl$, $R_2 = Cl$, $R_3 = H$, $R_4 = H$, $R_5 = H$, $R_6 = CH_3$, $R_7 = H$, $R_8 = H$
Fasamycin F $R_1 = H$, $R_2 = H$, $R_3 = H$, $R_4 = H$, $R_5 = H$, $R_6 = CH_3$, $R_7 = H$ $R_8 = COOH$
Fasamycin L $R_1 = Cl$, $R_2 = Cl$, $R_3 = H$, $R_4 = Cl$, $R_5 = H$, $R_6 = CH_3$, $R_7 = H$, $R_8 = H$
Fasamycin M $R_1 = Cl$, $R_2 = Cl$, $R_3 = H$, $R_4 = H$, $R_5 = CH_3$, $R_6 = H$ $R_7 = Cl$, $R_8 = H$
Fasamycin N $R_1 = Cl$, $R_2 = Cl$, $R_3 = Cl$, $R_4 = H$, $R_5 = H$, $R_6 = CH_3$, $R_7 = H$, $R_8 = H$
Fasamycin O $R_1 = Cl$, $R_2 = Cl$, $R_3 = H$, $R_4 = Cl$, $R_5 = CH_3$, $R_6 = CH_3$, $R_7 = H$, $R_8 = H$
Fasamycin P $R_1 = Cl$, $R_2 = Cl$, $R_3 = Cl$, $R_4 = H$, $R_5 = CH_3$, $R_6 = OH$ $R_7 = Cl$, $R_8 = H$
Fasamycin Q $R_1 = Cl$, $R_2 = Cl$, $R_3 = Cl$, $R_4 = Cl$, $R_5 = H$, $R_6 = CH_3$, $R_7 = H$, $R_8 = H$

Formicamycin A $R_1 = H$, $R_2 = Cl$, $R_3 = H$, $R_4 = H$, $R_5 = CH_3$, $R_6 = H$
Formicamycin B $R_1 = Cl$, $R_2 = Cl$, $R_3 = H$, $R_4 = H$, $R_5 = H$, $R_6 = H$
Formicamycin C $R_1 = H$, $R_2 = Cl$, $R_3 = Cl$, $R_4 = H$, $R_5 = CH_3$, $R_6 = H$
Formicamycin D $R_1 = Cl$, $R_2 = Cl$, $R_3 = Cl$, $R_4 = H$, $R_5 = H$, $R_6 = H$
Formicamycin E $R_1 = Cl$, $R_2 = Cl$, $R_3 = Cl$, $R_4 = H$, $R_5 = CH_3$, $R_6 = H$
Formicamycin F $R_1 = Cl$, $R_2 = Cl$, $R_3 = H$, $R_4 = Cl$, $R_5 = CH_3$, $R_6 = H$
Formicamycin G $R_1 = H$, $R_2 = Cl$, $R_3 = Cl$, $R_4 = Cl$, $R_5 = CH_3$, $R_6 = H$
Formicamycin H $R_1 = Cl$, $R_2 = H$, $R_3 = Cl$, $R_4 = Cl$, $R_5 = CH_3$, $R_6 = H$
Formicamycin I $R_1 = Cl$, $R_2 = Cl$, $R_3 = Cl$, $R_4 = Cl$, $R_5 = H$, $R_6 = H$
Formicamycin J $R_1 = Cl$, $R_2 = Cl$, $R_3 = Cl$, $R_4 = Cl$, $R_5 = CH_3$, $R_6 = H$
Formicamycin R $R_1 = Cl$, $R_2 = Cl$, $R_3 = Cl$, $R_4 = Cl$, $R_5 = H$, $R_6 = Cl$
Formicamycin S $R_1 = Cl$, $R_2 = Cl$, $R_3 = Cl$, $R_4 = Cl$, $R_5 = CH_3$, $R_6 = Cl$
Formicamycin T $R_1 = H$, $R_2 = Cl$, $R_3 = H$, $R_4 = Cl$, $R_5 = CH_3$, $R_6 = H$
Formicamycin U $R_1 = Cl$, $R_2 = H$, $R_3 = Cl$, $R_4 = H$, $R_5 = CH_3$, $R_6 = H$
Formicamycin V $R_1 = Cl$, $R_2 = H$, $R_3 = Cl$, $R_4 = H$, $R_5 = CH_3$, $R_6 = H$
Formicamycin W $R_1 = H$, $R_2 = Cl$, $R_3 = Cl$, $R_4 = Cl$, $R_5 = CH_3$, $R_6 = H$
Formicamycin X $R_1 = H$, $R_2 = Cl$, $R_3 = Cl$, $R_4 = Cl$, $R_5 = OH$, $R_6 = H$
Formicamycin Y $R_1 = H$, $R_2 = H$, $R_3 = Cl$, $R_4 = Cl$, $R_5 = OH$, $R_6 = H$

Formicalactone A $R_1 = H$, $R_2 = Cl$, $R_3 = H$, $R_4 = H$
Formicalactone B $R_1 = Cl$, $R_2 = Cl$, $R_3 = H$, $R_4 = H$
Formicalactone C $R_1 = Cl$, $R_2 = Cl$, $R_3 = H$, $R_4 = CH_3$
Formicalactone D $R_1 = Cl$, $R_2 = Cl$, $R_3 = Cl$, $R_4 = H$
Formicalactone E $R_1 = Cl$, $R_2 = Cl$, $R_3 = Cl$, $R_4 = CH_3$
Formicalactone F $R_1 = H$, $R_2 = Cl$, $R_3 = Cl$, $R_4 = H$
Formicalactone G $R_1 = Cl$, $R_2 = H$, $R_3 = Cl$, $R_4 = CH_3$

Figure 3.3 Structures of fasamycin, formicamycin and formicalactone congeners isolated from strains discussed in this thesis. The isolation of these compounds has been comprised of published and unpublished work. Blue green and pink coloured C rings denote key changes between different compound classes.

Fasamycin A R_1 = H
Fasamycin B R_1 = Cl

Fasamycin G R_1 = H, R_2 = CH_3, R_3 = Cl, R_4 = CH_3
Fasamycin H R_1 = H, R_2 = H, R_3 = H, R_4 = CH_3
Fasamycin I R_1 = Cl, R_2 = H, R_3 = H, R_4 = CH_3
Fasamycin J R_1 = Cl, R_2 = H, R_3 = H, R_4 = H
Fasamycin K R_1 = H, R_2 = CH_3, R_3 = Cl, R_4 = H

Streptovertimycin A R_1 = H, R_2 = H, R_3 = H, R_4 = CH_3, R_5 = H
Streptovertimycin B R_1 = Cl, R_2 = H, R_3 = H, R_4 = CH_3, R_5 = H
Streptovertimycin C R_1 = H, R_2 = Cl, R_3 = H, R_4 = CH_3, R_5 = H
Streptovertimycin D R_1 = H, R_2 = Cl, R_3 = H, R_4 = H, R_5 = H
Streptovertimycin E R_1 = Cl, R_2 = Cl, R_3 = H, R_4 = H, R_5 = H
Streptovertimycin F R_1 = H, R_2 = Cl, R_3 = Cl, R_4 = H, R_5 = H
Streptovertimycin G R_1 = H, R_2 = Cl, R_3 = Cl, R_4 = H, R_5 = CH_3
Streptovertimycin H R_1 = Cl, R_2 = Cl, R_3 = Cl, R_4 = H, R_5 = H

Accramycin A R_1 = CH_3, R_2 = CH_3, R_3 = H, R_4 = H, R_5 = H, R_6 = H , R_7 = H
Accramycin B R_1 = CH_3, R_2 = CH_3, R_3 = CH_3, R_4 = H, R_5 = H, R_6 = H , R_7 = H
Accramycin C R_1 = H, R_2 = CH_3, R_3 = H, R_4 = Cl, R_5 = H, R_6 = H , R_7 = H
Accramycin D R_1 = CH_3, R_2 = CH_3, R_3 = CH_3, R_4 = Cl, R_5 = H, R_6 = H , R_7 = H
Accramycin E R_1 = CH_3, R_2 = CH_3, R_3 = H, R_4 = Cl, R_5 = Cl, R_6 = H , R_7 = H
Accramycin F R_1 = CH_3, R_2 = H, R_3 = CH_3, R_4 = Cl, R_5 = Cl, R_6 = H, R_7 = H
Accramycin G R_1 = CH_3, R_2 = CH_3, R_3 = CH_3, R_4 = Cl, R_5 = Cl, R_6 = H, R_7 = H
Accramycin H R_1 = H, R_2 = H, R_3 = CH_3, R_4 = Cl, R_5 = H, R_6 = Cl, R_7 = Cl
Accramycin I R_1 = H, R_2 = CH_3, R_3 = CH_3, R_4 = Cl, R_5 = Cl, R_6 = Cl, R_7 = H
Accramycin J R_1 = H, R_2 = H, R_3 = CH_3, R_4 = Cl, R_5 = Cl, R_6 = Cl, R_7 = Cl
Accramycin K R_1 = H, R_2 = CH_3, R_3 = CH_3, R_4 = Cl, R_5 = Cl, R_6 = Cl, R_7 = Cl

Formicamycin N R_1 = H, R_2 = H, R_3 = Cl, R_4 = CH_3
Formicamycin O R_1 = Cl, R_2 = H, R_3 = H, R_4 = CH_3
Formicamycin P R_1 = H, R_2 = H, R_3 = Cl, R_4 = H
Formicamycin Q R_1 = Cl, R_2 = CH_3, R_3 = Cl, R_4 = CH_3

Figure 4.4 Structures of other identified formicamycin (N-Q) and fasamycin -like compounds, fasamycin (A-B and G-K) (Feng, Chakraborty et al. 2012, Yuan, Wang et al. 2020), streptovertimycins (A-H) (Yang, Li et al. 2020) and the accramycins (A-K) (Maglangit, Fang et al. 2019, Maglangit, Zhang et al. 2020). Structures are shown as have been reported in the literature.

3.2.2 Fasamycin and formicamycin display potent activity against archaeal species
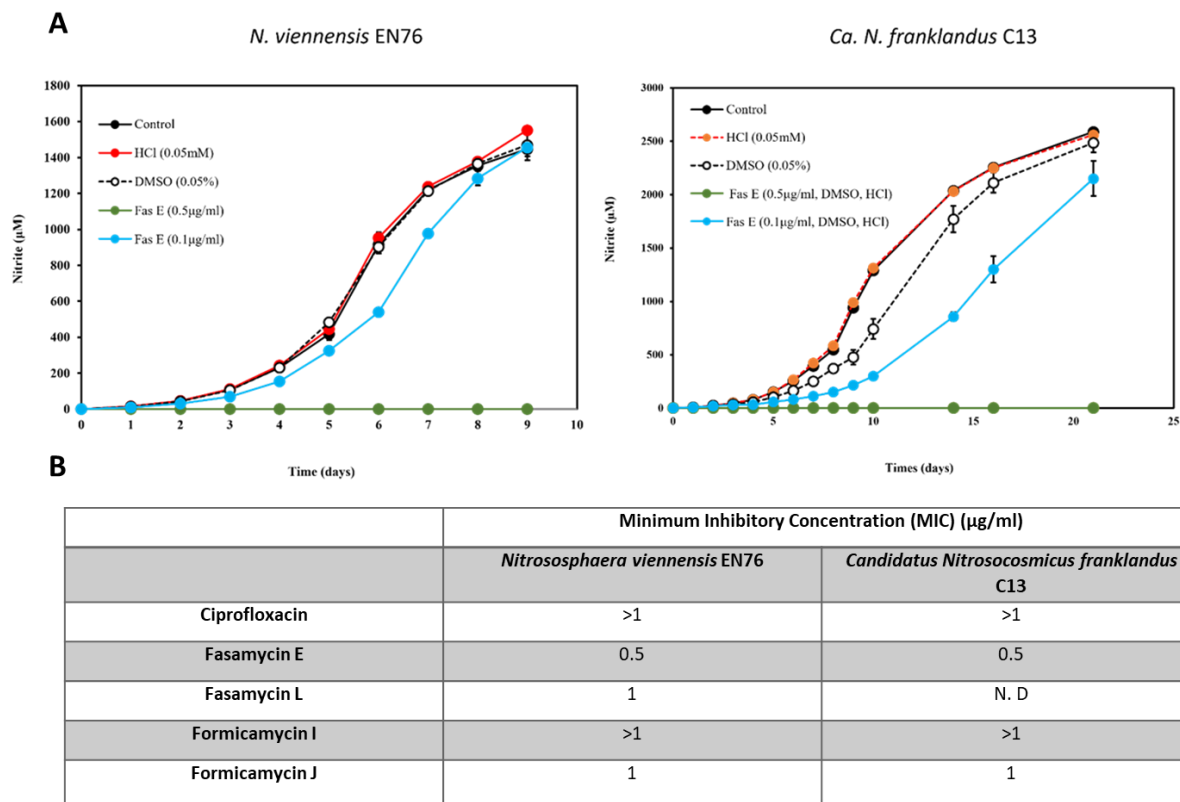
Archaea are singled celled organisms that were recognised as a third domain of life ~ 45 years ago (Woese and Fox 1977). They are a diverse group that can be found in most habitats including within human microbiomes and in extreme environments such as hot springs and salt lakes. The ability to thrive in extreme environments may be in part because they can utilise a large range of natural sources such as hydrogen, the reduction of metal ions and ammonia for growth. Interestingly, other than some minor associations in periodontitis, there are currently no identified archaeal species that are known to cause pathogenesis in humans; a lack of pathogenesis is fortunate because most archaea are resistant to the majority of antibacterial compounds (Khelaifia and Drancourt 2012). The lack of susceptibility to antibiotics may be due to several structural differences between bacteria and archaea such as the lack of peptidoglycan in archaeal cell walls and the fact that archaeal membranes are made up of isoprenoid lipids whereas bacterial membranes are made up of fatty acids (Villanueva, von Meijenfeldt et al. 2021). They do, however, share a few antibiotic targets including DNA replication and protein synthesis, where bacterial inhibitors of these targets, such as ciprofloxacin and rifampicin, do inhibit archaea (Khelaifia and Drancourt 2012).

To expand our bioactivity screen, we wanted to understand if either fasamycin or formicamycin displayed any inhibitory activity toward archaeal strains. Inhibitory growth assay experiments were conducted by Timothy Klein (UEA). Two fasamycin (E and L) and two formicamycin (I and J) congeners were assayed against two soil dwelling ammonium oxidising archaeal (AOA) species *Nitrososphera viennensis* EN76 and *Candidatus nitrosocosmicus franklandus* C13 (Stieglmeier, Klingl et al. 2014, Lehtovirta-Morley, Ross et al. 2016). As for the bacterial assays, the stock solutions of these compounds were prepared in DMSO to stock concentrations that gave a final DMSO concentration of 0.05 % (v/v) in liquid medium. Both archaeal species were exposed to three concentrations of each compound (0.1, 0.5 and 1 µg/ml), as well as ciprofloxacin (dissolved in 0.05 mM HCl and at the same concentrations), which targets topoisomerases – a validated archaeal target (Khelaifia and Drancourt 2012). Both AOA strains were also grown in the presence of 0.05% DMSO and 0.05 mM HCl (inhibitor

vehicle controls) to ensure inhibitory effects due to the compounds could be differentiated from activity attributed to the vehicles.

AOA strains were grown in liquid fresh-water medium, and growth of AOA cultures was monitored by measuring nitrite accumulation as these strains cannot be monitored by optical density due to their slow growth rate and therefore being practically invisible to standard assays in liquid medium. Nitrite concentrations were analysed using the Greiss colorimetric assay measuring absorbance at 540 nm, and performed daily for a total of 9 days and 21 days for *Nitrososphera viennensis* EN76 and *Candidatus nitrosocosmicus franklandus* C13 respectively (Lehtovirta-Morley, Ross et al. 2016). Growth curves were used to determine the MIC of the compounds used in this study against the AOA strains. The lowest concentration of compound in which the AOA strains exhibited no growth was determined to be the MIC. Representative examples of growth curves from both AOA strains in the presence of fasamycin E are shown in **Figure 3.5A**.

Both fasamycin congers (E and L) completely impeded the growth of *Nitrososphaera viennensis* EN76 with MICs of 0.5 and 1 μg/ml respectively (**Figure 3.5B**) and fasamycin E also showed inhibitory activity toward *Candidatus Nitrosocosmicus franklandus* C13 with a MIC of 0.5 μg/ml. Out of the two formicamycin congeners tested (J and I), formicamycin J also inhibited the growth of both archaeal species (MIC = 1 μg/ml) but formicamycin I showed no inhibitory activity against either strain at the concentrations tested (**Figure 3.5B**). Similarly, ciprofloxacin did not show any inhibitory activity towards either AOA strain up to 1 μg/ml (**Figure 3.5B**). Further testing would need to be undertaken to verify if ciprofloxacin and formicamycin I can inhibit growth of these AOA strains at higher concentrations than those tested in this experiment.

A

N. viennensis EN76

Ca. N. franklandus C13

B

	Minimum Inhibitory Concentration (MIC) (µg/ml)	
	Nitrososphaera viennensis EN76	*Candidatus Nitrosocosmicus franklandus* C13
Ciprofloxacin	>1	>1
Fasamycin E	0.5	0.5
Fasamycin L	1	N. D
Formicamycin I	>1	>1
Formicamycin J	1	1

Figure 3.5 A - Exemplar growth curves of *Nitrososphera viennensis EN76 and Candidatus nitrosocosmicus franklandus C13* in the presence of fasamycin E and the vehicles 0.05% DMSO and 0.05 mM HCl as determined by nitrite production. **B**- MIC values determined for all compounds against both archaeal species using the growth curve method. Error bars represent standard deviation   from biological triplicates. Growth assays were undertaken by Timothy Klein.

3.3 Discussion

The formicamycins and their biosynthetic intermediates the fasamycins were previously shown to be inhibitors of Gram-positive organisms and the work documented in this chapter expands these observations by showing that both sets of compounds are active against a range of Gram-positive organisms and to an *E. coli* strain with a permeabilised outer membrane. We found that chlorination of the fasamycin backbone increases bioactivity against Gram-positive bacteria, as inferred by increased bioactivity from chlorinated fasamycin congeners in comparison to the non-chlorinated fasamycin C, but there is no clear correlation between bioactivity and increasing chlorination. Activity relationships reported for other fasamycin and fasamycin-like compounds have found that mono-chlorination leads to the most favourable bioactivity profile (Feng, Chakraborty et al. 2012, Yang, Li et al. 2020). Unfortunately, we did not have enough material to undertake MIC testing with the mono-chlorinated fasamycin D, isolated from *S. formicae*, and therefore we cannot say for certain whether mono-chlorination leads to increased bioactivity in comparison to further chlorinated fasamycins isolated from *S. formicae.* Unlike the fasamycins, we did determine that increased chlorination of the formicamycin scaffold does correlate with increased potency against Gram-positive bacteria. In contrast, research by Yuan et al (2020) found that formicamycin O, a mono-chlorinated formicamycin has increased bioactivity to that of a di-chlorinated formicamycin, formicamycin Q. Our results and those reported in the literature indicate that the bioactivity of both fasamycin and formicamycin may be due to several factors, including the regiochemistry and number of different decorating groups (i.e., chlorines and *O*-methyl groups).

We also report that all the fasamycin and formicamycin congeners tested in this work do not exhibit bioactivity against the Gram-negative indicator strain *E. coli* with an intact outer membrane but were able to inhibit a membrane permeabilised *E. coli* strain, indicating that the outer-membrane of Gram-negative strain impedes the ability of these compounds to penetrate the cells and act upon their target, thus conferring intrinsic resistance. However, Yuan et al (2020) identified novel fasamycin (G-K) and formicamycin (N-Q) molecules that were found to be bioactive against *Escherichia coli*

ATCC 8099 which is a unique report in the literature for this class of compounds, these results may indicate that that distribution of chlorine atoms across the fasamycin scaffold may lead to the ability to cross the Gram-negative outer-membrane.

This characteristic antibacterial property of the compounds from the *for* BGC is particularly interesting considering that the intermediates in formicamycin biosynthesis, the fasamycins and formicalactones, also display activity against the same bacterial organisms as the end products of the pathway, the formicamycins. Given the energy cost to the host to extend the biosynthetic pathway from fasamycin intermediates to formicamycin end products we might expect increased biological activity for the formicamycins. However, we have shown that both classes of compound exhibit similar potency against the strains tested here and this may indicate that the fasamycin and formicamycin compounds have different antibacterial targets. Investigations into the biological target are discussed later in this thesis in Chapter 4 and 5.

An intriguing observation has been made that both fasamycin E and formicamycin J are potent inhibitors of two archaeal species. Although novel inhibitors of archaeal growth are not sought after, this is an extremely interesting observation because fasamycins have previously been found to inhibit the fatty acid synthase (FAS-II) pathway which is responsible for the synthesis of fatty acids for membranes in bacteria (Feng, Chakraborty et al. 2012). As archaea do not synthesise fatty acids (Villanueva, von Meijenfeldt et al. 2021), the inhibitory activity of the fasamycins is surprising and suggests the fasamycins may have an additional target, at least in archaea, or as the formicamycins, specifically formicamycin J, are also able to inhibit these two archaeal species and a range of Gram-positive bacteria, it may be hypothesised that the target of formicamycin must be present in both bacteria and archaea such as proteins involved in DNA replication or protein synthesis.

To further the work detailed in this chapter, efforts should focus on determining how both fasamycin and formicamycin inhibit bacterial growth and whether they inhibit the same bacterial target. To understand this, attempts at generating resistant mutants should be undertaken with both compounds to determine the target of each class of compound.

4.0 Investigating the target of fasamycin and formicamycin

4.1 Introduction

Determining the target and the mode of action of an antibiotic is extremely important in terms of a compound's clinical potential. Some compounds can be incredibly potent against bacteria, but their target and mode of action means they are potentially toxic to humans. For the example, the polymixins (colistin) are an incredibly potent class of antibiotics that inhibit Gram-negative bacteria, by disrupting the cell membrane, but are used as an antibiotic of last resort due to the fact that they cause nephrotoxicity and neurotoxicity in humans (Mohapatra, Dwibedy et al. 2021). The most successful antibiotics are those that inhibit a process or target that is unique to bacteria, e.g., DNA gyrase, peptidoglycan biosynthesis or the bacterial ribosome (discussed in Chapter 1).

The 'gold standard' for target determination of an antibacterial compound is through the generation of spontaneous resistant mutants, which can then be genome sequenced to identify mutations which should theoretically map to the gene that encodes the compounds target. This target can then be further validated *in vitro* using biochemical assays and/or structural studies. However, sometimes this gold standard of target determination cannot be achieved due to several factors such as the inability to generate resistant mutants or the generation of mutants that exhibit resistance due to a non-specific mechanism (e.g., efflux pumps).

As described in detail in Chapter 1, when the formicamycins were first identified they were novel to *S. formicae* but their biosynthetic precursors, the fasamycins, had been previously characterised. Research by Feng et al (2012) undertook a study of polyketide biosynthetic gene clusters cloned directly from soil and isolated two fasamycin congeners (A and B) with promising antibacterial properties. Resistant *E. faecalis* mutants, with increased MICs toward fasamycin A were generated by exposing cultures to concentrations of fasamycin A above the minimum inhibitory concentration and genome sequencing of resistant mutants revealed the presence of multiple mutations within the different strains. All strains contained loss of function mutations within FabT, the MarR-family repressor of the essential fatty acid synthase II (FAS-II) pathway which

led to over-expression of all the fatty acid biosynthesis genes under FabT control, indicating that the fasamycins inhibit FAS-II. *In vitro* fatty acid elongation assays were undertaken alongside *in vivo* target protein over-expression studies, whereby all of the genes of the FAS-II pathway were over-expressed individually, and the target of fasamycin A was determined to be FabF, an elongation condensation enzyme and over-expression of FabF led to fasamycin A resistance (Feng, Chakraborty et al. 2012). As the formicamycins have only recently been identified, no investigations have been undertaken on the target of these compounds

The aim of this work was to investigate possible *in vivo* targets of formicamycin using resistant mutants and then verifying potential targets *in vitro*. A further aim was to verify the previously identified target of fasamycin, FabF, with fasamycins isolated from *S. formicae*.
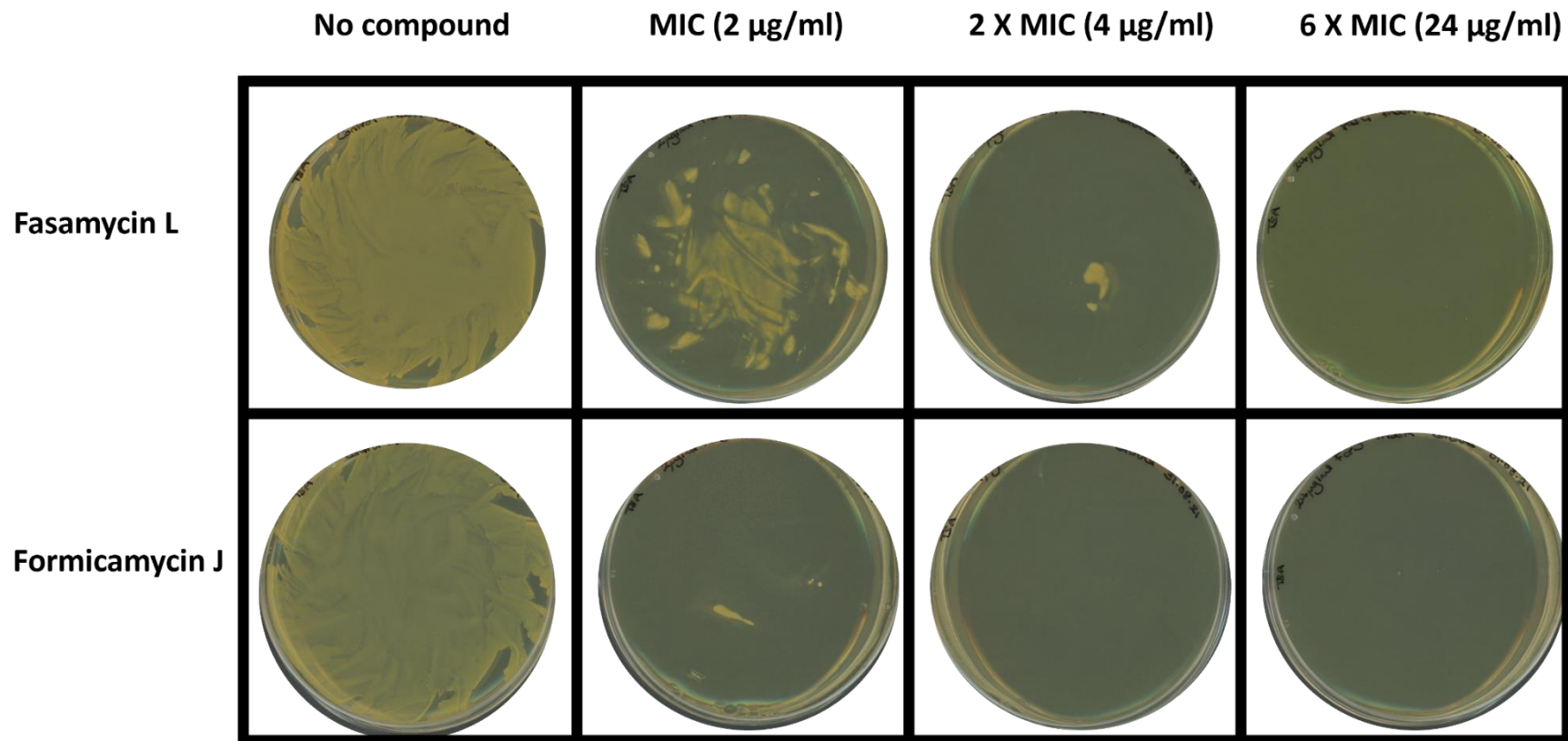
4.2 Results

4.2.1 Attempts to generate spontaneous resistance to fasamycin and formicamycin

Here, we attempted to replicate the work done by Feng et al (2012) with our fasamycin and formicamycin compounds, using *S. aureus* in replacement of *E. faecalis*. Resistant mutant generation was attempted by the author of this thesis and Dr Corinne Arnold (JIC) by exposing methicillin sensitive *S. aureus* (MSSA) to varying concentrations (1, 2, and 6 X MIC) of fasamycin L and formicamycin J congeners. Overnight cultures of MSSA were plated onto tryptic soy agar supplemented with either fasamycin L or formicamycin J (2, 4 and 24 µg/ml) and grown at 37˚C overnight. **Figure 4.1** shows representative results of these assays. In all cases either no colonies grew or the resulting colonies did not exhibit increases in MIC towards any of the fasamycin or formicamycin congeners tested and were therefore not resistant mutants.

Repeat experiments were conducted with different congeners of fasamycin and formicamycin and *B. subtilis* and *E. coli* NR698 (which has a leaky outer membrane) were also used for mutant generation but yielded the same results as for MSSA (not shown). After several unsuccessful attempts we concluded that, unlike fasamycin A, resistance to the fasamycin and formicamycin compounds tested in this study could not be

generated using this method. This may indicate that both compounds have an alternative target.

Figure 4.1 Representative results from spontaneous mutation generation. *S. aureus* (MSSA) grown on TS agar in the presence of increasing concentration of fasamycin L and formicamycin J. Plates show growth after overnight incubation at 37°C. No colonies were formed above MIC concentration for either compound. Experiments were undertaken by Hannah McDonald and Dr Corinne Arnold.

Research by Qin et al (2017) indicated that the formicamycin compounds exhibited a high barrier to resistance, inferred from the fact that no resistance was generated in *B. subtilis* after 20 days of serial passage at sub-MIC concentrations of formicamycin J. Here, a barrier to resistance experiment was conducted to extend this work, by increasing the time period of exposure, including fasamycin congeners and using a different test strain. Two *S. aureus* strains (MSSA and MRSA) were grown in triplicate in the presence of two congeners of fasamycin (E and L) and formicamycin (I and J) individually for 40 days. Sub-MIC concentrations that resulted in viable cultures (5 ml) were pre-determined prior to the experiment by growing MSSA and MRSA cultures in serial dilutions of each fasamycin and formicamycin congener; the highest concentration of fasamycin and formicamycin congeners that allowed for growth of MSSA and MRSA using this method was determined to be 0.5 µg/ ml (¼ MIC) for all congeners. To ensure any differences in MIC were attributable to fasamycin and formicamycin exposure, MSSA and MRSA were also sub-cultured in TSB medium + DMSO (inhibitor vehicle control) for the duration of the experiment. Overnight cultures were used to inoculate fresh medium supplemented with fasamycin or formicamycin congeners or DMSO daily; MIC testing was conducted every 10 days (day 0, 10, 20, 30 and 40) via resazurin assay for each of the cultures to determine if resistance had been generated in any of the strains (**Table 4.1**). Representative resazurin assay images can be seen in **SI figures 1-4**.

After 40 days of exposure there were no significant changes in MIC for any fasamycin or formicamycin congener in either the MSSA or MRSA strains and fasamycin/ formicamycin exposed cultures showed similar MICs to those treated with DMSO. Variation in MIC was observed across all conditions whereby the MIC would vary by approximately ± 2 µg/ml in comparison to MICs determined at day 0. However, this was also observed in the DMSO control so we attribute this to biological variation.

Assuming that *S. aureus* has a doubling time of 20 minutes (Missiakas and Schneewind 2013), these experiments roughly equate to 2880 generations and signifies that both classes of compound exhibit a very high barrier to resistance. Although this is unhelpful in determining the target of our compounds, it makes them promising candidates for clinical development.

Table 4.1 MIC determinations from day 0 and day 40 of MRSA and MSSA grown in the presence of either fasamycin (E and L), formicamycin (I and J) congeners or DMSO (control) for 40 days. Representative MIC data from triplicate experiments.

	Minimum inhibitory concentration (MIC) (µg/ml)					
	Day 0 (Pre-exposure)		40 days post compound exposure		40 days post DMSO exposure	
	MRSA	MSSA	MRSA	MSSA	MRSA	MSSA
Fasamycin E	2	4	4	4	4	2
Fasamycin L	4	2	4	4	2	2
Formicamycin I	4	4	2	2	2	2
Formicamycin J	4	2	2	2	2	2

4.2.2 Over-expression of fatty acid synthase II genes does not confer resistance to fasamycin or formicamycin

FabF was verified as the target of fasamycin A through the over-expression of each of the individual FAS-II genes under the control of FabT. As we cannot generate fasamycin or formicamycin resistant mutants in MSSA or MRSA, we wanted to determine if over-expression of any of the individual FAS-II genes in *S. aureus* increases resistance to these compounds. Therefore, MSSA strains containing over-expression constructs for the individual fatty acid synthase genes (*fabD, fabF, fabG, fabH, fabI* and *fabZ*) and an empty vector (EV) control were generated by expressing a second copy of each gene under the control of an oxytetracycline inducible promoter on a chloramphenicol resistant plasmid (pRAB11). Strain creation including vector construction, transformation and assays were conducted by Dr Corinne Arnold (JIC).

Over-expression strains (OD$_{600}$ 0.05) were used to inoculate soft nutrient agar (SNA) supplemented with chloramphenicol and oxytetracycline to induce expression of the FAS genes. Over-expression strains were subjected to spot on lawn MIC testing in triplicate, whereby compounds of interest are spotted directly onto agar plates containing bacterial strains, using a concentration range of fasamycin L (256 – 2 µg/ml), formicamycin J (256 – 2 µg/ml), two previously characterised fatty acid inhibitors,

triclosan (6-0.06 µg/ml) which inhibits FabI and platensimycin (256 – 2 µg/ml) which inhibits FabF and the protein synthesis inhibitor, apramycin (1.4 µg/ml) as a negative control. Plates were incubated overnight at 37°C and results were confirmed by eye.

As expected, over-production of FabI and FabF were able to inhibit the bioactivity of triclosan (MIC: EV – 2 µg/ml vs FabI - > 8 µg/ml) and platensimycin (MIC: EV – 32 µg/ml vs FabI - > 256 µg/ml) respectively in comparison to the MIC determined for the EV control but both compounds retained activity against all the other over-expression strains tested (**Figure 4.2**). As expected, the negative control apramycin retained activity against all strains tested. No significant increase in MICs were observed for either fasamycin L or formicamycin J in any of the over-expression strains. We did note however, that *fabH* over-expression increased the fasamycin L MIC from 32 µg/ml (EV control) to 64 µg/ ml but this increase in MIC was much reduced in comparison to observed changes in MIC for the platensimycin and triclosan controls. Furthermore, work by Feng et al (2012) observed a 2.5-fold change in MIC toward fasamycin A when *fabF* was over-expressed in *E. faecalis* which compared to similar increases in MIC for the FabF-inhibiting antibiotic controls, cerelurin and BABX. However, using *S. aureus* we observed a much more dramatic change in MIC for the platensimycin and triclosan controls and therefore did not define this 2-fold change as significant resistance in this experiment.

Two hypotheses can be proposed to explain these results; firstly, the compounds isolated from *S. formicae* do not inhibit fatty acid biosynthesis and have a different target or secondly, that the fasamycin compounds isolated from *S. formicae* do inhibit fatty acid synthesis but that over-expression of individual FAS proteins are not sufficient to confer resistance. We continued to investigate both hypotheses going forward.
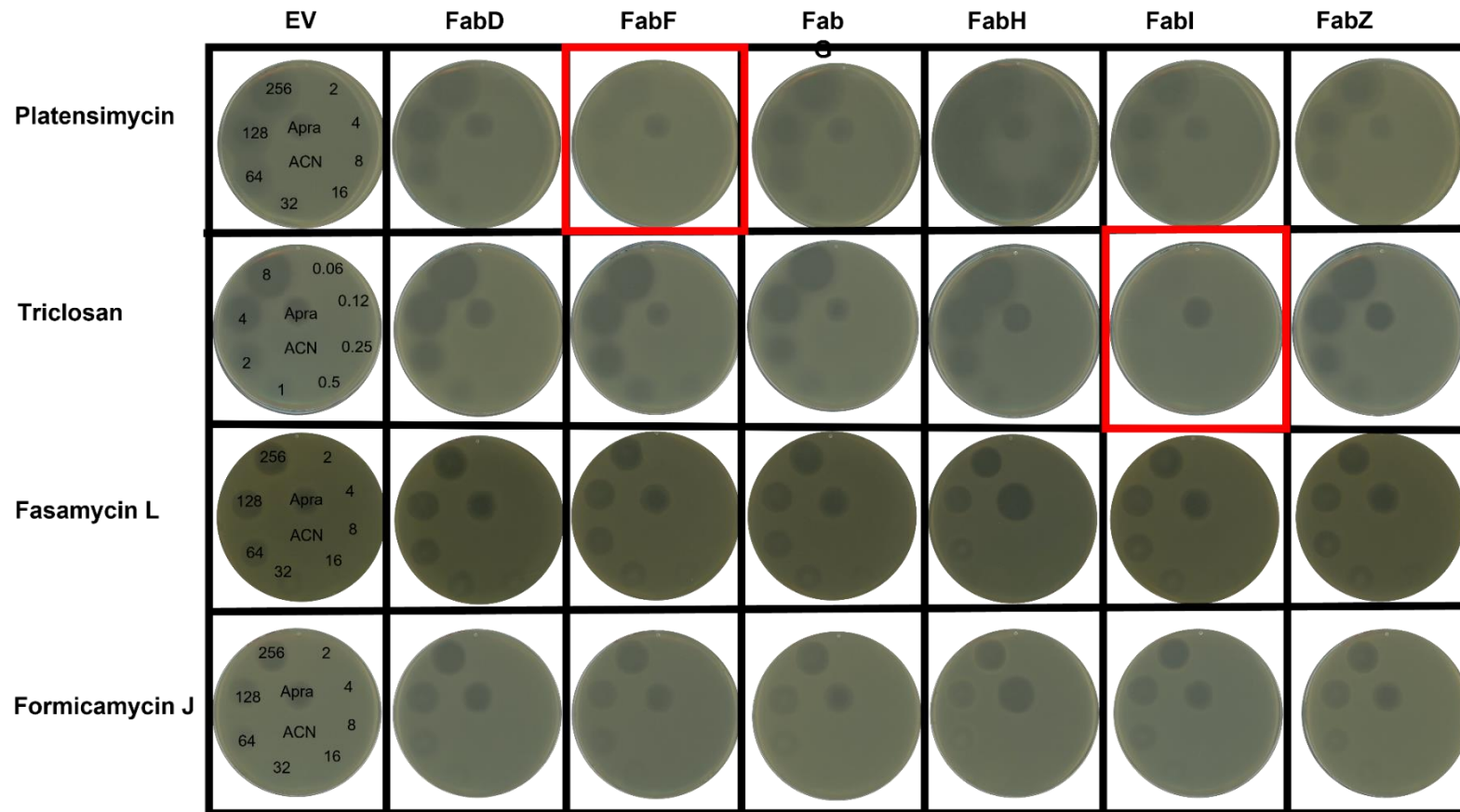
Figure 4.2 Representative results from triplicate experiments showing the effect of *fabD*, *fabF*, *fabG*, *fabH*, *fabI* and *fabZ* over expression on platensimycin, triclosan, formicamycin J and fasamycin L MIC. EV; empty vector control. Red boxes denote those strains that provide resistance. Apra – apramycin, ACN – acetonitrile. Numbers refer to compound concentration in μg/ml. Experiments were undertaken by Dr Corinne Arnold.

95

4.2.3 Reporter strains reveal multiple potential targets for fasamycins and formicamycins

Bacterial reporter strains are a useful tool to aid in identifying the cellular targets of antibacterial compounds. These strains typically contain fusions of reporter genes to gene promoters from specific biochemical pathways. When these pathways are inhibited, for example by exposure to an antibiotic, the expression of the reporter gene is increased due to an increase in promoter activity, resulting in the production of a reporter enzyme that is bioluminescent or reacts with an indicator compound in the agar to give a colorimetric marker that can be visualised by eye or measured.

A panel of *B. subtilis* reporter strains were gifted to us by Professor Jeff Errington (Newcastle University) and used to identify potential targets of the fasamycins and formicamycins. These strains have a *lacZ* gene fused to promoters that are responsive to the inhibition of several established antibacterial targets, such that inhibition leads to the production of the *lacZ* gene product, beta galactosidase, and this hydrolyses X-gal to produce a blue dye that forms a ring around the colony. These strains have been used to identify the target of vancoresmycin and therefore may provide useful information in target elucidation for both fasamycin and formicamycin (Kepplinger, Morton-Laing et al. 2018). Details of the individual strains and their positive controls are documented in **Table 4.2**.

Table 4.2 Details of *B. subtilis* reporter strains, including the antibacterial target they are used to report and their positive controls, used in this experiment
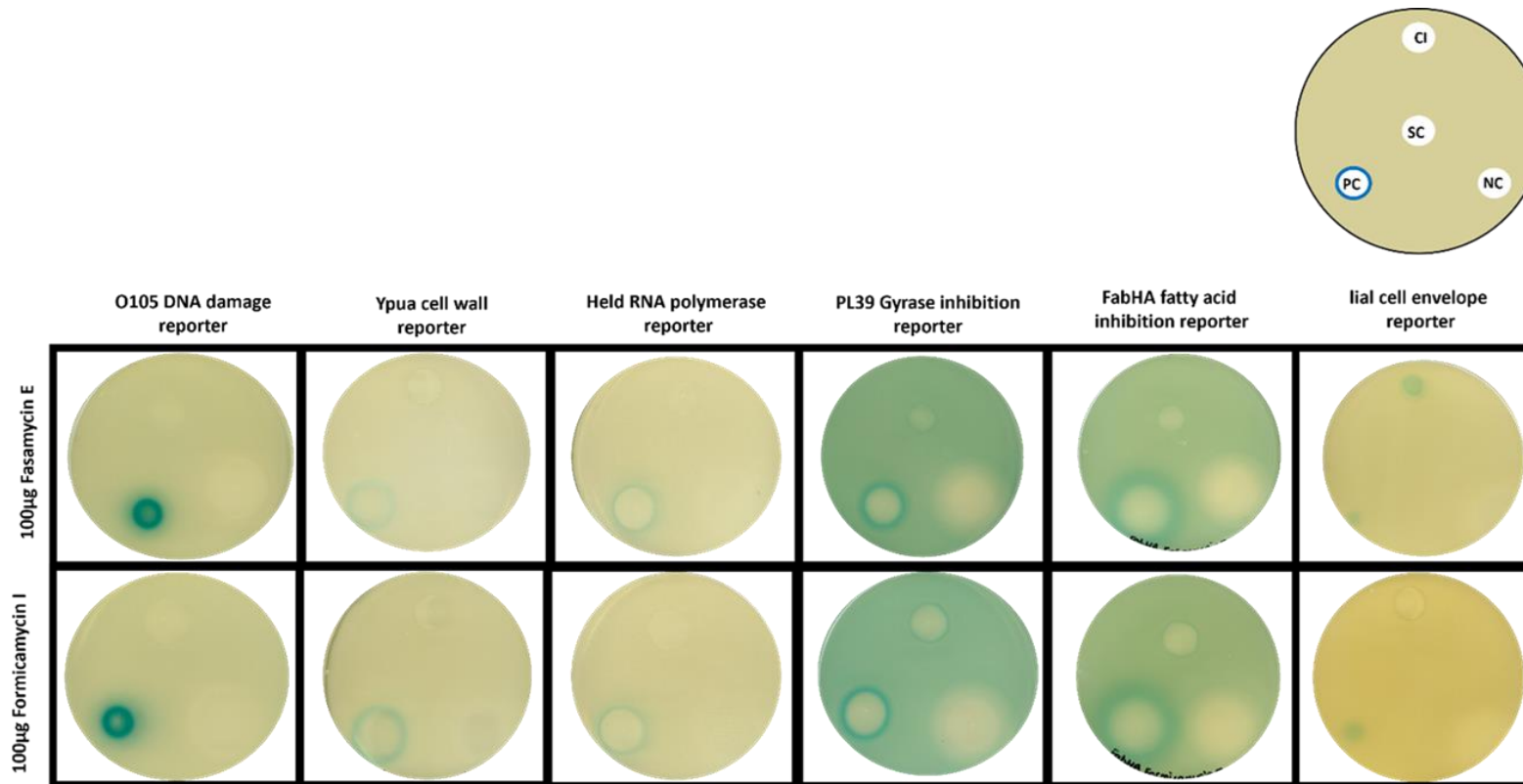
B. subtilis reporter strain	Target	Positive control
B. subtilis PL39	DNA Gyrase inhibition reporter	Novobiocin
B. subtilis ypuA	Cell Wall damage reporter	Cefotaxime
B. subtilis fabHA	Fatty acid synthase inhibition reporter	Triclosan
B. subtilis o105	DNA damage reporter	Doxorubicin
B. subtilis helD	RNA polymerase inhibition reporter	Rifampicin
B. subtilis lial	Cell envelope reporter	Bacitracin

Reporter strains were grown to exponential phase (OD_{600} 0.4) in triplicate before being added into SNA agar supplemented with X-gal (100 μg/ml). Fasamycin E (100 μg/ml), formicamycin I (100 μg/ml) both made up in 100 % methanol and the relevant controls for each reporter strain (positive, negative and methanol) were spotted onto the agar, plates were incubated overnight, and results were determined by eye. None of the negative controls gave any positive reporter activity as indicated by a lack of a blue ring around the zones of inhibition, similarly the DMSO (inhibitor vehicle control) control showed no evidence of inhibitory activity. The positive controls for each individual reporter strain all gave a blue ring around the zone of inhibition indicating that the reporter strains were reactive to specific stresses and no inhibitory activity was observed for the methanol solvent controls. In every assay conducted, both the fasamycins and formicamycins used in these experiments showed activity against the fatty acid, gyrase and cell envelope inhibition reporters. The gyrase and fatty acid inhibition reporter plates displayed a blue colour across the whole plate, which may be due to high concentrations of compounds used. However, darker blue rings could be distinguished around positive controls and fasamycin and formicamycin spots and so they were deemed to be positive results (**Figure 4.3**). For clarity, zoomed in images of the fatty acid and gyrase inhibition reporter plates can be found in **Figures 4.4 and 4.5**. We did not observe any activity for any of the other reporter strains tested against fasamycin and formicamycin.

Fatty acid inhibition reporter activity for fasamycin corroborates what is documented in the literature about the target of fasamycin and these results represent our first line of evidence that fasamycin compounds from *S. formicae* also inhibit fatty acid synthesis *in vivo*. The positive response for fatty acid inhibition of formicamycin is also not surprising as the fasamycins are intermediates in formicamycin biosynthesis and therefore, both compounds may be able to inhibit similar biological targets due to their related structures. However, positive responses for both gyrase and cell envelope inhibition reporter strains when exposed to both compounds were interesting as these results not only provided potential new targets to investigate but they also provide a potential explanation for why it is has proven so challenging to generate resistance to fasamycin and formicamycin; it is possible that these compounds inhibit multiple, distinct biochemical pathways *in vivo* and therefore generating spontaneous resistance to

multiple essential *in vivo* targets is biologically difficult. Furthermore, the results of this experiment represent the first line of evidence for what the target of formicamycin could be.

Although reporter strains are useful for indicating how an antibacterial is inhibiting bacteria *in vivo* they are not sufficient to confirm the target of an antibiotic on their own, so the results of these experiments must be validated using other methods. Investigations going forward, only focus upon fatty acid inhibition and gyrase inhibition as we hypothesised that the positive response of the cell envelope inhibition reporter strain may be a secondary response to fatty acid inhibition, as fatty acids are important components of the cell membrane (Vadia, Tse et al. 2017). Although we cannot exclude this as a true target, investigating three targets is outside the scope of a what can be achieved during this PhD project.

**Key: CI:** compound of interest, **SC:** Solvent control, **PC:** Positive Control, **NC:** Negative Control

Figure 4.3 Representative results from *B. subtilis* reporter assays. Reporter strains were grown in SNA supplemented with 100 µg/ml X-gal. Fasamycin E and formicamycin I (100 µg/ml) in methanol were spotted onto agar alongside a positive, negative and a solvent (methanol) control. Blue rings around zones of inhibition indicate a positive reporter response.

B. subtilis fatty acid inhibition reporter strain

Fasamycin E
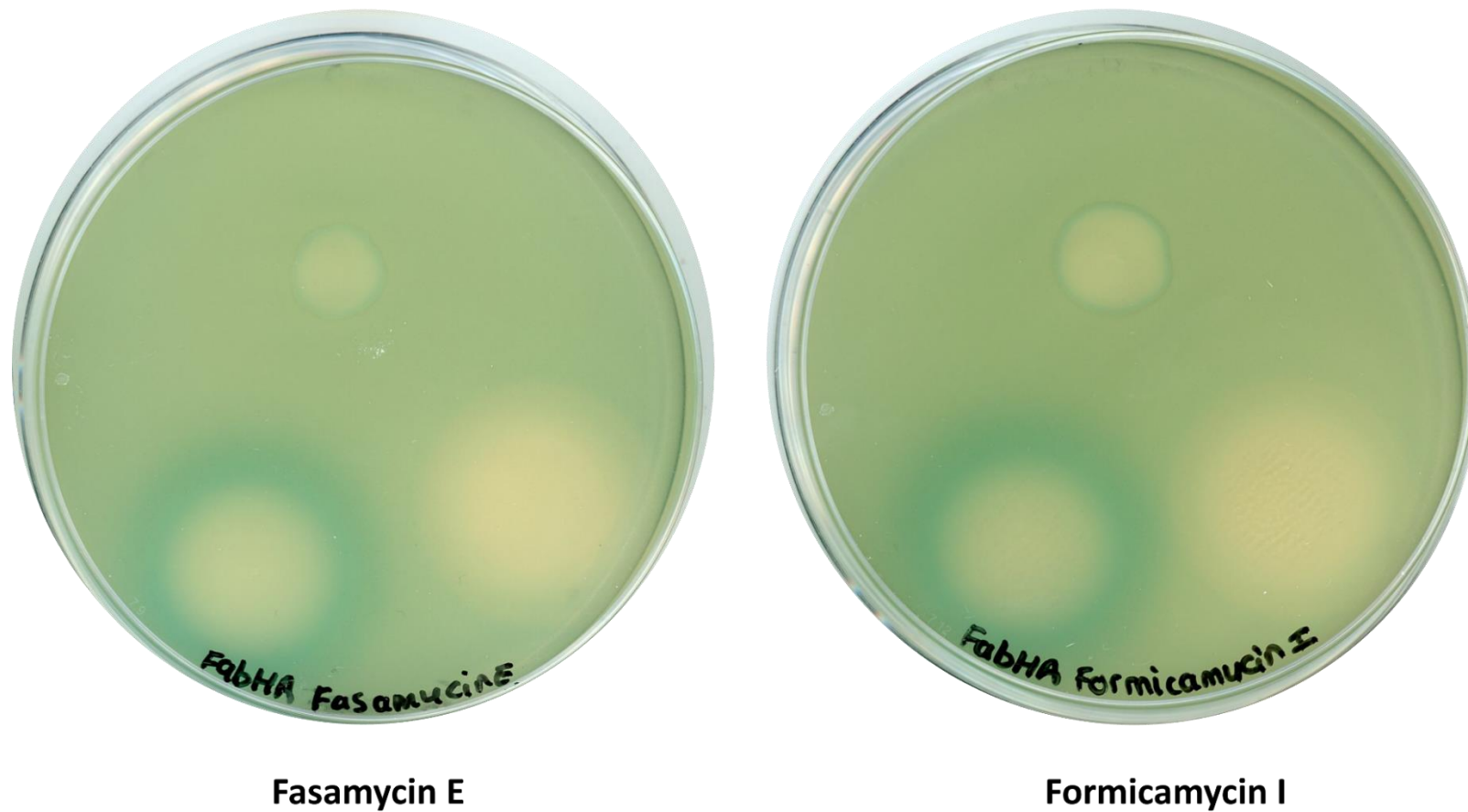
Formicamycin I

Figure 4.4: Zoomed in images of fatty acid inhibition reporter strains spotted with fasamycin E and formicamycin I, both 100 μg/ ml (top spot), triclosan (positive control – bottom left spot) and spectinomycin (negative control – bottom right spot).

B. subtilis gyrase inhibition reporter strain
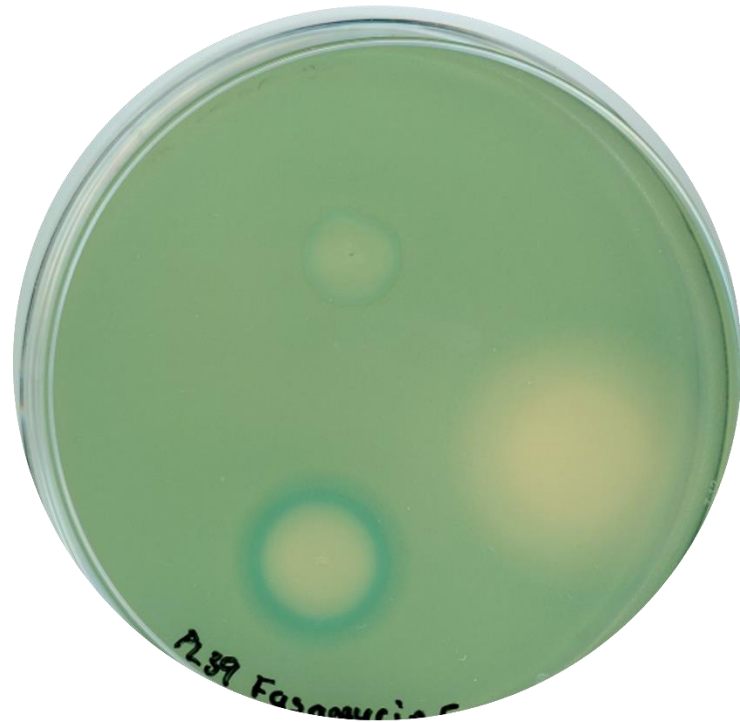
Fasamycin E

Formicamycin I

Figure 4.5: Zoomed in images of gyrase inhibition reporter strains spotted with fasamycin E and formicamycin I, both 100 µg/ml (top spot), novobiocin (positive control – bottom left spot) and spectinomycin (negative control – bottom right spot).

4.2.4 Transcriptome analysis of *S. aureus* exposed to fasamycin and formicamycin

To further investigate if our compounds have the proposed dual-target inhibitory effect *in vivo*, an RNA sequencing experiment was performed by Dr Rebecca Devine (JIC) whereby the transcriptomes of *S. aureus* cells exposed to either fasamycin and formicamycin, were compared to non-fasamycin/formicamycin treated (treated with DMSO which is the inhibitor vehicle control) *S. aureus*. Cultures were grown in triplicate to early exponential phase before addition of either fasamycin E (2 X MIC – 4 µg/ml), formicamycin J (2 X MIC – 4 µg/ml) or a methanol only control to the culture broth. Cultures were incubated for a further 15 minutes before a 1mL sample was cenitrfuged and the cell pellets used for RNA extraction. RNA sequencing was conducted by Novagene (Cambridge, UK) and the data were analysed to determine significance of changes (> 1-fold log change and < P 0.05), by Dr Govind Chandra (JIC). The results showed that fasamycin and formicamycin exposure caused a vast array of significant (> 1-fold log change and < P 0.05) changes in RNA transcript levels, as expected for stressed bacterial cells, such that pinning down potential targets from these data alone would prove challenging (**SI Figure 5**). However, with several potential targets indicated from the reporter strain experiments, we were able to assess any changes to specific genes related to these targets.

Analysis of genes involved in fatty acid biosynthesis 15 minutes post exposure to fasamycin and formicamycin was undertaken. As previously discussed, resistant mutants to fasamycin A were found to contain mutations within the *fabT* gene of the FAS-II pathway, however, the nomenclature of the FAS-II pathway differs in *S. aureus* in comparison to *E. faecalis* whereby the regulator of the FAS-II pathway is called FapR instead of FabT but has the same function. *S. aureus* FapR represses the transcription of several genes, including *fabDFGHI*, whose products are required for the FAS-II pathway (Schujman, Paoletti et al. 2003) (**Figure 4.6**) (Albanesi and de Mendoza 2016). Analysis of *fapR* expression revealed it is down regulated by a log-fold of 1.4 after exposure to fasamycin and down regulated by a log-fold of 2 after formicamycin treatment in comparison to the untreated control (**Figure 4.7A**). Given that FapR is a repressor, we would assume that down fold regulation would lead to the de-repression and therefore over-expression of FAS-II genes. However, even when *fapR* transcripts are

downregulated, increased transcripts for *fabDFGHI* are not observed at the significance level we assigned for this analysis with either fasamycin or formicamycin treatment. We do, however, see a log-fold of 2 decrease in *fabZ* transcripts after exposure to fasamycin. FabZ is a β-hydroxyacyl-(acyl-carrier-protein) dehydratase which acts upon β-hydroxyacyl-ACP, which is only present if the FAS-II pathway is functional. Down-regulation of this transcript and reduced levels of the protein would be expected if earlier proteins in the pathway were inhibited. Formicamycin exposed *S. aureus* also showed a reduction in transcripts of two genes involved in malonyl-CoA biosynthesis, which acts as the precursor in fatty acid biosynthesis (*accB* and *accC*) which also suggests an inhibitory effect on the FAS-II pathway. A hypothesis for this observation is that there may be either an accumulation of malonyl-CoA in the cell that is not being fed into FAS-II biosynthesis or that the biosynthesis pathway is no longer operational and therefore production of malonyl-CoA is not needed (**Figure 4.7A**).
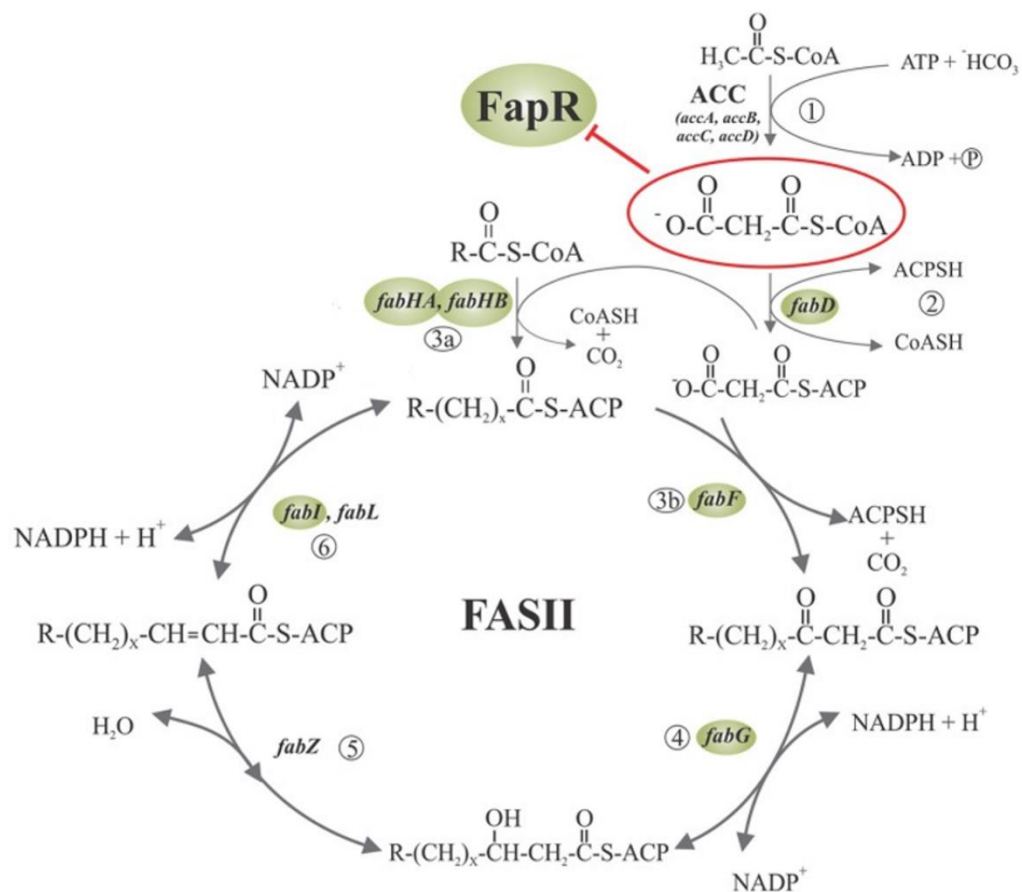

Figure 4.6 Fatty acid synthesis pathway. 1; Acetyl-CoA carboxylase (ACC) actus upon acetyl-CoA to form malonyl-CoA. 2; Malonyl-CoA is transferred to ACP by FabD, malonyl-CoA transacyclase 3a; Cycles of fatty acid elongation by condensation are initiated by

FabH producing a β-ketoester 4; FabG, a β-ketoacyl-ACP reductase, reduces the β-ketoester to β-hydroxyacyl-ACP, 5; β-hydroxyacyl-ACP is dehydrated to unsaturated acyl-ACP by FabZ, 6; finally the unsaturated acyl-ACP is reduced by FabI. 3b; subsequent elongation is initiated by FabF. Red circle indicates the ligand of FapR. Adapted from Albanesi and de Mendoza 2016

Transcripts of the *S. aureus* gyrase encoding genes, *gyrA* and *gyrB*, were found to be at least 1.5 log-fold up regulated after 15 minutes of exposure to fasamycin E and an over 2 log-fold increase in both *gyrA* and *gyrB* transcripts were seen after exposure to formicamycin J (**Figure 4.7B**). Increases in these transcripts may be in response to the antibiotics, i.e., the cell is increasing the levels of GyrA and GyrB proteins to combat inhibition from fasamycin and formicamycin. Increases in *lexA* and *recA* transcripts (> 1.5 log-fold) which encode DNA damaging sensing proteins involved in the SOS response, were also observed after fasamycin and formicamycin exposure. LexA is a repressor that acts upon ~ 20 genes involved in the SOS response and antibiotic treatment or stress to the cell produces a signal which activates RecA. Although LexA represses the SOS response, RecA cleaves LexA to relieve repression so the overall effect of fasamycin and formicamycin treatment may be to increase the SOS response in response to DNA gyrase inhibition. Increased expression of *S. aureus gyrA*, *gyrB*, *lexA* and *recA* is also induced by exposure to ciprofloxacin, a well characterised gyrase inhibitor (Cirz, Jones et al. 2007).

Taken together the results of the reporter assays and RNA sequencing indicate that DNA gyrase could be a target for fasamycins and formicamycins. The rest of the work in this chapter and Chapter 5 focuses on the characterisation of fasamycin and formicamycin inhibition of topoisomerases such as DNA gyrase.
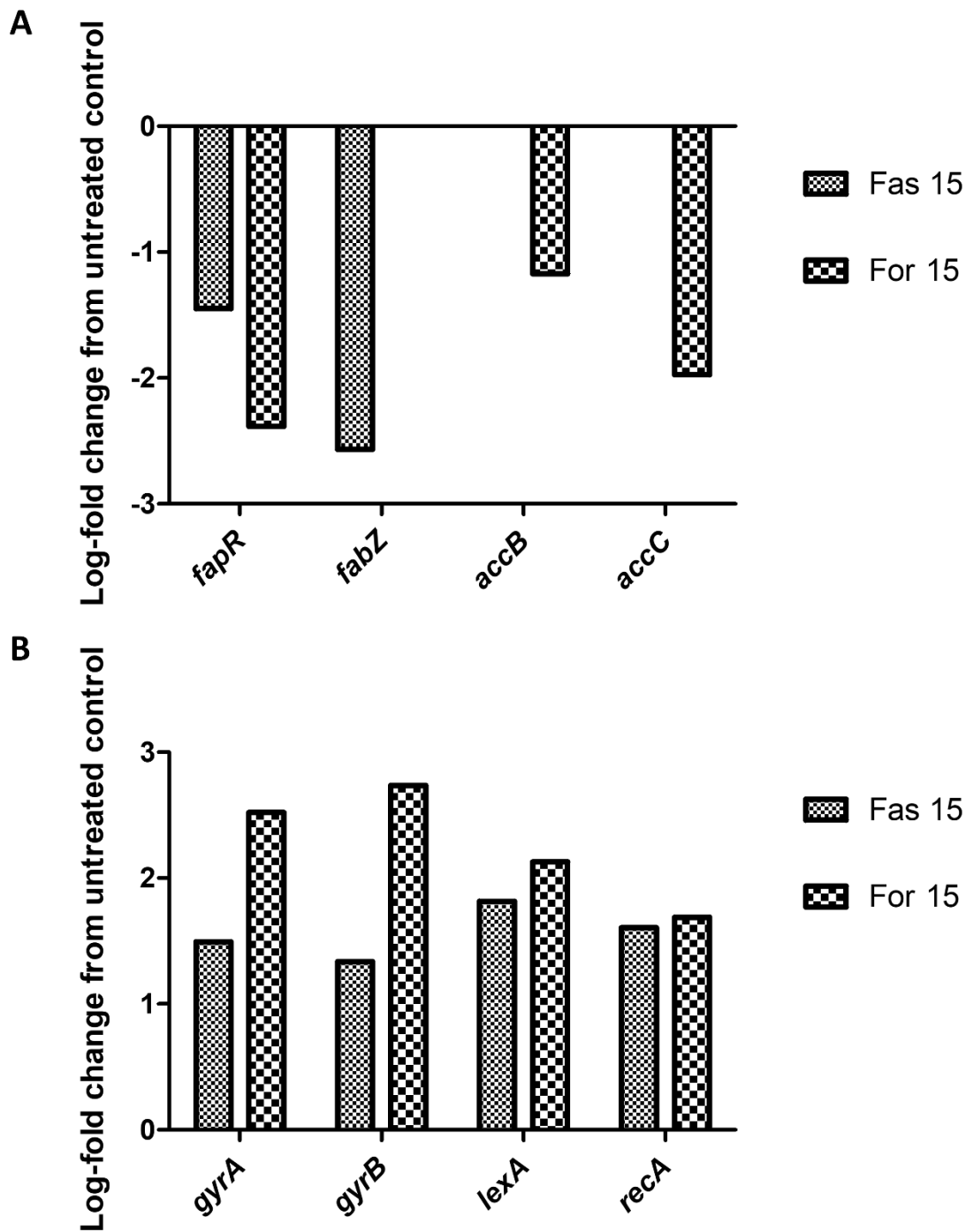
Figure 4.7 Log-fold change in transcript levels of genes involved in fatty acid biosynthesis (**A**) and DNA topology (**B**) of *S. aureus* treated with fasamycin (Fas15) and formicamycin (For15) in comparison to non-treated but solvent controlled *S. aureus.* RNA samples were prepared by Dr Rebecca Devine.

4.2.5 Fasamycin and formicamycin inhibit gyrase and topoisomerase IV *in vitro*

Gyrase is a type II topoisomerase that is essential in all bacterial cells as is topoisomerase IV (topo IV) which has high homology to gyrase. Both enzymes play a vital role in the cell by interconverting the topology of DNA between supercoiled and relaxed states through the use of double stranded (ds) DNA breaks (McKie, Neuman et al. 2021). In this chapter gyrase is defined as a topoisomerase that introduces supercoils into relaxed DNA and topo IV as a topoisomerase that relaxes supercoiled DNA; however, the activities of these enzymes are more complex than this and a comprehensive explanation of topoisomerases including gyrase, topo IV and the mechanism of DNA manipulation is given in Chapter 5 of this thesis.

These enzymes have been well studied and assays have been developed that can monitor and determine the topology of DNA after incubation with these enzymes, allowing inhibition of their activities to be determined and crudely quantified. The different topologies of DNA and the effects of gyrase and topo IV on DNA are shown in **Figure 4.8**. Assays to measure the inhibition of topo IV relaxation or gyrase supercoiling use the same principle of incubating the topoisomerase enzymes with a DNA substrate (supercoiled for topo IV and relaxed for gyrase) in the presence of potential inhibitors. DNA is extracted and separated on a 1 % TAE agarose gel in the absence of ethidium bromide (EtBr) which is excluded as it has DNA intercalating properties which would interfere with the topology of the DNA. In the presence of a gyrase inhibitor DNA remains in a relaxed state and conversely, in the presence of a topo IV inhibitor DNA remains in its supercoiled form.
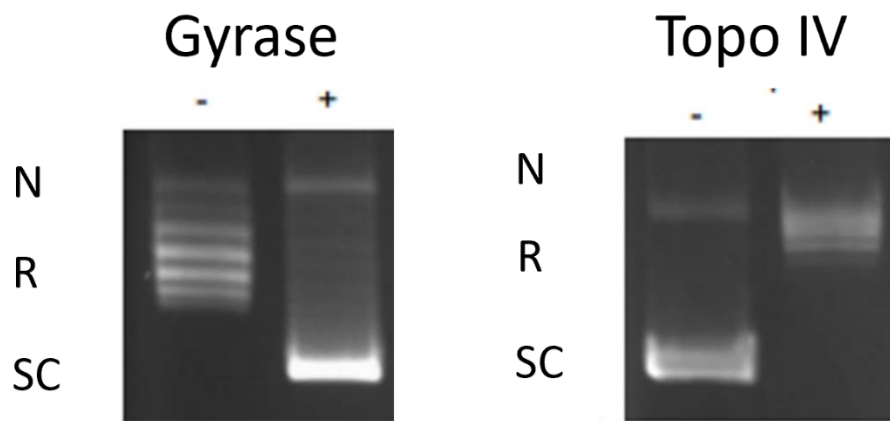
Figure 4.8 DNA topologies as determined by gel electrophoresis on a TAE 1% agarose gel run in the absence of EtBr. – no enzyme, + enzyme added, N; nicked DNA, R; relaxed DNA, SC; supercoiled DNA. Gyrase converts relaxed DNA to the supercoiled form and topo IV converts supercoiled DNA into its relaxed form.
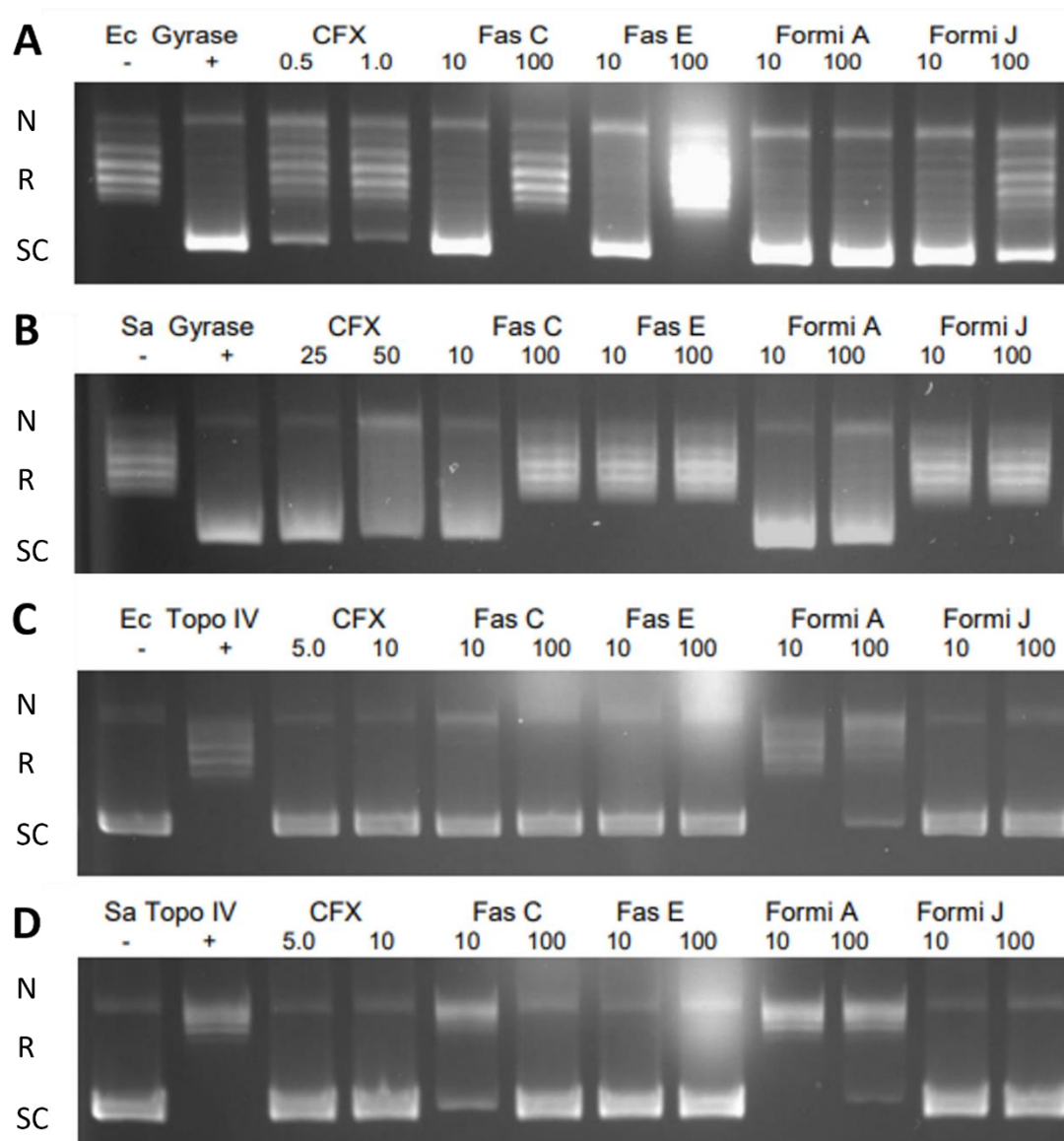
Figure 4.9 Supercoiling (gyrase) and relaxation (topo IV) assays in the presence of ciprofloxacin (CFX), fasamycin (C and E) and formicamycin (A and J). – no enzyme, + enzyme added, N; nicked DNA, R; relaxed DNA, SC; supercoiled DNA. Concentrations of compounds are expressed in μM. Experiments conducted by Inspiralis (UK).

To investigate if fasamycins or formicamycins inhibit topoisomerases, several congeners of both were sent to Inspiralis (Norwich Research Park) for preliminary biochemical assays. Two concentrations (100 μM and 10 μM) of fasamycin congeners (C and E) and formicamycin congeners (A and J) were assayed for inhibitory activity against topo IV and gyrase, from *E. coli* and *S. aureus*.

Gyrase and topo IV from both *E. coli* and *S. aureus* were incubated in assay buffer in the presence of plasmid DNA (supercoiled pBR322 in the case of topo IV and relaxed pBR322

for gyrase) and either 10 or 100 µM of a fasamycin or formicamycin congener, DMSO (inhibitor vehicle control) or ciprofloxacin (5 or 10 µM). Assays were incubated at 37°C for 30 minutes before the assay was stopped with STEB reagent and chloroform/isoamyl alcohol. To recover DNA, assays were centrifuged and the aqueous layer containing DNA was ran on a 1 % TAE agarose gel, gels were stained in EtBr before being visualised by UV and topology of DNA was determined.

As shown in **Figure 4.9A**, fasamycin C and E inhibit *E.coli* gyrase at 100 µM as shown by the complete absence of supercoiled DNA; neither of the formicamycin congeners inhibit this enzyme as *E.coli* gyrase was able to convert relaxed DNA to a supercoil state. Fasamycin E and formicamycin J both inhibited *S. aureus* gyrase at the lowest concentration tested (10 µM) (**Figure 4.9B**). Formicamycin A and fasamycin C however, showed little to no inhibitory activity against *E. coli* or *S. aureus* gyrase. These results confirm that both compounds can inhibit at least one of the gyrase enzymes *in vitro* but also indicate that there is a difference in inhibitory activity between *E. coli* or *S. aureus* gyrase enzymes.

Both fasamycin congeners (C and E) and formicamycin J completely inhibited the action of *E. coli* topo IV to relax the supercoiled DNA at both 100 and 10 µM as indicated by the presence of supercoiled DNA (**Figure 4.9C**). Similarly, fasamycin E and formicamycin J completely inhibit the relaxation activity of *S. aureus* topo IV at both concentrations tested (**Figure 4.9D**). Fasamycin C was a less potent inhibitor of *S. aureus* topo IV in comparison to fasamycin E and formicamycin as complete inhibition of topo IV activity was only observed at 100 µM. As with gyrase, formicamycin A had little effect on either *E. coli* or *S. aureus* topo IV.

These results show that some fasamycin and formicamycin congeners inhibit both topo IV and gyrase *in vitro*, especially in the case of the *S. aureus* enzymes. To further characterise the inhibitory activity of our compounds against gyrase and topo IV specific inhibitory concentrations were determined for one gyrase and topo IV enzyme.

4.2.6 Fasamycin and formicamycin display inhibitory activity against a range of topoisomerases

To determine the extent of the inhibitory activity of fasamycin and formicamycin against topo IV and gyrase in our own hands, relaxation and supercoiling assays using a sub-set

of fasamycin and formicamycin congeners were undertaken to determine the concentration of fasamycin and formicamycin that inhibits 50% of the supercoiling or relaxation activity of gyrase and topo IV respectively which is defined as the half maximal inhibitory concentration (IC_{50}). Going forward we decided to use *E. coli* topo IV and *S. aureus* gyrase so that detailed analysis could be undertaken across two different species. Topo IV was purified from *E. coli* K12, (described in Chapter 5) and *S. aureus* gyrase was purchased from Inspiralis. Supercoiling and relaxation assays were conducted using the same methods that were used above for the initial screening but using an extended concentration range of fasamycin and formicamycin compounds.
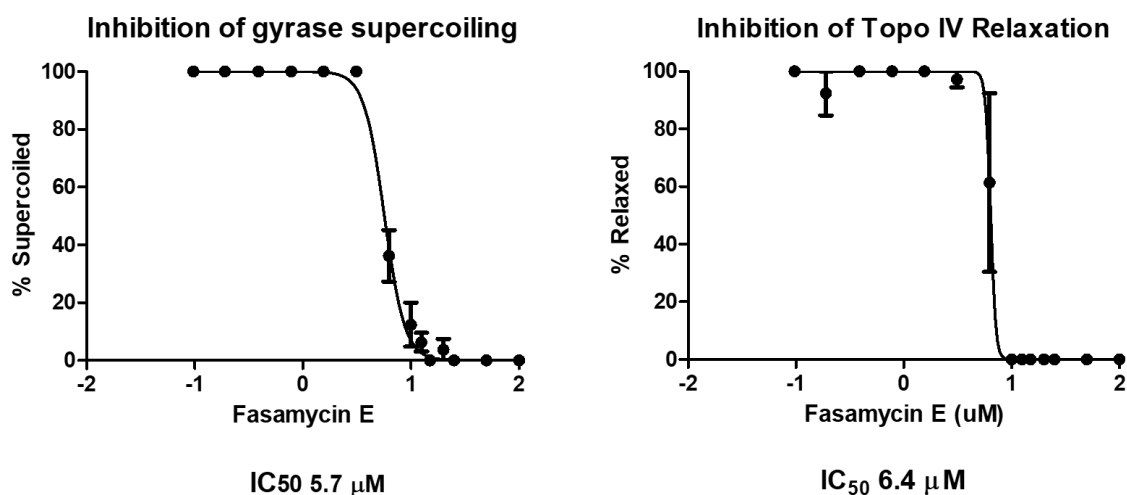
Figure 4.10 IC_{50} curves for fasamycin E determined from triplicate supercoiling (*S. aureus* gyrase) and relaxation (*E. coli* topo IV) assays. Error bars represent standard deviation from biological triplicates.

Three congeners of fasamycin (C, E and L) and formicamycin (A, I and J) were subjected to IC_{50} determination. Compounds were titrated in a serial dilution (100 – 0.1 µM) into both the *E. coli* topo IV and *S. aureus* gyrase assays. IC_{50} curves were plotted from the resulting gels by quantifying the different topologies of DNA as a percentage of total DNA on the gel and IC_{50} values were determined using GraphPad prism software, an example of IC_{50} curves for fasamycin E are shown in **Figure 4.10**. Representative examples of supercoiling and relaxation assays are shown in **SI Figures 6 and 7**.

Determined IC$_{50}$ values for all enzymes are shown in **Table 4.3**. All fasamycin congeners tested exhibited inhibitory activity toward both topo IV and gyrase, with fasamycin C exhibiting the highest IC$_{50}$ values (25.5 µM – topo IV and 23.3 µM – gyrase) and therefore determined to be the least active at inhibiting these enzymes. Fasamycins E and L showed at least 2-fold inhibitory activities towards both gyrase (fasamycin E - 5.7 µM, fasamycin L - 4.7 µM) and topo IV (fasamycin E - 6.4 µM, fasamycin L - 9.2 µM) in comparison to fasamycin C (**Table 4.3**).

Formicamycin A showed no inhibitory activity towards either enzyme at any concentration tested in this experiment whereas formicamycins I and J displayed potent activity against both enzymes; formicamycin J was determined to be the more potent inhibitor of both *E.coli* topo IV (6µM vs 11.3 µM) and *S. aureus* gyrase (7.1 µM vs 11.1 µM). Overall, the fasamycin congeners tested in this experiment were more potent towards *S. aureus* gyrase whereas formicamycins showed similar inhibitory activity to both enzymes. Overall, the fasamycin congeners are better inhibitors of the gyrase and topo IV enzymes tested here than the formicamycins.

Table 4.3 IC$_{50}$ determinations of fasamycin (C,E and L) and formicamycin (A, I and J) congeners against topo IV, gyrase and topo VI and human topo II. – Not determined. IC$_{50}$ values are determined from at least duplicate experiments.

	IC$_{50}$ (µM)				
	E. coli Topo IV	*S. aureus* gyrase	*M. mazei* Topo VI	Human Topo IIα	Human Topo IIβ
Fasamycin C	25.5	23.3	-	-	-
Fasamycin E	6.4	5.7	3.4	26.2	50
Fasamycin L	9.2	4.7	-	-	-
Formicamycin A	> 100	> 100	-	-	-
Formicamycin I	11.3	11.1	-	-	-
Formicamycin J	6	7.1	11.9	>100	>100
Ciprofloxacin	1.7	3.2	-	-	-

Next, an analysis of three other topoisomerase enzymes was undertaken with a representative fasamycin (E) and formicamycin (J) congener. In Chapter 3 of this thesis, it is shown that both fasamycin and formicamycin show potent bioactivity toward two archaeal species *N. viennesis* EN76 and *Ca. n. franklandus* C13. These archaeal species do not encode the FAS-II pathway but they do encode topoisomerases which suggests these are inhibited by fasamycins and formicamycins. We had at our disposal the purified archaeal *M. mazei* topoisomerase VI (topo VI), which was purified by Adam Allen (JIC). Topo VI is made up in A_2B_2 heterotetramer of two Top6A and two Top6B subunits and is a type II topoisomerase found predominantly in plants and in some single celled organisms, including some archaea (Nichols, DeAngelis et al. 1999). The function of topo VI is predominately to separate two-topologically linked daughter chromosomes (decatenate) and relax DNA in archaea by the generation of ds DNA breaks, making the activities of this enzyme essential (Bergerat, Gadelle et al. 1994).

In vitro assays conducted by Adam Allen (JIC) were undertaken with *M. mazei* topo VI. Assays were conducted using the same methods documented above and IC_{50}s were determined (**SI Figure 8**). Both compounds displayed inhibitory activity toward topo VI, but fasamycin E was determined to be a more potent inhibitor than formicamycin J (3.4 and 11.9 µM respectively, **Table 4.3**). Although the topo VI enzyme tested comes from a different archaeal species than those tested *in vivo*, these results support the hypothesis that *in vivo* archaeal inhibition may be due to inhibition of topoisomerases.

Human topoisomerase II enzymes α and β differ from the type II topoisomerases from bacteria as they are encoded by a single gene (TOP2A and TOP2B) in comparison to the dual subunit structure of topo IV and DNA gyrase (Lang, Mirski et al. 1998). However, both enzymes utilise double strand DNA breaks to change the topology of DNA and are thus classed as type II enzymes (Roca, Berger et al. 1996). Both enzymes (topo IIα and topo IIβ) have roles within chromosome condensation, chromatid separation, transcription and replication, the main difference between these enzymes is that the α form localises to chromosome 17 whereas the β form localises to chromosome 3. Additionally, both enzymes are validated targets for anti-cancer therapies however, the most clinically useful antibiotics have a higher selectivity towards bacterial topoisomerases in comparison to the human topoisomerases, to limit toxicity to the user.

Human topoisomerase proteins were purchased from Inspiralis (UK) and preliminary relaxation assays were conducted as described previously but in the presence of 4 concentrations of fasamycin E and formicamycin J (100, 25, 10 and 1 µM). Resulting DNA was subjected to electrophoresis and DNA topology was determined, gels were then used to crudely determine an IC_{50} value (**Figure 4.11**).
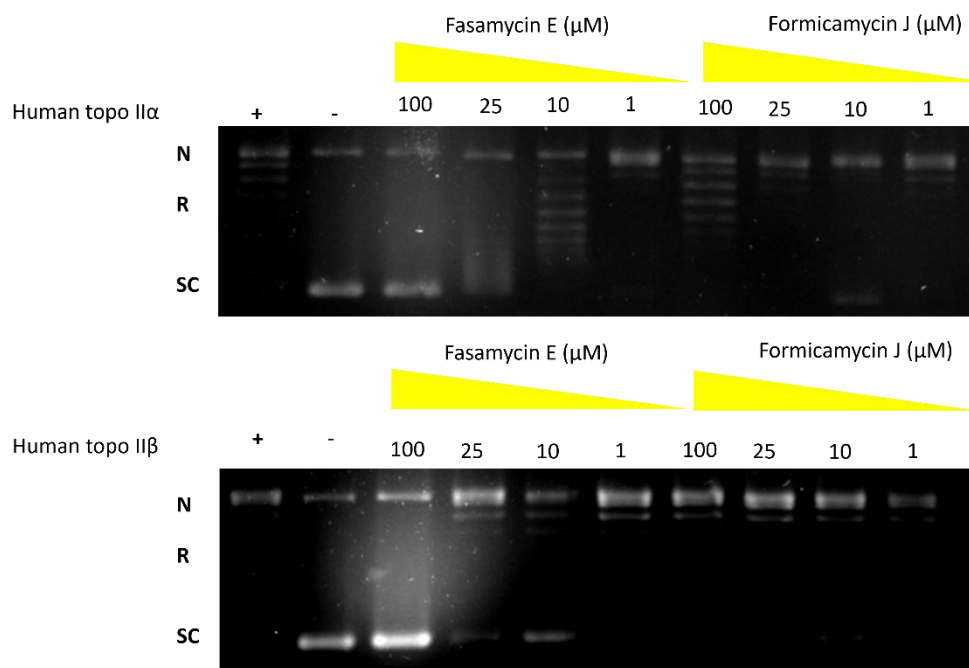
Figure 4.11 Effect of fasamycin E and formicamycin J on the ability of human topoisomerase α and β to relax DNA. Extracted DNA was ran on 1% TAE agarose gel. +/- enzyme; N - Nicked DNA; R - Relaxed DNA; SC - Supercoiled DNA.

Fasamycin E was found to weakly inhibit both human topo IIα and human topo IIβ relaxation, (IC_{50} 26.2 and 50 µM respectively, **Table 4.3**) exhibiting higher inhibitory activity toward human topo IIα. In contrast, formicamycin J showed minor inhibitory activity toward topo IIα and no activity toward topo IIβ at the highest concentration tested (100 µM). Both compounds clearly display a preference toward bacterial and archaeal enzymes, fasamycin E shows at least a 4-fold and formicamycin J shows at least a 10-fold higher affinity toward bacterial and archaeal topoisomerases tested in this work. These results for formicamycin J especially, show promising clinical relevance due to the preference toward non-human enzymes. To follow up this preliminary work, experiments should be undertaken with an increased concentration range of compounds, to allow for more accurate IC_{50} determination, and compared to other

bacterial topo II topoisomerase inhibitors (i.e., ciprofloxacin) and human topoisomerase inhibitors (I.e., etoposide).

4.2.7 Gyrase and topo IV inhibition is characteristic of fasamycin and formicamycin congeners

We wanted to understand if this inhibitory activity against gyrase and topo IV was a common feature of all fasamycin and formicamycin compounds. We were also intrigued to understand if any of the lactone intermediates that are produced during the conversion of fasamycin to formicamycin display any inhibitory activity towards these specific topoisomerases. Therefore, a selection of fasamycin, formicamycin and lactone congeners were assayed against *E. coli* topo IV and *S. aureus* gyrase at a single concentration (50 µM) using methods previously described for supercoiling and relaxation assays in this chapter. As only one high concentration was being tested, compounds were only classed as inhibiting if they were able to completely inhibit the action of the enzyme tested. **Table 4.4** shows the inhibitory activities of the compounds tested. Representative examples of supercoiling and relaxation assays are shown in **SI Figures 9 and 10**.

Overall fasamycins and formicamycins show inhibitory activity toward the topoisomerase enzymes. All fasamycin congeners tested showed inhibitory activity to both *E.coli* topo IV and *S. aureus* gyrase. Formicamycin congeners, however, showed a preference for activity against *E. coli* topo IV in comparison to *S. aureus* gyrase as inferred by half of the formicamycin congeners tested not displaying any inhibitory activity against *S. aureus* gyrase whilst exhibiting activity toward *E. coli* topo IV. Furthermore, none of the lactone intermediate compounds tested showed complete inhibitory activity against either enzyme at 50 µM.

Table 4.4 Inhibitory activities of fasamycin, formicamycin and formicalactone congeners against *E. coli* topo IV and *S. aureus* gyrase. +; inhibitory activity, -; no inhibitory activity

| Compound (50 µM)	*E. coli* topo IV	*S. aureus* gyrase
Formicamycin A	-	-
Formicamycin B	-	-
Formicamycin C	+	-
Formicamycin D	+	-
Formicamycin E	+	-
Formicamycin G	+	+
Formicamycin H	+	+
Formicamycin I	+	+
Formicamycin J	+	+
Formicamycin R	+	+
Formicamycin S	+	+
Formicamycin T	-	-
Formicamycin W	+	-
Fasamycin C	+	+
Fasamycin E	+	+
Fasamycin F	+	+
Fasamycin L	+	+
Fasamycin M	+	+
Fasamycin N	+	+
Fasamycin O	+	+
Fasamycin P	+	+
Lactone A	-	-
Lactone B	-	-
Lactone D	-	-
Lactone E	-	-
Lactone F	-	-
Lactone G	-	-
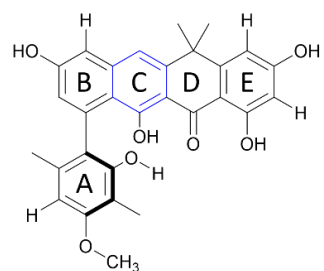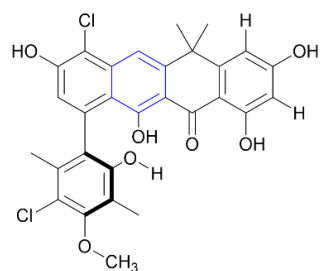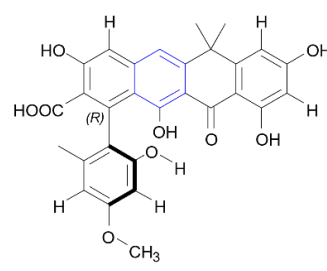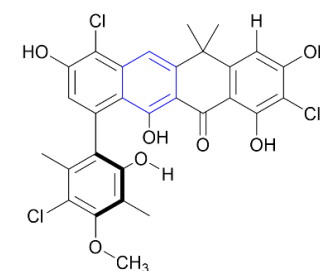
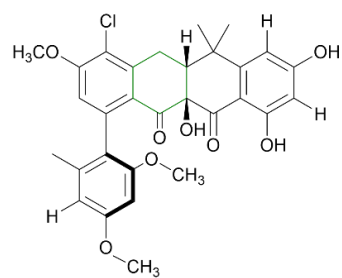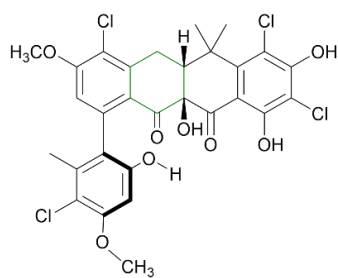Fasamycin C   Fasamycin E   Fasamycin F   Fasamycin L
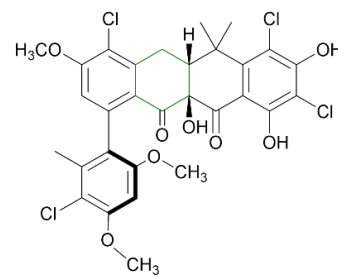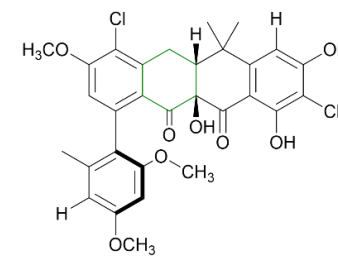
Formicamycin A   Formicamycin I   Formicamycin J   Formicamycin T

Figure 4.12 2D structures of several fasamycin (C, E, F and L) and formicamycin (A, I, J and I) congeners including labelling of compound rings.

These results, taken together with the IC_{50} determinations, can allow us to draw some conclusions on how the structures of these compounds may be affecting the inhibition of topoisomerase enzymes. Structures of fasamycin and formicamycin congeners discussed below are shown in **Figure 4.12**.

We can conclude that chlorination of the fasamycin backbone is not essential for the inhibitory activity seen against these enzymes as both fasamycin C and fasamycin F are able to inhibit the supercoiling and relaxation activities of *S. aureus* gyrase and *E.coli* topo IV respectively. However, fasamycin C has the weakest activity against these enzymes as shown by IC_{50} determination in comparison to the chlorinated fasamycins E and L, which may indicate that although chlorination of fasamycin is not essential for inhibitory activity, chlorination appears to aid in the potency of fasamycin inhibition of topoisomerases, a phenomenon which is also seen in terms of biological activity (discussed in Chapter 3).

As fasamycin E and fasamycin L, both of which show similar IC_{50} values, have chlorination on different rings of the fasamycin structure, it is hard to determine if the regiochemistry of these atoms is important for topoisomerase inhibition. Furthermore, fasamycin F, a non-halogenated fasamycin congener with a carboxylic acid group on C24 of the B ring, shows little to no biological activity and yet exhibits inhibitory activity towards both enzymes indicating that although the carboxylic acid group abolishes bioactivity, the positioning of this group on the B ring may not interfere with the fasamycin-topoisomerase interaction implying that the B ring may not be important in topoisomerase binding.

Formicamycin A and T show no inhibitory activity towards either topoisomerase enzyme however no obvious structural similarity between these two compounds that may be responsible for the lack of activity has been determined. Overall, formicamycins appear to display slightly less activity toward topoisomerases than fasamycins which we hypothesise may be due to the 3D structural differences between the two classes of compounds. Fasamycins have a more planar structure than that of the formicamycins, which display a twisted structure due to their chiral centres. The relatively planar structure of fasamycins is also a feature of several topoisomerase inhibitors such as

doxorubicin and mAMSA (**Figure 4.13**) and therefore may aid in the binding of the compound to a pocket on topoisomerases (Yang, Teves et al. 2014).
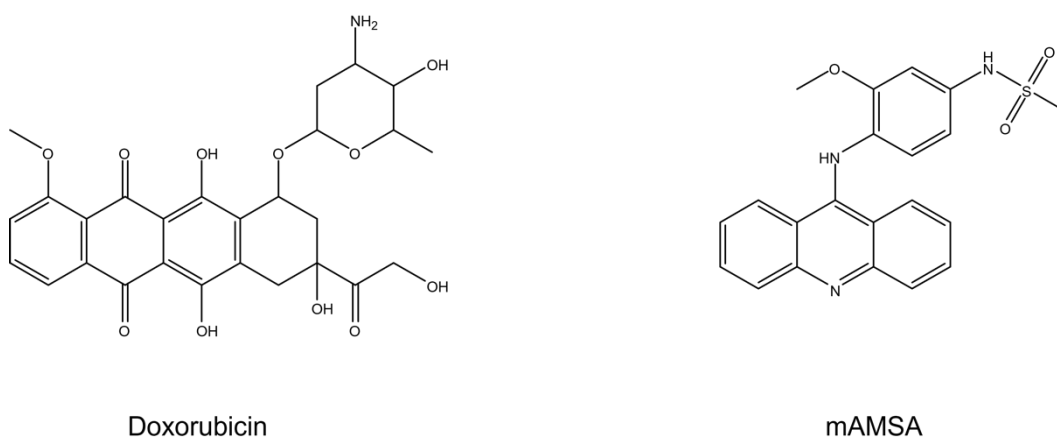
Doxorubicin   mAMSA

Figure 4.13 Structures of planar DNA gyrase inhibitors doxorubicin and amsacrine.

4.3 Discussion

As discussed in Chapter 1, the antibiotic pipeline has been diminishing over the last 60 years meaning that any new antibiotic is valuable, but antibiotics with novel targets or mechanisms of inhibition and a high barrier to resistance should be given priority for development.

The work in this chapter has determined that both fasamycins and formicamycins show an incredibly high barrier to resistance against *S. aureus* strains as well as being unsuccessful at generating resistance across several different bacterial strains using conventional methods. However, using a series of techniques we have shown that both compounds show indications of inhibiting the essential fatty acid synthesis pathway, concurring with what is stated in the literature, as well as inhibiting type II topoisomerases which has not been reported before. We show that over-expressing the individual genes of the FAS-II pathway, including FabF, does not lead to significant resistance to our compounds, a finding that contradicts published reports. However, we hypothesise that this lack of resistance seen by over-expression of the FAS-II genes is due to the inhibition of the second target. If fasamycins and formicamycins are indeed inhibiting multiple biological targets *in vivo* then this could explain why resistance to either fasamycin or formicamycin has not been observed; multiple biological targets has proven to be the cause of lack of resistance with several characterised compounds such as the synthetic antibiotic SCH 79797 which inhibits folate metabolism and bacterial

membrane integrity in tandem (Martin, Sheehan et al. 2020). Although several dual-targeting antibiotics are reported in the literature, the majority are synthetic or semi-synthetic compounds. A search of the literature indicates that there are no examples of natural product derived dual-targeting antibiotics. If fasamycin and formicamycin do indeed inhibit two *in vivo* targets involved in different cell processes; this may be a novel report in the literature.

The results reported in this chapter identify topoisomerases as a target of both fasamycin and formicamycin. Both sets of molecules are inhibitors of bacterial topo IV relaxation and gyrase supercoiling activities as well as exhibiting inhibitory activity toward archaeal topo VI. Compounds that can inhibit both gyrase and topo IV at approximately equimolar concentrations are referred to as dual-targeting antibiotics such as the synthetic ULD1 and ULD2 compounds (Nyerges, Tomašič et al. 2020). Although we have not confirmed that our compounds can inhibit both gyrase and topo IV at the same time *in vivo*, we have shown that both classes of compounds have the ability to inhibit both gyrase and topo IV from *S. aureus* in biochemical assays. Furthermore, we know that archaea do not synthesise fatty acids, they instead favour isoprenoid lipids, and therefore we know that the bioactivity of fasamycin against archaea is not due to inhibition of the FAS-II pathway. We have shown that our compounds inhibit one of the types of topoisomerases (topo VI) encoded by archaea, in vitro. These data support our hypothesis that topoisomerase inhibition is a true *in vivo* mechanism of inhibition of fasamycin and formicamycin.

Further support of this multiple target theory stems from the fact that the IC_{50} values determined *in vitro* for the individual enzymes are equal to or higher than that of the MIC values determined in Chapter 3 (**SI Table 1**), generally IC_{50} values *in vitro* are much lower than MICs as the compound has direct access to its target, we therefore hypothesise that inhibition of multiple targets is the cause for lower MICs in comparison to determined IC_{50}s due to the fact that that the topoisomerases appear to be valid *in vivo* targets due to the results of the reporter and RNA sequencing experiments.

The biochemical assays reported here show that fasamycin and formicamycin compounds display a higher affinity for the prokaryotic topoisomerases tested in this study in comparison to the human enzymes. Formicamycin J appears to specifically

inhibit bacterial and archaeal topoisomerases in comparison to the human topoisomerases, which further increases the attractiveness of these compounds for clinical development. Fasamycin E has some inhibitory activity toward human topo IIα and to a limited extent toward topo IIβ. However, fasamycin E having some inhibitory effects on human topoisomerases is not the end of potential clinical development; several clinically used antibiotics such as gemifloxacin also show some inhibitory activity toward these enzymes but have a higher affinity for bacterial topoisomerases (Fief, Hoang et al. 2019). Furthermore, many antineoplastic (cancer) therapies are compounds that target and inhibit human topo IIα. The most valuable of these drugs selectively inhibit human topo IIα in comparison to human topo IIβ. Fasamycin E has a higher affinity for topo IIα and therefore may prove to be a useful basis for potential anti-cancer therapeutics (Nitiss 2009). However, only one congener of fasamycin and formicamycin was tested against these human enzymes and therefore more congeners should be tested to see if any of the fasamycin congeners show no activity toward the human topos.

To continue this research the mechanism of inhibition of the topoisomerase enzymes needs to be identified and fatty acid inhibition needs to be verified, e.g., using biochemical assays and structural studies.

5.0 Investigating the mechanism of topoisomerase inhibition by fasamycins and formicamycins
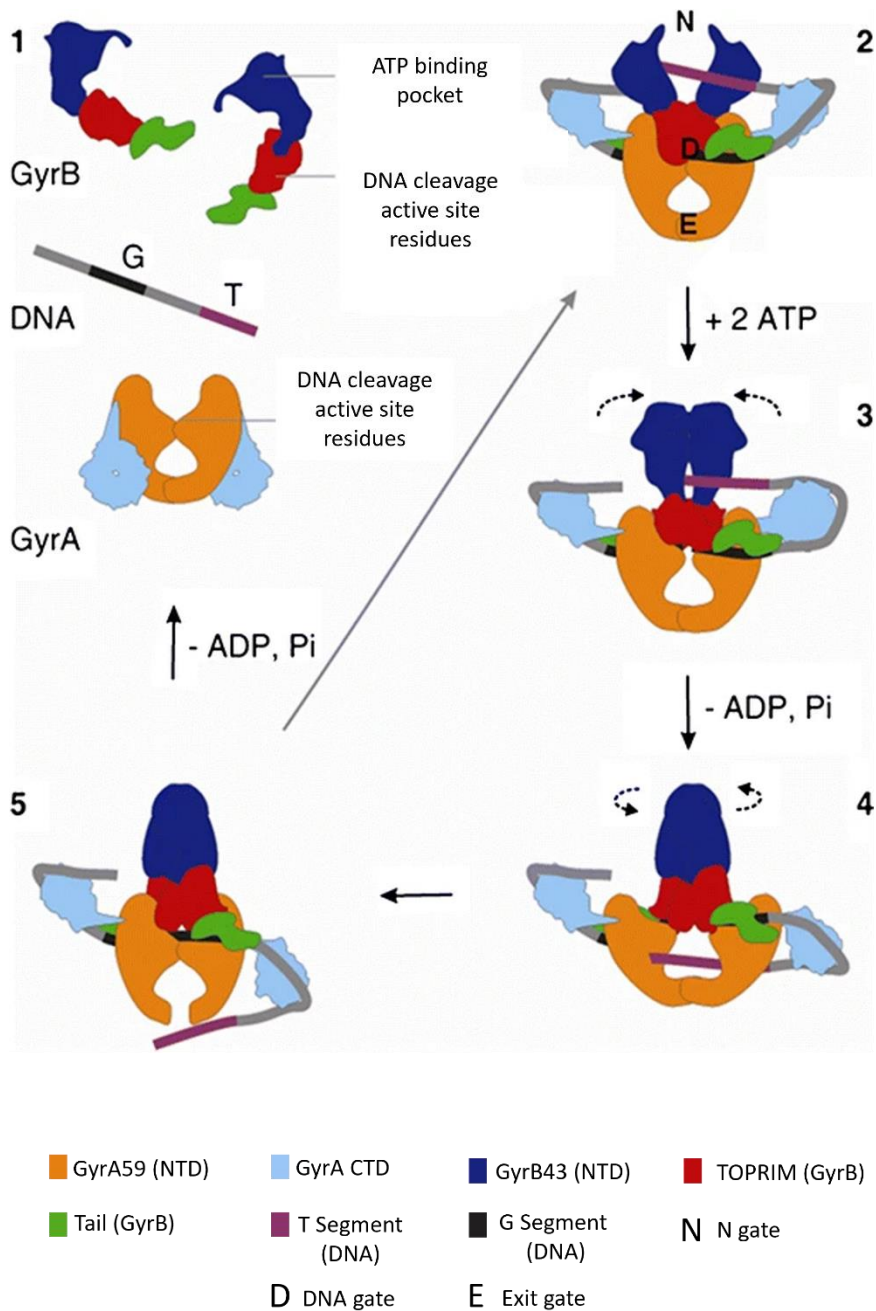
5.1 Introduction

5.1.1 DNA gyrase and topoisomerase IV

DNA topoisomerases are fundamental for manipulating and maintaining DNA topology, making them ubiquitous enzymes essential for all living organisms (Bates and Maxwell 2005). Although most topoisomerases (topos) perform a similar function, interconverting DNA topological states via DNA breakage mediated by a phosphotyrosyl linkage to the DNA backbone, the mechanism by which this is orchestrated is dependent upon the class of enzyme. There are two main types of topos, type I and type II, which are characterised by the ability to generate single stranded (ss) DNA breaks and double stranded (ds) DNA breaks respectively (Liu, Liu et al. 1980). The work in this chapter predominately focuses on two type II topoisomerases, DNA gyrase and topoisomerase IV (topo IV) which are predominately found in bacteria.

Gyrase and topo IV are attractive antimicrobial targets as they are absent in humans and play a fundamental role in the bacterial cell (Bradbury and Pucci 2008, Buzun, Bielawska et al. 2020). DNA gyrase was discovered in 1976 and is predominately found in bacteria, some plants and archaea (Gellert, Mizuuchi et al. 1976). The functional enzyme is comprised of two protein subunits GyrA (97 kDa, *E. coli*) and GyrB (90 kDa, *E.coli*) in an A_2B_2 complex. In simple terms the GyrA subunit is responsible for DNA interactions and cleavage, and GyrB is an ATPase which catalyses the hydrolysis of ATP to ADP to provide energy for the enzymes activity (Reece and Maxwell 1991). Similarly, topo IV, which was discovered in 1990, is made up of two subunits ParC (84 kDa, *E.coli*) and ParE (70 kDa, *E.coli*) with ParC being homologous to GyrA and ParE to GyrB (Kato, Nishimura et al. 1990). Although the enzymes exhibit high homology to each other, their roles in the cell are different; DNA gyrase introduces negative supercoils into DNA, relaxes positive supercoils, decatenates DNA in the presence of Mg^{2+} and ATP and relaxes negative

supercoils whereas topo IV is responsible for decatenation (unlinking of the daughter chromosomes) and relaxation of positive or negative supercoiled DNA in bacteria.

5.1.2 Two gate mechanism of type II topoisomerases

GyrA59 (NTD) GyrA CTD GyrB43 (NTD) TOPRIM (GyrB)

Tail (GyrB) T Segment (DNA) G Segment (DNA) N N gate

D DNA gate E Exit gate

Figure 5.1 Two gate mechanism (adapted from Collin et al 2011). 1) Architecture of GyrA, GyrB and DNA. 2) Wrapping activities of gyrase positions the transported (T) segment over the gate (G) segment of DNA. 3) GyrB dimerises in the presence of ATP causing the transient cleavage of the G segment and the capture of the T segment. 4) ATP hydrolysis allows for strand passage to occur and the T segment is transported through the cleaved

G segment. 5) G segment is religated introducing two negative supercoils into DNA. T segment is released and the hydrolysis of a second ATP to ADP resets the enzyme.

The proposed mechanism for dsDNA cleavage by type II topos is called the 'two-gate mechanism' which is explained below and in **Figure 5.1** (Roca and Wang 1992, Roca and Wang 1994, Collin, Karkare et al. 2011). The mechanism relies upon three interfaces of gyrase which can either be in an open or closed conformation; the N-gate which is the N-terminal domain of GyrB, the DNA-gate which comprises of the GyrA-GyrB-DNA interface and lastly the C-terminal area of coiled coils of GyrA which is also referred to as the exit gate. To start the reaction a portion of DNA, referred to as the gate (G) segment interacts with gyrase between the GyrA dimer N-terminus and the topoisomerase primase domain (TOPRIM) of GyrB (Cabral, Jackson et al. 1997). DNA is wrapped around gyrase to form a right-handed supercoil, and this wrapping in turn causes a second segment of the same DNA, called the transported segment (T), to reach the N gate where it is placed above the G segment to prepare for strand passage (Heddle, Mitelheiser et al. 2004). Closure of the N gate takes place in the presence of ATP, which traps the T segment. In turn, to make the dsDNA break, the G segment is cleaved through the formation of phosphotyrosyl bonds 4 bp apart on the DNA resulting in a DNA-GyrA covalent attachment. The T segment passes through the broken DNA G segment (strand passage), which is driven by the hydrolysis of ATP, and through the exit gate. Hydrolysis of a second ATP to ADP resets the enzyme by opening up the N gate. This 'two gate mechanism' is also the proposed mechanism for topo IV mediated dsDNA breakage but unlike gyrase, topo IV does not wrap DNA around itself meaning it cannot supercoil DNA. As these enzymes are critical to any process involving DNA such as DNA replication and transcription, any perturbations in topoisomerase function can lead to unresolved dsDNA breaks and ultimately cell death.

5.1.3 Inhibitors of type II topoisomerases

The essential nature of type II topoisomerases in bacteria makes them incredibly attractive antibacterial targets and therefore a large number of inhibitors have been characterised or synthesised which exhibit different mechanisms of inhibiting these crucial enzymes. A selection of inhibitor classes and their mechanism of action is summarised in **Table 5.1**. The most successful class of DNA gyrase inhibitors are the quinolones, which originate from nalidixic acid, an agent used to treat urinary tract

infections, which was discovered as a synthesis by-product of another compound (the antimalarial chloroquine) (Lesher, Froelich et al. 1962). Successive generations of drug development using the structure of nalidixic acid ultimately led to the discovery of the early quinolones and then the fluroquinolones (Buchbinder and Webb 1962, Koga, Itoh et al. 1980, Davis, Markham et al. 1996). Ciprofloxacin (**Table 5.1**), a second-generation fluroquinolone, is one of the most widely used gyrase inhibitors and can also inhibit topo IV in some organisms, sometimes with greater potency. The inhibitory activities of quinolones are generally attributed to their ability to stabilise the gyrase–DNA (or topo IV-DNA) cleavage complex, making them gyrase poisons. By blocking resolution of the cleavage complex dsDNA breaks are not resolved leading to induction of the SOS response and ultimately cell death (Gellert, Mizuuchi et al. 1977, Sato, Inoue et al. 1986, Bryan, Bedard et al. 1989, Laponogov, Sohi et al. 2009). Ciprofloxacin and other quinolone-based gyrase inhibitors have been used clinically for many years; however, this has led to an inevitable increase in quinolone resistance in pathogenic bacteria which has been extensively studied and is determined by point mutations within specific regions, called the quinolone-resistance-determining regions (QRDRs), in both subunits of gyrase and topo IV. These mutations lead to changes within the protein structure and reducing the ability of the quinolones to bind to the enzyme and stabilise the cleavage complex (Yoshida, Bogaki et al. 1990, Yoshida, Bogaki et al. 1991).

The aminocoumarins are another well studied class of inhibitors and are characterised by the presence of a 3-amino-4,7-dihydroxycoumarin moiety (shown in **Table 5.1**) (Smith, Dietz et al. 1956). The exemplar aminocoumarin, novobiocin was originally isolated from a *Streptomyces* species, *Streptomyces nive*us, and the aminocoumarin scaffold has been subjected to extensive structural elaboration through both chemical synthesis and biosynthetic manipulation (Heide 2009). Similar, to the fluroquinolones, novobiocin has potent antimicrobial activity due to the inhibition of gyrase (and topo IV) but unlike fluoroquinolones, novobiocin acts as a competitive inhibitor of ATP for binding sites on GyrB (Gellert, O'Dea et al. 1976, Sugino, Higgins et al. 1978). However, the mechanism of competitive inhibition by novobiocin (and other analogues) is unusual as these compounds bind in an overlapping binding pocket to that of ATP rather than acting as an ATP mimic (Gilbert and Maxwell 1994). Like fluoroquinolones resistance to

aminocoumarins is also determined by point mutations leading to amino acid changes but in this case to the GyrB binding site.

Like the aminocoumarins, cyclothialidines (**Table 5.1**) are cyclic peptides produced by *Streptomyces* spp. which also target DNA gyrase by binding to GyrB and inhibit ATP hydrolysis through the overlapping of the ATP binding site but generally have little antimicrobial activity *in vivo* due to poor penetration into the cell membrane and thus have had limited potential as a clinical therapeutic in its current form. However, this compound showed incredibly potent inhibitory activities against *E.coli* gyrase *in vitro*, displaying IC_{50} values for up to 29-fold higher activity than the quinolones (Goetschi, Angehrn et al. 1993, Nakada, Gmünder et al. 1995). As the *in vitro* inhibitory activity of this class of compound was so promising, 14-membered lactone analogues were synthesised which possessed potent gyrase inhibitory activity as well as promising antibacterial activity. As would be anticipated resistance determinants to these compounds map to mutations within *gyrB* and are hypothesised to inhibit the cyclothialidines from binding to GyrB.(Stieger, Angehrn et al. 1996).
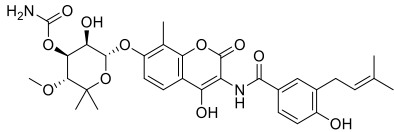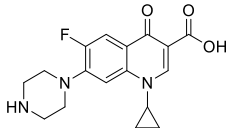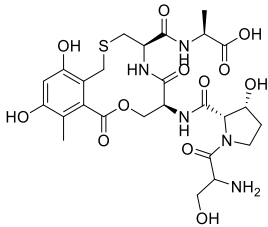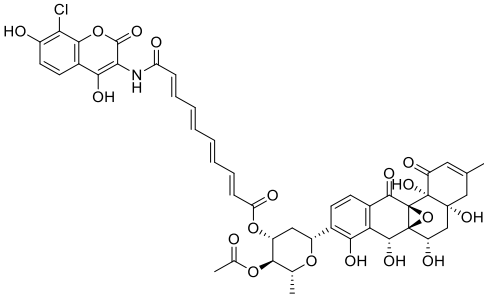
A number of additional inhibitors of gyrase have been reported and include the proteinaceous microcin B17 and CcdB (Miki, Chang et al. 1984, Davagnino, Herrero et al. 1986), the majority of which act as poisons and inhibit gyrase and topo IV through stabilisation of the cleavage complex (Bahassi, O'Dea et al. 1999, Heddle, Blance et al. 2001). A class of inhibitors that do not inhibit gyrase or topo IV through stabilisation of cleavage complexes or competitive inhibition is the simocylinones (**Table 5.1**). These compounds were isolated from *Streptomyces antibioticus* and have an interesting bifunctional chemical structure comprised of distinct aminocoumarin and polyketide moeities (Holzenkämpfer, Walker et al. 2002). Antimicrobial activity of simocyclinones is observed against Gram-positive organisms but not Gram-negative bacteria, although antimicrobial activity can be observed in an *E.coli* strain which has a deficient outer membrane which suggests that the membrane of Gram-negatives impedes the activity of the simocyclinones. Simocyclinones were found to show inhibitory activity toward both *E. coli* and *S. aureus* gyrase supercoiling activity *in vitro* and were determined to inhibit gyrase by interfering with its ability to bind DNA by binding to two separate binding pockets on the N-terminal domain of GyrA (Buttner, Schäfer et al. 2018). Although simocylinones display a novel mechanism of action, resistance can be
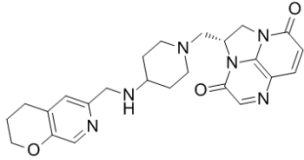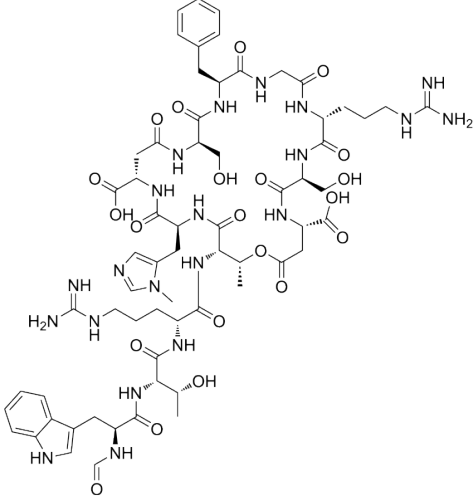
attributed to mutations within the binding site on *gyrA* which impede the ability of SD8 to bind to gyrase (Flatman, Howells et al. 2005). These compounds have met with little clinical success as antibiotics due to their significant inhibitory activities toward human topoisomerase II which leads to significant toxicity. However, this novel mechanism of action could be exploited in the future through the production of new analogues through chemical synthesis or through the biosynthetic engineering of natural products.

There is currently a global need for the discovery of novel antimicrobials, especially those with novel mechanisms of action in order to combat the growing problem of AMR. Despite this gyrase and topo IV are still considered as important targets for the development of new antimicrobials due to their essential nature in microbes and their absence in humans, and any newly discovered synthetic or naturally derived small molecules would be considered useful starting points for antibiotic development.

In Chapter 4 of this thesis, the inhibitory activities of fasamycin and formicamycin on topoisomerase mediated supercoiling and relaxation of DNA have been characterised. Both fasamycin and formicamycin display preferred inhibitory activity against gyrase, topo IV and archaeal topo VI in comparison to type II human topoisomerases, showing promise for further investigation. In this chapter, the mechanism by which they inhibit these enzymes is investigated using a combination of biochemical techniques including DNA topology assays and protein chromatography.

Table 5.1 Classes of different type II topoisomerase inhibitors including details of their origin and mechanism of action.

Class	Example	Structure	Mechanism of action	Origin	Reference
Aminocoumarins	Novobiocin		Competitive inhibition of ATP hydrolysis	Natural – *Streptomyces* spp	(Smith, Dietz et al. 1956)
(Fluoro)quinolones	Ciprofloxacin		Stabilisation of the DNA gyrase cleavage complex and formation of double stranded DNA breaks	Synthetic	(Koga, Itoh et al. 1980, Davis, Markham et al. 1996)
Cyclothialidines	Cyclothialidine		Inhibition of ATPase activity	Natural – *Streptomyces* spp.	(Goetschi, Angehrn et al. 1993)
Simocylinones	Simocylinone D8		Inhibition of topoisomerase – DNA binding	Natural – *Streptomyces* Spp	(Holzenkämpfer, Walker et al. 2002)

| Triazaacenaphthylenes	Gepotidacin		Production of gyrase mediated single stranded DNA breaks.	Synthetic	(Gibson, Bax et al. 2019)
Evybactins	Evybactin		Stabilisation of the DNA gyrase cleavage complex and formation of double stranded DNA breaks. Exhibits a unique mode of entry into *Mycobacterial* cells via transport through the BacA transporter.	Natural - *Photorhabdus noenieputensis*	(Imai, Hauk et al. 2022)

5.2 Results

5.2.1 Purification of Topo IV for mechanism of action studies

In Chapter 4, the *in vitro* inhibitory activities of fasamycin and formicamycin on gyrase and topo IV were characterised with the finding that both compounds showed preferential inhibition toward *E.coli* topo IV as well as both gyrase and topo IV from *S. aureus.* We decided to undertake the mechanistic work documented in this chapter, on topo IV from *E.coli* due to the previously published purification procedures and the relative ease of purification, we also noted that there were limited examples of protein structures of full length *E.coli* topo IV either on its own or in complex with inhibitors. Our ultimate aim of this work for the future is to obtain a cryogenic electron microscopy (Cryo-EM) structure of our compounds, both fasamycin and formicamycin, bound to topo IV.

For the purification of *E.coli* topo IV, DNA sequences for the two subunits ParC and ParE were PCR amplified from *E. coli* K12 and cloned separately into a modified pET28b protein expression plasmid, containing an N-terminal polyhistidine-tag and a C-terminal strep-tag (Trp-Ser-His-Pro-Gln-Phe-Glu-Lys). Plasmids were transformed into the IPTG inducible *E. coli* BL21(DE3) Star strain which is a protein expression host strain designed for enhanced protein stability and yield. Both subunits were subjected to purification by fast protein liquid chromatography (FPLC), using nickel and streptavidin affinity columns before being further purified by anion exchange to reduce contamination of other proteins (**Figure 5.2**). During purification it was noted that ParC requires at least 150 mM NaCl to remain folded, therefore all purification steps had to be undertaken in buffers containing at least 150 mM NaCl. Affinity tags were cleaved from both purified ParC and ParE using TEV and 3C proteases to ensure correct future complex formation.

To generate the active enzyme complex, the two subunits (ParC and ParE) were combined together at an equimolar concentration and subjected to size exclusion chromatography (SEC) to form the topo IV holoenzyme in the A_2B_2 configuration (**Figure 5.2**). Purified holo-topo IV was subjected to relaxation assays to confirm its activity (indicated by 100% relaxation of supercoiled substrate at 12.5 nM).
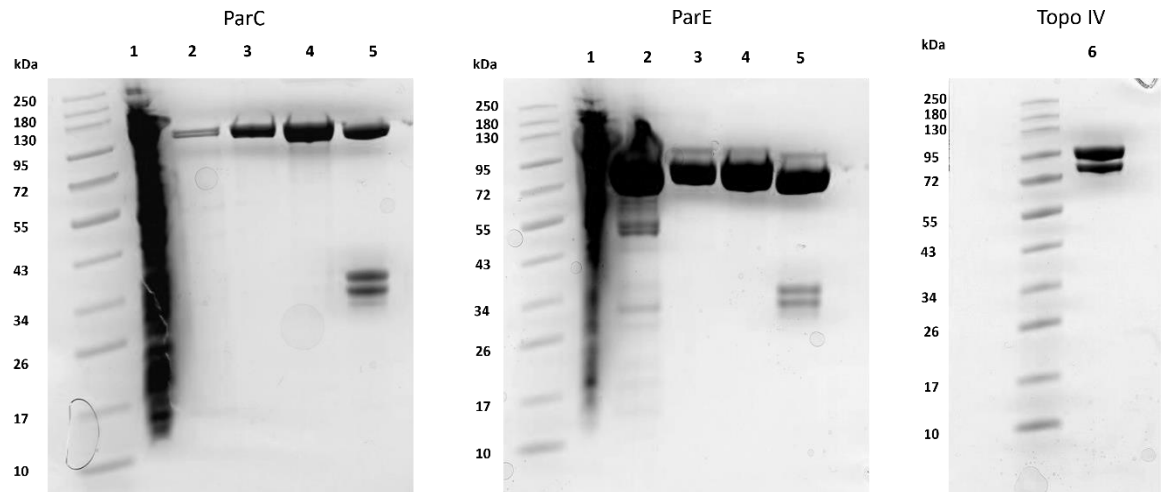
Figure 5.2 SDS page gels of the purification steps of the individual subunits of topoisomerase IV ParC and ParE and the reconstituted A$_2$B$_2$ holoenzyme complex. **1:** Cell lysate; **2**: Nickel(HisTrap) column elution; **3**: Streptavidin (StepTrap) column elution; **4**: Anion exchange column elution; **5**: Post cleavage with TEV and 3C proteases; and **6**: Final purified complex after size exclusion column. Ladder is a 250-10 kDa Color Prestained Protein Standard.

5.2.2 Fasamycin and formicamycin do not stabilise the cleavage complex of topo IV

As discussed in Chapter 4, topoisomerases have been extensively studied since their discovery, and many techniques have been developed to analyse their effect on DNA topology. Some of the most useful techniques are assays developed to analyse the different topological states of DNA after exposure to topos and include cleavage assays which are used in this chapter. Cleavage assays are used to determine if the cleavage complexes of gyrase and topo IV have been stabilised by exposure to a chemical agent whereby they are inhibited from resolving dsDNA breaks leading to an accumulation of linear DNA products.

Cleavage assays involve incubating either supercoiled or relaxed DNA substrates with topoisomerases for e.g., 60 minutes in the presence or absence of inhibitors. Proteinase K and SDS are added to the assay to trap any cleavage complexes and incubated for a further 30 minutes. Assays are stopped by addition of a chloroform/isoamyl alcohol mixture and STEB (40 % (w/v) sucrose, 100 mM Tris-HCl pH8, 10 mM EDTA, 0.5 mg/ml Bromophenol Blue) after which the DNA resulting from the assays are ran on a 1%

agarose TAE gel (1μg /ml EtBr) in TAE buffer containing 1μg /ml EtBr. Linear DNA products arising from inhibition of the cleavage complex are visualised on gels containing EtBr as the presence of a DNA intercalator allows for distinction between relaxed topoisomers and linear DNA to be made, as, in the absence of a DNA intercalator both relaxed and linear DNA resolves at similar places on the gel (**Figure 5.3**).
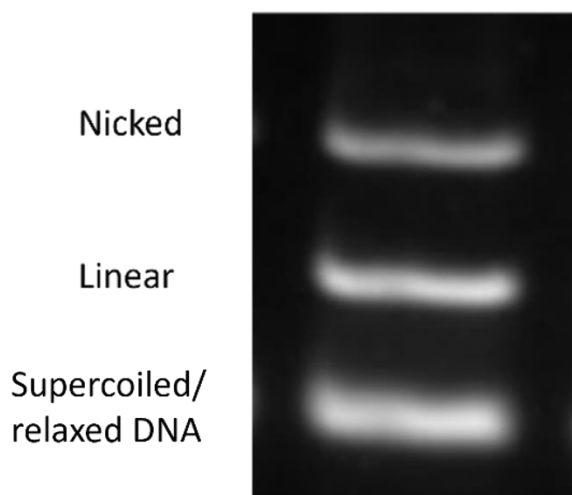
Figure 5.3 Topological states of DNA after cleavage assays as visualised after separation on a 1% agarose TAE gel in the presence of ethidium bromide (EtBr) (1 μg/ml).
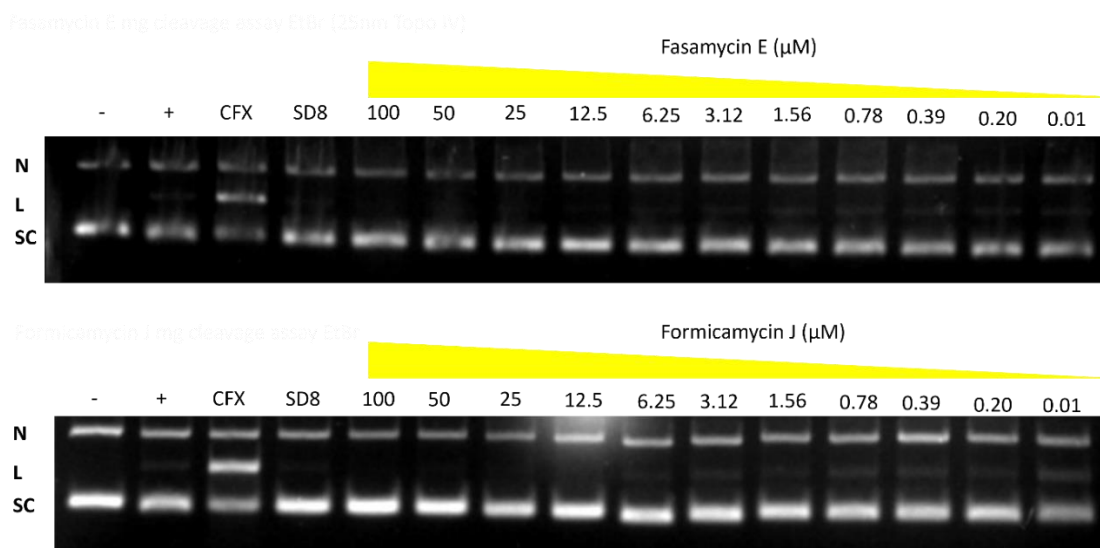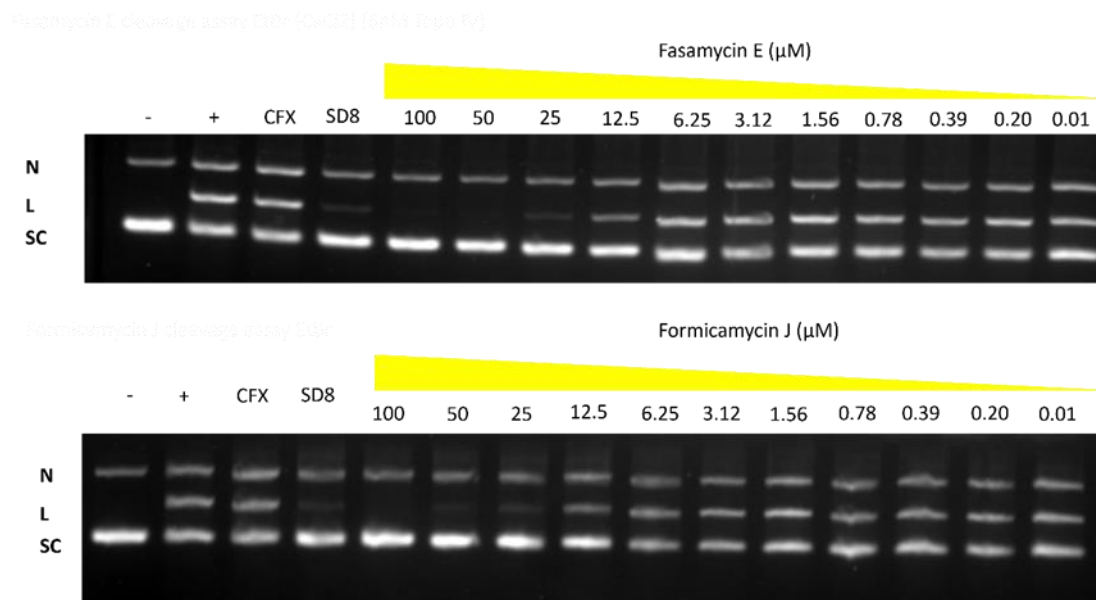

Figure 5.4 DNA cleavage assays run in the presence of decreasing concentrations of fasamycin E and formicamycin J. Extracted DNA was ran on 1% TAE agarose gel (EtBr 1μg/ mL). +/- enzyme; CFX- ciprofloxacin (20 μM) and SD8 (50 μM) used as positive and negative controls respectively; **N** - Nicked DNA; **L** - Linear DNA; **SC** - Supercoiled DNA;

EtBR – ethidium bromide. Neither fasamycin E or formicamycin J show evidence of stalling the cleavage complex and the accumulation of linear DNA at the concentrations tested.

Cleavage assays, in duplicate, were undertaken to determine if fasamycin and formicamycin inhibit topo IV by stabilisation of the cleavage complex as is observed for the fluroquinolones. Topo IV and supercoiled DNA were incubated in the presence of fasamycin E and formicamycin J (100-0.01 µM) before DNA was extracted and ran on a 1% TAE gel (1 µg/ml EtBr). Ciprofloxacin (20 µM), which causes increased levels of ds DNA breaks, due to its mechanism of action, was used as a positive control, and SD8 (50 µM) was used as a negative control as its mechanism of inhibition does not yield ds DNA breaks and linear DNA. As shown in **Figure 5.4**, neither fasamycin E or formicamycin J (up to 100 µM) showed any signs of increased linear DNA accumulation in comparison to the DMSO only control, indicating that these compounds do not inhibit topo IV through the stabilisation of the cleavage complex.

5.2.3 Fasamycin and formicamycin protect DNA from Ca^{2+} mediated topo IV cleavage


Figure 5.5 Ca^{2+} DNA cleavage assays run in the presence of decreasing concentrations of fasamycin E and formicamycin J. Extracted DNA was ran on 1% TAE agarose gel (EtBr 1μg/ mL). +/- enzyme; CFX (20 μM) and SD8 (50 μM) used as positive and negative controls respectively; **N** - Nicked DNA; **L** - Linear DNA; **SC** - Supercoiled DNA; EtBr – ethidium bromide. Both fasamycin and formicamycin protect from dsDNA break formation mediated by topo IV.

During several the studies undertaken for this project it was noted that the inclusion of either fasamycin E or formicamycin J in cleavage assays appeared to reduce the presence of linear DNA products, even under conditions when linear DNA products should be present. This suggested that both compounds may confer a protective effect against the formation of linear DNA, i.e., fasamycin and formicamycin completely inhibit the ability of topo IV to cause ds DNA breaks, and we therefore attempted to determine if this was an actual phenomenon or an artifact of the assay conditions.

One approach to determine if a compound can inhibit the cleavage activity of a topoisomerase is to incubate the enzyme in conditions that encourage these cleavage events. Type II topos require divalent metal ions, such as Mg^{2+} to carry out dsDNA

cleavage (Kato, Suzuki et al. 1992), and replacement of Mg^{2+} with Ca^{2+} stimulates topo IV to induce high levels of cleavage events causing an increased formation of linear DNA products (Pitts, Liou et al. 2011). Cleavage assays, as described above, can be amended by replacing Mg^{2+} with Ca^{2+} in the cleavage assay buffer to encourage topo IV mediated dsDNA break formation. Therefore, to understand if our compounds protect against cleavage mediated ds DNA break formation, fasamycin and formicamycin were titrated into topo IV cleavage assays in a buffer containing Ca^{2+} in replacement of Mg^{2+}, methods were then followed as described for cleavage assays; resulting plasmid DNA was ran on a 1% agarose TAE gel (1µg/ml EtBr), and DNA was visualised by UV. **Figure 5.5** shows that as expected, in the presence of Ca^{2+} topo IV (+ DMSO) mediates the formation of linear DNA products, with approximately 30 % of resulting total DNA recovered being linear (**Figure 5.6A**), Ciprofloxacin (20 µM) exposure also yielded linear DNA products making up approximately 25 % of total recovered DNA (**Figure 5.6A**). DNA taken from SD8 (50 µM) treated topo IV showed a reduction in linear DNA products (< 10 % total DNA) in comparison to DNA recovered from the topo IV (+DMSO) control which was expected as SD8 impedes the ability of topo IV to bind DNA and therefore cleavage cannot take place. Both fasamycin and formicamycin were able to inhibit the formation of linear DNA products in a concentration dependant manner as shown in **Figure 5.6B**. At 50 µM fasamycin and formicamycin almost completely inhibited the formation of linear DNA products (**Figure 5.6A**) indicating that both compounds can protect against Ca^{2+} mediated cleavage. This protective effect of fasamycins and formicamycins could be due to them inhibiting the interaction between topo IV and DNA, as has been shown for SD8.
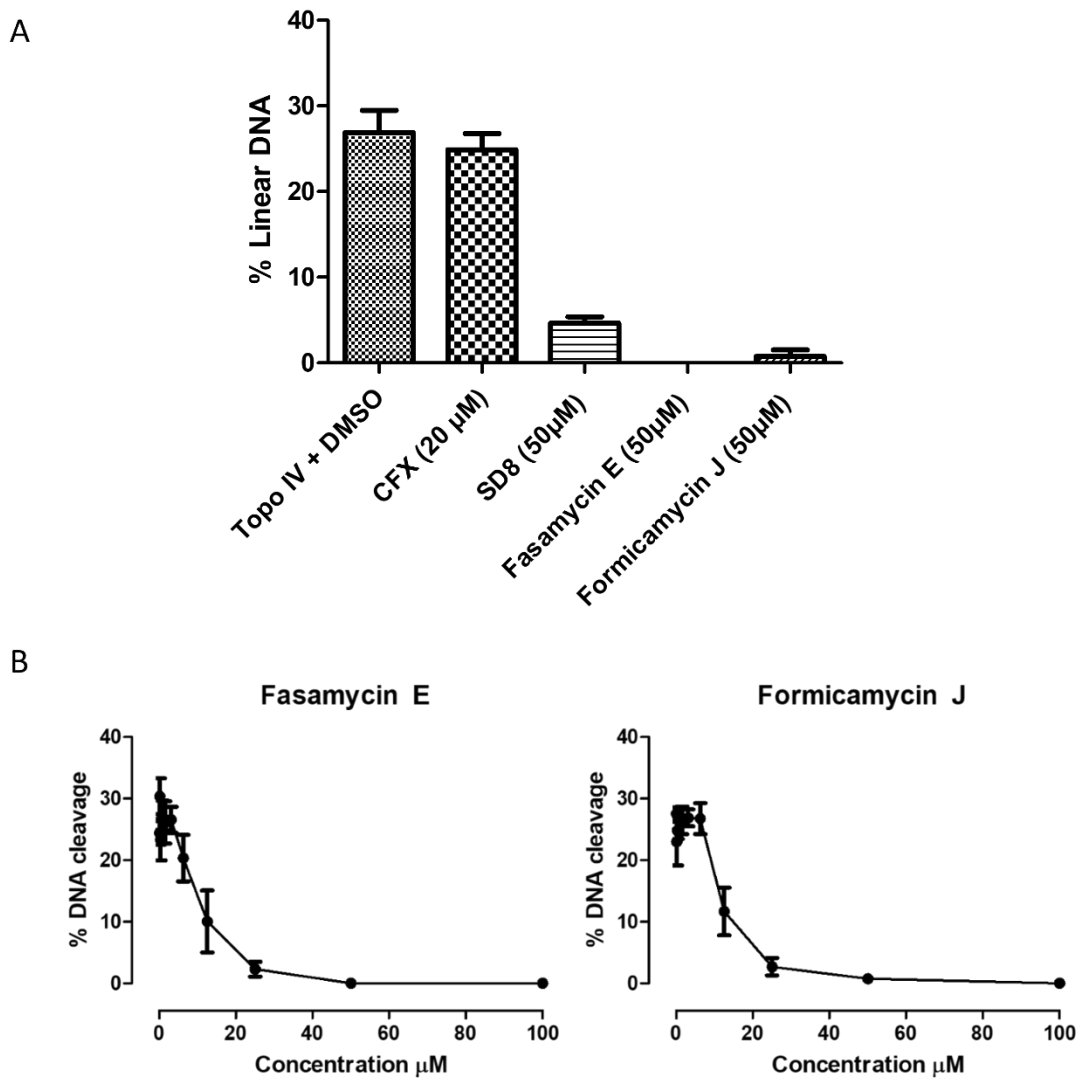
Figure 5.6 Effect of fasamycin and formicamycin exposure on linear DNA products from Ca^{2+} cleavage assays. **A** - Percentage of cleaved DNA in the presence of Ca2+ and either fasamycin and formicamycin, CFX – ciprofloxacin, SD8 – simocylinone. **B** – Analysis of percentage of linear DNA at different concentrations of fasamycin E and formicamycin J exposure during Ca2+ cleavage assays. Data shown is average of duplicate experiments and error bars represent standard deviation.

## 5.2.4 Investigating the ability of fasamycin E and formicamycin J to inhibit topoisomerase-DNA binding
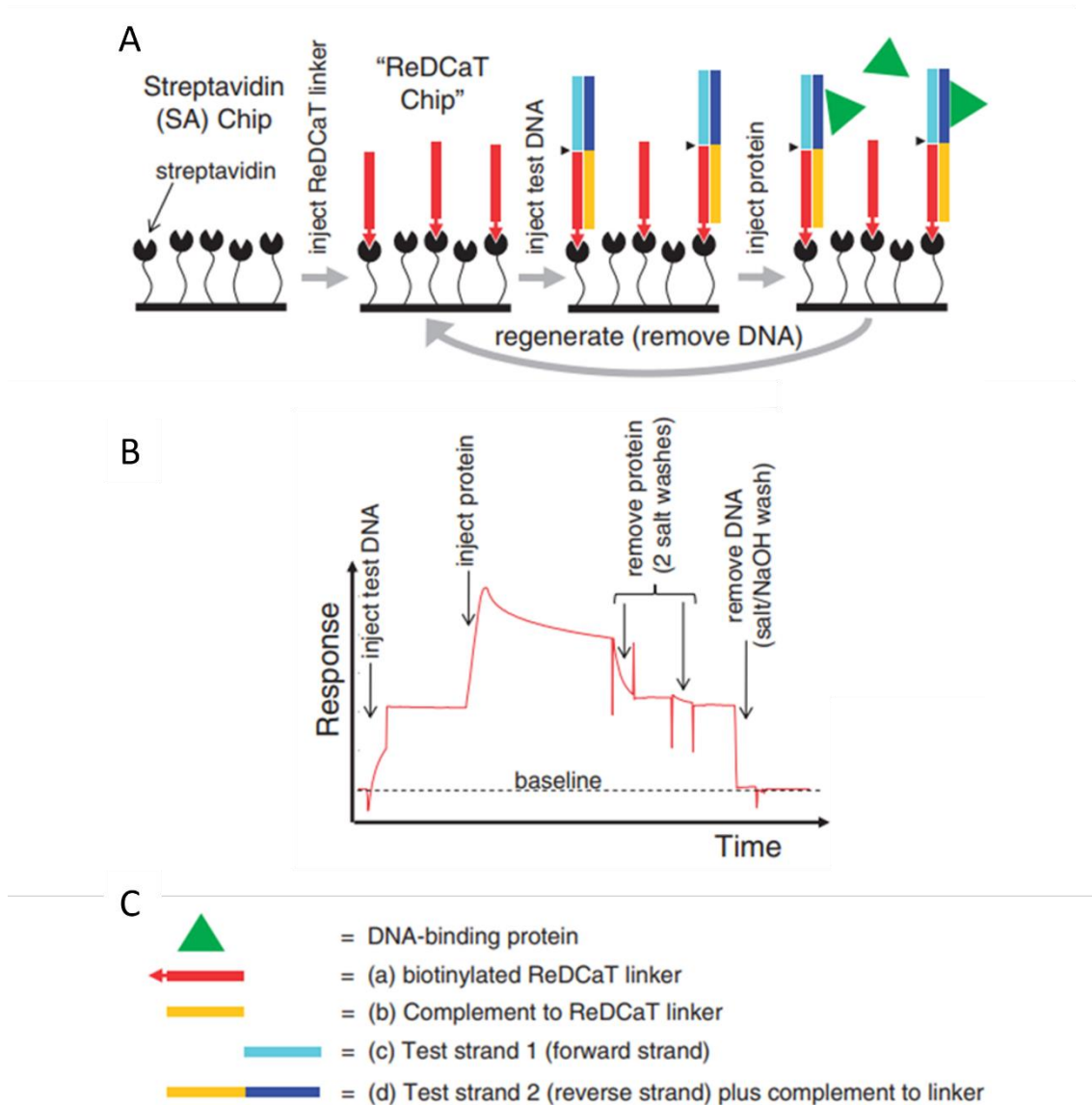
Figure 5.7 Methodology of ReDCaT SPR. **A** – Diagrammatic representation of events taking place in the flow cell of the SPR including DNA binding to the chip and protein binding of bound DNA. **B**- Sensorgram of a protein that binds to immobilised DNA. **C** – Diagram key. (Adapted from Stevenson, Assaad et al. 2013).

Reusable DNA capture technique surface plasmon resonance (ReDCaT SPR) experiments were undertaken to further investigate whether fasamycin E and formicamycin J inhibit the DNA binding activity of topo IV. The ReDCaT SPR method is shown in diagrammatic form **Figure 5.7** and uses a streptavidin chip to bind dsDNA through a biotinylated linker on the reverse strand of DNA. Once DNA is bound to the chip, the protein of interest is

flowed over the bound DNA and a response is recorded if the protein of interest binds to the DNA.

Protein binding in this experiment is expressed as R_{max}, which is defined as the percentage of the maximum response that would be generated if every single piece of immobilised ds DNA on the chip had one protein bound, therefore the R_{max} value can be over 100% if more than one protein unit can bind to one dsDNA unit (Stevenson, Assaad et al. 2013). We theorised that if fasamycin and formicamycin are inhibiting the DNA binding ability of topo IV, then protein (holoenzyme topo IV) in buffer containing either of these compounds should show a reduced affinity for DNA.
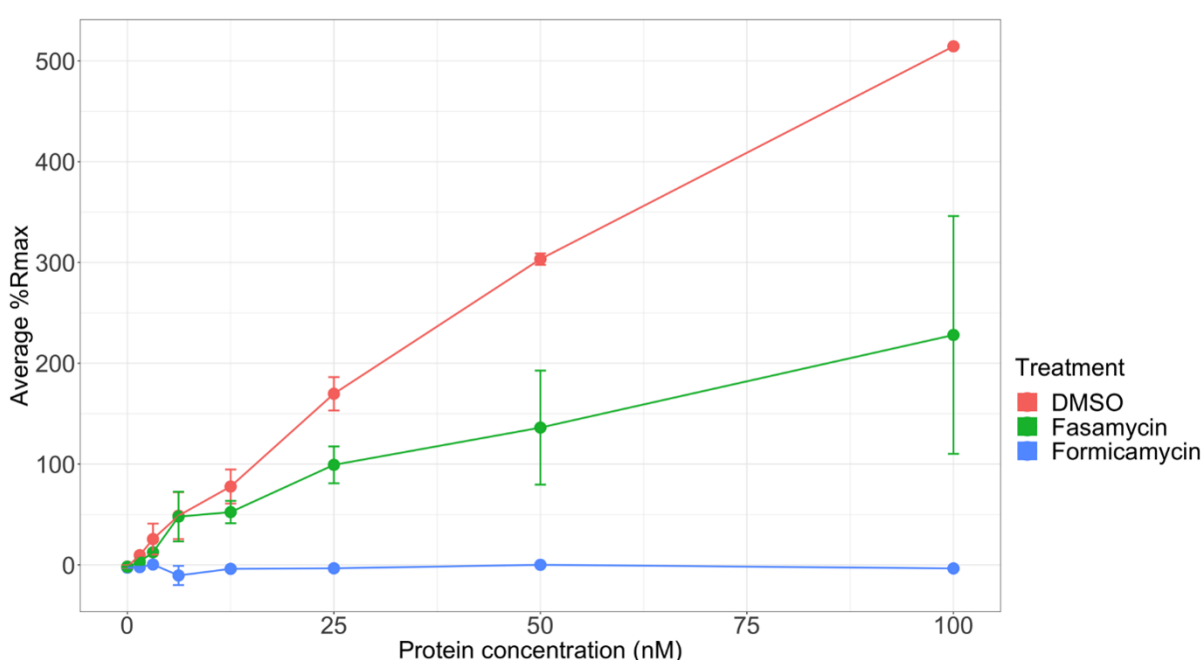
Figure 5.8 Effect of increased protein (topo IV) concentration on DNA binding ability and effect on DNA binding due to addition of fasamycin and formicamycin (both 100 μM). Error bars represent standard deviation from triplicate experiments.

A concentration gradient of holoenzyme topo IV (0, 1, 5, 25, 50 and 100 nM) was flowed over the 34 bp DNA, which had been immobilised onto the streptavidin chip, in HBS-EP+ buffer (150 mM NaCl, 3 mM EDTA, 0.05% (v/v) surfactant P20, 10 mM HEPES (pH 7.4); GE Healthcare) containing either DMSO (inhibitor vehicle control), fasamycin E (100 μM) and formicamycin J (100 μM). As shown in **Figure 5.8**. DMSO treated topo IV displayed a concentration dependant DNA binding response as indicated by the increase in % R_{max} as protein concentration increases. Addition of 100 μM fasamycin E reduced the ability

of topo IV to bind DNA by approximately half at every protein concentration whereas addition of 100 μM formicamycin J completely abolished all DNA binding ability of topo IV at every protein concentration tested. Although these results are preliminary, they indicate that the inhibitory activities of both fasamycin and formicamycin to topo IV may be due to the compounds impeding the ability of topo IV to bind DNA. Further experiments will be needed to confirm this data including determination of IC_{50} values for inhibition of DNA binding in the presence of fasamycins and formicamycins.

5.2.5 Fasamycin and formicamycin do not intercalate DNA

Table 5.2 Degree of intercalation of DNA of fasamycin, formicamycin and mAMSA at different concentrations. − no intercalation, + low intercalation, ++ medium intercalation, +++ high intercalation.

|	Degree of intercalation		
	1 uM	10 uM	100 uM
mAMSA	-	++	+++
Fasamycin C	-	-	-
Fasamycin E	-	-	-
Formicamycin A	-	-	-
Formicamycin J	-	-	-

The next step in investigating the mechanism of action of these compounds was to determine if fasamycin and formicamycin act as DNA intercalators instead of binding to the enzyme itself. The ability of a compound to intercalate DNA, by slotting into the DNA double-helix or binding to the minor grove of DNA, can be assessed using an intercalation assay. The intercalation assay works by monitoring the ability of wheatgerm topoisomerase I to change the topology of DNA, from supercoiled to relaxed DNA, after DNA has been treated with a compound. In the presence of an intercalating compound wheatgerm topoisomerase I is unable to relax the DNA and therefore, the DNA will be in a supercoiled topological state which can be determined by electrophoresis by analysing the topology of DNA. However, DNA from samples treated with compounds that give a positive result for an intercalator must also be tested to

ensure that the result is not due to the compounds inhibiting the wheatgerm topoisomerase I itself.

Intercalation assays were performed for us by the Norwich based company Inspiralis who are experts in topoisomerase assays. supercoiled DNA was incubated individually in the presence of three concentrations (1, 10 and 100 µM) of two fasamycin congeners (C and E), two formicamycin congeners (A and J) and the known DNA intercalator amsacrine (mAMSA) at room temperature for 5 minutes before wheatgerm topoisomerase I was added into each assay and incubated at 37˚C for 30 minutes. DNA was extracted from each of the assays and ran on a 1% TAE agarose gel. Gels were stained in EtBr before DNA was visualised by UV. Intercalation ability is scored by the amount of supercoiled topoisomers present after electrophoresis and the ability of a compound to intercalate can be assigned as either displaying no intercalation (-); low intercalation (+); medium intercalation (++); or high intercalation (+++).

Results of intercalation assays are displayed in **Table 5.2**. mAMSA showed medium and high intercalation activity at 10 and 100 µM respectively, whereas both fasamycin (C and E) and both formicamycin (A and J) congeners showed no intercalation activity at the concentrations tested in this experiment. As none of the fasamycin or formicamycin treated DNA samples tested in this study showed the presence of supercoiled DNA, they were not investigated as inhibitors of wheatgerm topoisomerase I. These results indicate that fasamycin and formicamycin do not intercalate DNA and their ability to inhibit the activity of topoisomerase activity (such as gyrase and topo IV) is likely through a specific enzyme interaction.

5.2.6 Fasamycin E predominately interacts with ParC
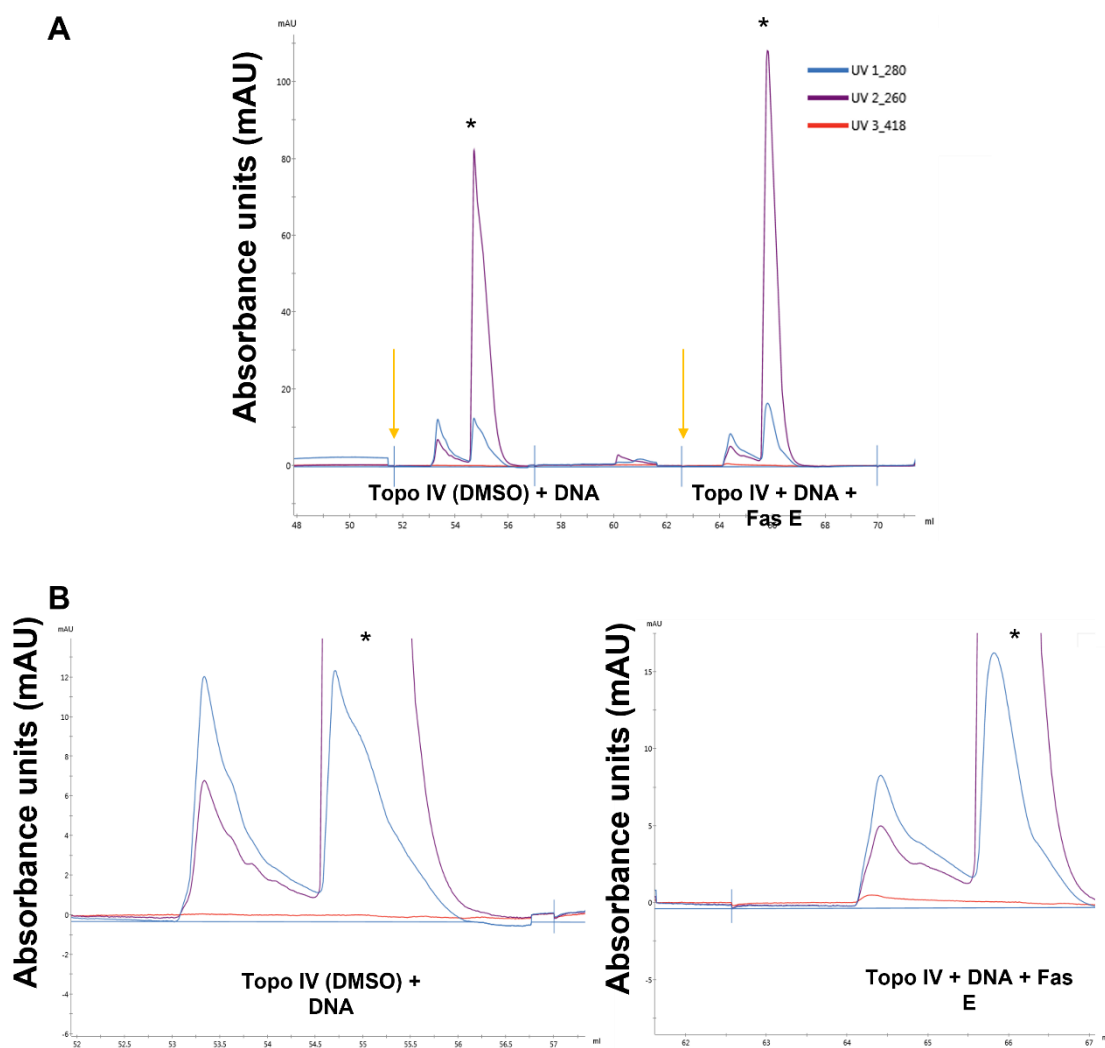
Figure 5.9 Chromatograms of topo IV with DNA in the presence of either DMSO (inhibitor vehicle control) or 25 µM fasamycin E. Samples were consecutively injected one after the other onto the column, injections are designated by yellow arrows. Elution of topo IV is monitored at 280 nm (blue), of DNA at 260 nm (purple), and of fasamycin E at 418 nm (red). **A**: topo IV (DMSO) complex with DNA and topo IV complex with DNA and fasamycin E; **B**, enlarged peaks from **A** of topo IV (DMSO) + DNA and topo IV + DNA + fasamycin E; In all cases the first peak in each sample corresponds to the topo IV

complex, the second peak designated with an ***** can be attributed to excess DNA, AMP-NP and buffer constituents.

Inhibitors of type II topoisomerases, that do not intercalate DNA, bind to one or both subunits of the enzyme. We therefore, wanted to determine if we could observe the fasamycin compounds, due to their characteristic absorbance at 418 nm, binding to topo IV and the individual subunits ParC and ParE using chromatography methods by monitoring different UV-vis wavelengths specific for proteins (280 nm), DNA (260 nm) and fasamycin (418 nm) compounds by FPLC.

Investigations were first undertaken with holoenzyme to ensure we could identify binding of fasamycin E whereby topo IV (400 nM) was incubated in elution buffer (buffer A + 150 mM NaCl + 4 mM MgCl) in the presence of 34 bp ds DNA (sequence above) (200 nM) for 30 minutes before the addition of 0.5 mM of the non-hydrolysable analogue of ATP 5'-adenylyl beta,gamma-imidodiphosphate (AMP-NP) to ensure that the enzyme is in a closed confirmation. After a further 30 minutes of incubation either DMSO (inhibitor vehicle control) or fasamycin E (25 µM) was added to the sample and further incubated for 15 minutes at room temperature. Samples were individually injected onto a SEC Superdex 200 (5/150 GL) column, eluted in a column volume (3 ml) of elution buffer (buffer A + 150 mM NaCl + 4 mM MgCl) and resulting peak wavelengths were analysed. Any peaks eluting after a column volume (3 ml) of buffer were found to be unbound assay constituents I.e., unbound DNA and AMP-NP, these peaks have been labelled (*****) on each of the chromatograms and therefore will not be discussed henceforth. All samples were ran consecutively on the same run with each new sample injected after a column volume of buffer had passed through the column (as indicated by yellow arrows on **Figure 5.9 and 5.10**). To ensure no aspect of the assay conditions led to interference of any monitored wavelength, all components of the assay (protein, DNA, fasamycin E and AMP-NP) were ran through the column individually and traces recorded.

We hypothesise that if fasamycin E is able to bind to topo IV we would expect to see an observable 418 nm peak co-eluting with the protein and DNA. As expected**,** no peak at 418 nm was observed in the topo IV + DMSO control, however, an identifiable peak at 418 nm on the chromatogram is observed co-eluting with topo IV in the fasamycin E treated sample (**Figure 5.10**). For further reassurance that fasamycin E is indeed bound

to topo IV and not eluting at the same retention time (within the 3 mL elution) on this column, we compared the topo IV + fasamycin E chromatograms with those of fasamycin E only. Interestingly, fasamycin E (25 µM) in elution buffer does not give an identifiable peak at 418 nm during the run which we hypothesise is due to the hydrophobic nature of the compounds and that any unbound fasamycin is being retained on the column, this hypothesis was further supported by the column being stained yellow, the characteristic colour of fasamycin compounds.
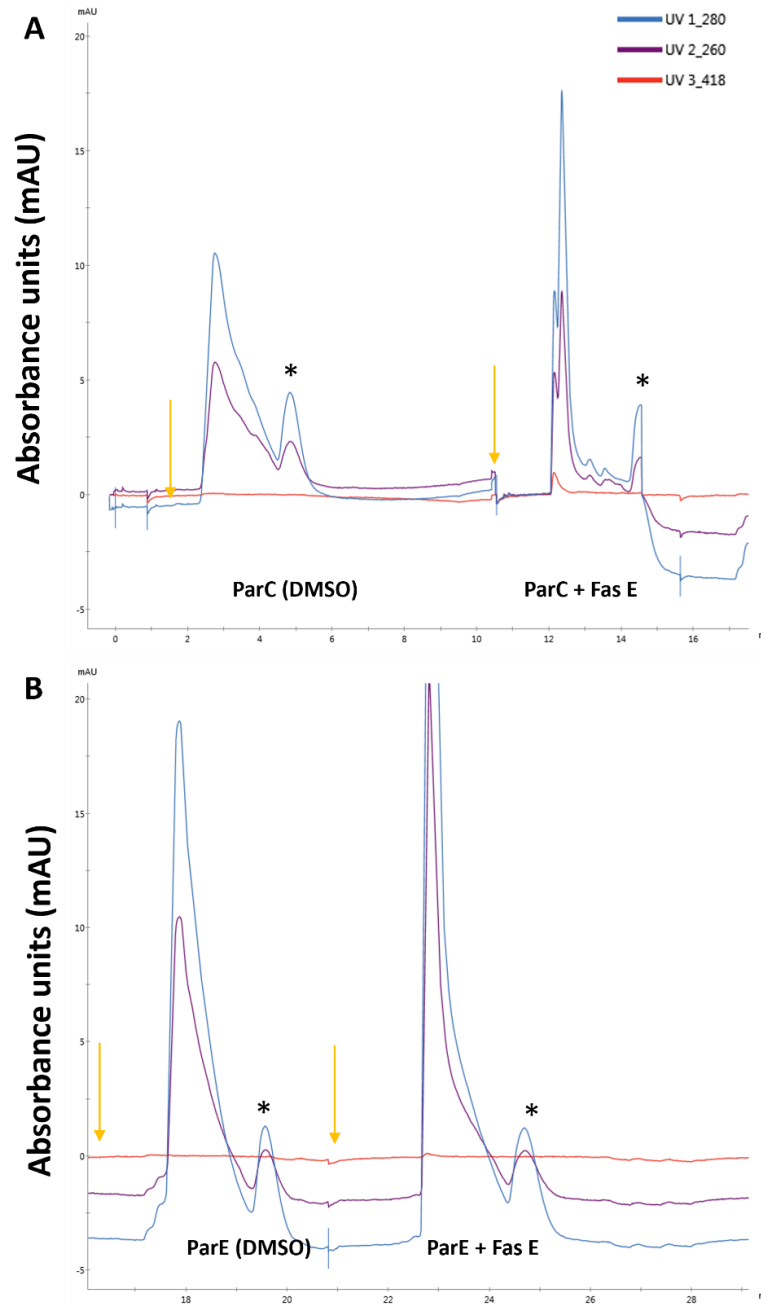
Figure 5.10 Chromatograms of ParC and ParE in the presence of either DMSO (inhibitor vehicle control) or 25 µM fasamycin E. Samples were consecutively injected one after the other onto the column, injections are designated by yellow arrows. Protein (ParC and ParE) is monitored at 280 nm (blue), DNA monitored at 260 nm (purple) and fasamycin E is monitored at 418 nm (red) which is a characteristic absorption wavelength of fasamycin. **A**- ParC + DMSO and ParC + fasamycin E; **B**, ParE + DMSO and ParE with fasamycin E. In all cases the first peak in each sample corresponds to the protein (ParC or ParE), the second peak designated with an ***** can be attributed to buffer constituents.

As previously described, topo IV is made up of two subunits ParC and ParE, and we wanted to determine which subunit fasamycin E interacts with. Therefore, ParC and ParE were individually incubated in the presence of either fasamycin E or DMSO (inhibitor vehicle control) for 30 minutes at room temperature before being directly injected onto the SEC column as described above. As expected, no peak at 418 nm was observed for either ParC or ParE incubated with DMSO. However, an identifiable peak corresponding to the 418 nm wavelength was observed co-eluting with the ParC protein (**Figure 5.10A**), and upon close inspection of ParE + fasamycin E samples we also observed a minor peak at 418 nm indicating that fasamycin E was bound to ParE but to a lesser extent than that observed for ParC (**Figure 5.10A** and **Figure 5.10B**). To characterise the preference of fasamycin E binding, peak height analysis using mAU values was undertaken which revealed that there was over 2-fold more fasamycin E bound to ParC in comparison to ParE (**SI Figure 11**). Interestingly, after exposure to fasamycin E, ParC eluted as two identifiable peaks which we hypothesise corresponds to the dimeric and monomeric forms of ParC respectively, fasamycin E was found to elute with what we consider to be the dimeric form of ParC. These results indicate that fasamycin E can bind and interact with both subunits of topo IV but with a higher binding affinity toward ParC. To ensure that this binding of fasamycin E to ParE is not an artefact of the experiment, increased concentrations of fasamycin E should be incubated with ParE, if fasamycin E does truly bind to ParE we would expect to see a concentration dependant increase in peak height at 418 nm co-eluting with ParE. Unfortunately, this method could not be used with the formicamycin compounds due to the wavelength at which formicamycin absorbs, 285 nm, as there is interference at this wavelength from other experimental constituents. Further methods will have to be used to confirm formicamycin binding such as SPR and ITC which can monitor protein – small molecule interactions.

5.2.7 Fasamycin and formicamycin retain activity against *in vivo* simocyclinone D8 resistant organisms and against *in vitro* ciprofloxacin and simocyclinone D8 resistant gyrase proteins

Given its mechanism of action, we wished to understand if simocyclinone D8 resistance could impact the antibacterial potency of fasamycin and formicamycin. *E.coli* NR698 mutants resistant to simocyclinone D8 were gifted from Dr Tung Le (JIC); these mutants were generated previously by exposing *E. coli* NR698 overnight cultures to SD8 at 10 µg/

ml on agar plates (Edwards, Flatman et al. 2009). Mutants isolated in this study encoded amino acid changes within GyrA of gyrase, and 5 amino acid changes were identified: V44G (**SP 8.1**), H45Y (**SP 8.6**), H45Q (**SP 6.6**), G81S (**SP5**) and D87Y (**SP 1**). These mutated amino acids map to the binding site of simocyclinone D8, as determined by protein crystallography, and these mutations are hypothesised to stop simocyclinone D8 being able to bind within its binding pocket on the gyrase enzyme (Edwards, Flatman et al. 2009).

Table 5.4 MIC values of fasamycin and formicamycin against simocyclinone D8 resistant mutants. Representative resazurin assays are shown in **SI Figure 12.**

Strain	Mutated residue	Fasamycin L MIC (µg/ml)	Formicamycin J MIC (µg/ ml)	Simocyclinone D8 (µg/ ml)
E. coli **NR698**	SD8 sensitive strain	8	4	0.25
E. coli **NR698 SP 1**	D87Y	8	4	>32
E. coli **NR698 SP 5**	G81S	8	4	>32
E. coli **NR698 SP 6.6**	H45Q	8	4-8	>32
E. coli **NR698 SP 8.1**	V44G	8	4-8	>32
E. coli **NR698 SP 8.6**	H45Y	8	4-8	>32

Simocyclinone D8 resistant mutants were tested using resazurin assays against fasamycin L and formicamycin J. As shown in **Table 5.4**, none of the simocyclinone D8 gyrase resistant mutants conferred cross-resistance which would be indicated by significantly increased MICs to the fasamycin or formicamycin congeners. This result is particularly interesting, as our earlier results indicated that fasamycin and formicamycin inhibit the interaction of type II topos with DNA, similarly to simocyclinone D8. Thus, the lack of cross resistance suggests that fasamycins/formicamycins and simocyclinone D8 interact with different binding sites within type II topos, or with a different binding mode.

After determining *in vivo* that characterised simocyclinone D8 mutants did not confer any resistance to either fasamycin or formicamycin, we wanted to understand if gyrase mutants that confer resistance to known gyrase inhibitors *in vitro* could also exhibit cross-resistance to our compounds. To examine this, biochemical experiments were undertaken by Inspiralis using a selection of four *E. coli* gyrase mutant proteins. These enzymes, *E.coli* gyrase **S83L**, *E.c*oli gyrase **D87A**, *E.coli* gyrase **D426N** and *E.coli* gyrase **R91Q** all contain single amino acid substitutions within the GyrA subunit which confer resistance to fluroquinolones (**S83L**, **D87A** and **D426N**) or simocyclinone D8 (**R91Q**). Supercoiling assays, as described in detail in Chapter 4, with mutant enzymes and the *E. coli* native enzymes were conducted in the presence of fasamycin E and formicamycin J alongside the controls of ciprofloxacin and simocyclinone D8. IC_{50} values for the inhibition of supercoiling determined were calculated, and fold changes in IC_{50} compared to the native enzyme were determined as shown in **Table 5.5**. Given the inherent variability of these assays that arises due to several factors such as protein concentration as well as protein and compound batch, we determined a minimum 5-fold increase in IC_{50} as indicating resistance. As expected, ciprofloxacin displayed increased IC_{50} values for fluroquinolone resistant gyrase proteins (**S83L**, **D87A** and **D426N**) with increases in supercoiling IC_{50} values ranging from 8- to 53-fold and indicating a high level of resistance in comparison to the wild type protein. Similarly, the IC_{50} values for simocyclinone D8 against the **R91Q** mutant gyrase were increased 44-fold, again indicating a high level of resistance. None of the mutations tested had a significant effect on the sensitivity to fasamycin E or formicamycin J as seen by the minimal changes in IC_{50}s indicating that none of these amino acid substitutions are sufficient to confer resistance to either of our compounds *in vitro*. Lack of resistance due to fluroquinolone resistance mutations (**S83L**, **D87A** and **D426N**) was not surprising due to the different mechanism of action of fasamycin and formicamycin as hypothesised by previous experiments. However, it was interesting to see that the SD8 resistant gyrase conferred no resistance to either compound due to our hypothesis that fasamycin and formicamycin may inhibit the topoisomerase-DNA interaction similarly to simocyclinone D8.

Table 5.5. Fold-change in IC_{50} values for inhibition of mutated gyrase proteins by fasamycin E, formicamycin J, ciprofloxacin and simocyclinone D8 in comparison to wild type *E. coli* gyrase. Values highlighted in red are deemed to be resistant to compound exposure. Green highlighted values indicate no resistance. Experiments were conducted by Inspiralis (UK).

	Fold change in supercoiling inhibition (IC_{50} WT enzyme/IC_{50} mutant enzyme)			
	E. coli S83L	*E. coli* D87A	*E. coli* D426N	*E. coli* R91Q
Resistance	Fluroquinolones	Fluroquinolones	Fluroquinolones	SD8
Ciprofloxacin	53	8	25	
Simocyclinone D8				44
Fasamycin E	1.3	1.3	1.8	1
Formicamycin J	2	3	3.5	1.5

Although the mutant enzymes tested in this experiment do not give a comprehensive representation of the mutations that can confer resistance to both ciprofloxacin and simocyclinone D8, taken together with the *in vivo* data for strains resistant to ciprofloxacin and simocyclinone D8, it seems a reasonable assumption that fasamycin/ formicamycin do not bind in the same binding pockets, or with the same binding mode, as ciprofloxacin and simocyclinone D8. To develop further this work, homologous mutants in topo IV to the ones described here should be investigated as inhibition assays have indicated that fasamycin and formicamycin are more potent inhibitors of *E.coli* topo IV in comparison to *E. coli* gyrase.

### 5.2.8 Formicamycin inhibits ciprofloxacin induced DNA cleavage

Throughout this chapter we have demonstrated that both fasamycin and formicamycin show similar behaviour to simocyclinone D8 in a range of *in vitro* assays designed to probe their mechanism of inhibition of DNA gyrase and topo IV. Research by Flatman et al (2005), found that simocyclinone D8 was able to protect from ciprofloxacin induced dsDNA break formation, through the stabilisation of the cleavage complex which they

inferred further supported the finding that simocyclinone D8 inhibits topoisomerase-DNA binding.

To study this phenomenon further we conducted a cleavage assay, in duplicate, in the presence of a defined concentration of ciprofloxacin (10 µM) which stabilises the DNA-enzyme cleavage complex leading to increased levels of DNA cleavage and the accumulation of linear DNA. Thus, fasamycin and formicamycin were titrated into the assay (100 – 1.6 µM) and after appropriate incubation, the resulting distribution of DNA topologies was analysed. If fasamycins and formicamycins block DNA binding to type II topos as we hypothesise, then their presence in the assay should inhibit the formation of linear DNA in a dose dependant manner.

 As expected, DNA incubated with topo IV in the absence of ciprofloxacin, showed minimal amounts of linear DNA whereas DNA from ciprofloxacin treated topo IV assays showed high levels of cleavage, as determined by increased linear DNA products (**Figure 5.7**). Formicamycin J was found to be able to protect from ciprofloxacin induced cleavage in a concentration dependant manner as determined by a complete absence of linear DNA above a concentration of 25 µM. In contrast fasamycin E showed a modest protective effect of ciprofloxacin induced linear DNA as indicated by the less intense band for linear DNA. This band intensifies in a concentration dependant manner and therefore we conclude that fasamycin E does confer some protection against ciprofloxacin induced linear DNA formation. As exposure to fasamycin E does not completely abolish linear DNA formation in the presence of ciprofloxacin, we hypothesise that ciprofloxacin outcompetes fasamycin E and thus some linear products are observed.

The binding of ciprofloxacin stabilises DNA-gyrase cleavage complexes and, therefore, the ability of formicamycin J to protect against ciprofloxacin mediated cleavage suggests two hypotheses. In the first scenario formicamycin competitively binds to topo IV before ciprofloxacin is able to bind or, alternatively, formicamycin has the ability to displace ciprofloxacin that has already bound to topo IV. To distinguish between these possibilities, experiments could be designed to determine if formicamycin can displace ciprofloxacin from a pre-formed ciprofloxacin-topo IV complex.
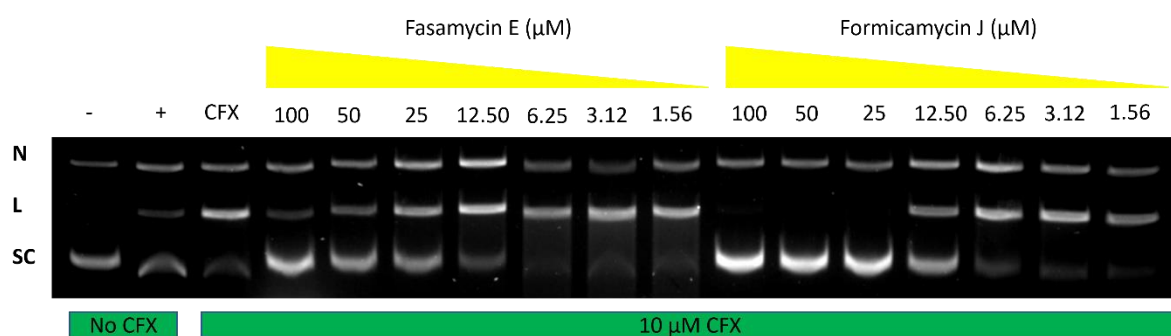
Figure 5.11. The effect of fasamycin E and formicamycin J on ciprofloxacin (CFX) induced DNA cleavage. Fasamycin and formicamycin were titrated into a topo IV-DNA cleavage assay containing 10 μM of CFX. Following incubation, the resulting DNA was run on an agarose in the presence of 1 μg/ ml EtBr. **-** control (no enzyme or drug); **+** Topo IV and DMSO; **N**, nicked circle; **L**, linear; **SC**, supercoiled DNA.

5.3 Discussion

Since the golden age of antibiotic discovery, the antibiotic pipeline has declined significantly, with only 27 new antibiotics undergoing clinical investigations in 2021, a much-reduced figure in comparison to previous years. Moreover, the increasing problem of antimicrobial resistance means that antibiotics with new mechanisms of action, or which are effective against resistant strains, are in high demand.

As the control of DNA topology is a fundamental prerequisite for all processes requiring DNA, new gyrase and topo IV inhibitors are some of the most sought-after antibiotics; as such several new gyrase/topo IV inhibitors are undergoing clinical trials. These include molecules such as gepotidacin and zoliflodacin, both of which are of synthetic origin (Bax, Murshudov et al. 2019, Kolarič, Anderluh et al. 2020). The majority of clinically used gyrase/topo IV inhibitors, and most notably the fluoroquinolones, stabilise the enzyme-DNA cleavage complex and as such are considered as gyrase poisons (Miki, Chang et al. 1984, Bryan, Bedard et al. 1989, Heddle, Blance et al. 2001). Unfortunately, as discussed at the start of this chapter, many bacteria have acquired resistance to these types of antibiotics through mutations leading to amino acid changes within the fluoroquinolone binding sites of these enzymes.

Taken together with the results of Chapter 4, we have shown that both fasamycin and formicamycin inhibit the essential activities of both bacterial gyrase and topo IV. We have further demonstrated that neither of these compounds show indications of being

able to stabilise the cleavage complex of topoisomerases, like that seen with ciprofloxacin. We therefore propose that the formicamycins represent new a class of compounds that act as catalytic inhibitors which retain inhibitory activity towards gyrase proteins containing several fluoroquinolone and simocyclinone D8 resistance mutations, as well as bacterial strains resistant to simocyclinone D8. We further hypothesise that the fasamycins and formicamycins are not ATPase inhibitors, like the aminocoumarins, as they preferentially interact with the ParC subunit of topo IV instead of the ATPase domain, ParE.

Through intercalation assays we have shown that neither fasamycins nor formicamycins bind or intercalate with DNA directly, but that they do appear to impede DNA binding of topo IV, taken together with the SEC chromatography experiments which indicated that fasamycin E preferentially binds to ParC (GyrA) but binding to ParE (GyrB) can also be observed, we hypothesise that both classes of compound bind to topo IV in such a way that they hinder DNA binding. Therefore, an educated guess suggests that fasamycin compounds bind at the ParC-ParE-DNA interface (DNA gate). Furthermore, although we propose our fasamycins and formicamycins bind to gyrase/topo IV and inhibit the binding of DNA, as does simocyclinone D8, we have also shown that mutant strains and enzymes that are resistant to simocyclinone D8 remain sensitive to both types of compounds indicating that fasamycin/formicamycin likely bind at a different binding site to simocyclinone D8. Additionally, we also cannot rule out the possibility that fasamycins and formicamycins having different binding sites/modes to each other due to their different 3D structures.

 In summary, the work in this chapter contributes to the ongoing investigation of the mechanism of action of fasamycin and formicamycin antibiotics and will guide future structural work to elucidate the fasamycin and formicamycin binding site and completely define the mechanism of action.

Part II: Chemical analysis of *S. formicae* mutants and heterologous expression of the formicamycin biosynthetic gene cluster.

6.0 Re-wiring the regulation of the formicamycin biosynthetic gene cluster leads to high producing formicamycin strains
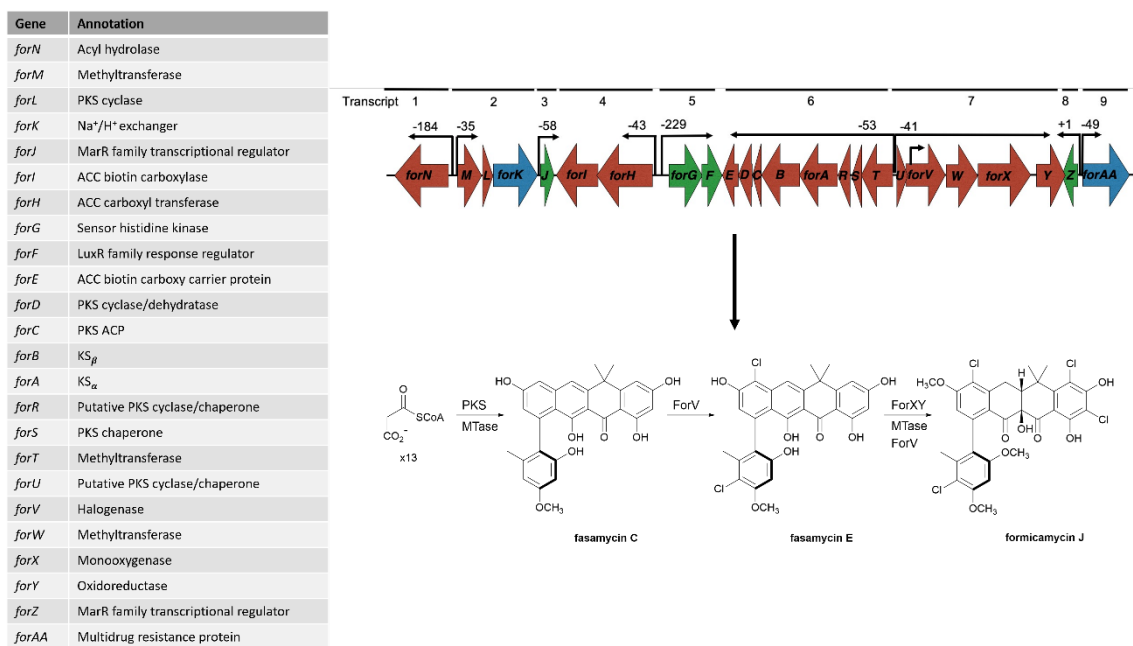
6.1 Introduction
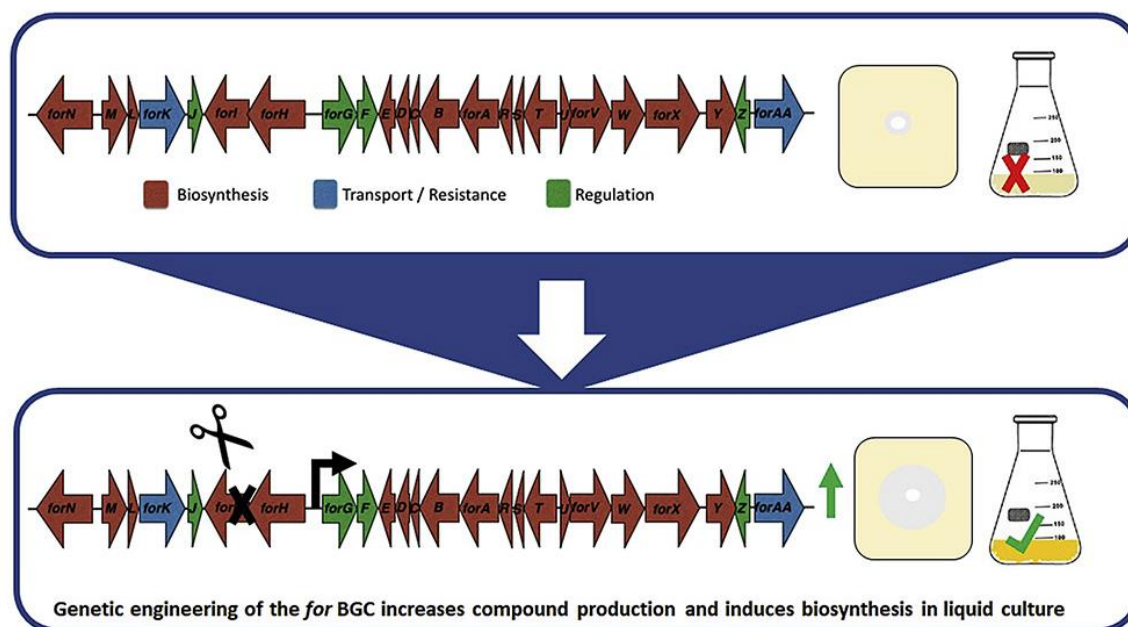
Graphical abstract: Diagrammatic representation of how deletion of the MarR regulator ForJ leads to compound production in liquid media and increased formicamycin production. Scissors represent the deletion of *forJ* by CRISPR (Devine, McDonald et al. 2021).

The search for novel natural products is especially significant in present day due to the increased prevalence of antimicrobial resistance (AMR) (Walker, Barrett et al. 2009). A common bottleneck in the search for new clinically useful natural products is the low production levels observed for microbial fermentation and the involved methods needed to isolate these compounds. Formicamycin compounds and their biosynthetic precursors, the fasamycins, have previously been identified to be potent antimicrobials with a high barrier for the selection of resistance, making them attractive as potential new antibiotics (Qin, Munnoch et al. 2017). However, formicamycins are no exception from the productivity bottleneck. To enhance compound production, natural product producers such as *Streptomyces* spp. can be genetically modified to provide high yielding strains which can begin to overcome this bottleneck (Aigle and Corre 2012).

This chapter will discuss the creation of high-producing *S. formicae* strains via genetic modification using CRISPR-Cas9 technology and formed the basis of a publication entitled '*Re-wiring the regulation of the formicamycin biosynthetic gene cluster to enable the development of promising antibacterial compounds*'

This paper describes the effect of targeted gene deletions within the formicamycin biosynthetic gene cluster (BCG) and reveals the importance of three regulators of the *for* BGC, two MarR-family transcriptional regulators ForJ and ForZ, and the two-component system ForGF, which together regulate the expression of genes required for both biosynthesis and export of fasamycins and formicamycins (Devine, McDonald et al. 2021). The three regulatory genes had been given putative annotations (**Figure 6.1**) but deletion mutants were vital in confirming their specific roles in the *for* BGC (Qin, Munnoch et al. 2017). Using this knowledge, we generated strains that exhibit increased titres, formicamycin compounds in liquid medium (which has never been reported before in the wild-type strain), alongside the isolation of novel fasamycin and formicamycin congeners.

This chapter will focus on my work to determine the titre of the *S. formicae* mutants described in this paper and provide a discussion of what this analysis can tell us about the regulation of the formicamycin BGC and how this information guided us in creating enhanced formicamycin and fasamycin producing strains.
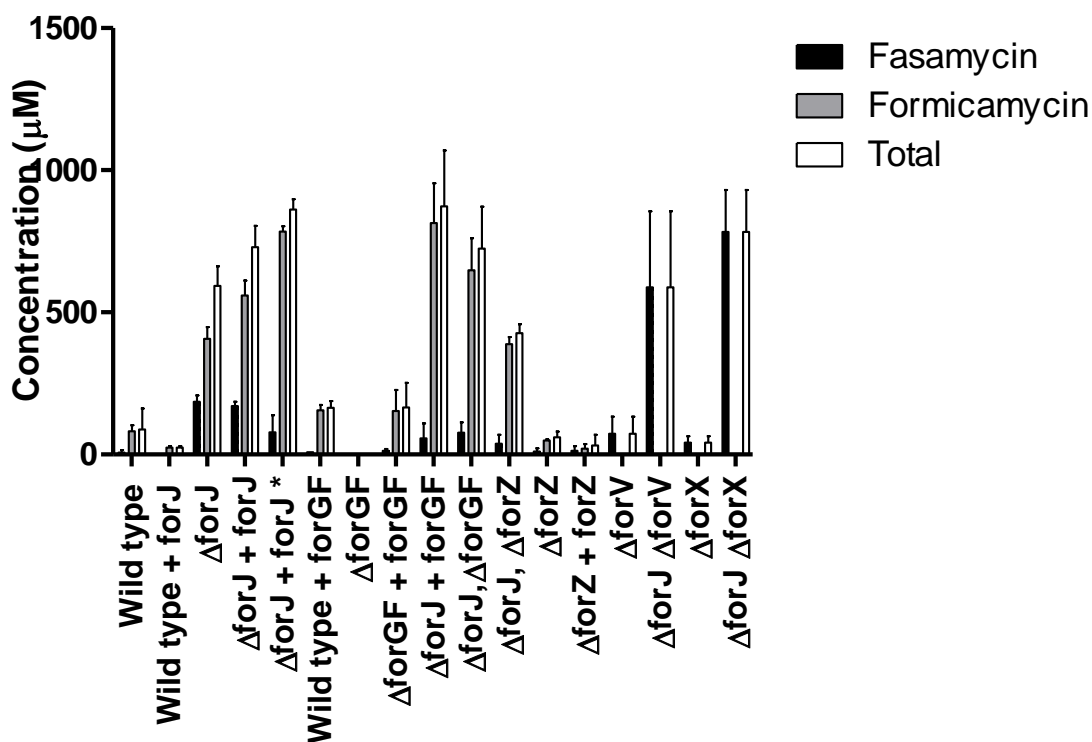
Gene	Annotation
forN	Acyl hydrolase
forM	Methyltransferase
forL	PKS cyclase
forK	Na+/H+ exchanger
forJ	MarR family transcriptional regulator
forI	ACC biotin carboxylase
forH	ACC carboxyl transferase
forG	Sensor histidine kinase
forF	LuxR family response regulator
forE	ACC biotin carboxy carrier protein
forD	PKS cyclase/dehydratase
forC	PKS ACP
forB	KS$_\beta$
forA	KS$_\alpha$
forR	Putative PKS cyclase/chaperone
forS	PKS chaperone
forT	Methyltransferase
forU	Putative PKS cyclase/chaperone
forV	Halogenase
forW	Methyltransferase
forX	Monooxygenase
forY	Oxidoreductase
forZ	MarR family transcriptional regulator
forAA	Multidrug resistance protein

Figure 6.1 Formicamycin biosynthesis was found to require 24 genes encoded on 9 different transcripts. Arrows represent the individual genes of the cluster. Red = biosynthetic genes, blue = the two transporters of the cluster, green = regulators. Formicamycin biosynthesis occurs by the formation of fasamycins through the combined action of the polyketide synthase (PKS), methyltransferases (MTase), *for* encoded gene products, and a single halogenase (ForV). Hydroxylation and ring expansion undertaken by ForX leads to a lactone intermediate, the flavin-dependent oxidoreductase ForY then catalyses a reductive ring contraction to yield the formicamycin backbone. Reproduced with permission from Devine et al 2021.

6.2 Results

6.2.1 Titre analysis of *S. formicae* mutants

All *S. formicae* mutants and complementation strains in this chapter were made by Dr Rebecca Devine (JIC) using CRISPR/Cas 9 methodology to generate start to stop codon deletions of the genes of interest. These mutants were generally phenotypically similar to that of *S. formicae* wild-type (white sporulation pigment), except in the case of any strain that contained a deletion of the MarR regulator *forJ*. Deletion of *forJ* yielded strains which lacked white spore pigment indicating the inability to sporulate and excreted a yellow substance indicating a developmental defect in this strain possibly due to toxicity due to over production of *for* BGC compounds (**Figure 6.2**). Complementation for all knockouts was conducted by re-introducing a copy of the deleted gene under their

native promoters using site specific integrative vectors. Full details of strain generation are reported in Devine *et al* (2021)(Devine, McDonald et al. 2021).

Figure 6.2 Phenotypes of *S. formicae* wild-type and *S. formicae ΔforJ*

Titre analysis was undertaken by growing *S. formicae* strains on SFM agar and analysing the compounds produced via HPLC of ethyl acetate extracts. Titres were determined by measuring the relevant peak areas from HPLC traces at wavelengths specific for both fasamycin and formicamycin (**SI Figure 13**) and calibrated using a standard curve of known concentrations of a representative fasamycin and formicamycin congener (**SI Figures 14-15** and **SI Tables 2- 3**). Titres for the mutant strains were compared to that of the parental strain and formicamycin producer, henceforth referred to as *S. formicae* wild-type *(***Figure 6.3** and **Table 6.1***).

Figure 6.3 Genetic manipulation of the formicamycin BGC in *S. formicae* results in changes to total fasamycin and total formicamycin production on solid SFM media. Combined metabolites refer to fasamycin and formicamycin production together. Error bars represent standard deviation from biological triplicates.

To quantify the effect of mutations within biosynthetic genes on the products of the formicamycin BGC, production of fasamycin and formicamycin by the parental strain had to be characterised. Analysis of fasamycin and formicamycin titres of multiple replicates (*n*= 16) of *S. formicae* wild-type revealed variable titres for the combined levels of fasamycin and formicamycin production. To understand the basis of this variability, individual fasamycin and formicamycin production was analysed (**Figure 6.4**).

Titres of formicamycins were always higher than those of fasamycins, which was expected as fasamycins are biosynthetic precursors of the formicamycins. However, while fasamycin titres were stable (6.5 ± 9.6 µM) the formicamycin titres of individual replicates were highly variable (81.3 ± 21.6 µM). It is thus important to bear in mind the biological variability of fasamycin and formicamycin production by the *S. formicae* wild-type strain during all further analysis.
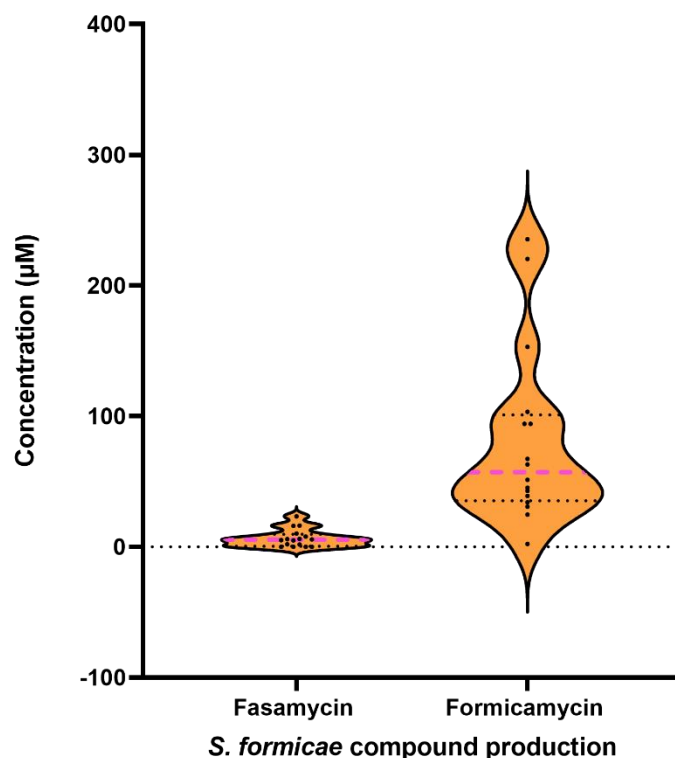
Figure 6.4 Violin plots displaying the variation in fasamycin and formicamycin production by the *S. formicae* wild-type strain (*n*=16). The pink dotted line indicates the median

6.2.2 MarR – family transcriptional regulators

Multiple Antibiotic Resistant Regulator (MarR) family regulators are a group of transcriptional regulators that generally repress gene transcription and are often found in natural product BGCs. The formicamycin BGC contains two MarR-family transcriptional regulators, ForJ and ForZ.

Deletion of *forJ* (*S. formicae* Δ*forJ)* results in a significant increase in both fasamycin and formicamycin titres in comparison to *S. formicae* wild-type. *S.formicae* Δ*forJ* exhibits a 6.7-fold increase in total fasamycin/ formicamycin titres in comparison to *S. formicae* wild-type (592.7 ± 69.4 µM vs 87.9 ± 74.2 µM) (**Table 6.1**). ForJ was hypothesised to be a negative regulator of the *for* pathway and thus increased titres were expected due to de-repression of the pathway; our results confirm this hypothesis.

Two attempts to complement the *forJ* deletion were attempted using both the native and the *ermE** promoter, the results of which were both unsuccessful and compound production was comparable to that of *S. formicae* Δ*forJ*. It is unclear why the

complementation of this mutant was unsuccessful, but we were able to demonstrate that over-expression of *forJ* in the wild-type strain was able to reduce fasamycin production to un-quantifiable levels and formicamycin biosynthesis to ~ 30 % of wild type titres (24.8 ± 4.7 µM vs 87.9 ± 74.2 µM) (**Table 6.1**).

Upon deletion of the second BGC situated MarR regulator gene, *forZ*, a ~ 30 % reduction in combined fasamycin/ formicamycin titres was seen in comparison to the *S. formicae* wild-type strain. Complementation of *forZ* did not restore wild type levels of production as was observed for the *forJ* complementation. Upon first inspection we hypothesised that this reduction in metabolite production might be attributed to biological variation, as seen with the *S. formicae* wild-type controls. However, when both *forJ* and *forZ* are deleted together, a reduction in metabolites is still observed in comparison to the over-producing *S. formicae ΔforJ* strain (427.1 ± 31.6 µM vs 592.7 ± 69.4 µM total metabolites).

6.2.3 Two-component system ForGF

Two-component signal transduction systems (TCS) are widespread in prokaryotes but are not found in the animal kingdom. Consisting of a sensor kinase and a cognate response regulator, they are one of the major ways that bacteria sense environmental changes and are therefore important in the production of *Streptomyces* secondary metabolites. *Streptomyces* genomes have been shown to encode a higher number of TCSs than other bacteria and many are involved in antibiotic biosynthesis. TCS can affect antibiotic biosynthesis in two ways, the first is by acting as pleiotropic regulators, whereby one regulator can influence several antibiotic producing BGCs. In more rare cases, they can be cluster-situated regulators (CSRs) that are encoded within the BGC that they control.

The *for* BGC contains a cluster-situated TCS which is made up of ForG and ForF, a sensor histidine kinase and a LuxR response family regulator respectively. Deletion of the operon containing *forF* and *forG* was undertaken to produce *S. formicae ΔforGF*. Titre analysis revealed that deletion of these genes completely abolished fasamycin and formicamycin production indicating an essential role in formicamycin biosynthesis (**Figure 6.3**). Restoration of formicamycin biosynthesis was seen when *ΔforGF* was complemented with *forGF* under the control of the native promoter, with titres that

were higher than that of *S. formicae* wild-type (165.7 ± 86.1 μM vs 87.9 ± 74.2 μM total metabolites). This is consistent with overexpression of *forGF* in *S. formicae* which was found to almost double the production of total metabolites in comparison to *S. formicae* wild-type (164.3 ± 23.7 μM vs 87.9 ± 74.2 μM), further indicating a crucial role of this TCS in formicamycin biosynthesis.

However, when a deletion of the two-component system (*ΔforGF*) and the negative regulator (*ΔforJ)* were combined in one strain to produce *S. formicae ΔforJΔforGF*, metabolite analysis revealed a high producing formicamycin strain with titres comparable to that of the de-repressed *ΔforJ* strain. This was unexpected due to the observation that *forGF* is essential for formicamycin biosynthesis in the wild-type strain. This indicates that although ForGF is important in the production of formicamycins, its effect can be circumvented by the de-repression of the BGC. Combining an extra copy of ForGF in the de-repressed strain (*S.formicae ΔforJ + forGF)* resulted in a 10-fold increase in combined fasamycin and formicamycin titre in comparison to wild-type titres (873.4 ± 195.9 μM vs 87.9 ± 74.2 μM). This strain also exhibited a 1.5-fold increase in total metabolites in comparison to Δ*forJ* making this the highest yielding strain created.

6.2.4 Deletion of forV and forX in a de-repressed background yields high producing fasamycin strains

Flavin-dependant halogenase ForV

A common denominator between the majority of fasamycin and formicamycin congeners is that they are all chlorinated, except for the non-halogenated fasamycin C, and various congeners have been isolated carrying up to four chlorine atoms. Analysis of the genes within the *for* BGC indicates only a single halogenase ForV is encoded, it has been shown that deletion of *forV* leads to accumulation of fasamycin C demonstrating that ForV is a promiscuous enzyme capable of performing multiple chlorination events (Qin, Devine et al. 2020). Furthermore, due to the absence of any formicamycin molecules produced by this strain, it appears that chlorination, and therefore ForV, plays a gate-keeping role for the conversion of fasamycins to formicamycins. Halogenation is not only important for the conversion of fasamycins to formicamycins but also affects the antibacterial potency of the various congeners and

will be discussed in a later chapter. With this knowledge in hand, we created an over-producing fasamycin C strain by combining the *ΔforV* and *ΔforJ* mutations into one strain. *S. formicae ΔforJV* only produced the fasamycin C congener at concentrations 8-fold higher than that of *S. formicae ΔforV* (587.5 ± 268.1 µM vs 72.8 ± 60.3 µM)*.

Flavin-dependant monooxygenase ForX

An important step in the conversion of fasamycin to formicamycin is the Baeyer-Villiger like oxidation step carried out by the monooxygenase ForX on chlorinated fasamycin congeners. It has been shown that deletion of *forX* leads to accumulation of chlorinated fasamycin congeners and completely abolishes formicamycin production (Qin, Devine et al. 2020). To build on this previous research titre analysis of *S. formicae ΔforX* was undertaken and found to produce fasamycins at a higher titre than that of wild type (~6-fold) but total titres are reduced by approximately half due to the absence of formicamycins. This suggests that in *S. formicae* fasamycin accumulation cannot replace missing formicamycin accumulation which could indicate that accumulation of fasamycins in high quantities may have a toxic effect. As above, we combined a *forX* and *forJ* mutation to yield a high yielding fasamycin producing strain. *S. formicaeΔforJX* produced several fasamycin congeners at high levels at approximately 18-fold higher than the *forX* mutant (782.6 ± 147.8 µM vs 42.3 ± 22.6 µM).

Table 6.1 Fasamycin, formicamycin and total titres of *S. formicae* mutants grown on solid SFM media. * Complemented with native promotor, ** complemented with ErmE* promoter. Wild-type *n* =16, all other strains *n* =3

Strain	Fasamycin titre (µM)	Formicamycin titre (µM)	Combined titre (µM)
Wild-type	6.5 ± 9.6	81.3 ± 21.6	87.9 ± 74.2
Wild-type + *forJ*	0	24.8 ± 4.7	24.8 ± 4.7
Δ*forJ*	186.2 ± 22.2	406.5 ± 42.1	592.7 ± 69.4
Δ*forJ* + *forJ**	170.8 ± 15.4	558.8 ± 53.5	729.6 ± 74.8
Δ*forJ* + *forJ***	78.0 ± 60.2	784.0 ± 18.9	862.0 ± 36.6
Wild-type + *forGF*	8.6 ± 0.02	155.7 ± 18.7	164.3 ± 23.7
Δ*forGF*	0	0	0
Δ*forGF* + *forGF*	13.1 ± 6.7	153.7 ± 73.6	165.7 ± 86.1
Δ*forJ* + *forGF*	56.7 ± 52.9	814.2 ± 139.8	873.4 ± 195.9
Δ*forJ* Δ*forGF*	76.3 ± 36.8	648.1 ± 112.7	724.5 ± 147.8
Δ*forJ* Δ*forZ*	38.6 ± 31.2	388.5 ± 24.8	427.1 ± 31.6
Δ*forZ*	11.1 ± 10.6	49.8 ± 3.7	60.9 ± 19.7
Δ*forZ* + *forZ*	13.6 ± 15.8	21.0 ± 15.7	31.8 ± 38
Δ*forV*	72.8 ± 60.3	0	72.8 ± 60.3
Δ*forJ*Δ*forV*	587.5 ± 268.1	0	587.5 ± 268.1
Δ*forX*	42.3 ± 22.6	0	42.3 ± 22.6
Δ*forJ*Δ*forX*	782.6 ± 147.8	0	782.6 ± 147.8

6.2.5 Deletion of the negative regulator gene *forJ* leads to the discovery of new fasamycin and formicamycin congeners

Careful reanalysis of the various strains containing the *forJ* deletion using HPLC and LCMS revealed the presence of several new fasamycin and formicamycin congeners. Isolation and structural elucidation of these new compounds was performed by Dr Zhiwei Qin (JIC).

We observed several new peaks from extracts of *S. formicae ΔforJX*, compared to *S. formicae* wild-type, which had the characteristic chromophore of fasamycin congeners (**Figure 6.5**) Individual peaks were purified leading to the identification of six new fasamycin congeners that were characterised. Structural elucidation by NMR and high-resolution MS methods revealed that these new fasamycin congeners (L-Q) were differentially chlorinated in comparison to previously identified fasamycins from *S. formicae* (**Figure 6.6**).

C	Fasamycin C
E	Fasamycin E
1	Fasamycin L
2	Fasamycin M
3	Fasamycin N
4	Fasamycin O
5	Fasamycin P
6	Fasamycin Q
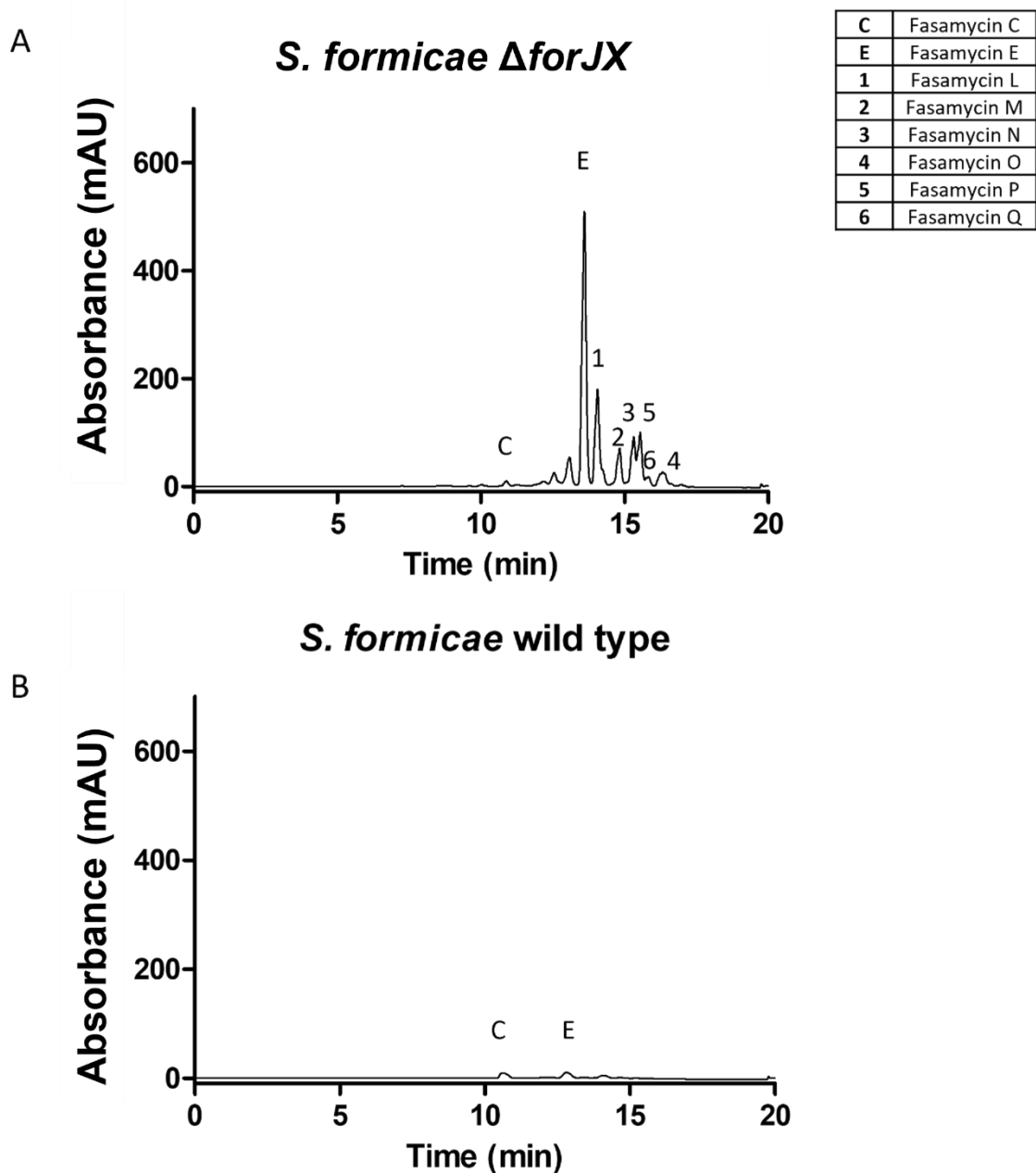
Figure 6.5 Chromatogram traces at 418nm of ethyl acetate extracts from *S. formicae* ΔforJX (A) compared to *S. formicae* wild-type (B) grown on solid SFM. Deletion of *forJ* and *forX* leads to the presence of several new chlorinated fasamycin congeners. Fasamycin E (E) and fasamycin C (C) had been previously isolated from *S. formicae*, compounds 1-6 represent new congeners.

Previously we had only seen up to two chlorine atoms on the fasamycin backbone (fasamycin E) whereas these new congeners contained up to 4 chlorine atoms. Similarly, two new formicamycin molecules (R and S) were uncovered in extracts taken from *S. formicae ΔforJ*, once again following the same pattern of increased halogenation as seen in the new fasamycin congeners. Formicamycins R and S displayed 5 halogenation events orchestrated by the halogenase ForV in comparison to the 4 previously observed for formicamycin I and J.
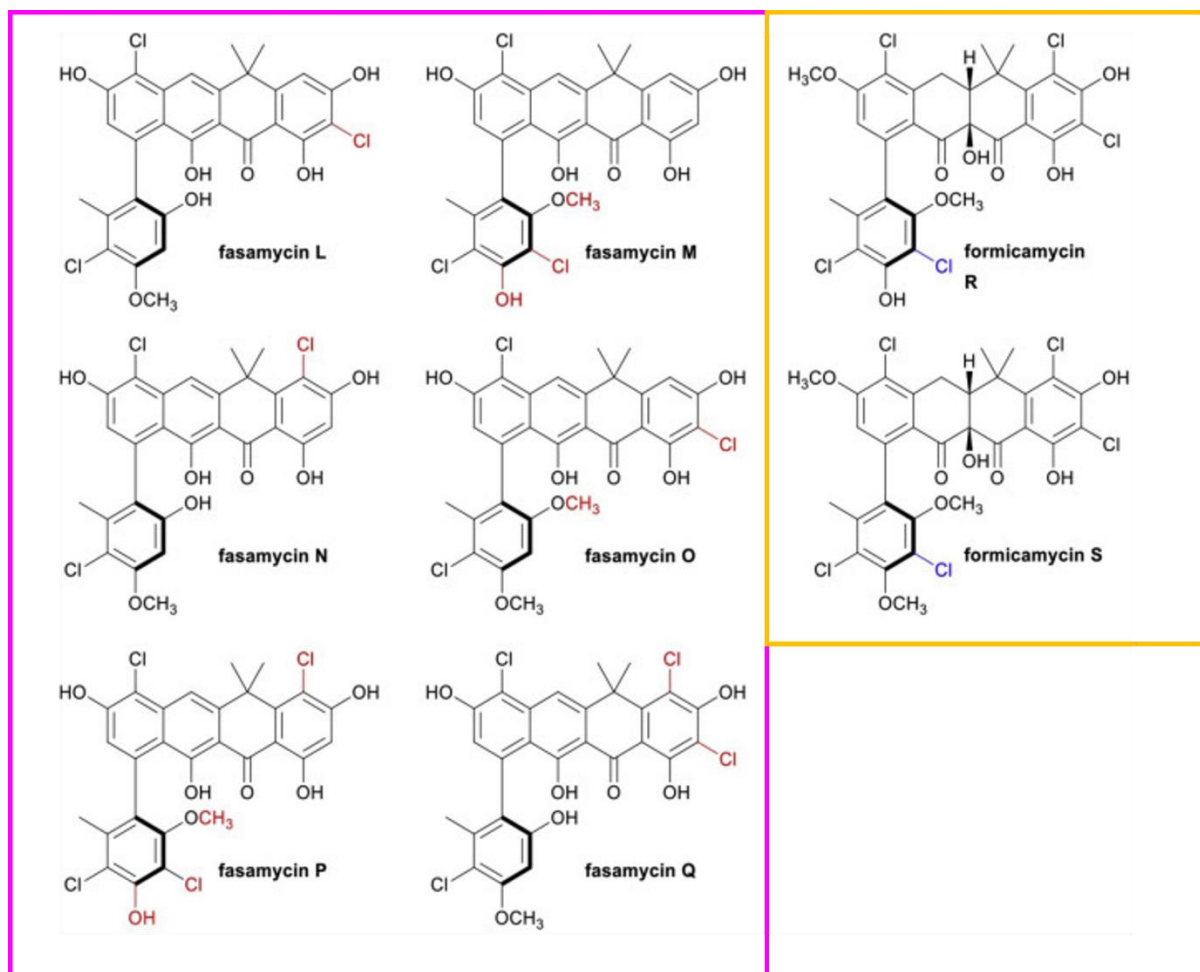
Figure 6.6 Six new fasamycin congeners (L-Q) were isolated from *S. formicae ΔforJX* and two new formicamycin congeners (R and S) were isolated from *S. formicae ΔforJ*. Fasamycin structures are highlighted in pink and formicamycin structures are highlighted in orange. Isolation and structural elucidation of new compounds was undertaken by Dr Zhiwei Qin (JIC) Changes in new fasamycins in comparison to previously identified congeners (C-E) are shown in red and changes in formicamycin structure in comparison to formicamycins A-J are shown in blue (Reproduced with consent from Devine et al 2021).

6.2.6 Deletion of *forJ* induces formicamycin production in liquid media

Fasamycins and formicamycins have only previously been isolated when the wild-type *S. formicae* strain was grown on solid media, and, despite extensive testing, we had not been able to observe their production when grown in liquid media. This limits our ability to develop these compounds further, for example in a preclinical context due to the time consuming and involved extraction processes. Liquid culture is preferred for promising natural products due to the ability to perform larger scale fermentations with simpler downstream processing.

To our surprise, whilst growing the *S. formicae* regulator gene mutants in liquid culture it was noted that derepressed (*ΔforJ)* strains turned the liquid medium a yellow colour which is characteristic of products from the fasamycin/formicamycin pathway.
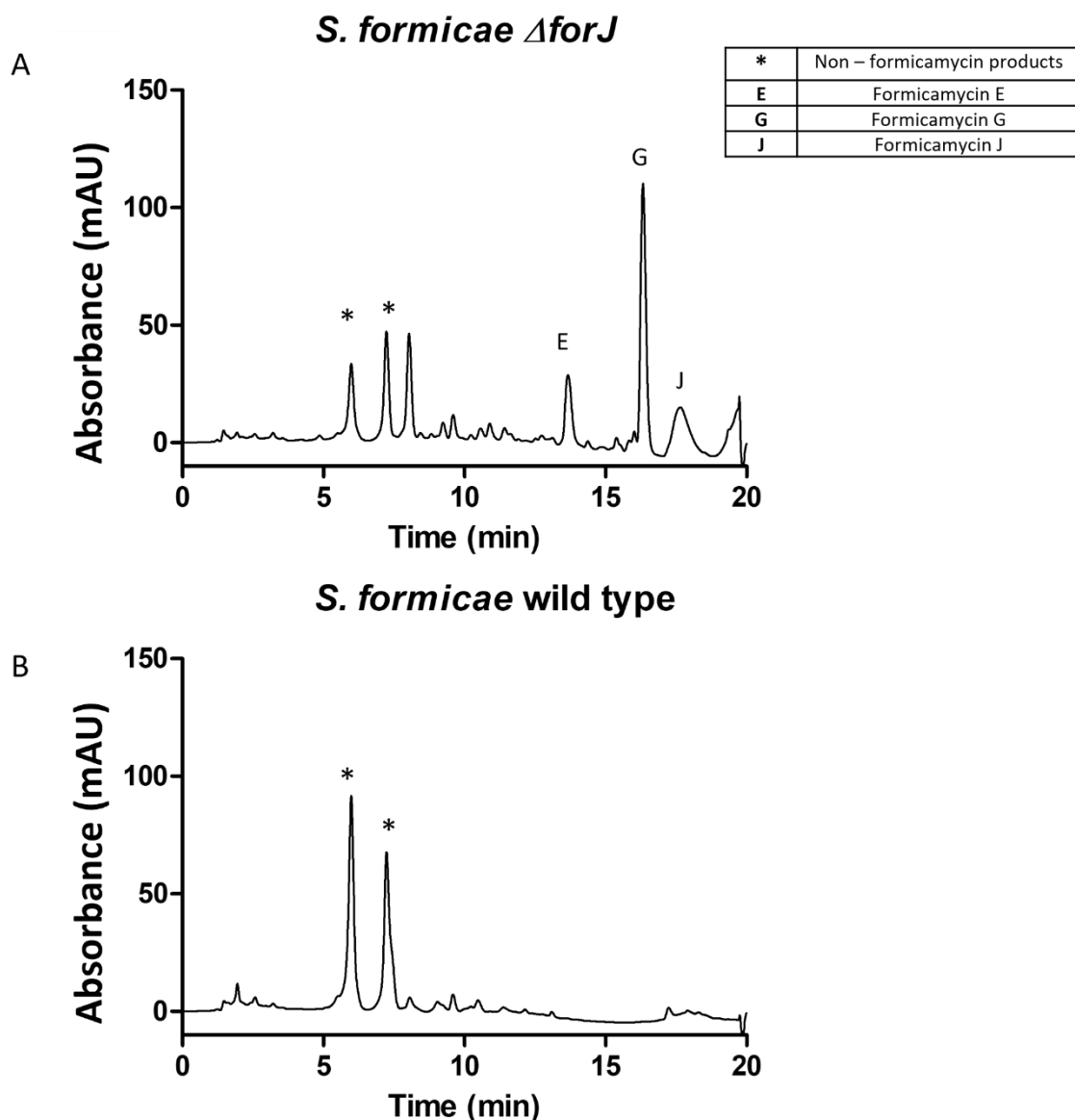
Figure 6.7 HPLC traces at 285 nm for extracts *of S. formicae ΔforJ* (**A**) and *S. formicae* wild-type (**B**) strains grown in liquid SFM media. The wild-type strain does not produce any compounds in liquid media but deletion of *forJ* leads to the switching on of formicamycin biosynthesis in liquid media, major formicamycin peaks have been labelled.

We hypothesised that any strain containing the *forJ* deletion should in theory be able to produce compounds in liquid media. An analysis of titres was conducted, all titres data for liquid SFM analysis are shown in **Figure 6.8** and **SI Table 4.**

Our analysis revealed that on average all strains containing the *forJ* deletion produced higher titres of fasamycin and formicamycin in liquid media, even when

complementation of the deletion has been attempted, in comparison to solid agar. Interestingly, fasamycin production by *S. formicae ΔforJ* was significantly reduced in liquid media when compared to agar titres, but the combined formicamycin titre was increased ~ 1.5-fold in comparison to agar production leading to a higher combined titre overall. In contrast, the high-producing *S. formicae ΔforJ+forGF* strain retained similar formicamycin titres when grown in liquid media whereas fasamycin titres increased by ~ 5-fold in comparison to agar.
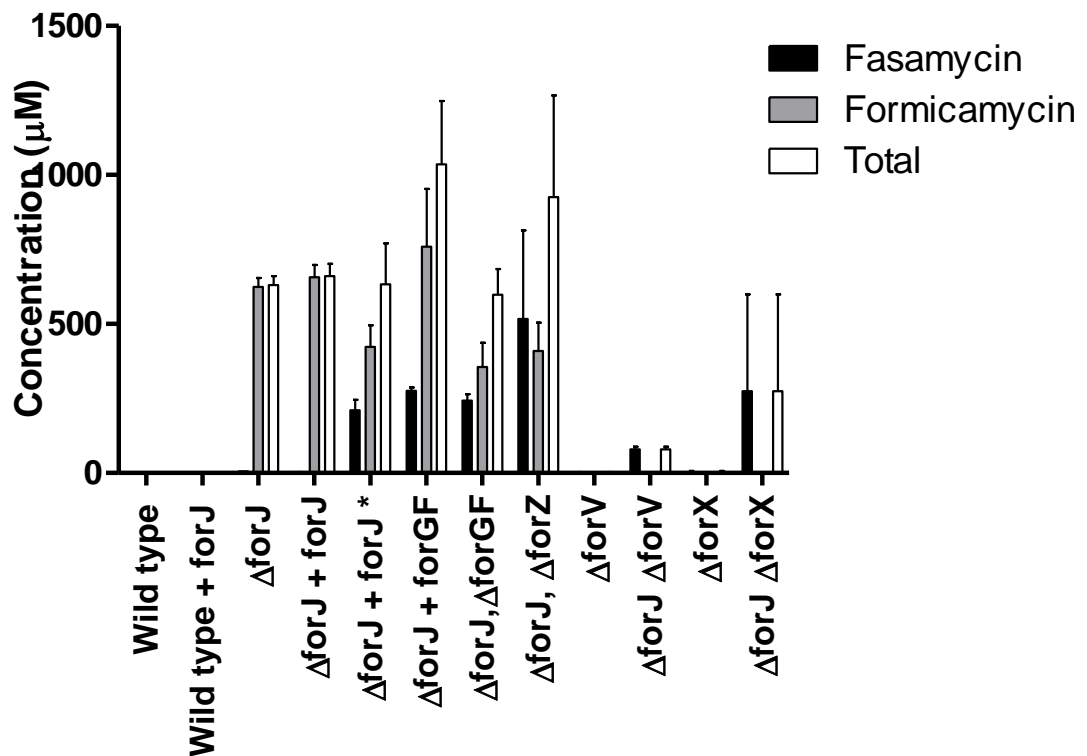
Figure 6.8 *S. formicae* strains containing deletion of *forJ* show high titres of fasamycin and formicamycin when grown in liquid SFM media. Error bars represent standard deviation from biological triplicates.

6.3 Discussion

The work in this chapter demonstrates the importance of understanding the roles played by the genes encoded within a natural product BGC. Building on a preliminary understanding of the formicamycin BGC we were able to make targeted mutations that led to an understanding of gene product function, and to the production of high yielding fasamycin and formicamycin producing strains. We showed that deletion of the two-component system (TCS), ForGF, abolished production of all metabolites from this pathway and therefore that ForGF must be important for formicamycin biosynthesis. Work by Devine *et al* (2021) has also determined that ForGF specifically activates transcription of the *for* BGC in comparison to other TCS which regulate several processes such as life-cycle development and secondary metabolism making ForGF a rare example of a cluster-situated TCS. Although rare, an example of another cluster-situated TCS is CinKR which specifically activates transcription of the cinnamycin gene cluster in *Streptomyces cinnamoneus*. Similarly to ForGF, deletion of *CinKR* also abolishes production of cinnamycin (O'Rourke, Widdick et al. 2017). ForGF clearly plays an important role in formicamycin biosynthesis however since de-repression of the *for* BGC can circumvent the loss of ForGF, it is clearly not the master regulator of the pathway.

ForJ represses the *for* BGC and deletion of *forJ* leads to increased production of formicamycin and the induction of biosynthesis during liquid culture of *S. formicae*. Several examples in the literature show that deletion of CSRs, specifically repressors, also lead to the over-production of natural products from BGCs such as the deletion of *mmyR* and *scbR2* regulators in *S. coelicolour* which causes increased production of methylenomycin and abCPK respectively (O'Rourke, Wietzorrek et al. 2009, Gottelt, Kol et al. 2010, Aigle and Corre 2012). MarR regulators generally only regulate the expression of themselves and a divergently encoded gene (Grove 2013), ChIP sequencing experiments documented in Devine et al 2021 however, show that ForJ is a rare MarR repressor in the fact that it binds several promoter regions within the *for* BGC, repressing the entire *for* BGC suggesting ForJ is the master regulator of the *for* BGC. Recent work on the fasamycin like molecules, the accramycins, also found that the MarR regulator AccJ was the master regulator of the pathway and that deletion of *accJ* from

the *acc* BGC led to not only increased compounds of accramycin A, but also the discovery of several new accramycins and several previously identified napthacemycin and fasamycin molecules (Maglangit, Zhang et al. 2020).

The third regulator of the *for* BGC, ForZ, acts in a more common way for MarR regulators in the fact that ChIP sequencing analysis determined that ForZ binds to intergenic regions to regulate its own gene expression and the expression of the gene that encodes ForAA, a transporter within this pathway (Devine, McDonald et al. 2021). We hypothesise that that formicamycin biosynthesis is a positive feedback loop and that the reduction in total metabolites seen in the *forZ* deletion strain is due to the de-repression of the transporter ForAA causing formicamycin to be constantly exported out of the cell and ultimately reducing formicamycin biosynthesis.

The formicamycins have potent bioactivity and attempts to generate resistant mutants by exposure to sub-MIC concentrations have been unsuccessful indicating a high barrier to resistance making these compounds potentially interesting clinical candidates. We have now created high producing strains that can produce the formicamycins in liquid media which is the preferred isolation method for industrially produced antibiotics. We also show that deletions of regulatory genes lead to the production of several new congeners of fasamycin and formicamycin, increasing our repertoire of analogues for investigation. The work in this chapter also contributes to several other pieces of work as documented in this thesis.

7.0 Heterologous expression of the formicamycin biosynthetic gene cluster unveils new glycosylated fasamycin compounds

7.1 Introduction

As discussed in Chapter 6, genetic manipulation of the *for* BGC yielded high-titer formicamycin producing strains due to de-repression of the BGC by deletion of *forJ* which encodes a MarR repressor that controls expression of the BGC (strain *S. formicae* D*forJ*) Devine, McDonald et al. 2021). To compliment this work, we wanted to investigate if the *for* BGC could be heterologously expressed, a technique that is used to both increase compound titers and provide a cleaner metabolic 'background' to aid purification of compounds (Huo, Hug et al. 2019).

Heterologous expression is generally undertaken in strains which have been genetically modified to reduce the number of secondary metabolites they themselves produce. This means important biosynthetic precursors, such as malonyl-CoA, can be diverted for the production of the desired compound (Gomez-Escribano and Bibb 2011). *Streptomyces* is a popular genus for the heterologous expression of large BGCs due to their natural ability to produce a wide range of structurally diverse natural products (Nah, Pyeon et al. 2017). Many techniques and *Streptomyces* heterologous expression strains have already been reported, and generally these include variants of *S. coelicolor*, *S. albus* and *S. lividans* (Gomez-Escribano and Bibb 2011). Furthermore, other rare actinomycetes have also been used as hosts, including *Saccharopolyspora erythraea* (Martin, Timoney et al. 2003, Rodriguez, Hu et al. 2003). With this knowledge in hand, we wanted to assess the ability of two heterologous host strains, *S. coelicolor* M1146 and *S. erythraea Δery* to produce the products of the formicamycin BGC. Although we did not see increased titers of formicamycins when compared to the derepressed strain *S. formicae ΔforJ*, several new compounds were identified during the course of this work and therefore a further aim of this chapter was to isolate and characterize these new molecules.

7.2 Results

7.2.1 Assessing heterologous hosts for formicamycin compound production
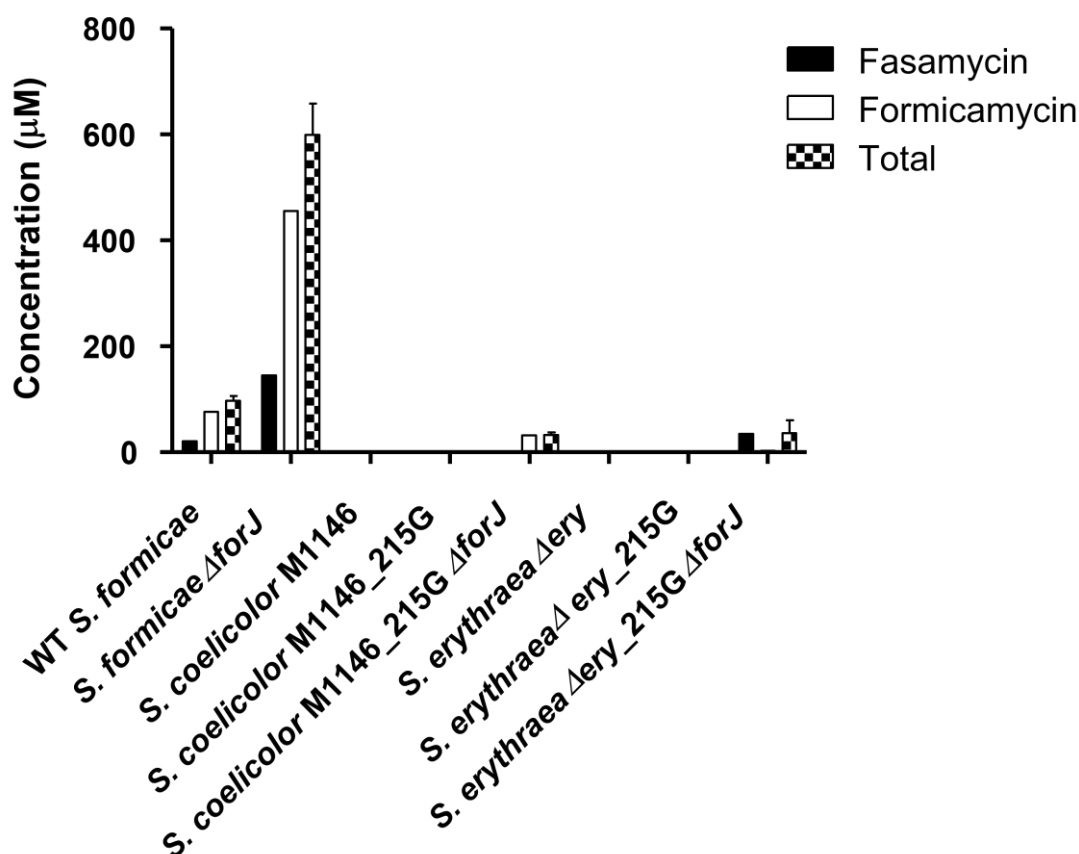
Figure 7.1 Analysis of total fasamycin, formicamycin and combined titres from *S. formicae*, *S. coelicolor* M1146 and *S. erythraea* Δ*ery* strains grown on SFM agar. Error bars represent standard deviation from biological triplicates.

Heterologous host strain construction was undertaken by Dr Abigail Alford and Dr Rebecca Devine (both JIC) using the previously engineered *Streptomyces coelicolor* M1146 (Rodriguez, Hu et al. 2003, Gomez-Escribano and Bibb 2011) and *Saccharopolyspora erythraea* Δ*ery* (a gift from Isomerase Therapeutics, Cambridge UK) strains. The previously reported phage-derived artificial chromosome (PAC) (pESAC13_215G) containing the whole formicamycin BGC (plus ~40-80 kb of additional DNA from either side of the BGC) was successfully integrated into the φC31 phage-1 integration site of both host strains via tri-parental mating into *Escherichia coli* ET12567

using the pR9604 transfer plasmid, followed by conjugal transfer to the actinomycete host yielding strains *S. coelicolor* M1146_215G and *S. erythraea* Δ*ery*_215G respectively. Given that deletion of the gene encoding the MarR regulator ForJ increases metabolite production in *S. formicae*, *forJ* was replaced with an apramycin gene in the PAC using a PCR targeting approach to yield pESAC13_215GΔ*forJ*. pEASC13_215GΔ*forJ* was then introduced into the two heterologous hosts by conjugal transfer to yield *S. coelicolor* M1146_215GΔ*forJ* and *S. erythraea* Δ*ery*_215GΔ*forJ*.

To investigate the ability of these strains to produce fasamycin and formicamycin compounds, all strains, including *S. formicae* wild-type and *S. formicae* Δ*forJ* as compound production controls, were grown in biological triplicate for 10 days at 30°C on SFM agar. Agar plugs were taken from each plate and metabolites were extracted using ethyl acetate. The solvent was removed under reduced pressure before the residues were resuspended in methanol. Extracts were subjected to liquid-chromatography mass spectroscopy (LCMS) and high-performance liquid chromatography (HPLC). Quantitative metabolite analysis to determine titres of combined fasamycin and formicamycin production (**Figure7.1** and **Table 7.1**) was achieved by comparing peak areas from HPLC analysis to those of predetermined standard calibration curves using purified fasamycin and formicamycin congeners (**SI Figures 14- 15** and **SI Tables 2- 3**).

Table 7.1 Table of titres of fasamycin, formicamycin and combined titres produced from *S. formicae*, *S. coelicolor* and *S. erythraea* strains grown on SFM agar. (*S. coelicolor M1146_215GΔforJ n=2*; all other strains *n*=3)*.

Strain	Titre (µM)		
	Fasamycins	Formicamycins	Combined fasamycins and formicamycins
WT *S. formicae*	20.6 ± 6.1	75.5 ± 3.5	96.1 ± 9.6
S. formicae Δ*forJ*	144.3 ± 21.0	455.0 ± 38.1	599.3 ± 59.1
S. coelicolor M1146	0	0	0
S. coelicolor M1146_215G	0	0	0
S. coelicolor M1146_215GΔ*forJ*	0.4 ± 0.3	31.2 ± 5.1	31.6 ± 5.4
S. erythraea Δ*ery*	0	0	0
S. erythraea Δ*ery*_215G	0	0	0

|			
S. erythraea Δ*ery_*215GΔ*forJ*	33.4 ± 21.1	2.1± 1.3	35.5 ± 24.4

The control strains *S. formicae*, and *S. formicae* Δ*forJ* produced the expected levels of fasamycin and formicamycin congeners as reported previously (Devine, McDonald et al. 2021) (**Table 7.1**). *S. coelicolor* M1146_215G and *S. erythraea* Δ*ery_*215G showed no evidence of fasamycin or formicamycin production, but both de-repressed strains *S. coelicolor* M1146_215GΔ*forJ* and *S. erythraea* Δ*ery_*215GΔ*forJ* showed evidence of compound production. *S. coelicolor* M1146_215GΔ*forJ* produced several previously identified fasamycin (C-E) and formicamycin (A-D and H) congeners. Upon titre analysis it was found that fasamycin production was severely reduced in this strain in comparison to *S. formicae* wild-type (0.4 ± 0.3 vs 20.6 ± 6.1 µM) and formicamycin congener production was found to be approximately half that of *S. formicae* wild-type (31.2 ± 5.1 vs 75.5 ± 3.5 µM). *Streptomyces coelicolor* M1146_215GΔ*forJ* global production fell short of *S. formicae* Δ*forJ* total metabolite production by approximately 20-fold, indicating that *Streptomyces coelicolor* M1146_215GΔ*forJ* is not a suitable heterologous host for over-expression to scale up the production of formicamycin congeners (**Table 7.1**).

S. erythraea Δ*ery_*215GΔ*forJ* showed even less potential as a heterologous host strain with very low levels of fasamycins, mostly fasamycin C, and only two formicamycins (A and B) being produced in trace quantities. Global titres from *S. erythraea* Δ*ery_*215GΔ*forJ* were found to be approximately 3-fold less than *S. formicae* wild-type, although the fasamycin titres were comparable to that of *S. formicae* wild-type (33.4 ± 21.1 vs 20.6 ± 6.1 µM) while formicamycin production was severely reduced. The titres for *S. erythraea* Δ*ery_*215GΔ*forJ* also fell dramatically short of those observed from *S. formicae* Δ*forJ.* These results indicate that neither of these strains are suitable heterologous hosts for the scale-up of fasamycin and formicamycin production.

7.2.2 Identification of new fasamycin like congeners

Close inspection of the *S. erythraea* Δ*ery_*215GΔ*forJ* HPLC chromatograms indicated the presence of six previously unidentified peaks which displayed the characteristic fasamycin chromophore (λ_{max} 250, 290, 350 and 420 nm) (**SI Figure 16**). These were

notable for their early elution times on reverse phase chromatography, indicating that they were more polar than all other characterised fasamycin congeners (**Figure 7.2**).
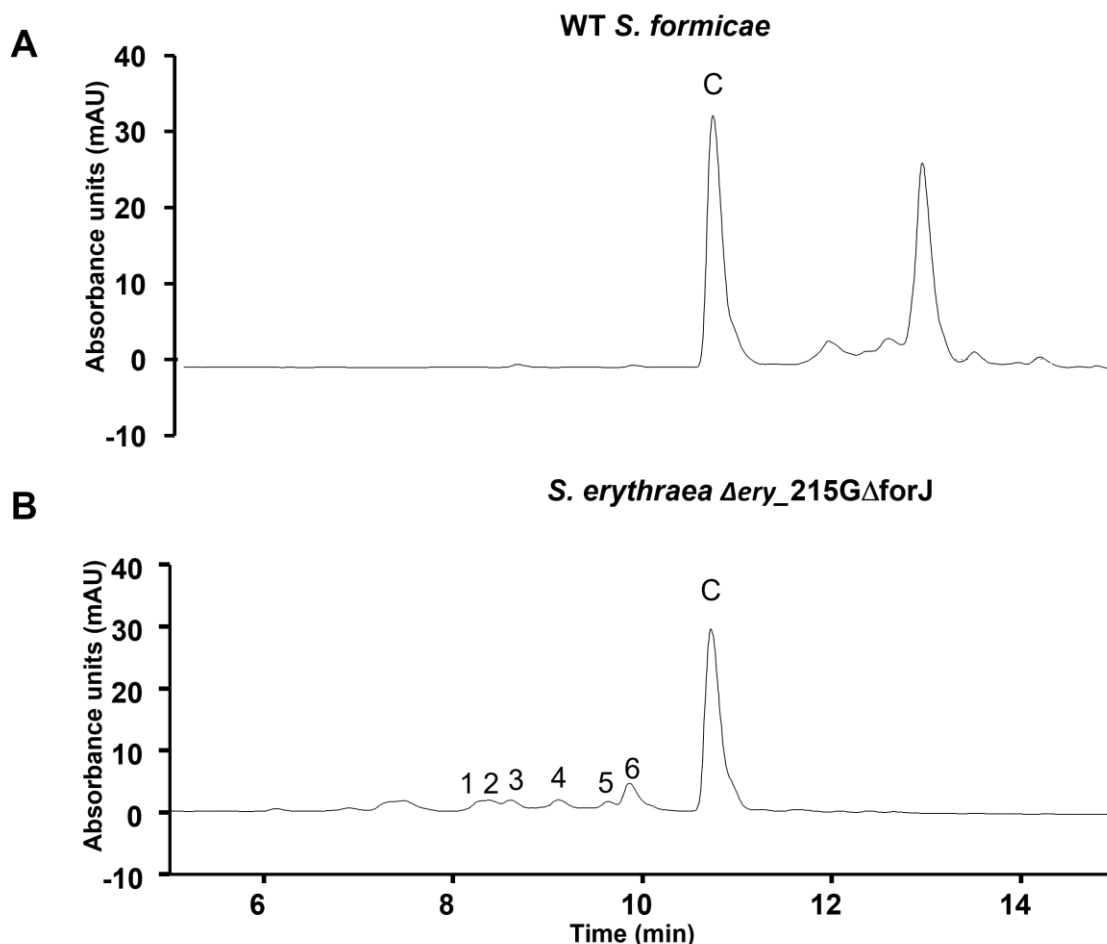

Figure 7.2 Chromatograms at 418 nm of *S. formicae* wild-type (**A**) and *S. erythraea* Δ*ery*_215GΔ*forJ* (**B**) grown on SFM agar. Labels 1-6 indicate previously unidentified peaks; C- fasamycin C. Extracts were analysed by HPLC using a Phenomenex Gemini NX C18 column (150 × 4.6 mm).

Preliminary LCMS analysis revealed that these six new peaks (1-6) contained compounds with mass to charge ratios indicative of the glycosylation of known fasamycins (e.g. increases of *m/z* values by 162 Da over the known fasamycin, indicative of hexose addition). To confirm that these new potential compounds were indeed glycosylated fasamycins we set out to isolate and characterise them.

Growth of *S. erythraea* Δ*ery*_215GΔ*forJ* was upscaled (1 L) on SFM agar and grown at 30°C. After for 10 days the agar was extracted with ethyl acetate and the resulting organic extract was purified by flash chromatography and preparative HPLC.

Surprisingly, after this purification we were only able to isolate the previously identified peak 2 observed during analytical analysis (**Figure 7.2**) and two further new peaks 7 and 8 from this fermentation; peaks 7 and 8 showed masses indicative of fasamycin congeners glycosylated with a uronic acid (**Figure 7.3**). Upon re-inspection of the original upscaled extract by LCMS, it became clear that the previous peaks 1,3,4,5 and 6 (identified by analytical HPLC) were present in only trace quantities; retrospective analysis of analytical samples revealed that peaks 7 and 8 were also present in the original analytical fermentations but only at trace levels. On this basis a second upscaled (6 L) fermentation of *S. erythraea* Δ*ery*_215GΔ*forJ* was undertaken; analysis of the resulting extract showed it matched the original HPLC profile with peaks 1-6 present (but not 7 and 8). Compounds 1-6 were then purified from this extract by flash chromatography and reversed-phase chromatography as described for the first upscaled extract.
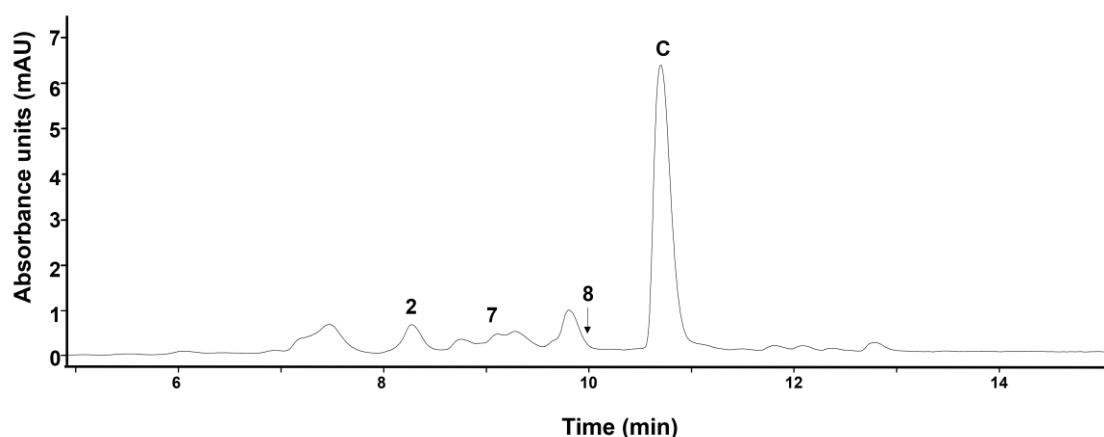
Figure 7.3 LCMS chromatogram from first *S. erythraea* Δ*ery*_215GΔ*forJ* upscaled fermentation. 2, previously identified peak; 7 and 8, new peaks; C, fasamycin C. Extracts were analysed by HPLC using a Phenomenex Gemini NX C18 column (150 × 4.6 mm).

## 7.2.3 Isolation and mass spectrometry analysis of new compounds

As noted, eight samples were isolated from the two upscaled growths of *S. erythraea* Δ*ery*_215GΔ*forJ*. These were subjected to detailed chemical analysis using LCMS/MS, high-resolution MS/MS fragmentation, 1D and 2D NMR, and high-performance anion

exchange chromatography with pulsed amperometric detection (HPAEC-PAD) experiments. On this basis the structures of these new compounds were determined, although for two samples it became clear that more than one compound was present in the sample; for these the structures of some components could not be determined with certainty, although proposals were made. **Table 7.2** summarises each of the sample's identities including which upscaled fermentation each sample was identified in and the compounds present.

As shown in **Table 7.2**, fraction 1 contained three distinguishable compounds **1 a-c** and fraction 5 contained 2 compounds (**5a** and **5b**). Both fractions 1 and 5 contained a major compound, **1c** and **5a** respectively; the other identified compounds (**1a-b** and **5b**) were of insufficient quantity for full structural elucidation. On this basis, only compounds **1c**, **2**, **3, 4**, **5a**, **6**, **7** and **8** will be discussed henceforth.

Table 7.2 Compounds identifiable from LCMS analysis in each of the 8 fractions obtained.

Analytical HPLC Chromatogram Peak	Preparative HPLC Fraction Number	Compounds in sample
Figure 7.2B, Peak 1	1	**1a, 1b, 1c**
Figure 7.2B, Peak 2	2	**2**
Figure 7.2B, Peak 3	3	**3**
Figure 7.2B, Peak 4	4	**4**
Figure 7.2B, Peak 5	5	**5a, 5b**
Figure 7.2B, Peak 6	6	**6**
Figure 7.3, Peak 7	7	**7**
Figure 7.3, Peak 8	8	**8**
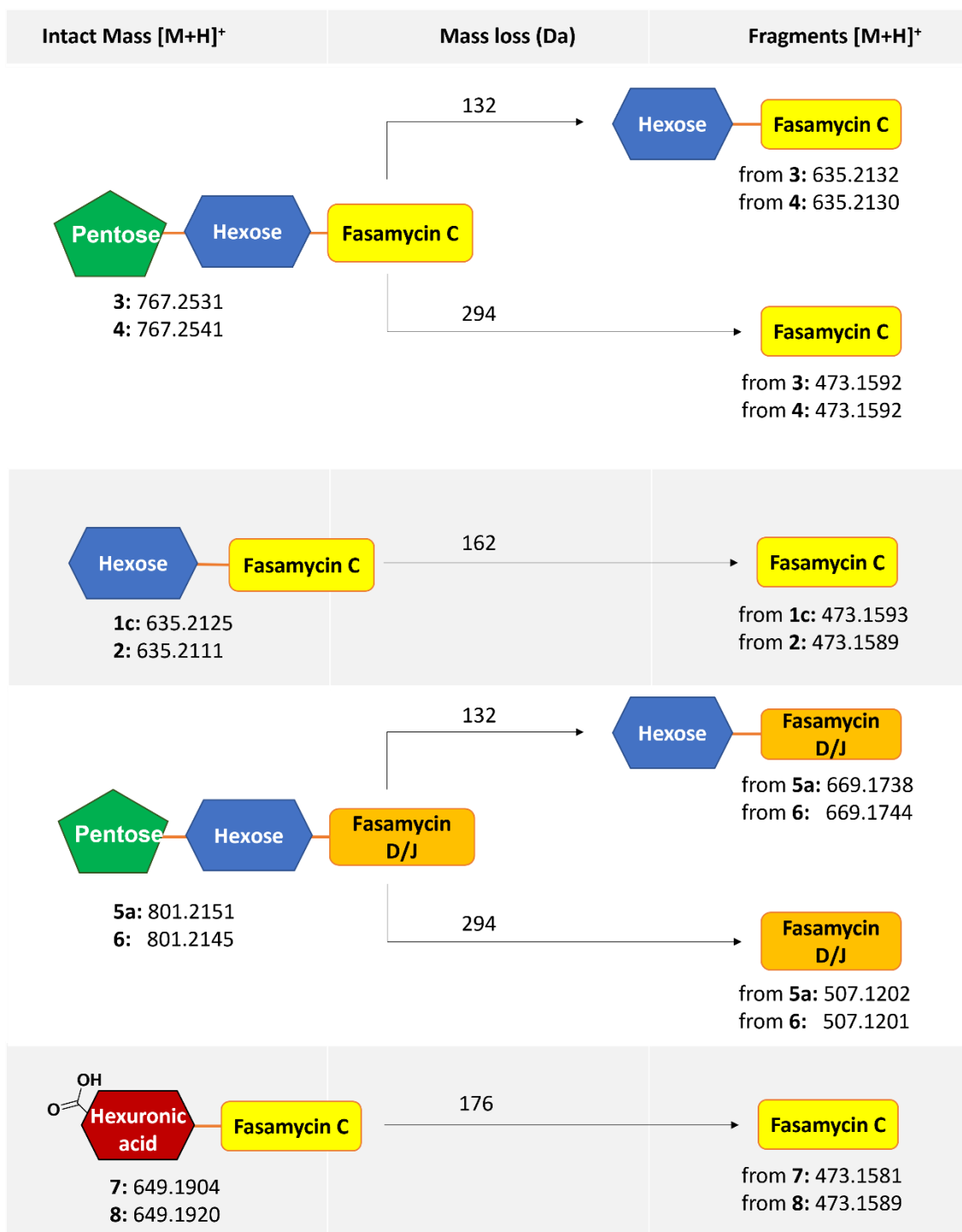
Figure 7.4 Diagrammatic representation of LCMS/MS analysis of fractions 1-8 which reveals masse to charge ratios of new compounds **1c**-**5a** and **6**-**8**; predicted aglycones and sugars are shown.

Each fraction (1-8) was subjected to Liquid Chromatography with tandem mass spectrometry (LCMS/MS). The identified intact m/z [M+H]$^+$ of the main species of each fraction are shown in **Figure 7.4**, using these mass-to-charge ratios and fragmentation data we were able to propose which of the fasamycin congeners comprised the

aglycones and whether the intact mass-to-charge ratios corresponded to the potential addition of an individual hexose, a disaccharide (hexose-pentose) or a hexuronic acid for each of the individual compounds.

High-resolution mass spectrometry (HRMS) of the fraction containing **compound 1c** indicated the presence of species with molecular formulae $C_{34}H_{34}O_{12}$ (**1c**: m/z 635.2125 $[M+H]^+$, calc. for $C_{34}H_{35}O_{12}^+$ 635.2123, Δ = 0.3 ppm). LCMS/MS fragmentation of the molecular ion with m/z 635.2125 showed a fragment with m/z 473.1593 $[M+H]^+$ generated from the loss of 162 Da which we propose corresponds to a single hexose unit. We propose that the fragment with m/z 473.1593 $[M+H]^+$ corresponds to the mass of a fasamycin C adduct.

HRMS of the fraction containing **compound 2** indicated the presence of species with molecular formulae $C_{34}H_{34}O_{12}$. (m/z 635.2111 $[M+H]^+$ calc. for $C_{34}H_{35}O_{12}^+$ 635.2123, Δ= -1.9 ppm). Similar to **1c**, a fragment was observed with a loss of 162 Da, indicative of a hexose, to give an aglycone fragment with m/z of 473.1589 ($C_{28}H_{24}O_7$) consistent with an fasamycin C adduct.

Compound 3 differed from **1c** and **2** as the species was determined to have an m/z of 767.2531 $[M+H]^+$ (calc for $C_{39}H_{43}O_{16}^+$ 767.2546, Δ = -2.0 ppm) which indicated a molecular formula of $C_{39}H_{42}O_{16}$. MS/MS analysis revealed two fragments. The first showed m/z of 635.2132 $[M+H]^+$ corresponding to a loss of 132 Da suggesting loss of a pentose and m/z of 473.1592 $[M+H]^+$ corresponding to loss of 294 Da suggesting loss of a pentose plus hexose (disaccharide). As we did not observe an ion for loss of a hexose without loss of the pentose we hypothesise a proximal hexose with terminal pentose.

Compound 4 was determined to have a molecular formulae of $C_{39}H_{42}O_{16}$ (m/z 767.2541 $[M+H]^+$ calc for $C_{39}H_{43}O_{16}^+$ 767.2546, Δ = -0.7 ppm). Like **compound 3**, two diagnostic fragments were identified with m/z of 635.2130 $[M+H]^+$ corresponding to a loss of 132 Da suggesting a pentose, and m/z of 473.1592 $[M+H]^+$ corresponding to loss of 294 Da suggesting loss of a disaccharide (pentose plus hexose). As with **3** we did not observe an ion for loss of a hexose without loss of the pentose and together these data suggested a proximal hexose with terminal pentose.

HRMS of fraction 5 found **compound 5a** to have a *m/z* 801.2151 [M+H]$^+$. This species showed a characteristic isotope pattern for a singly chlorinated molecule, and the molecular formulae was proposed to be $C_{39}H_{41}ClO_{16}$ (calc for $C_{39}H_{42}ClO_{16}^+$ 801.2126, Δ= 3.1 ppm). Two fragments were seen by MS/MS, the first with *m/z* of 669.1738 [M+H]$^+$ corresponding to a loss of 132 Da and suggesting loss of a pentose, and a second with *m/z* of 507.1202 [M+H]$^+$ corresponding to loss of 294 Da and suggesting loss of a disaccharide (pentose plus hexose). This indicated the aglycone to be either fasamycin D (isolated from *S. formicae*) or fasamycin J isolated from *Streptomyces* sp. KIB-1414 (Yuan, Wang et al. 2020). Again we did not observe an ion for loss of a hexose without loss of the pentose by MS/MS, and together this data suggested a proximal hexose with terminal pentose.

HRMS of **Compound 6** indicated a species with *m/z* 801.2145 [M+H]$^+$ corresponding to the molecular formulae $C_{39}H_{41}ClO_{16}$ (calc for $C_{39}H_{42}ClO_{16}^+$ 801.2156, D = -1.4 ppm). As with **compound 5a**, the isotope pattern indicated a singly chlorinated species. MS/MS analysis of **6** revealed two diagnostic fragments with *m/z* of 669.1744 [M+H]$^+$, corresponding to a loss of 132 Da suggesting loss of a pentose, and *m/z* of 507.1201 [M+H]$^+$ corresponding to loss of 294 Da suggesting loss of a disaccharide (pentose plus hexose); we did not observe an ion for loss of a hexose without loss of the pentose by MS/MS and together this data suggested a proximal hexose with terminal pentose.

The intact ion of **compound 7** was found to have *m/z* 649.1904 [M+H]$^+$ indicating a molecular formulae of $C_{34}H_{32}O_{13}$ (calc for $C_{34}H_{33}O_{13}^+$ 649.1916, Δ= -1.8 ppm). In-source fragmentation revealed a fragment with a *m/z* of 473.1581 [M+H]$^+$, indicating a fasamycin C aglycone and a loss of 176 Da which is indicative of a hexauronic acid.

We propose **compound 8** is a structural isomer of **7** as HRMS gave a parent ion with *m/z* 649.1920 [M+H]$^+$ (calc for $C_{34}H_{33}O_{13}^+$ 649.1916, Δ = 0.6 ppm) indicating a molecular formula of $C_{34}H_{32}O_{13}$. In source-fragmentation gave a single fragment with *m/z* of 473.1589 [M+H]$^+$ (calc for $C_{28}H_{25}O_7^+$ 473.1595, Δ= -1.3 ppm) consistent with an fasamycin C aglycone. Again, we propose a hexauronic acid is responsible for the 176 Da loss.

Although LCMS/MS analysis had provided us with a detailed understanding of these compounds, there were limitations and structural details that we could not determine by these methods alone. Therefore, further structural investigations were undertaken.

7.2.4 Structural elucidation by NMR and carbohydrate analysis.
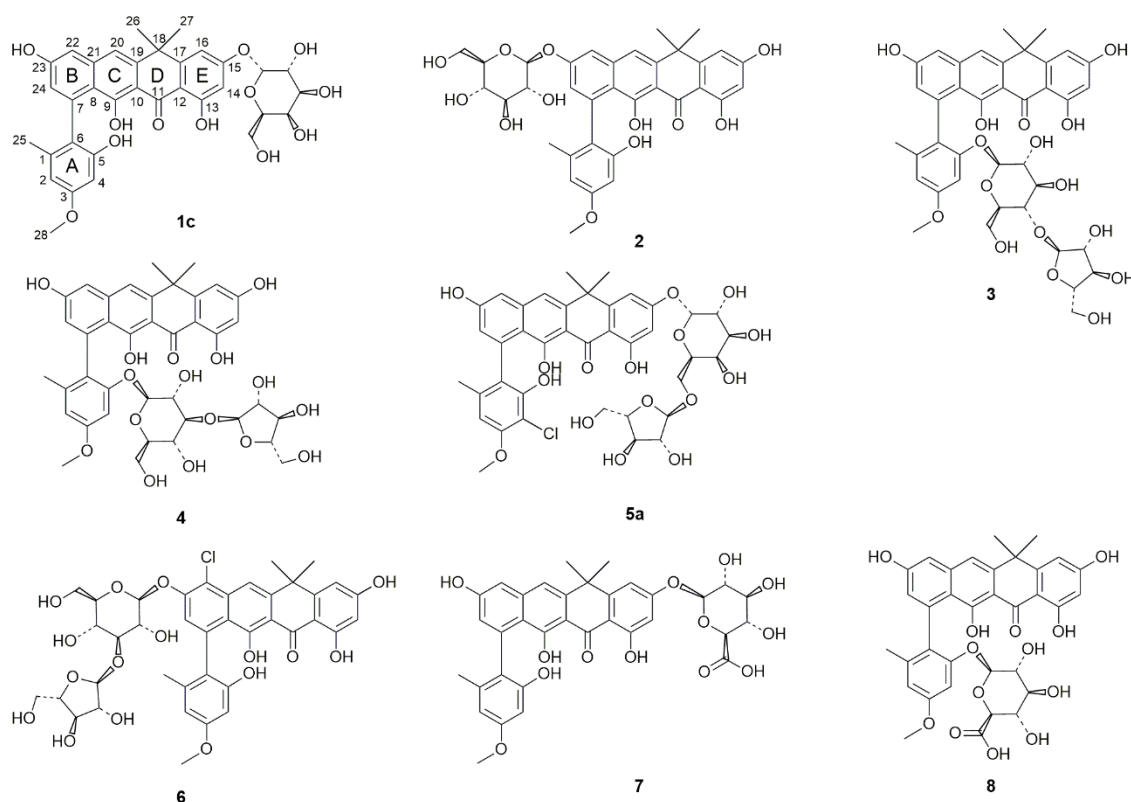
Figure 7.5 Chemical structures of new glycosylated fasamycins as determined by 1D and 2D NMR, LCMS/MS, and carbohydrate analysis.

To enable the structural characterisation of the newly identified compounds, 1D (^{1}H and ^{13}C) and 2D (COSY, NOESY, HSQC-edited, HSQC-coupled, HMBC and ROESY) NMR spectra were recorded for each sample. NMR analysis and experiments were undertaken by Dr Sergey Nepogodiev of the NMR Platform at JIC with the help of Dr Edward Hems. Overall, analysis of chemical shifts and coupling constants of the fasamycin aglycone in the ^{1}H NMR spectra of samples 1-8 revealed close similarity to the ^{1}H NMR spectra reported for fasamycin C or the monochlorinated fasamycins D and J (Qin, Munnoch et al. 2017,

Yuan, Wang et al. 2020). However, as a result of glycosylation, some chemical shifts displayed noticeable changes. Those changes, together with ROESY and HMBC correlations (if available), were used to elucidate the regiochemistry of O-glycosylation; fasamycin aglycones have a total of five hydroxy groups that are potentially available to form O-glycosidic linkages. Furthermore, the ring size and anomeric configuration of the saccharide units were established using characteristic carbohydrate J couplings and chemical shifts of anomeric signals in the ^{1}H and ^{13}C NMR spectra (Agrawal 1992). While relative configurations of glycoside residues attached to the compounds in samples 1-8 were determined with great confidence, the assignment of absolute configurations was not determined. As such we represent the carbohydrate units with the configurations most commonly found in nature (D-Glc, D-Gal and L-Ara) but with hollow wedges and dashed lines following accepted convention (Maehr 2002).

Carbohydrate analysis and aglycone identity was confirmed by Dr Edward Hems (JIC) using high performance anion exchange chromatography with pulsed amperometric detection (HPAEC-PAD) and LCMS respectively. For carbohydrate and aglycone analysis, samples were first hydrolysed by heating in 1.0 M aqueous trifluoroacetic acid and the resulting polar monosaccharides were separated from the lipophilic fasamycin aglycone using a C18 SPE cartridge. The identity of the fasamycin aglycone for samples 1-4 was confirmed by LCMS in comparison with an authentic fasamycin C standard. The identity of the fasamycin aglycone for sample 5 was confirmed by NMR analysis, although there was insufficient material from sample 6 for NMR. Aglycone analysis was not performed after hydrolysis of samples 7 and 8 but inferred from other data including the NMR data for the glycoside.

Table 7.3 Fasamycin aglycone and carbohydrate identities of isolated compounds **1-8**.

Compound	Fasamycin aglycone	Carbohydrate
1c	Fasamycin C	Galactose
2	Fasamycin C	Glucose
3	Fasamycin C	Glucose and arabinose
4	Fasamycin C	Glucose and arabinose
5a	Fasamycin J	Galactose and arabinose
6	Fasamycin D	Galactose and arabinose
7	Fasamycin C	Glucuronic acid
8	Fasamycin C	Glucuronic acid

The proposed structures of the new compounds are shown in **Figure 7.5** and determined fasamycin aglycone and constituent carbohydrates of each of the compounds are detailed in **Table 7.3**.

Compound 1c was confirmed to consist of a fasamycin C aglycone by analysing the liberated aglycone (post acid hydrolysis for carbohydrate analysis) via LCMS in comparison to an authentic standard. Additionally, ^{1}H NMR resonances were consistent with this aglycone being fasamycin C. Due to the multiple species present in this sample, HPAEC-PAD analysis revealed the presence of three carbohydrates: glucose, galactose and arabinose. The glycosidic region of **1c** contained seven signals consistent with the single hexose glycoside as proposed by LCMS analysis. Glycosidic signals were assigned using COSY spectra and correlated with ^{13}C chemical shifts using HSQC spectra. Chemical shift of the ^{13}C anomeric signal and *J* coupling values suggested a pyranose with a 1,2-*cis*-configuration and comparison of the measured ^{1}H and ^{13}C data for **1c** alongside data of various glycopyranosides in the literature allowed us to define the glycosidic component as 1,2-*cis*-galactopyranoside indicating that galactose was the carbohydrate attached to this compound (Uhrínova, Uhrían et al. 1991). ROESY spectra were used to confirm the regiochemistry of the linkage to fasamycin C and we propose glycosylation at O15 on ring E of fasamycin C. The structure of **1c** has therefore been defined as 15-*O*-(α-galactopyranosyl)-fasamycin C.

The aglycone of **compound 2** was determined to be fasamycin C by LCMS analysis of the aglycone produced by acid hydrolysis. HPAEC-PAD analysis indicated a single carbohydrate that was confirmed to be glucose by comparison with an authentic standard and this was further supported by characteristic ^{13}C and ^{1}H NMR signals which determined the identity as 1,2-*trans*-glucopyranose. The regiochemistry of glycosylation was determined to be O23 of ring B on fasamycin C using HMBC cross peak data and through-space interactions indicated by ROESY spectra. We therefore propose the structure to be 23-*O*-β-glucopyranosyl-fasamycin C.

The **compound 3** aglycone was confirmed to be fasamycin C by LCMS analysis after hydrolysis, and this was supported by characteristic ^{1}H data in comparison to fasamycin C. Furthermore, HPAEC-PAD analysis indicated the presence of two carbohydrates: glucose and arabinose in a 1:1 ratio. Analysis of COSY and HSQC spectra established that the disaccharide component consisted of a terminal 1,2-*trans*-arabinofuranose residue attached to O4 of a proximal 1,2-*trans*-glucopyaranose. The 1,4-glycosidic linkage was supported by the ROESY spectra and HMBC cross peak analyses. The regiochemistry of glycosylation of fasamycin C by the disaccharide was assigned by an HMBC cross peak, as well as a through-space interaction in the ROESY spectra which indicated glycosylation of ring A at O5 of fasamycin C. Taken together compound 3 was determined to be 5-*O*-(4-*O*-(α-arabinofuranosyl)-β-glucopyranosyl)-fasamycin C.

HPAEC-PAD analysis of **compound 4** showed the presence of glucose and arabinose peaks in a 1:1 ratio. The resulting aglycone from acid hydrolysis was confirmed to be fasamycin C by LCMS by comparison to an authentic standard. Similar to **compound 3**, the disaccharide was determined to consist of a terminal 1,2-*trans*-arabinofuranose moiety with a proximal 1,2-*trans*-glucopyranose. HMBC correlations allowed us to determine that α-arabinofuranose is attached to the β-glucopyranose at O3 and from the ROESY spectra it was apparent that the glucosyl residue is attached to O5 of ring A of the fasamycin C aglycone. Therefore **compound 4** was determined to be 5-*O*-(3-*O*-(α-arabinofuranosyl)-β-glucopyranosyl)-fasamycin C.

The aglycone of **compound 5a** had been hypothesised to be either fasamycin D or fasamycin J, but due to lack of authentic standards of either compound the aglycone was determined by ^{1}H NMR and comparison to the previously published spectra. We had already determined that this sample contained a major (**5a**) and minor (**5b**) species and HPAEC-PAD analysis indicated the presence of three carbohydrates: galactose, glucose and arabinose (1:1:1). MS/MS analysis had previously indicated a species containing a disaccharide but no evidence of a trisaccharide and we therefore propose one of the carbohydrates belongs to the minor species. ^{1}H NMR spectra and HSQC spectra determined the presence of an α-galactopyranosyl residue. Furthermore, analysis of HSQC and HMBC spectra identified chemical shifts that were characteristic for furanosides which we assigned to an α-arabinofuranosyl residue and this residue was determined to be attached to the α-galactopyranosyl residue at O6 as determined by ROESY spectra and HMBC. Furthermore, the glycosylation was found to be at O15 on ring E of fasamycin J. HPAEC-PAD analysis revealed the presence of three carbohydrates and we propose that the presence of glucose can be attributed to the presence of the minor species **5b**. Taken together we assign the structure of **compound 5a** to be 15-*O*-(6-*O*-(α-arabinofuranosyl)-α-galactopyranosyl)-fasamycin J.

HPAEC-PAD analysis of **compound 6** showed the presence of two carbohydrate peaks corresponding to galactose and arabinose in a 1:1 ratio. We had previously shown that the aglycone of **6** was either the monochlorinated fasamycin D or fasamycin J. Careful inspection of NMR spectra allowed us to assign the aglycone of this compound to be fasamycin D. This was further supported by the observation that aglycones from **5a** and **6** had different retention times by LCMS. Analysis of COSY and HSQC spectra established a disaccharide which consisted of a terminal 1,2-*trans*-arabinofuranose residue attached to O3 of a proximal 1,2-*trans*-glucopyaranose, and the 1,3-glycosidic linkage was further supported by cross peaks in the ROESY spectra. The regiochemistry of fasamycin glycosylation was determined by ROESY correlations and HMBC cross peak data which indicated glycosylation of O23 on ring B of fasamycin D. The structure of **6** was thus determined as 23-*O*-(3-*O*-α-arabinofuranosyl)-β-glucopyranosyl)-fasamycin D.

The aglycone of **compound 7** was determined to be fasamycin C by comparison to previously published fasamycin C NMR spectra. However, noticeable differences

between the aromatic proton shifts of **7** and fasamycin C suggested the glycosylation of O15 on ring E of fasamycin C. HPAEC-PAD analysis revealed the presence of a single carbohydrate species, glucuronic acid. The carbohydrate region of the ^{13}C spectra of **7** showed resonances consistent with glucopyranosiduronic acid. We thus propose the structure of **7** to be 15-*O*-(β -glucopyranosyluronic acid)-fasamycin C**.**

HPAEC-PAD analysis of **compound 8** revealed the presence of a single carbohydrate, and, like **7**, this was determined to be glucuronic acid. The carbohydrate region of the ^{1}H NMR spectra of **8** showed resonances that were consistent with a glucopyranosiduronic acid moiety, similar to **7**. HMBC spectra provided support for O5 on ring A of fasamycin C as the site of glycosylation, and this was further supported by ROESY data. The combined data for **compound 8** allowed us to assign its structure as 5-*O*-(β-glucopyranosyluronic acid)-fasamcyin C.

7.2.5 Bioactivity of compounds 1-6

The newly identified compounds were tested for their antibacterial activity against a panel of indicator strains including *Bacillus subtilis, Staphylococcus aureus* and *Escherichia coli*. Compounds **1**-**6** exhibited no bioactivity against any of the bioassay strains at concentrations up to 120 μg/ml. These results contrasted strongly with the recent description of two structurally related molecules called naphthacemycins D_1 and D_2 that were isolated from *Streptomyces* sp. N12W1565. These are glycosylated fasamycin congeners that were reported to be moderately bioactive against MRSA (MIC ~ 17 μg/ml), *B. subtilis* (MIC ~ 24 μg/ ml), *E. coli* (MIC ~ 30 μg/ ml) and *Pseudomonas aeruginosa* (MIC ~ 40 μg/ ml) (Gao, Nie et al. 2022)*.* We hypothesise that either alteration of the fasamycin backbone via glycosylation, a known detoxification mechanism in microorganisms, abolishes the bioactivity of our glycosylated compounds, or that the concentrations that our compounds were tested at were not sufficient to observe antibacterial activity.

7.3 Discussion

In this chapter we showed that the heterologous expression of the *for* BGC does not lead to improved titers of formicamycin and fasamycins, at least for the two strains described

here. Despite this it does highlight the phenomenon that heterologous expression of BGCs can lead to the production of new congeners. It also demonstrated the power of metabolomics methods to identify new compounds. Mass spectroscopy (MS) is a century old technology, however, in the huge improvements in the resolution and accuracy of MS have revolutionized the way scientists, especially natural products scientists, are able to characterize complex biological samples (Bouslimani, Sanchez et al. 2014). MS methods are of fundamental importance for processes such as the identification of known compounds (dereplication) from new antimicrobial extracts and for determining accurate (<5 ppm) mass-to-charge ratios. Furthermore, the addition of highly sensitive chromatographic methods, such as liquid and gas chromatography, alongside MS has added an extra dimension to the power of the individual techniques and allowed for accurate and sensitive analyses of biological samples to be made (Pitt 2009). In recent years, MS methods, particularly MS/MS, have been used in combination with NMR and X-ray crystallography to determine the structures of compounds such as cyclic peptides (Ng, Bandeira et al. 2009). Furthermore, several frameworks have now been developed to aid in structural elucidation using MS fragmentation data such as the fragmentation tree basic local alignment search tool (FT-BLAST) (Rasche, Scheubert et al. 2012). The work presented here further highlights the usefulness of MS methods for the determination of natural product structures. We show that relatively accurate chemical structures can be predicted for samples of low quantity and which contain multiple components just using HRMS and MS/MS methods. These projections provide an excellent framework for which structures can be confirmed using 1D and 2D NMR. Bioassays found that none of the compounds described in this study had antimicrobial properties at any concentration below 120 µg/ml, therefore these compounds would have been missed using the usual activity guided fractionation methods, further proving the usefulness of MS methods for discovery of new chemistry.

Although the compounds detailed in this chapter are novel, the finding of glycosylated fasamycin-like compounds is not. Two glycosylated napthacemycins, napthacemycin D_1 and napthacemycin D_2, were recently reported from *Streptomyces* sp. N12W1565 (Gao, Nie et al. 2022). A glycosyltransferase, NatY, not encoded within the napthacemycin BGC, was shown to be responsible for the glycosylation of these particular compounds. Analysis of the *S. erythraea* genome identified a homologue of NatY (with 43% identity) which is a member of the Yjic family of flavonoid glycosyltransferases. We hypothesize

this homologue may be responsible for at least some of the glycosylation reactions needed to generate compounds **1**-**8**. We found no homologue of NatY encoded in the native producer of formicamycins, *S. formicae*.

We determined that one of the glycosylated compounds discovered in this work (**compound 5a)** has fasamycin J as the aglycone. This is a singly halogenated congener that had previously been reported from *Streptomyces* sp. KIB-1414 (Yuan, Wang et al. 2020) but not from *S. formicae*. This interesting observation indicates that *S. formicae* has further potential to produce additional fasamycin congeners to the ones we have previously identified.

Overall, the work in this chapter highlights the ability to find compounds with interesting chemistry from the heterologous expression of well characterized BGCs. Furthermore, this work contributes to the plethora of fasamycin and fasamycin-like compounds that have been discovered from different actinomycetes (Fukumoto, Kim et al. 2017, Maglangit, Zhang et al. 2020, Yang, Li et al. 2020, Yuan, Wang et al. 2020).

8.0 Conclusions and further work

8.1 The formicamycin compounds are potentially clinically interesting compounds exhibiting a dual-targeting mode of action

Prior to the start of this project, work in the Wilkinson and Hutchings labs had identified a new class of pentacyclic polyketide compounds, the formicamycins, from *Streptomyces formicae,* a novel strain isolated from a plant-ant symbiosis (Qin, Munnoch et al. 2017). These new compounds, alongside their biosynthetic intermediates, the fasamycins, had been found to display potent bioactivity against clinically relevant pathogens such as MRSA and VRE. Formicamycins were also found to display a high barrier to resistance, with no resistance generated to *B. subtilis* strains after 20 days of sub inhibitory concentration exposure. Although the fasamycin compounds isolated from *S. formicae* were novel, the class of compounds had previously reported by Feng et al. (2012), who isolated fasamycin A and B from the heterologous expression of environmental DNA. Fasamycin A and B were identified to be inhibitors of bacterial type II fatty acid synthesis (FAS-II) through the inhibition of the essential elongation condensation enzyme FabF (Feng, Chakraborty et al. 2012). However, prior to the start of this project there had been no attempts at characterising the target and mechanism of action of the formicamycin compounds.

During this work, MIC determination of 9 fasamycin, 14 formicamycin and 6 formicalactone compounds isolated from wild-type and mutated *S. formicae* strains has allowed us to gain a preliminary understanding of the effect of compound structure, of both fasamycin and formicamycin, on the ability to inhibit specific bacterial strains. Furthermore, we have determined that both classes of compound inhibit growth of two archaeal species which may shed light on the cellular targets of fasamycin and formicamycin due to the fact that archaea are known to be intrinsically resistant to many antibacterial compounds and are generally only susceptible to antibiotics targeting ribosomes or topoisomerases (Khelaifia and Drancourt 2012). We have also identified that both classes of compounds are able to inhibit a permeabilised *E. coli* strain, indicating that Gram-negative resistance is due to the inability of the compounds to gain access into the cell and exert their effects on the cellular target(s). As many of the critical

priority pathogens identified by the World Health Organisation are Gram-negative and there is a global need for new anti-Gram-negative antibiotics. The work presented here may provide a clear starting point for the development of synthetic derivatives of fasamycin and formicamycin that can gain entry into Gram-negative cells. Derivatives of a FAS-II inhibitor, Debio-1452, which only exhibits bioactivity against Gram-positive organisms, have recently been synthesised, through substitutions of chemical groups, which inhibit a broad-range of Gram-negative pathogens (Parker, Cain et al. 2022), therefore similar investigations could be undertaken with both fasamycin and formicamycin compounds.

Throughout this PhD, we set out to identify and characterise the target and mode of action of the formicamycin compounds and to determine whether the fasamycin compounds isolated from *S. formicae* were also inhibitors of FAS-II. During the course of this work, all attempts, including exposure to high concentrations of fasamycin and formicamycin compounds and the barrier to resistance, to generate resistant bacterial mutants to either class of compound were unsuccessful. Furthermore, to add to work by Qin et al (2017), no resistance was observed in *S. aureus* strains grown in the presence of sub inhibitory concentrations of fasamycin or formicamycin for 40 days, demonstrating that these compounds display a high barrier to resistance. Our results, at least for the fasamycin compounds, conflict with what is reported in the literature as resistant bacterial mutants were generated toward fasamycin A. However, we hypothesise that these differences in findings can be attributed to the differences in experimental design, including the different congeners of fasamycin used and the fact that our experiments were conducted using *S. aureus* strains whereas mutants to fasamycin A were generated in *E. faecalis.* To confirm this hypothesis, resistant mutant generation should be attempted using *E. faecalis* and using fasamycin molecules as structurally similar to fasamycin A as possible. If resistant mutant generation is still unsuccessful, then targeted mutation of FabT in *E. faecalis* should also be undertaken and the resulting strain should be assayed for the ability to confer resistance to both fasamycin and formicamycin compounds. We also observed that, unlike reports documented for fasamycin A, over-expression of individual fatty acid synthesis proteins was not sufficient to provide significant resistance to either class of compounds isolated from *S. formicae*, indicating that if fatty acid inhibition is a true *in vivo* target of these

compounds, then these compounds also inhibit further cellular processes. Although this high barrier to resistance is an incredibly attractive characteristic in terms of clinical potential of these compounds and indicates the potential for a novel mechanism of action, this meant that characterising the cellular target(s) of these compounds was extremely difficult. However, through the use of several *in vivo* and *in vitro* techniques, we have demonstrated that both fasamycin and formicamycin compounds show evidence of inhibiting multiple cellular targets, specifically type II fatty acid synthesis and topoisomerases such as gyrase and topo IV, which may explain why generating resistant mutants to these compounds is practically impossible. Further support for this dual target theory, especially for the fasamycins comes from the observations described in this thesis that show that fasamycin compounds inhibit archaeal species, which do not synthesise fatty acids and therefore inhibition of fatty acid synthesis cannot be responsible for observed bioactivity against these species.

Although we have shown that both classes of compounds indicate inhibition of FAS-II through the use of *in vivo B. subtilis* reporter strains, a limitation of this work has been the lack of characterisation of the ability of both fasamycin and formicamycin compounds isolated from *S. formicae* to inhibit the bacterial FAS-II pathway. Therefore, ongoing work will need to verify the inhibitory activities of both fasamycin and formicamycin compounds on the synthesis of fatty acids through the use of biochemical and structural studies. *In vitro* fatty acid elongation assays should be undertaken to characterise whether the fasamycin compounds isolated here, alongside the formicamycins, inhibit the production of elongated fatty acids as shown with fasamycin A (Feng, Chakraborty et al. 2012). If successful, research efforts going forward should aim to obtain a crystal structure of both compounds bound to FabF, with the ultimate aim of generating FabF mutants that are resistant to both classes of compounds. Although there have been computational docking studies of fasamycin A bound to FabF, there are currently no reports in the literature of fasamycin bound FabF crystal structures and thus would be a novel report.

A large proportion of the work presented in this thesis has been focussed on characterising the ability of fasamycin and formicamycin to inhibit topoisomerases such as bacterial gyrase and topo IV. We have shown, using biochemical experiments, that both fasamycin and formicamycin inhibit the essential activities of both gyrase and topo

IV enzymes *in vitro*. We have further demonstrated that both compounds retain inhibitory activity against gyrase enzymes encoding for resistance to ciprofloxacin and simocyclinone SD8 indicating that cross resistance to other topoisomerase inhibitors is not observed, at least with those tested in this work. We further conclude that topoisomerase inhibition is most likely a valid *in vivo* target of these compounds, owing to the fact that positive responses for gyrase inhibition are seen in *in vivo B. subtilis* reporter strains and the fact that RNA transcript analysis of *S. aureus* strains exposed to both fasamycin and formicamycin showed significant changes in genes encoding gyrase proteins, as well as genes coding for important proteins in the SOS response. Furthermore, as both fasamycin and formicamycin compounds inhibit archaeal species and we have demonstrated that both compounds inhibit topoisomerase VI relaxation in *in vitro* assays, we believe this further indicates that topoisomerase inhibition is a valid *in vivo* target of both compounds. To develop this work further, a comprehensive investigation into the inhibitory ability of fasamycin and formicamycin should be undertaken with topoisomerases from different bacterial and eukaryotic species. We have shown in preliminary assays that both classes of compounds, especially in the case of formicamycin J, display a specificity for prokaryotic topoisomerases in comparison to those isolated from humans but further investigations are required to confirm these findings.

An in-depth characterisation of the mechanism of topoisomerase inhibition has been undertaken. We have determined that neither fasamycin or formicamycin exposure to topoisomerases results in the stabilisation of cleavage complexes, as seen with the fluroquinolones, instead appearing to limit the ability of topoisomerases to bind DNA but our results indicate that this is not achieved through the binding of fasamycin or formicamycin in the same binding pocket as simocyclinone SD8. We therefore propose that both fasamycin and formicamycin represent novel catalytic inhibitors of topoisomerases with a potentially undocumented binding site. These findings indicate that not only are the fasamycin and formicamycin compounds dual-targeting compounds, a novel report for natural product antibiotics, but that they also may display a novel mechanism of action toward topoisomerases.

While the work in this thesis represents significant progress in understanding how the formicamycins exert their inhibitory effects, a great deal of work needs to be undertaken

to verify the interaction between these compounds and topoisomerases. As there are many examples in the literature of crystal structures of gyrase complexes and inhibitors (Mustaev, Malik et al. 2014, Buttner, Schäfer et al. 2018), we wanted to attempt to obtain structures of fasamycin and formicamycin bound to topo IV. However, the fasamycin compounds do not freely crystalise and therefore we hypothesised that this would limit the success of our experiments. Therefore, during the course of this PhD, preliminary work has begun attempts at obtaining a cryogenic electron microscopy (CryoEM) structure of fasamycin E bound to topo IV purified from *E. coli*, which eliminates the need for crystallised compound and has been used to solve the structure of gyrase from *E. coli* (Vanden Broeck, Lotz et al. 2019). As of yet we have not been able to obtain high resolution structural data from these experiments to be able to say with any certainty where fasamycin E is binding within the topo IV structure. It is also unknown to date, whether fasamycin and formicamycin compounds bind and inhibit topoisomerases in the same way as each other and therefore, future work should continue these attempts to obtain structures of *E. coli* topo IV with both fasamycin and formicamycin inhibitors bound. Once a binding site has been identified, it should be further characterised through the use of targeted mutations within the binding site to obtain fasamycin/ formicamycin resistant topo IV enzymes. Biophysical analysis experiments should also be conducted such as isothermal titration calorimetry (ITC) to determine fasamycin and formicamycin binding affinity (KD) for purified topoisomerase subunits, as well as undertaking further SPR experiments to fully characterise the ability of both compounds to inhibit topo IV – DNA binding.

Throughout this work, in all experiments conducted, we have found that both fasamycin and formicamycin appear to inhibit the same cellular targets. However, these results do not make sense when contemplating the project in an evolutionary context. Bioinformatic analysis documented in Qin et al (2020) compared the *for* BGC to gene clusters with high homology in *Streptomyces kanamyceticus* and the producing organism of the fasamycin-like accramycin A compounds (Maglangit, Fang et al. 2019). Analyses revealed that none of these predicted fasamycin producing strains contained the genes *forX, forY, forZ* and *forAA* which encode for proteins essential in the conversion or of fasamycin to formicamycin compounds or for export of formicamycin compounds (Qin, Devine et al. 2020). However, the gene products of *forY, forZ* and

forAA, show high homology to sequences encoded in the genomes of *Actinomadura* species which suggests that *S. formicae* may have encoded for the production of fasamycin molecules and then acquired these genes via horizontal gene transfer from *Actinomadura* species. If we accept this hypothesis, then the cost of extending the fasamycin biosynthetic pathway to the formicamycin compounds must confer an additional benefit that the fasamycin compounds do not confer to *S. formicae* for the genes to have been retained. These findings, taken together with the observations that the fasamycin compounds generally exhibit more potent inhibitory activities towards topoisomerases and the vastly different 3D structure of formicamycin in comparison to fasamycin, we propose there may be a further target of the formicamycin molecules. To further this theory, we will need to determine IC_{50} values for fatty acid synthesis inhibition to confirm whether FAS-II is a valid target of the formicamycins, or whether the positive responses seen in reporter strains are off target effects due to structural similarity between fasamycin and formicamycin. Investigations into the biological differences between both compounds should be undertaken, including identifying any potential further cellular targets of formicamycin. Proteomics based approaches such as thermal proteomics could be employed to investigate further targets of formicamycin compounds, these experiments work by treating cell lysates with a compound of interest, interactions between the compound and a protein target should protect the protein from degradation and therefore can indicate antibiotic targets (Mateus, Kurzawa et al. 2020). During the course of this work, we discovered that a few formicamycin molecules did not inhibit the activities of either gyrase or topo IV enzymes and yet retain biological activity, albeit less potent, toward bacterial strains. Preliminary investigations into these formicamycin compounds, specifically formicamycin A, has determined that exposure of *S. aureus* to high concentrations of formicamycin A leads to the formation single colonies. Several of these single colonies have been found to grow on concentrations of formicamycin A four times (32 μg/ml) higher than the pre-determined MIC (8 μg/ml) (**Figure 8.1**). We therefore hypothesise that this compound only inhibits one of the proposed cellular targets, explaining why it exhibits higher MICs in comparison to the other formicamycin compounds and why we are able to generate potential resistant mutants. Further work should assess the MIC of these formicamycin A exposed strains, if increased, these strains should be subjected to full genome sequencing to uncover the reason for increased resistance.

A

Formicamycin A
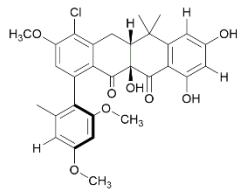
Topo IV IC$_{50}$: >100 μM

Gyrase IC$_{50}$: >100 μM

S. aureus MIC: 8 μg/ml

B
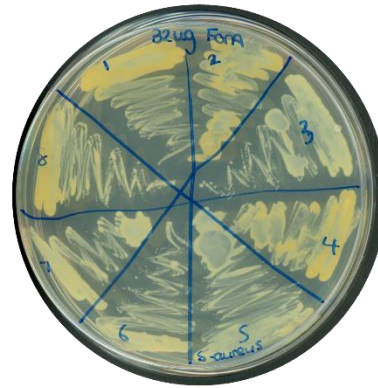
After exposure to formicamycin A

Figure 8.5 Formicamycin A shows no inhibition of either *E. coli* topo IV or *S. aureus* gyrase under 100 μM but still retains biological activity against bacterial strains (**A**). *S. aureus* exposed to high concentrations of formicamycin A leads to the formation of single colonies. Single colonies have been found to grow at concentrations 4 times higher than previously determined MIC (**B**).

8.2 Investigating the effect of targeted mutation within the formicamycin biosynthetic gene cluster on the production of fasamycin and formicamycin

The aim of this work was to understand how different mutations within genes encoded by the *for* BGC effected the production of the fasamycin and formicamycin compounds. Prior to this work products of formicamycin biosynthesis had only been isolated in small quantities and observed after growth of *S. formicae* on solid agar. We have now shown that deletion of the genes encoding the MarR regulator, ForJ, derepresses the *for* BGC and leads to not only increased yields of these compounds, but also the production of them in liquid medium. Furthermore, using this knowledge we have been able to combine targeted mutations of *for* BGC encoded genes within this derepressed background such as over-expression of the two-component system, ForGF, to generate high yielding formicamycin strains that have been observed to produce formicamycin compounds at a 9-fold higher titre than that of the wild-type *S. formicae* strain. These findings may provide useful for the development of formicamycins as potential clinical candidates due to the fact that most industrial production of natural products is done using large scale batch fermentations in liquid culture. Investigations should be undertaken to determine if the production of these compounds from modified *S.*

formicae strains, such as *S. formicae ΔforJ* + ForGF, are suitable for industrial style production methods. If these investigations indicate that modified *S. formicae* strains are not suitable then further work should focus on identifying potential heterologous host strains that can produce these compounds to yields required for industrial style fermentations. We have already shown in Chapter 7 that attempts at heterologous expression of the *for* BGC using *S. coelicolor* M1146 and *S. erythraea Δery* did not lead to improved titres of either fasamycin or formicamycin compounds and therefore other actinomycete hosts would need to be investigated. Although heterologous expression of the *for* BGC in these strains was unsuccessful in terms of improved formicamycin titre, these investigations led to the isolation and characterisation of several glycosylated analogues of the fasamycin molecules. These findings highlight the ability to find compounds with interesting chemistry from heterologous expression and, as glycosylation of fasamycin C, D and J led to the abolishment of bioactivity, we can infer that the specific positions of glycosylation may be important in terms of the molecule's bioactivity, which may further aid in synthetic derivatives of these compounds.

8.3 Final conclusions

The work in this thesis demonstrates the formicamycin compounds and their biosynthetic intermediates, the fasamycins, are clinically interesting compounds. We have shown that both fasamycin and formicamycin not only exhibit potent bioactivity towards clinically relevant bacterial species, but we also demonstrate that they display a high barrier to resistance which is most likely because they exhibit a dual-targeting mechanism of action which is a novel report in the literature. The findings from our work may help to uncover a new potential binding site on the validated antibacterial target, gyrase, which could be exploited for the production of synthetic analogues. The knowledge that has been gained through the course of this PhD further solidifies the formicamycins as potential clinical candidates and investigations into their suitability for clinical use for example, toxicity testing and infection models, should be a priority of future work. This work highlights the talented nature of *S. formicae* as species of interest in the search for novel bioactive molecules. As this work has only focussed upon a single BGC of this strain which has yielded two classes of bioactive compounds and has not even touched upon investigations into the other potentially novel BGCs of this strain which may provide fruitful in the hunt for novel chemistry and compounds. Importantly,

we show that nature is not a dried-up resource in terms of discovering novel antimicrobials and highlights the importance of investigating different niches for natural product producing microorganisms.

9.0 Supplementary information

SI Figure 1: MSSA formicamycin I and J Day 0 and Day 40 resazurin assays. MSSA strains are grown in TSB liquid media containing a serial dilution of the compound of either formicamycin I or formicamycin J. Plates were grown overnight at 37˚C before the addition of resazurin dye. Blue wells indicate no viable cells. Pink ce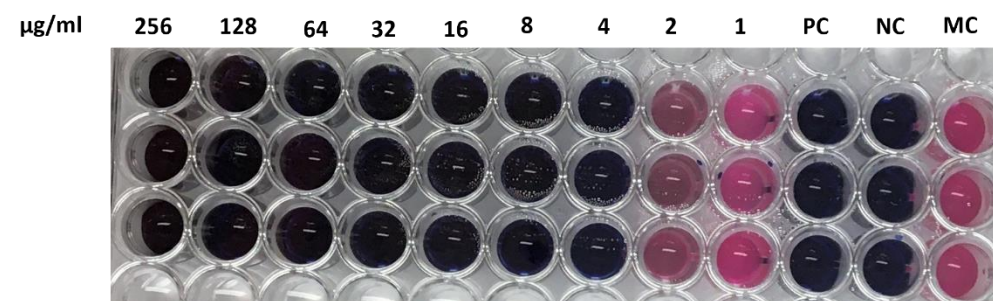lls indicate viable cells. PC – positive control (apramycin 50 µg/mL), NC – negative control (no inoculation of bacteria) and MC – Media control (indicator strain grown in the media containing 5% DMSO to ensure the strain can grow).
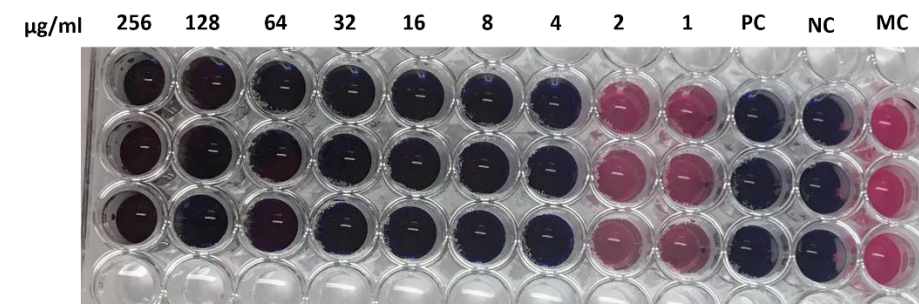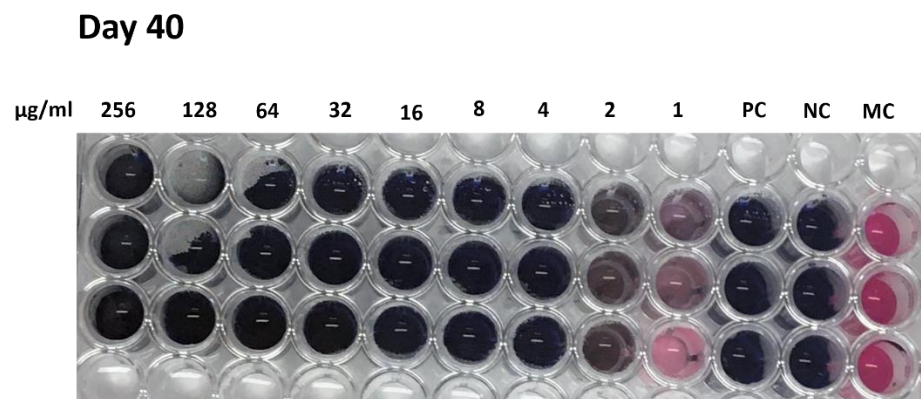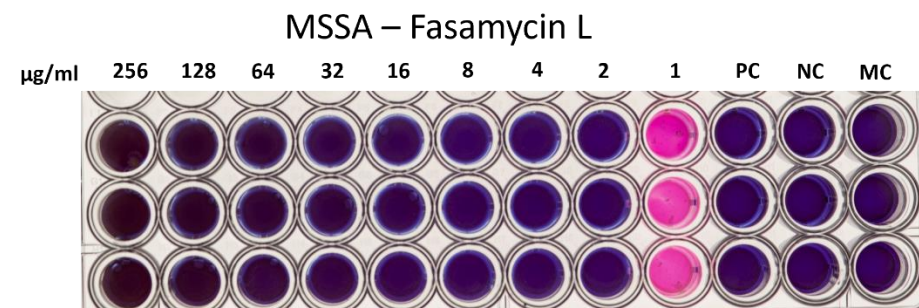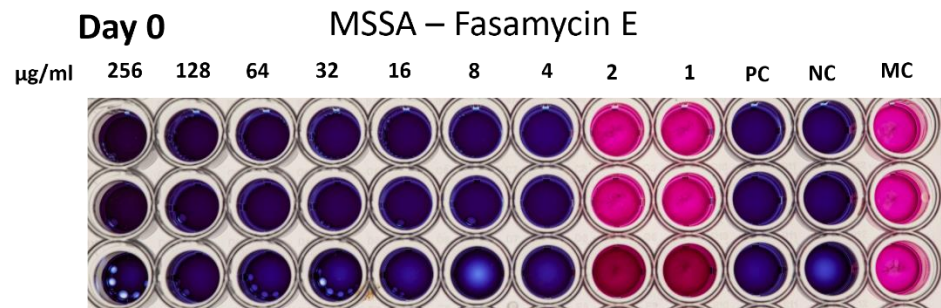
SI Figure 2: MSSA fasamycin E and L Day 0 and Day 40 resazurin assay. MSSA strains are grown in TSB liquid media containing a serial dilution of the compound of either fasamycin E or fasamycin L. Plates were grown overnight at 37°C before the addition of resazurin dye. Blue wells indicate no viable cells. Pink cells indicate viable cells. PC – positive control (apramycin 50 μg/mL), NC – negative control (no inoculation of bacteria) and MC – Media control (indicator strain grown in the media containing 5% DMSO to ensure the strain can grow).
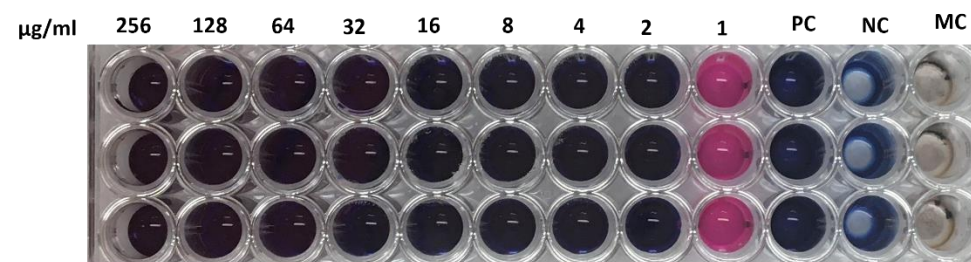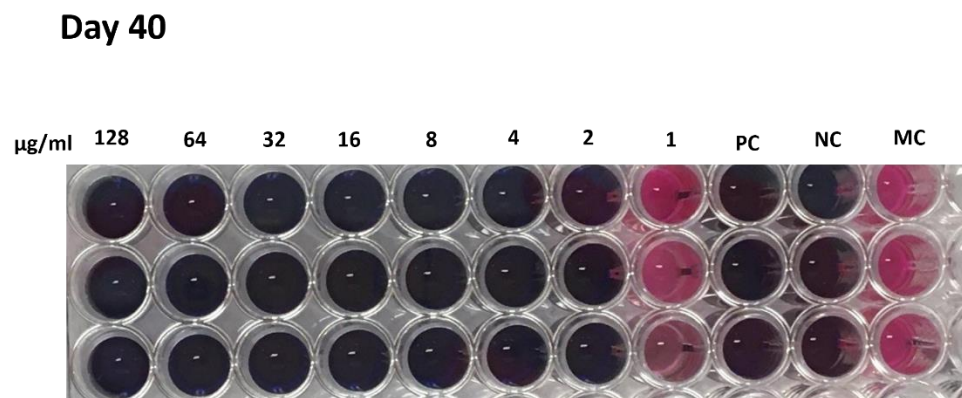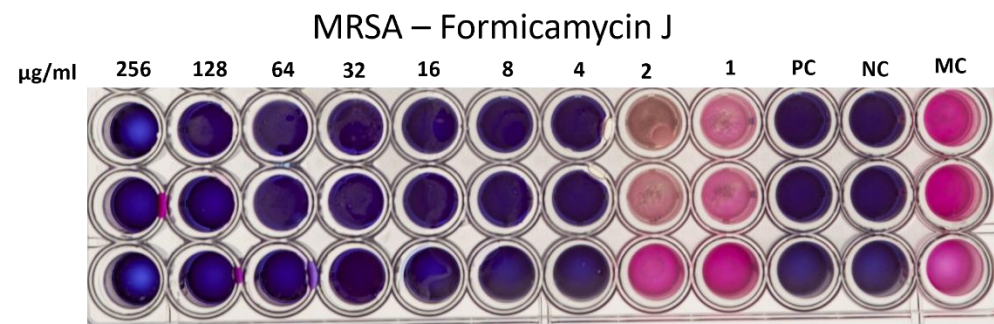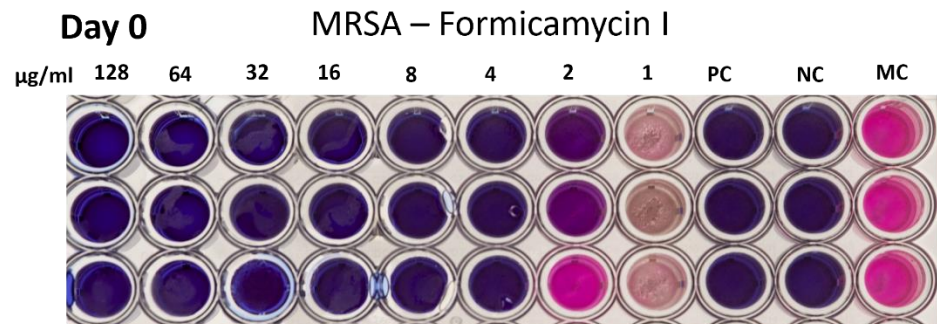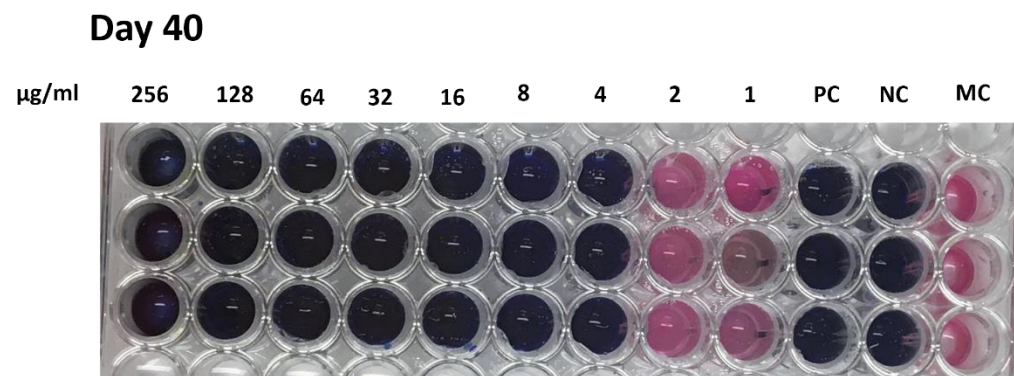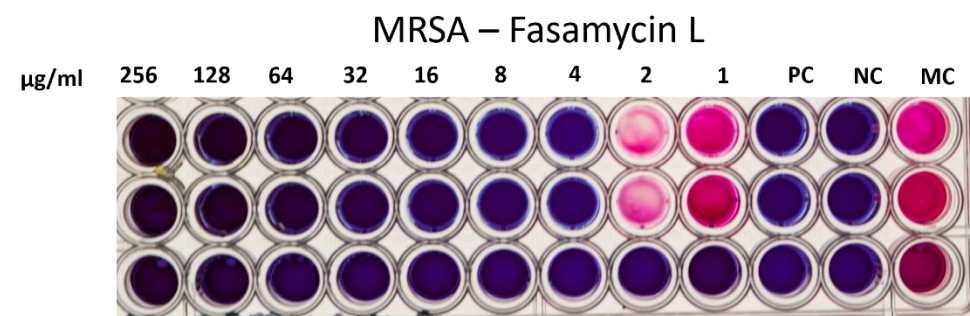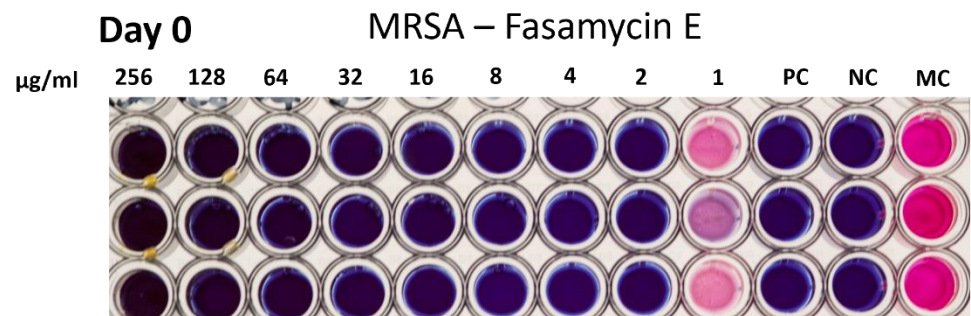
SI Figure 3: MRSA formicamycin I and J Day 0 and Day 40 resazurin assays. MRSA strains are grown in TSB liquid media containing a serial dilution of the compound of either formicamycin I or formicamycin J. Plates were grown overnight at 37°C before the addition of resazurin dye. Blue wells indicate no viable cells. Pink cells indicate viable cells. PC – positive control (apramycin 50 µg/mL), NC – negative control (no inoculation of bacteria) and MC – Media control (indicator strain grown in the media containing 5% DMSO to ensure the strain can grow).

Day 0

MRSA – Fasamycin E

µg/ml 256 128 64 32 16 8 4 2 1 PC NC MC

MRSA – Fasamycin L

µg/ml 256 128 64 32 16 8 4 2 1 PC NC MC

Day 40

µg/ml 256 128 64 32 16 8 4 2 1 PC NC MC

µg/ml 256 128 64 32 16 8 4 2 1 PC NC MC

SI Figure 4: MRSA fasamycin E and L Day 0 and Day 40 resazurin assays. MRSA strains are grown in TSB liquid media containing a serial dilution of the compound of either fasamycin E or fasamycin L. Plates were grown overnight at 37˚C before the addition of resazurin dye. Blue wells indicate no viable cells. Pink cells indicate viable cells. PC – positive control (apramycin 50 µg/mL), NC – negative control (no inoculation of bacteria) and MC – Media control (indicator strain grown in the media containing 5% DMSO to ensure the strain can grow.
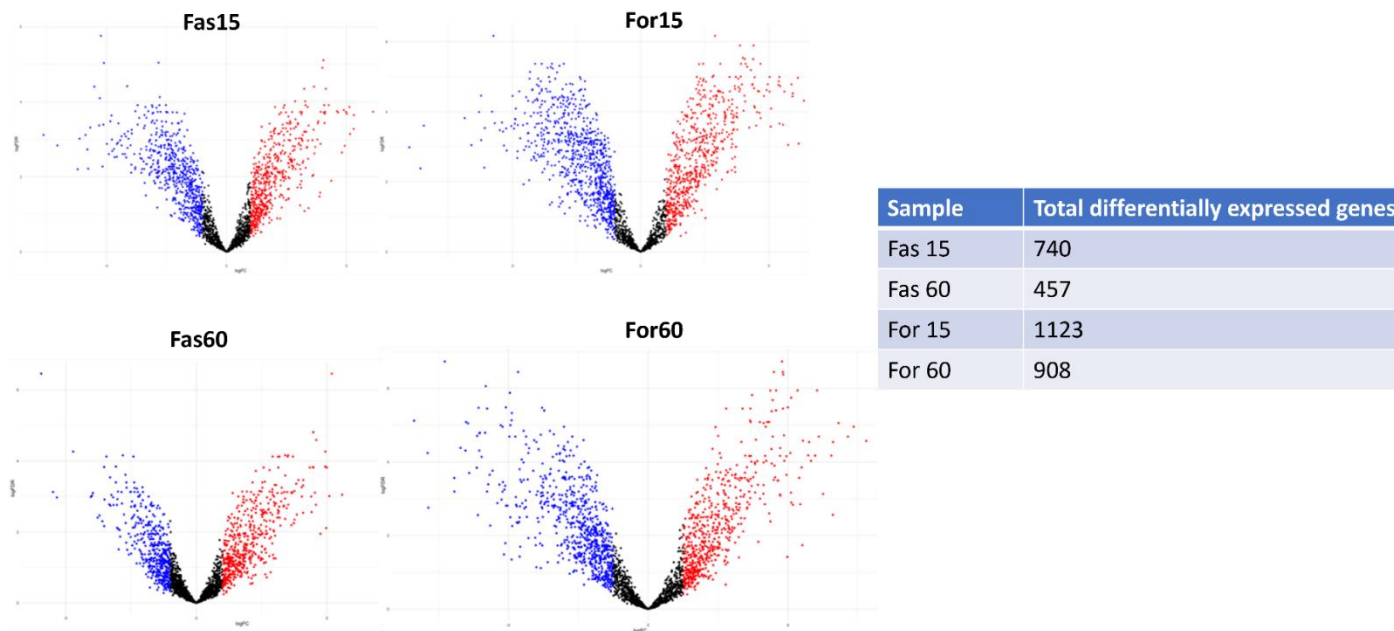
Differential gene expression (LogFC >1, p<0.05) in all samples compared to un-treated control

Sample	Total differentially expressed genes
Fas 15	740
Fas 60	457
For 15	1123
For 60	908

SI Figure 5   Volcano plots documenting differential gene expression (log-fold change >1 and at a significance value of p<0.05) of RNA transcripts from fasamycin and formicamycin exposed *S. aureus* in comparison to a solvent controlled *S. aureus* control. Both fasamycin and formicamycin treated *S. aureus* showed a vast array of changes after 15- and 60-minutes post exposure in comparison to the solvent controlled *S. aureus* control.
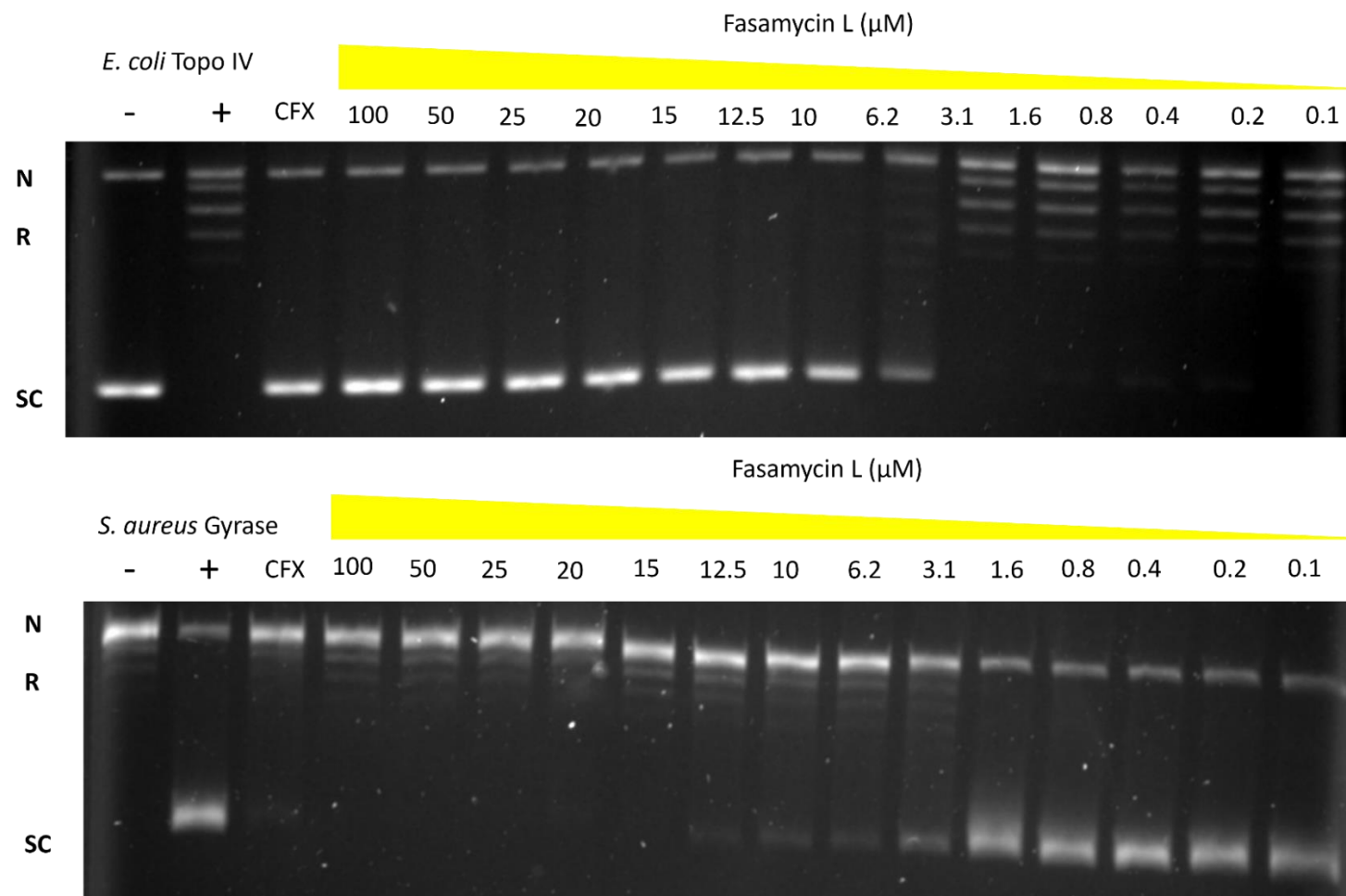
SI Figure 6: Examples of *E.coli* topo IV relaxation assays and *S. aureus* gyrase supercoiling assays in the presence of decreasing concentrations of fasamycin L. CFX- ciprofloxacin – no enzyme, + enzyme added, N; nicked DNA, R; relaxed DNA, SC; supercoiled DNA.
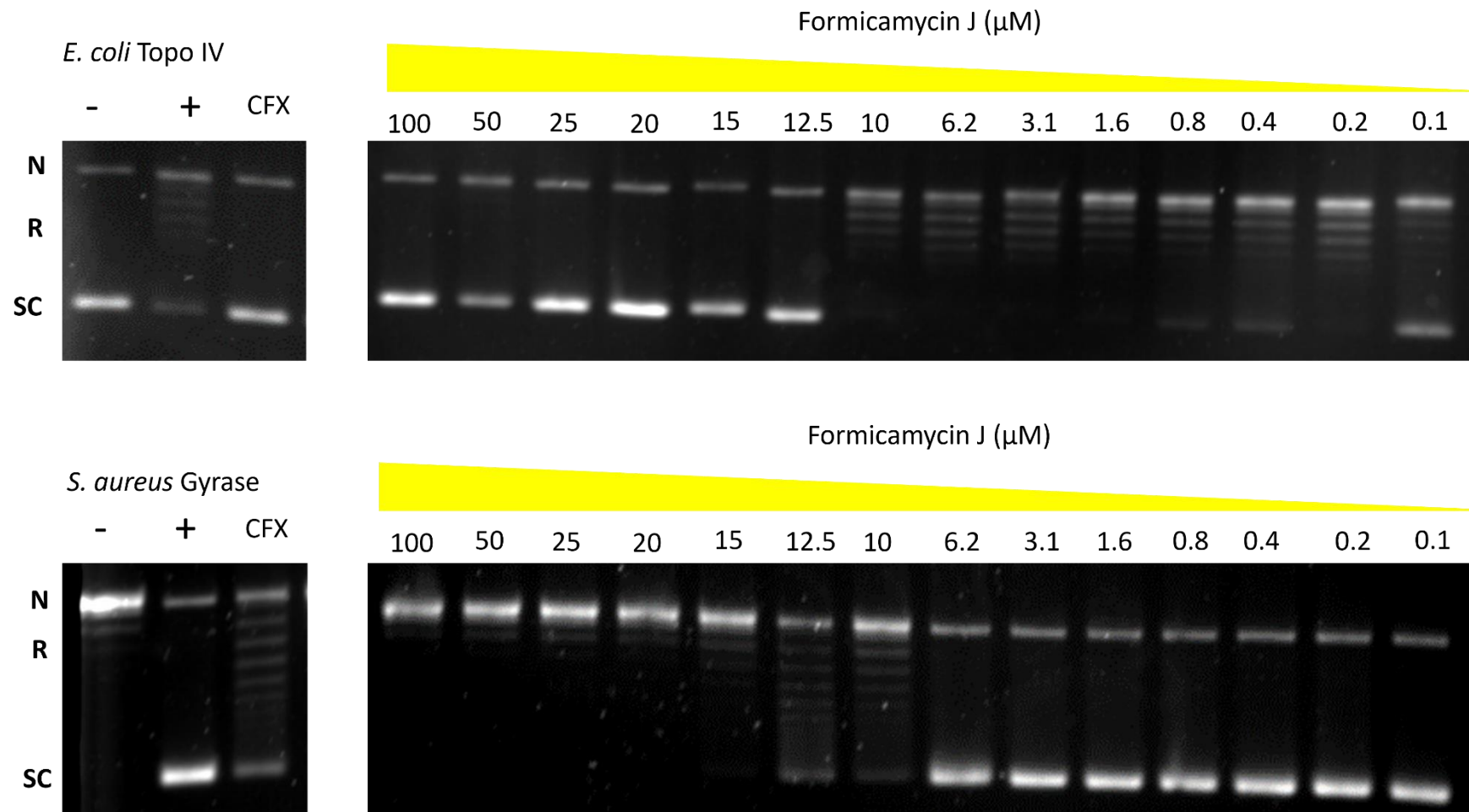
SI Figure 7: Representative examples of *E. coli* topo IV relaxation assays and *S. aureus* gyrase supercoiling assays in the presence of decreasing concentrations of formicamycin J. CFX- ciprofloxacin – no enzyme, + enzyme added, N; nicked DNA, R; relaxed DNA, SC; supercoiled DNA.
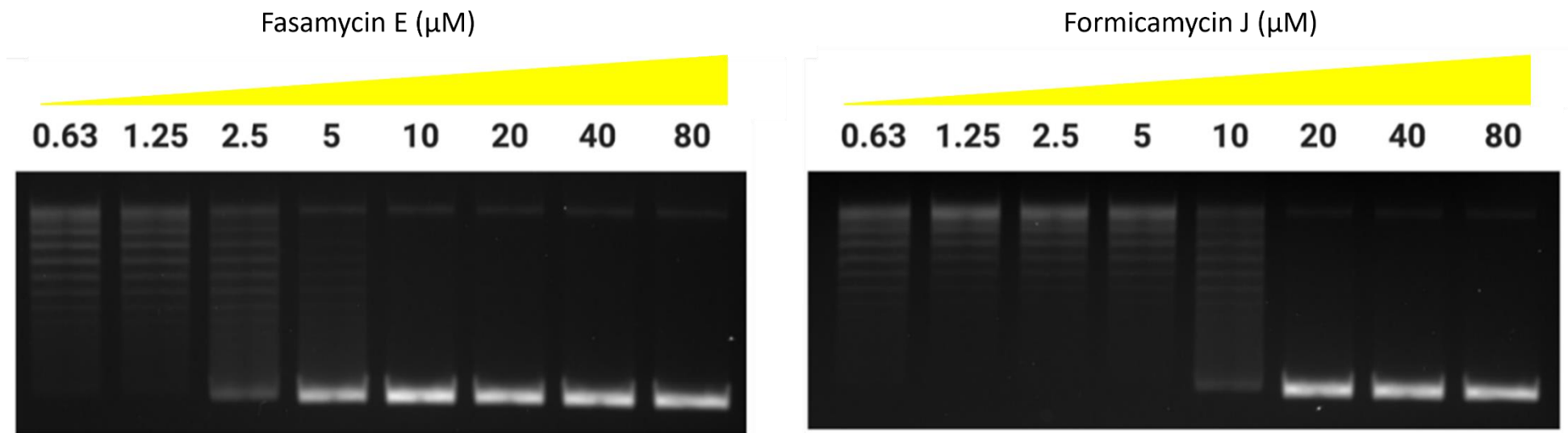
SI Figure 8: Representative examples of *M. maze*i Topo VI relaxation assays in the presence of increasing concentrations of fasamycin E and formicamycin J. Assays were conducted by Adam Allen.
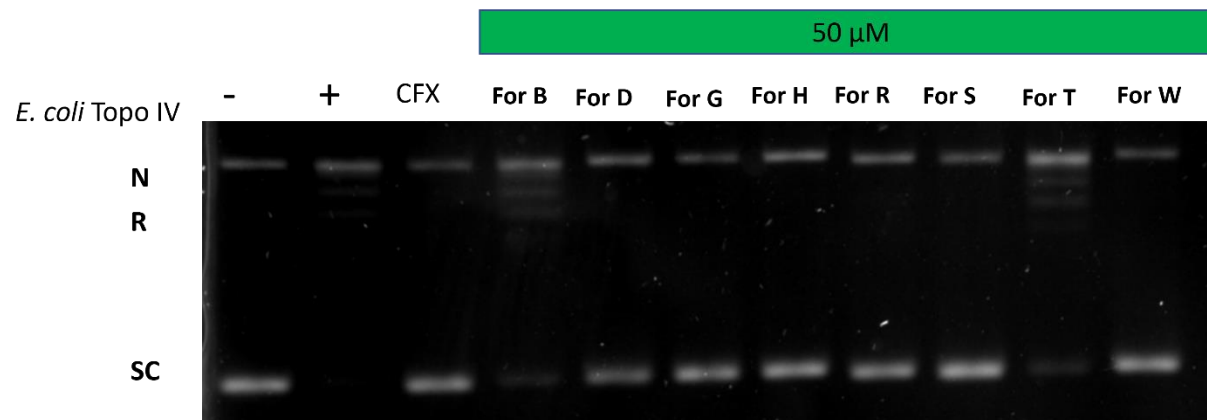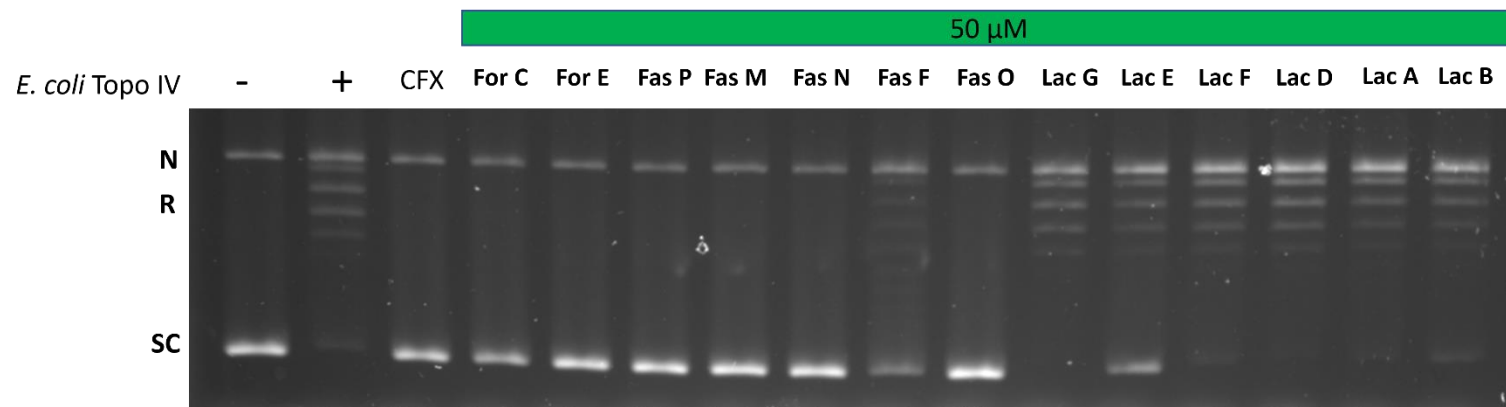
SI Figure 9: Examples of *E.coli* topo IV relaxation assays in the presence of different fasamycin (fas), formicamycin (for) and formicalactone (lac) congeners at 50 μM. CFX- ciprofloxacin – no enzyme, + enzyme added, N; nicked DNA, R; relaxed DNA, SC; supercoiled DNA.
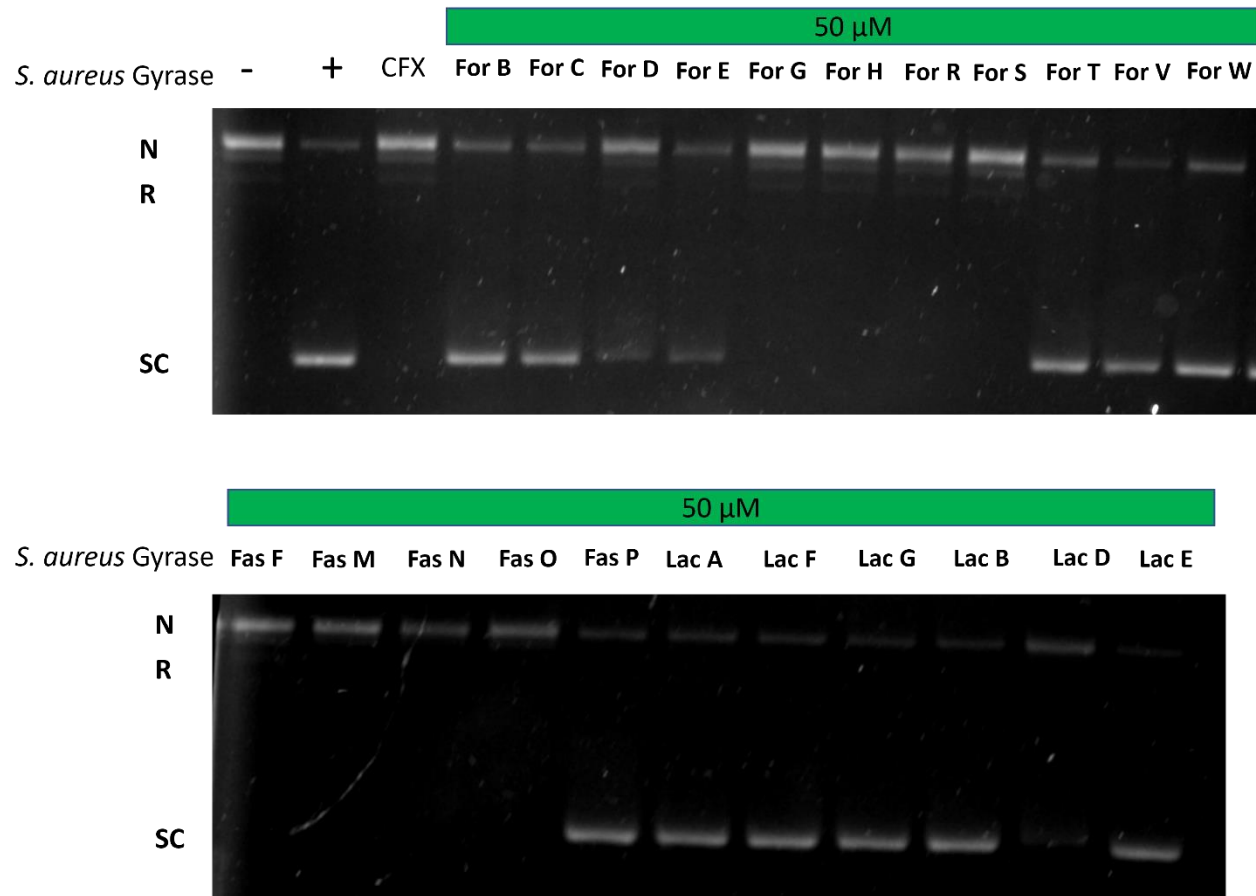
SI Figure 10: Examples of *S. aureus* gyrase supercoiling assays in the presence of different fasamycin (fas), formicamycin (for) and formicalactone (lac) congeners at 50 μM. CFX- ciprofloxacin – no enzyme, + enzyme added, N; nicked DNA, R; relaxed DNA, SC; supercoiled DNA.

SI Table 1: Comparison of MIC and IC$_{50}$ values determined for inhibition of topoisomerase enzymes tested in this work.

	IC$_{50}$ (µM)					MIC (µg/ mL)	
	E. coli Topo IV	*S. aureus* gyrase	*M. mazei* Topo VI	Human Topo IIα	Human Topo IIβ	*S. aureus* (MRSA)	*E.coli* NR698
Fasamycin C	25.5 (12 µg/ml)	23.3 (11 µg/ml)	-	-	-	16	16
Fasamycin E	6.4 (3.5 µg/ml)	5.7 (3 µg/ml)	3.4 (1.8 µg/ml)	26.2 (14 µg/ml)	50 (27 µg/ml)	2	8
Fasamycin L	9.2 (5.2 µg/ml)	4.7 (2.6 µg/ml)	-	-	-	2	8
Formicamycin A	> 100 (55 µg/ml)	> 100 (55 µg/ml)	-	-	-	16	>256
Formicamycin I	11.3 (7.2 µg/ml)	11.1 (7.2 µg/ml)	-	-	-	4	8
Formicamycin J	6 (4 µg/ml)	7.1 (4.6 µg/ml)	11.9 (7.7 µg/ml)	>100 (>65 µg/ml)	>100 (>65 µg/ml)	2	4
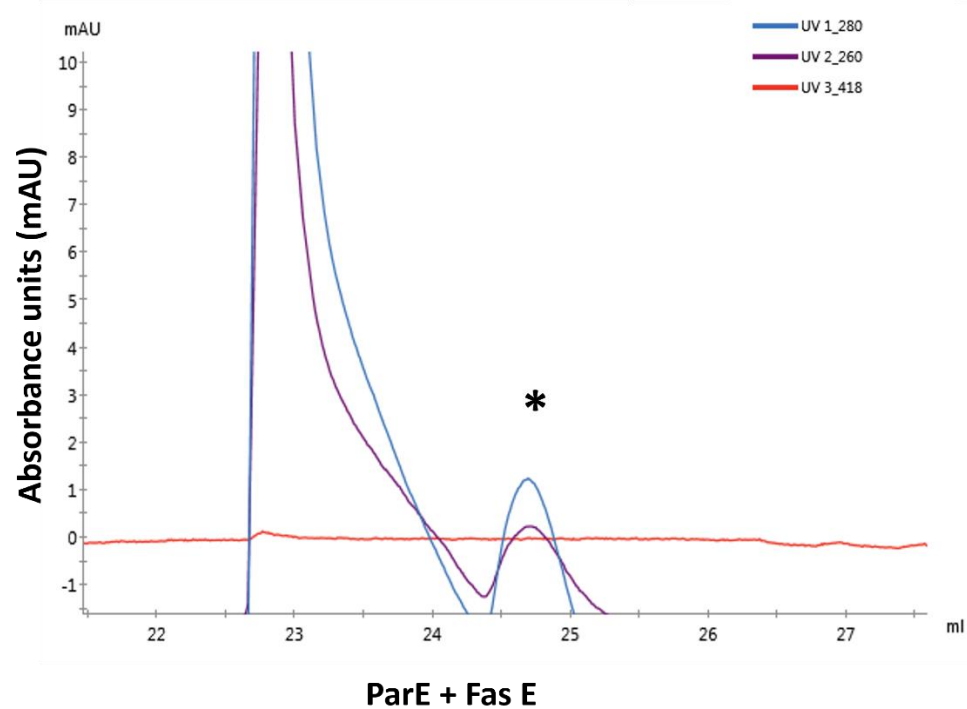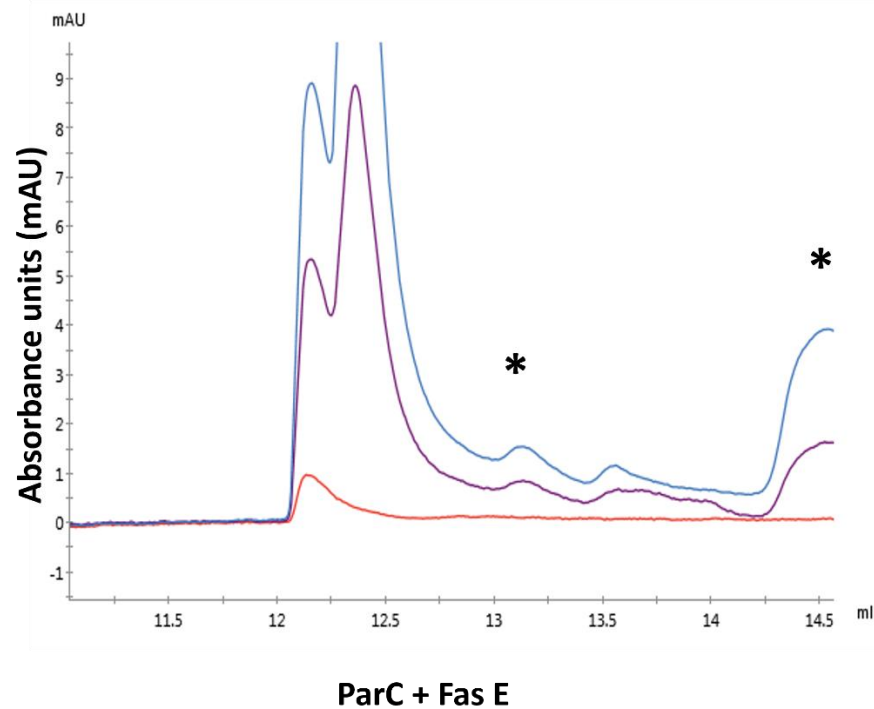
SI Figure 11: Close up of chromatograms of ParC and ParE in the presence of 25 µM fasamycin E. Samples were consecutively injected one after the other onto the column. Protein (ParC and ParE) is monitored at 280 nm (blue), DNA monitored at 260 nm (purple) and fasamycin E is monitored at 418 nm (red) which is a characteristic absorption wavelength of fasamycin. **A**- ParC + fasamycin E; **B**, ParE with fasamycin E. In all cases the first peak in each sample corresponds to the protein (ParC or ParE), the second peak designated with an * can be attributed to buffer constituents.
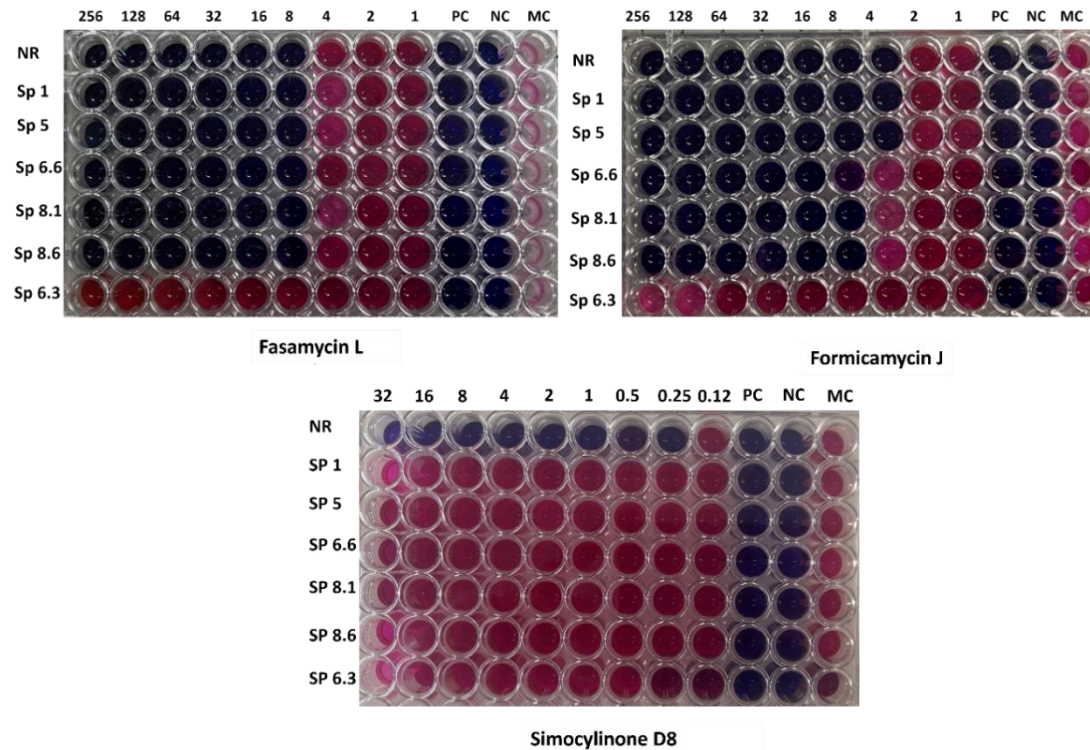
SI Figure 12: *E.coli* NR698 and resistant simocyclinone D8 strains were grown in LB liquid media containing a serial dilution of the compound of either formicamycin J, fasamycin L or simocyclinone D8. Plates were grown overnight at 37°C before the addition of resazurin dye. Blue wells indicate no viable cells. Pink cells indicate viable cells. PC – positive control (apramycin 50 µg/mL), NC – negative control (no inoculation of bacteria) and MC – Media control (indicator strain grown in the media containing 5% DMSO to ensure the strain can grow).
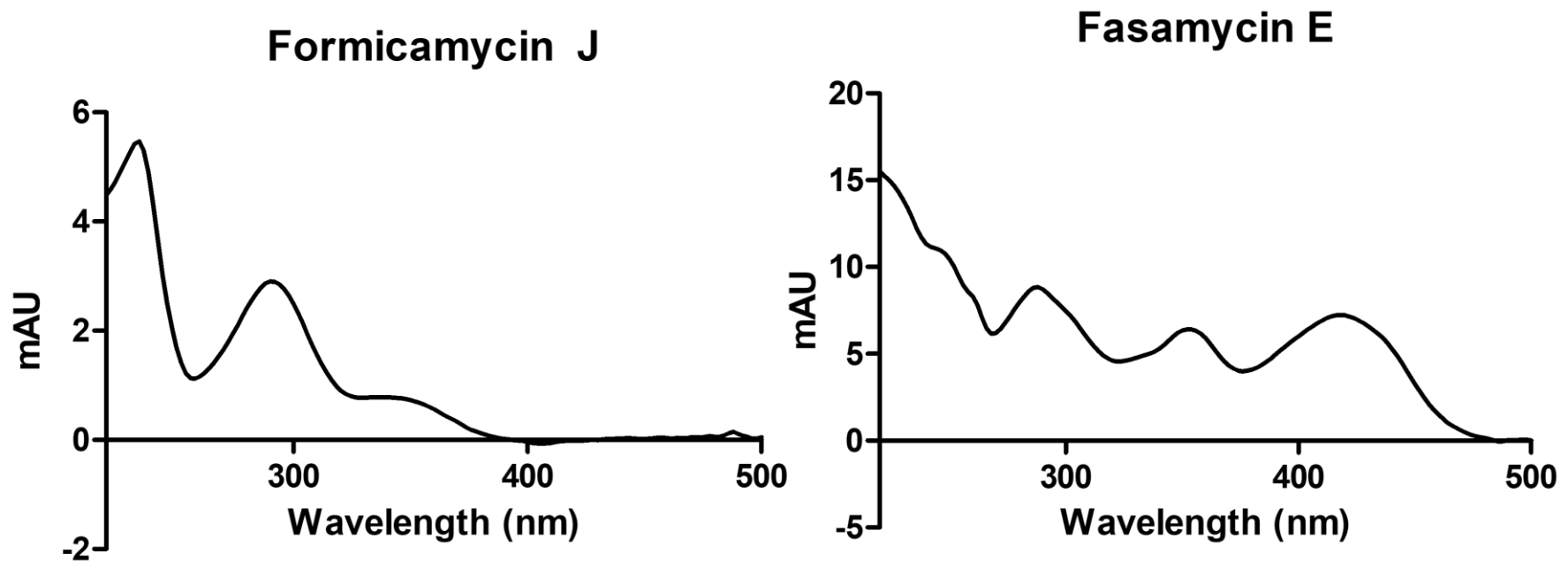
SI Figure 13 Characteristic chromophores of formicamycin J and fasamycin E.
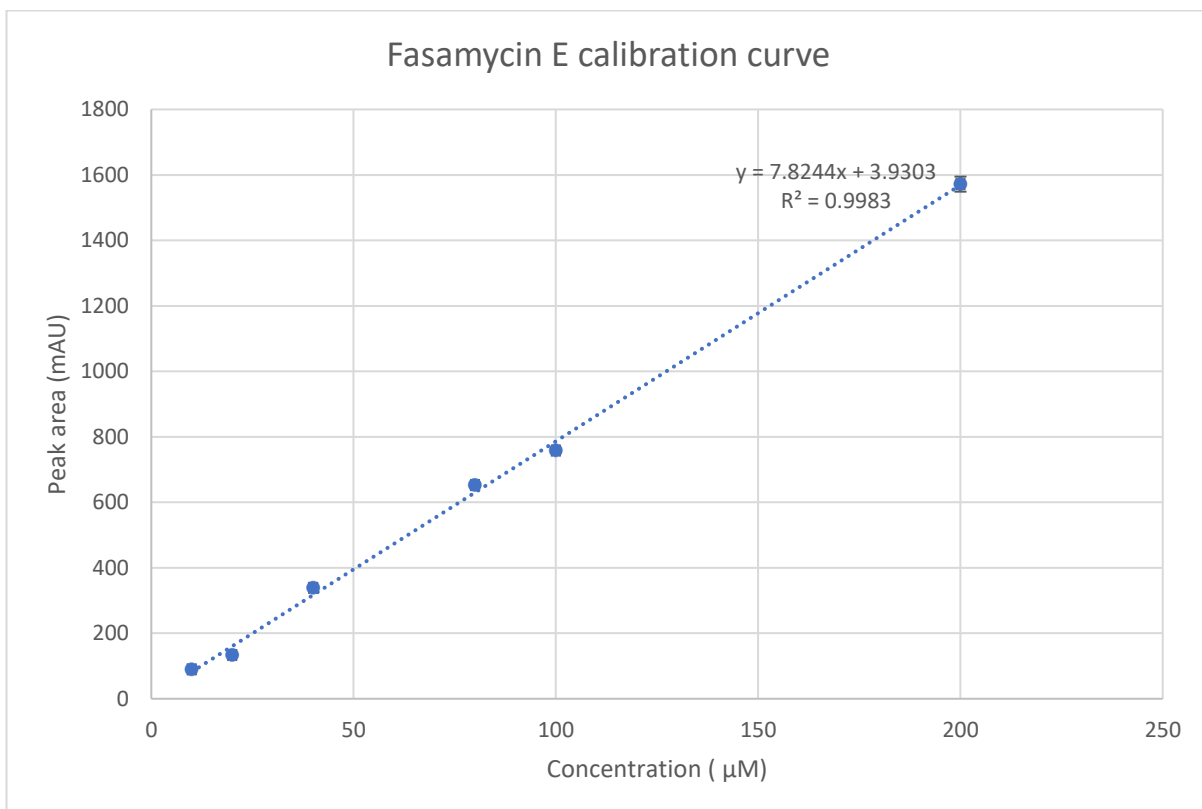
SI Figure 14: Calibration curve of fasamycin E

SI Table 2: Calibration table of fasamycin E

Fas E (µM)	mAU	Standard deviation	Standard error
10	89.8	1.5	0.866025404
20	133.6	2.696293753	1.556705924
40	338.7	4.750789408	2.742869544
80	652.5666667	11.58461624	6.688381302
100	758.0666667	12.01055092	6.934294805
200	1571.833333	39.68341383	22.91122966
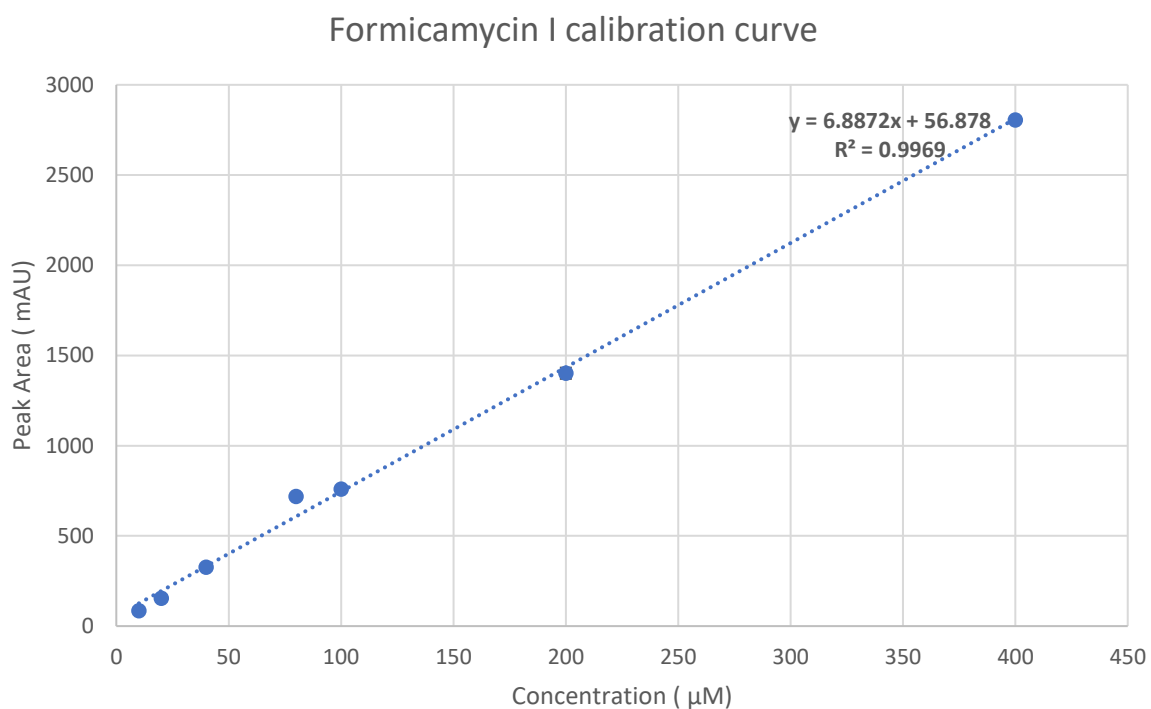
SI Figure 15: Calibration curve of formicamycin I

SI Table 3: calibration table of formicamycin I

For I (µM)	mAU	Standard deviation	Standard error
10	84.73333333	0.115470054	0.066666667
20	153.8666667	0.472581563	0.272845092
40	326.8333333	1.6563011	0.956265886
80	719.7	12.26499083	7.081195756
100	759.8333333	6.961561128	4.019259191
200	1401.366667	53.72525787	31.01829209
400	2805.9	27.43501412	15.83961279

SI Table 4: Fasamycin, formicamycin and total titres of *S. formicae* mutants grown in liquid SFM media (*n* =3). * Complemented with native promoter. ** complimented with ermE* promoter.

Strain	Fasamycins titre (µM)	Formicamycin titre (µM)	Combined titre (µM)
Wild-type	0	0	0
Wild-type + *forJ*	0	0	0
Δ*forJ*	6 ± 0.2	624.5 ± 29.4	628.4 ± 34.9
Δ*forJ* + *forJ**	2.7 ± 0.6	657.3 ± 40.7	662.1 ± 47.1
Δ*forJ* + *forJ***	210 ± 36.0	423.1 ± 72.4	633.1 ± 138.1
Δ*forJ* + *forGF*	275.4 ± 11.6	759.8± 193.8	1035.2 ± 212.6
Δ*forJ* Δ*forGF*	242.9 ± 21.6	355.3 ± 82.1	598.1 ± 85.7
Δ*forJ* Δ*forZ*	516.48 ± 297.4	409.1 ± 95.4	925.6 ± 341.2
Δ*forV*	1.3 ± 1.8	0	1.3 ± 1.8
Δ*forJ*Δ*forV*	79.4 ± 8.1	0	79.4 ± 8.1
Δ*forX*	2.54 ± 4.6	0	2.54 ± 4.6
Δ*forJ*Δ*forX*	274.3 ± 325.4	0	274.3 ± 325.4
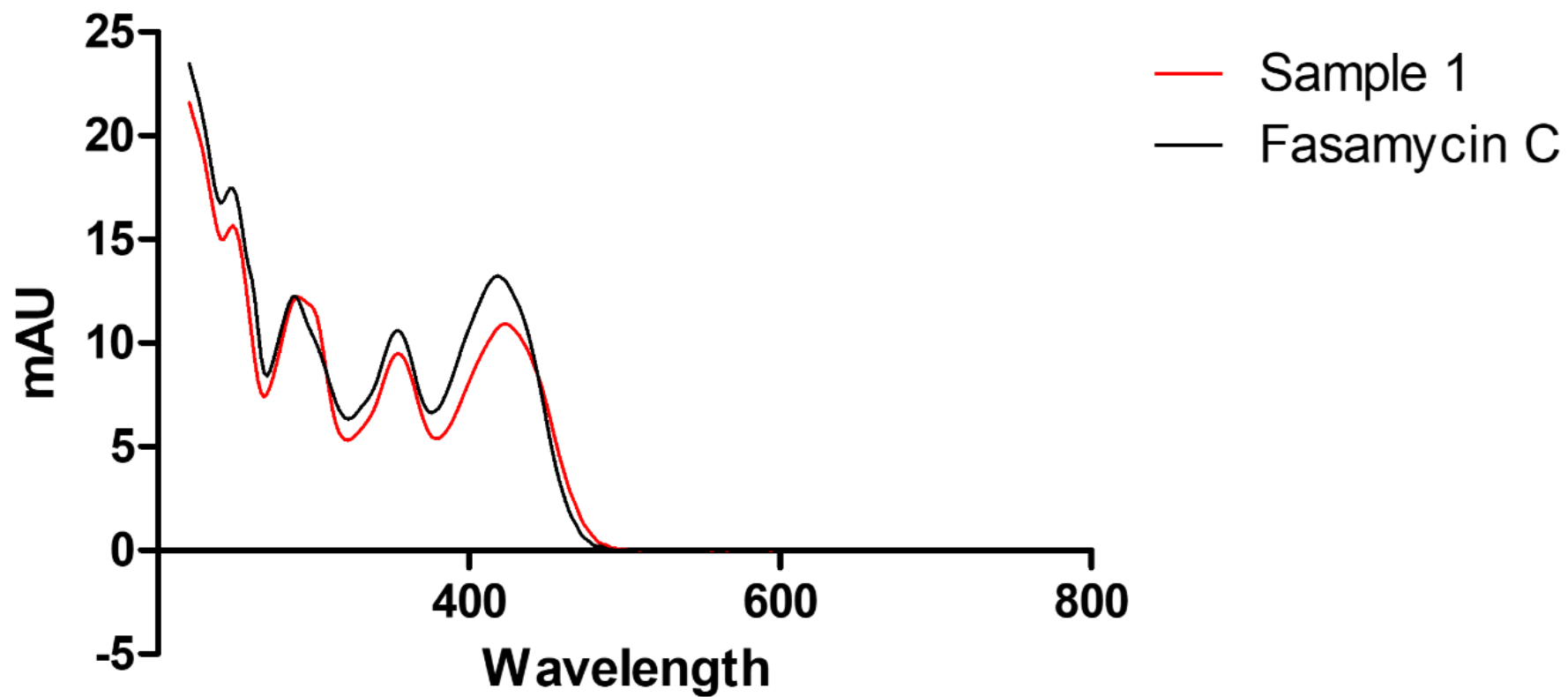
SI Figure 16: Overlay of UV-vis spectra of fasamycin C and sample 1 (contains compound **1c** and minor compounds **1a** and **1b**). Samples containing fasamycin derivatives were first identified by the presence of characteristic UV-Vis spectra of fasamycin chromophore.

10.0 Bibliography

Aigle, B. and C. Corre (2012). Chapter Seventeen - Waking up Streptomyces Secondary Metabolism by Constitutive Expression of Activators or Genetic Disruption of Repressors. Methods in Enzymology. D. A. Hopwood, Academic Press. **517:** 343-366.

Albanesi, D. and D. de Mendoza (2016). "FapR: From Control of Membrane Lipid Homeostasis to a Biotechnological Tool." Front Mol Biosci **3**: 64.

Albarano, L., R. Esposito, N. Ruocco and M. Costantini (2020). "Genome Mining as New Challenge in Natural Products Discovery." Mar Drugs **18**(4).

Atanasov, A. G., S. B. Zotchev, V. M. Dirsch, I. E. Orhan, M. Banach, J. M. Rollinger, D. Barreca, W. Weckwerth, R. Bauer, E. A. Bayer, M. Majeed, A. Bishayee, V. Bochkov, G. K. Bonn, N. Braidy, F. Bucar, A. Cifuentes, G. D'Onofrio, M. Bodkin, M. Diederich, A. T. Dinkova-Kostova, T. Efferth, K. El Bairi, N. Arkells, T.-P. Fan, B. L. Fiebich, M. Freissmuth, M. I. Georgiev, S. Gibbons, K. M. Godfrey, C. W. Gruber, J. Heer, L. A. Huber, E. Ibanez, A. Kijjoa, A. K. Kiss, A. Lu, F. A. Macias, M. J. S. Miller, A. Mocan, R. Müller, F. Nicoletti, G. Perry, V. Pittalà, L. Rastrelli, M. Ristow, G. L. Russo, A. S. Silva, D. Schuster, H. Sheridan, K. Skalicka-Woźniak, L. Skaltsounis, E. Sobarzo-Sánchez, D. S. Bredt, H. Stuppner, A. Sureda, N. T. Tzvetkov, R. A. Vacca, B. B. Aggarwal, M. Battino, F. Giampieri, M. Wink, J.-L. Wolfender, J. Xiao, A. W. K. Yeung, G. Lizard, M. A. Popp, M. Heinrich, I. Berindan-Neagoe, M. Stadler, M. Daglia, R. Verpoorte, C. T. Supuran and T. the International Natural Product Sciences (2021). "Natural products in drug discovery: advances and opportunities." Nature Reviews Drug Discovery **20**(3): 200-216.

Bahassi, E. M., M. H. O'Dea, N. Allali, J. Messens, M. Gellert and M. Couturier (1999). "Interactions of CcdB with DNA gyrase. Inactivation of Gyra, poisoning of the gyrase-DNA complex, and the antidote action of CcdA." J Biol Chem **274**(16): 10936-10944.

Baker, C. C., D. J. Martins, J. N. Pelaez, J. P. Billen, A. Pringle, M. E. Frederickson and N. E. Pierce (2017). "Distinctive fungal communities in an obligate African ant-plant mutualism." Proc Biol Sci **284**(1850).

Bates, A. D. and A. Maxwell (2005). DNA topology, Oxford University Press, USA.

Bax, B. D., G. Murshudov, A. Maxwell and T. Germe (2019). "DNA topoisomerase inhibitors: Trapping a DNA-cleaving machine in motion." Journal of molecular biology **431**(18): 3427-3449.

Bergerat, A., D. Gadelle and P. Forterre (1994). "Purification of a DNA topoisomerase II from the hyperthermophilic archaeon Sulfolobus shibatae. A thermostable enzyme with both bacterial and eucaryal features." Journal of Biological Chemistry **269**(44): 27663-27669.

Bibb, M. J. (2005). "Regulation of secondary metabolism in streptomycetes." Current Opinion in Microbiology **8**(2): 208-215.

Blanco, P., S. Hernando-Amado, J. A. Reales-Calderon, F. Corona, F. Lira, M. Alcalde-Rico, A. Bernardini, M. B. Sanchez and J. L. Martinez (2016). "Bacterial Multidrug Efflux Pumps: Much More Than Antibiotic Resistance Determinants." Microorganisms **4**(1).

Blin, K., S. Shaw, A. M. Kloosterman, Z. Charlop-Powers, G. P. van Wezel, Marnix H. Medema and T. Weber (2021). "antiSMASH 6.0: improving cluster detection and comparison capabilities." Nucleic Acids Research **49**(W1): W29-W35.

Borelli, D. and M. Middelveen (1986). "Actinomycetoma Caused by Streptomyces somaliensis." Archives of Dermatology **122**(10): 1097-1098.

Bosch, F. and L. Rosich (2008). "The contributions of Paul Ehrlich to pharmacology: a tribute on the occasion of the centenary of his Nobel Prize." Pharmacology **82**(3): 171-179.

Bradbury, B. J. and M. J. Pucci (2008). "Recent advances in bacterial topoisomerase inhibitors." Current Opinion in Pharmacology **8**(5): 574-581.

Bradford, P. A. (2001). "Extended-spectrum beta-lactamases in the 21st century: characterization, epidemiology, and detection of this important resistance threat." Clin Microbiol Rev **14**(4): 933-951, table of contents.

Breijyeh, Z., B. Jubeh and R. Karaman (2020). "Resistance of Gram-Negative Bacteria to Current Antibacterial Agents and Approaches to Resolve It." Molecules **25**(6).

Bryan, L., J. Bedard, S. Wong and S. Chamberland (1989). "Quinolone antimicrobial agents: mechanism of action and resistance development." Clinical and Investigative medicine. Medecine Clinique et Experimentale **12**(1): 14-19.

Buchbinder, M. and J. Webb (1962). "Anderson. LV and McCabe, W. R.: Laboratory studies and clinical pharmacology of nalidixic acid." Antimicrob. Agents Chemother: 308.

Burkholder, P. R. and N. H. Giles Jr (1947). "Induced biochemical mutations in Bacillus subtilis." American journal of botany: 345-348.

Bush, M. J., N. Tschowri, S. Schlimpert, K. Flärdh and M. J. Buttner (2015). "c-di-GMP signalling and the regulation of developmental transitions in streptomycetes." Nat Rev Microbiol **13**(12): 749-760.

Buttner, M. J., M. Schäfer, D. M. Lawson and A. Maxwell (2018). "Structural insights into simocyclinone as an antibiotic, effector ligand and substrate." FEMS Microbiol Rev **42**(1).

Buzun, K., A. Bielawska, K. Bielawski and A. Gornowicz (2020). "DNA topoisomerases as molecular targets for anticancer drugs." Journal of Enzyme Inhibition and Medicinal Chemistry **35**(1): 1781-1799.

Cabral, J. H. M., A. P. Jackson, C. V. Smith, N. Shikotra, A. Maxwell and R. C. Liddington (1997). "Crystal structure of the breakage–reunion domain of DNA gyrase." Nature **388**(6645): 903-906.

Calfee, D. P. (2012). "Methicillin-resistant Staphylococcus aureus and vancomycin-resistant enterococci, and other Gram-positives in healthcare." Curr Opin Infect Dis **25**(4): 385-394.

Chater, K. F., S. Biró, K. J. Lee, T. Palmer and H. Schrempf (2010). "The complex extracellular biology of Streptomyces." FEMS microbiology reviews **34**(2): 171-198.

Cirz, R. T., M. B. Jones, N. A. Gingles, T. D. Minogue, B. Jarrahi, S. N. Peterson and F. E. Romesberg (2007). "Complete and SOS-mediated response of Staphylococcus aureus to the antibiotic ciprofloxacin." J Bacteriol **189**(2): 531-539.

Clardy, J., M. A. Fischbach and C. R. Currie (2009). "The natural history of antibiotics." Current Biology **19**(11): R437-R441.

Collin, F., S. Karkare and A. Maxwell (2011). "Exploiting bacterial DNA gyrase as a drug target: current state and perspectives." Applied Microbiology and Biotechnology **92**(3): 479-497.

Cummings, M., R. Breitling and E. Takano (2014). "Steps towards the synthetic biology of polyketide biosynthesis." FEMS Microbiology Letters **351**(2): 116-125.

Currie, C. R., J. A. Scott, R. C. Summerbell and D. Malloch (1999). "Fungus-growing ants use antibiotic-producing bacteria to control garden parasites." Nature **398**(6729): 701-704.

D'Costa, V. M., C. E. King, L. Kalan, M. Morar, W. W. Sung, C. Schwarz, D. Froese, G. Zazula, F. Calmels and R. Debruyne (2011). "Antibiotic resistance is ancient." Nature **477**(7365): 457-461.

Das, A. and C. Khosla (2009). "Biosynthesis of Aromatic Polyketides in Bacteria." Accounts of Chemical Research **42**(5): 631-639.

Datsenko, K. A. and B. L. Wanner (2000). "One-step inactivation of chromosomal genes in <i>Escherichia coli</i> K-12 using PCR products." Proceedings of the National Academy of Sciences **97**(12): 6640-6645.

Davagnino, J., M. Herrero, D. Furlong, F. Moreno and R. Kolter (1986). "The DNA replication inhibitor microcin B17 is a forty-three-amino-acid protein containing sixty percent glycine." Proteins: Structure, Function, and Bioinformatics **1**(3): 230-238.

Davies, J. (2006). "Where have All the Antibiotics Gone?" The Canadian journal of infectious diseases & medical microbiology = Journal canadien des maladies infectieuses et de la microbiologie medicale **17**(5): 287-290.

Davies, J. and D. Davies (2010). "Origins and evolution of antibiotic resistance." Microbiol Mol Biol Rev **74**(3): 417-433.

Davis, R., A. Markham and J. A. Balfour (1996). "Ciprofloxacin." Drugs **51**(6): 1019-1074.

de Mendoza, D. and G. E. Schujman (2009). Lipid Biosynthesis. Encyclopedia of Microbiology (Third Edition). M. Schaechter. Oxford, Academic Press**:** 219-228.

Devine, R., H. P. McDonald, Z. Qin, C. J. Arnold, K. Noble, G. Chandra, B. Wilkinson and M. I. Hutchings (2021). "Re-wiring the regulation of the formicamycin biosynthetic gene cluster to

enable the development of promising antibacterial compounds." <u>Cell Chemical Biology</u> **28**(4): 515-523.e515.

Dharmaraj, S. (2010). "Marine Streptomyces as a novel source of bioactive substances." <u>World Journal of Microbiology and Biotechnology</u> **26**(12): 2123-2139.

Doroghazi, J. R. and W. W. Metcalf (2013). "Comparative genomics of actinomycetes with a focus on natural product biosynthetic genes." <u>BMC genomics</u> **14**(1): 1-13.

Du, D., Z. Wang, N. R. James, J. E. Voss, E. Klimont, T. Ohene-Agyei, H. Venter, W. Chiu and B. F. Luisi (2014). "Structure of the AcrAB–TolC multidrug efflux pump." <u>Nature</u> **509**(7501): 512-515.

Dutta, S., J. R. Whicher, D. A. Hansen, W. A. Hale, J. A. Chemler, G. R. Congdon, A. R. Narayan, K. Håkansson, D. H. Sherman, J. L. Smith and G. Skiniotis (2014). "Structure of a modular polyketide synthase." <u>Nature</u> **510**(7506): 512-517.

Edwards, M. J., R. H. Flatman, L. A. Mitchenall, C. E. M. Stevenson, T. B. K. Le, T. A. Clarke, A. R. McKay, H.-P. Fiedler, M. J. Buttner, D. M. Lawson and A. Maxwell (2009). "A Crystal Structure of the Bifunctional Antibiotic Simocyclinone D8, Bound to DNA Gyrase." <u>Science</u> **326**(5958): 1415-1418.

Feng, Z., D. Chakraborty, S. B. Dewell, B. V. B. Reddy and S. F. Brady (2012). "Environmental DNA-encoded antibiotics fasamycins A and B inhibit FabF in type II fatty acid biosynthesis." <u>Journal of the American Chemical Society</u> **134**(6): 2981-2987.

Feng, Z., D. Kallifidas and S. F. Brady (2011). "Functional analysis of environmental DNA-derived type II polyketide synthases reveals structurally diverse secondary metabolites." <u>Proc Natl Acad Sci U S A</u> **108**(31): 12629-12634.

Fief, C. A., K. G. Hoang, S. D. Phipps, J. L. Wallace and J. E. Deweese (2019). "Examining the Impact of Antimicrobial Fluoroquinolones on Human DNA Topoisomerase IIα and IIβ." <u>ACS Omega</u> **4**(2): 4049-4055.

Fishovitz, J., J. A. Hermoso, M. Chang and S. Mobashery (2014). "Penicillin-binding protein 2a of methicillin-resistant Staphylococcus aureus." <u>IUBMB Life</u> **66**(8): 572-577.

Flatman, R. H., A. J. Howells, L. Heide, H.-P. Fiedler and A. Maxwell (2005). "Simocyclinone D8, an Inhibitor of DNA Gyrase with a Novel Mode of Action." Antimicrobial Agents and Chemotherapy **49**(3): 1093-1100.

Fleming, A. (1944). "THE DISCOVERY OF PENICILLIN." British Medical Bulletin **2**(1): 4-5.

Flórez, L. V., P. H. W. Biedermann, T. Engl and M. Kaltenpoth (2015). "Defensive symbioses of animals with prokaryotic and eukaryotic microorganisms." Natural Product Reports **32**(7): 904-936.

Fukumoto, A., Y. P. Kim, A. Matsumoto, Y. Takahashi, M. Suzuki, H. Onodera, H. Tomoda, H. Matsui, H. Hanaki, M. Iwatsuki, S. Ōmura and K. Shiomi (2017). "Naphthacemycins, novel circumventors of β-lactam resistance in MRSA, produced by Streptomyces sp. KB-3346-5. I. The taxonomy of the producing strain, and the fermentation, isolation and antibacterial activities." J Antibiot (Tokyo) **70**(5): 562-567.

Gaynes, R. (2017). "The Discovery of Penicillin—New Insights After More Than 75 Years of Clinical Use." Emerging Infectious Diseases **23**(5): 849-853.

Gellert, M., K. Mizuuchi, M. H. O'Dea, T. Itoh and J.-I. Tomizawa (1977). "Nalidixic acid resistance: a second genetic character involved in DNA gyrase activity." Proceedings of the National Academy of Sciences **74**(11): 4772-4776.

Gellert, M., K. Mizuuchi, M. H. O'Dea and H. A. Nash (1976). "DNA gyrase: an enzyme that introduces superhelical turns into DNA." Proceedings of the National Academy of Sciences **73**(11): 3872-3876.

Gellert, M., M. H. O'Dea, T. Itoh and J.-I. Tomizawa (1976). "Novobiocin and coumermycin inhibit DNA supercoiling catalyzed by DNA gyrase." Proceedings of the National Academy of Sciences **73**(12): 4474-4478.

Gelpi, A., A. Gilbertson and J. D. Tucker (2015). "Magic bullet: Paul Ehrlich, Salvarsan and the birth of venereology." Sexually transmitted infections **91**(1): 68-69.

Gerber, N. and H. Lechevalier (1965). "Geosmin, an earthy-smelling substance isolated from actinomycetes." Applied microbiology **13**(6): 935-938.

Gibson, E. G., B. Bax, P. F. Chan and N. Osheroff (2019). "Mechanistic and Structural Basis for the Actions of the Antibacterial Gepotidacin against Staphylococcus aureus Gyrase." ACS Infectious Diseases **5**(4): 570-581.

Gilbert, E. J. and A. Maxwell (1994). "The 24 kDa N-terminal sub-domain of the DNA gyrase B protein binds coumarin drugs." Molecular microbiology **12**(3): 365-373.

Goetschi, E., P. Angehrn, H. Gmuender, P. Hebeisen, H. Link, R. Masciadri and J. Nielsen (1993). "Cyclothialidine and its congeners: a new class of DNA gyrase inhibitors." Pharmacol Ther **60**(2): 367-380.

Gomez-Escribano, J. P. and M. J. Bibb (2011). "Engineering Streptomyces coelicolor for heterologous expression of secondary metabolite gene clusters." Microbial Biotechnology **4**(2): 207-215.

Gottelt, M., S. Kol, J. P. Gomez-Escribano, M. Bibb and E. Takano (2010). "Deletion of a regulatory gene within the cpk gene cluster reveals novel antibacterial activity in Streptomyces coelicolor A3(2)." Microbiology **156**(8): 2343-2353.

Grove, A. (2013). "MarR family transcription factors." Current Biology **23**(4): R142-R143.

Guerrero-Garzón, J. F., M. Zehl, O. Schneider, C. Rückert, T. Busche, J. Kalinowski, H. Bredholt and S. B. Zotchev (2020). "Streptomyces spp. From the Marine Sponge Antho dichotoma: Analyses of Secondary Metabolite Biosynthesis Gene Clusters and Some of Their Products." Frontiers in Microbiology **11**.

Gust, B., G. Chandra, D. Jakimowicz, T. Yuqing, C. J. Bruton and K. F. Chater (2004). λ Red-Mediated Genetic Manipulation of Antibiotic-Producing Streptomyces. Advances in Applied Microbiology, Academic Press. **54:** 107-128.

Gygli, S. M., S. Borrell, A. Trauner and S. Gagneux (2017). "Antimicrobial resistance in Mycobacterium tuberculosis: mechanistic and evolutionary perspectives." FEMS Microbiology Reviews **41**(3): 354-373.

Haas, L. (1999). "Papyrus of Ebers and Smith." Journal of Neurology, Neurosurgery & Psychiatry **67**(5): 578-578.

Haeder, S., R. Wirth, H. Herz and D. Spiteller (2009). "Candicidin-producing Streptomyces support leaf-cutting ants to protect their fungus garden against the pathogenic fungus Escovopsis." <u>Proceedings of the National Academy of Sciences</u> **106**(12): 4742.

Hawkey, P. M. (1998). "The origins and molecular basis of antibiotic resistance." <u>Bmj</u> **317**(7159): 657-660.

Heddle, J. G., S. J. Blance, D. B. Zamble, F. Hollfelder, D. A. Miller, L. M. Wentzell, C. T. Walsh and A. Maxwell (2001). "The antibiotic microcin B17 is a DNA gyrase poison: characterisation of the mode of inhibition11Edited by J. Karn." <u>Journal of Molecular Biology</u> **307**(5): 1223-1234.

Heddle, J. G., S. Mitelheiser, A. Maxwell and N. H. Thomson (2004). "Nucleotide Binding to DNA Gyrase Causes Loss of DNA Wrap." <u>Journal of Molecular Biology</u> **337**(3): 597-610.

Heide, L. (2009). "Genetic engineering of antibiotic biosynthesis for the generation of new aminocoumarins." <u>Biotechnology advances</u> **27**(6): 1006-1014.

Helle, L., M. Kull, S. Mayer, G. Marincola, M. E. Zelder, C. Goerke, C. Wolz and R. Bertram (2011). "Vectors for improved Tet repressor-dependent gradual gene induction or silencing in Staphylococcus aureus." <u>Microbiology (Reading)</u> **157**(Pt 12): 3314-3323.

Hertweck, C., A. Luzhetskyy, Y. Rebets and A. Bechthold (2007). "Type II polyketide synthases: gaining a deeper insight into enzymatic teamwork." <u>Natural Product Reports</u> **24**(1): 162-190.

Holmes, N. A., R. Devine, Z. Qin, R. F. Seipke, B. Wilkinson and M. I. Hutchings (2018). "Complete genome sequence of Streptomyces formicae KY5, the formicamycin producer." <u>Journal of Biotechnology</u> **265**: 116-118.

Holzenkämpfer, M., M. Walker, A. Zeeck, J. Schimana and H. P. Fiedler (2002). "Simocyclinones, novel cytostatic angucyclinone antibiotics produced by Streptomyces antibioticus Tü 6040 II. Structure elucidation and biosynthesis." <u>J Antibiot (Tokyo)</u> **55**(3): 301-307.

Hooper, D. C. and G. A. Jacoby (2015). "Mechanisms of drug resistance: quinolone resistance." <u>Ann N Y Acad Sci</u> **1354**(1): 12-31.

Hopwood, D. A. (1997). "Genetic contributions to understanding polyketide synthases." Chemical reviews **97**(7): 2465-2498.

Huang, M., J.-J. Lu and J. Ding (2021). "Natural Products in Cancer Therapy: Past, Present and Future." Natural Products and Bioprospecting **11**(1): 5-13.

Hutchings, M. I., A. W. Truman and B. Wilkinson (2019). "Antibiotics: past, present and future." Current Opinion in Microbiology **51**: 72-80.

Imai, Y., G. Hauk, J. Quigley, L. Liang, S. Son, M. Ghiglieri, M. F. Gates, M. Morrissette, N. Shahsavari, S. Niles, D. Baldisseri, C. Honrao, X. Ma, J. J. Guo, J. M. Berger and K. Lewis (2022). "Evybactin is a DNA gyrase inhibitor that selectively kills Mycobacterium tuberculosis." Nature Chemical Biology **18**(11): 1236-1244.

Kato, J.-i., Y. Nishimura, R. Imamura, H. Niki, S. Hiraga and H. Suzuki (1990). "New topoisomerase essential for chromosome segregation in E. coli." Cell **63**(2): 393-404.

Kato, J., H. Suzuki and H. Ikeda (1992). "Purification and characterization of DNA topoisomerase IV in Escherichia coli." J Biol Chem **267**(36): 25676-25684.

Katsuyama, Y. and Y. Ohnishi (2012). "Type III polyketide synthases in microorganisms." Methods Enzymol **515**: 359-377.

Katz, L. and R. H. Baltz (2016). "Natural product discovery: past, present, and future." Journal of Industrial Microbiology & Biotechnology **43**(2): 155-176.

Kepplinger, B., S. Morton-Laing, K. H. Seistrup, E. C. L. Marrs, A. P. Hopkins, J. D. Perry, H. Strahl, M. J. Hall, J. Errington and N. E. E. Allenby (2018). "Mode of Action and Heterologous Expression of the Natural Product Antibiotic Vancoresmycin." ACS Chem Biol **13**(1): 207-214.

Kepplinger, B., S. Morton-Laing, K. H. Seistrup, E. C. L. Marrs, A. P. Hopkins, J. D. Perry, H. Strahl, M. J. Hall, J. Errington and N. E. E. Allenby (2018). "Mode of Action and Heterologous Expression of the Natural Product Antibiotic Vancoresmycin." ACS Chemical Biology **13**(1): 207-214.

Khan, T., K. Sankhe, V. Suvarna, A. Sherje, K. Patel and B. Dravyakar (2018). "DNA gyrase inhibitors: Progress and synthesis of potent compounds as antibacterial agents." Biomedicine & Pharmacotherapy **103**: 923-938.

Khelaifia, S. and M. Drancourt (2012). "Susceptibility of archaea to antimicrobial agents: applications to clinical microbiology." Clinical Microbiology and Infection **18**(9): 841-848.

Klassen, J. L. (2014). "Microbial secondary metabolites and their impacts on insect symbioses." Current opinion in insect science **4**: 15-22.

Koga, H., A. Itoh, S. Murayama, S. Suzue and T. Irikura (1980). "Structure-activity relationships of antibacterial 6, 7-and 7, 8-disubstituted 1-alkyl-1, 4-dihydro-4-oxoquinoline-3-carboxylic acids." Journal of medicinal chemistry **23**(12): 1358-1363.

Kolarič, A., M. Anderluh and N. Minovski (2020). "Two Decades of Successful SAR-Grounded Stories of the Novel Bacterial Topoisomerase Inhibitors (NBTIs) Miniperspective." Journal of medicinal chemistry **63**(11): 5664-5674.

Kowalska-Krochmal, B. and R. Dudek-Wicher (2021). "The Minimum Inhibitory Concentration of Antibiotics: Methods, Interpretation, Clinical Relevance." Pathogens **10**(2).

Lang, A. J., S. E. Mirski, H. J. Cummings, Q. Yu, J. H. Gerlach and S. P. Cole (1998). "Structural organization of the human TOP2A and TOP2B genes." Gene **221**(2): 255-266.

Laponogov, I., M. K. Sohi, D. A. Veselkov, X.-S. Pan, R. Sawhney, A. W. Thompson, K. E. McAuley, L. M. Fisher and M. R. Sanderson (2009). "Structural insight into the quinolone–DNA cleavage complex of type IIA topoisomerases." Nature Structural & Molecular Biology **16**(6): 667-669.

Lehtovirta-Morley, L. E., J. Ross, L. Hink, E. B. Weber, C. Gubry-Rangin, C. Thion, J. I. Prosser and G. W. Nicol (2016). "Isolation of 'Candidatus Nitrosocosmicus franklandus', a novel ureolytic soil archaeal ammonia oxidiser with tolerance to high ammonia concentration." FEMS Microbiology Ecology **92**(5).

Lesher, G. Y., E. J. Froelich, M. D. Gruett, J. H. Bailey and R. P. Brundage (1962). "1, 8-Naphthyridine derivatives. A new class of chemotherapeutic agents." Journal of Medicinal Chemistry **5**(5): 1063-1065.

Lewis, K. (2020). "The Science of Antibiotic Discovery." Cell **181**(1): 29-45.

Liang, M., L. Liu, F. Xu, X. Zeng, R. Wang, J. Yang, W. Wang, L. Karthik, J. Liu, Z. Yang, G. Zhu, S. Wang, L. Bai, Y. Tong, X. Liu, M. Wu, L.-X. Zhang and G.-Y. Tan (2022). "Activating cryptic biosynthetic gene cluster through a CRISPR–Cas12a-mediated direct cloning approach." Nucleic Acids Research **50**(6): 3581-3592.

Liu, L. F., C.-C. Liu and B. M. Alberts (1980). "Type II DNA topoisomerases: Enzymes that can unknot a topologically knotted DNA molecule via a reversible double-strand break." Cell **19**(3): 697-707.

Lu, Y. J. and C. O. Rock (2006). "Transcriptional regulation of fatty acid biosynthesis in Streptococcus pneumoniae." Mol Microbiol **59**(2): 551-566.

MacNeil, D. J., K. M. Gewain, C. L. Ruby, G. Dezeny, P. H. Gibbons and T. MacNeil (1992). "Analysis of Streptomyces avermitilis genes required for avermectin biosynthesis utilizing a novel integration vector." Gene **111**(1): 61-68.

Maglangit, F., Q. Fang, V. Leman, S. Soldatou, R. Ebel, K. Kyeremeh and H. Deng (2019). "Accramycin A, A New Aromatic Polyketide, from the Soil Bacterium, Streptomyces sp. MA37." Molecules **24**(18): 3384.

Maglangit, F., Y. Zhang, K. Kyeremeh and H. Deng (2020). "Discovery of New Antibacterial Accramycins from a Genetic Variant of the Soil Bacterium, Streptomyces sp. MA37." Biomolecules **10**(10): 1464.

Martin, J. K., J. P. Sheehan, B. P. Bratton, G. M. Moore, A. Mateus, S. H.-J. Li, H. Kim, J. D. Rabinowitz, A. Typas, M. M. Savitski, M. Z. Wilson and Z. Gitai (2020). "A Dual-Mechanism Antibiotic Kills Gram-Negative Bacteria and Avoids Drug Resistance." Cell **181**(7): 1518-1532.e1514.

Mateus, A., N. Kurzawa, I. Becher, S. Sridharan, D. Helm, F. Stein, A. Typas and M. M. Savitski (2020). "Thermal proteome profiling for interrogating protein interactions." Mol Syst Biol **16**(3): e9232.

McKie, S. J., K. C. Neuman and A. Maxwell (2021). "DNA topoisomerases: Advances in understanding of cellular roles and multi-protein complexes via structure-function analysis." BioEssays **43**(4): 2000286.

Medema, M. H., K. Blin, P. Cimermancic, V. de Jager, P. Zakrzewski, M. A. Fischbach, T. Weber, E. Takano and R. Breitling (2011). "antiSMASH: rapid identification, annotation and analysis of secondary metabolite biosynthesis gene clusters in bacterial and fungal genome sequences." Nucleic Acids Research **39**(suppl_2): W339-W346.

Meyer, E., P. Gastmeier, M. Deja and F. Schwab (2013). "Antibiotic consumption and resistance: data from Europe and Germany." International Journal of Medical Microbiology **303**(6-7): 388-395.

Miki, T., Z.-T. Chang and T. Horiuchi (1984). "Control of cell division by sex factor F in Escherichia coli: II. Identification of genes for inhibitor protein and trigger protein on the 42.84–43.6 F segment." Journal of molecular biology **174**(4): 627-646.

Missiakas, D. M. and O. Schneewind (2013). "Growth and laboratory maintenance of Staphylococcus aureus." Curr Protoc Microbiol **Chapter 9**: Unit 9C.1.

Mohapatra, S. S., S. K. Dwibedy and I. Padhy (2021). "Polymyxins, the last-resort antibiotics: Mode of action, resistance emergence, and potential solutions." J Biosci **46**(3).

Mustaev, A., M. Malik, X. Zhao, N. Kurepina, G. Luan, L. M. Oppegard, H. Hiasa, K. R. Marks, R. J. Kerns, J. M. Berger and K. Drlica (2014). "Fluoroquinolone-gyrase-DNA complexes: two modes of drug binding." J Biol Chem **289**(18): 12300-12312.

Nakada, N., H. Gmünder, T. Hirata and M. Arisawa (1995). "Characterization of the Binding Site for Cyclothialidine on the B Subunit of DNA Gyrase ∗." Journal of Biological Chemistry **270**(24): 14286-14291.

Newman, D. J. and G. M. Cragg (2016). "Natural products as sources of new drugs from 1981 to 2014." Journal of natural products **79**(3): 629-661.

Nichols, M. D., K. DeAngelis, J. L. Keck and J. M. Berger (1999). "Structure and function of an archaeal topoisomerase VI subunit with homology to the meiotic recombination factor Spo11." The EMBO journal **18**(21): 6177-6188.

Nitiss, J. L. (2009). "Targeting DNA topoisomerase II in cancer chemotherapy." Nat Rev Cancer **9**(5): 338-350.

Nyerges, A., T. Tomašič, M. Durcik, T. Revesz, P. Szili, G. Draskovits, F. Bogar, Ž. Skok, N. Zidar, J. Ilaš, A. Zega, D. Kikelj, L. Daruka, B. Kintses, B. Vasarhelyi, I. Foldesi, D. Kata, M. Welin, R. Kimbung, D. Focht, L. P. Mašič and C. Pal (2020). "Rational design of balanced dual-targeting antibiotics with limited resistance." PLOS Biology **18**(10): e3000819.

O'Neill, J. (2016). Tackling drug-resistant infections globally: final report and recommendations, Government of the United Kingdom.

O'Rourke, S., A. Wietzorrek, K. Fowler, C. Corre, G. L. Challis and K. F. Chater (2009). "Extracellular signalling, translational control, two repressors and an activator all contribute to the regulation of methylenomycin production in Streptomyces coelicolor." Molecular Microbiology **71**(3): 763-778.

O'Rourke, S., D. Widdick and M. Bibb (2017). "A novel mechanism of immunity controls the onset of cinnamycin biosynthesis in Streptomyces cinnamoneus DSM 40646." Journal of Industrial Microbiology and Biotechnology **44**(4-5): 563-572.

Pankey, G. A. and L. D. Sabath (2004). "Clinical Relevance of Bacteriostatic versus Bactericidal Mechanisms of Action in the Treatment of Gram-Positive Bacterial Infections." Clinical Infectious Diseases **38**(6): 864-870.

Parker, E. N., B. N. Cain, B. Hajian, R. J. Ulrich, E. J. Geddes, S. Barkho, H. Y. Lee, J. D. Williams, M. Raynor, D. Caridha, A. Zaino, M. Shekhar, K. A. Muñoz, K. M. Rzasa, E. R. Temple, D. Hunt, X. Jin, C. Vuong, K. Pannone, A. M. Kelly, M. P. Mulligan, K. K. Lee, G. W. Lau, D. T. Hung and P. J. Hergenrother (2022). "An Iterative Approach Guides Discovery of the FabI Inhibitor Fabimycin, a Late-Stage Antibiotic Candidate with In Vivo Efficacy against Drug-Resistant Gram-Negative Infections." ACS Central Science **8**(8): 1145-1158.

Peng, H. and K. J. Marians (1999). Overexpression and Purification of Bacterial Topoisomerase IV. DNA Topoisomerase Protocols: Volume I: DNA Topology and Enzymes. M.-A. Bjornsti and N. Osheroff. Totowa, NJ, Humana Press**:** 163-169.

Perry, J., N. Waglechner and G. Wright (2016). "The Prehistory of Antibiotic Resistance." Cold Spring Harb Perspect Med **6**(6).

Pitts, S. L., G. F. Liou, L. A. Mitchenall, A. B. Burgin, A. Maxwell, K. C. Neuman and N. Osheroff (2011). "Use of divalent metal ions in the DNA cleavage reaction of topoisomerase IV." Nucleic Acids Research **39**(11): 4808-4817.

Qin, Z., R. Devine, T. J. Booth, E. H. E. Farrar, M. N. Grayson, M. I. Hutchings and B. Wilkinson (2020). "Formicamycin biosynthesis involves a unique reductive ring contraction." Chemical Science **11**(31): 8125-8131.

Qin, Z., J. T. Munnoch, R. Devine, N. A. Holmes, R. F. Seipke, K. A. Wilkinson, B. Wilkinson and M. I. Hutchings (2017). "Formicamycins, antibacterial polyketides produced by Streptomyces formicae isolated from African Tetraponera plant-ants." Chemical Science **8**(4): 3218-3227.

Quezada, M., C. Licona-Cassani, P. Cruz-Morales, A. A. Salim, E. Marcellin, R. J. Capon and F. Barona-Gómez (2017). "Diverse Cone-Snail Species Harbor Closely Related Streptomyces Species with Conserved Chemical and Genetic Profiles, Including Polycyclic Tetramic Acid Macrolactams." Frontiers in Microbiology **8**.

Quintana, E. T., K. Wierzbicka, P. Mackiewicz, A. Osman, A. H. Fahal, M. E. Hamid, J. Zakrzewska-Czerwinska, L. A. Maldonado and M. Goodfellow (2008). "Streptomyces sudanensis sp. nov., a new pathogen isolated from patients with actinomycetoma." Antonie Van Leeuwenhoek **93**(3): 305-313.

Reece, R. J. and A. Maxwell (1991). "DNA Gyrase: Structure and Function." Critical Reviews in Biochemistry and Molecular Biology **26**(3-4): 335-375.

Reygaert, W. C. (2018). "An overview of the antimicrobial resistance mechanisms of bacteria." AIMS Microbiol **4**(3): 482-501.

Roca, J., J. M. Berger, S. C. Harrison and J. C. Wang (1996). "DNA transport by a type II topoisomerase: direct evidence for a two-gate mechanism." Proceedings of the National Academy of Sciences **93**(9): 4057-4062.

Roca, J. and J. C. Wang (1992). "The capture of a DNA double helix by an ATP-dependent protein clamp: A key step in DNA transport by type II DNA topoisomerases." Cell **71**(5): 833-840.

Roca, J. and J. C. Wang (1994). "DNA transport by a type II DNA topoisomerase: Evidence in favor of a two-gate mechanism." Cell **77**(4): 609-616.

Ruiz, N., B. Falcone, D. Kahne and T. J. Silhavy (2005). "Chemical conditionality: a genetic strategy to probe organelle assembly." Cell **121**(2): 307-317.

Rutledge, P. J. and G. L. Challis (2015). "Discovery of microbial natural products by activation of silent biosynthetic gene clusters." Nature reviews microbiology **13**(8): 509-523.

Sato, K., Y. Inoue, T. Fujii, H. Aoyama and S. Mitsuhashi (1986). "Antibacterial activity of ofloxacin and its mode of action." Infection **14**(4): S226-S230.

Schujman, G. E., L. Paoletti, A. D. Grossman and D. de Mendoza (2003). "FapR, a Bacterial Transcription Factor Involved in Global Regulation of Membrane Lipid Biosynthesis." Developmental Cell **4**(5): 663-672.

Seipke, R. F., J. Barke, C. Brearley, L. Hill, D. W. Yu, R. J. M. Goss and M. I. Hutchings (2011). "A Single Streptomyces Symbiont Makes Multiple Antifungals to Support the Fungus Farming Ant Acromyrmex octospinosus." PLOS ONE **6**(8): e22028.

Seipke, R. F., J. Barke, D. Heavens, D. W. Yu and M. I. Hutchings (2013). "Analysis of the bacterial communities associated with two ant-plant symbioses." MicrobiologyOpen **2**(2): 276-283.

Seipke, R. F., M. Kaltenpoth and M. I. Hutchings (2012). "Streptomyces as symbionts: an emerging and widespread theme?" FEMS Microbiology Reviews **36**(4): 862-876.

Shaw, W. V. (1983). "Chloramphenicol acetyltransferase: enzymology and molecular biology." CRC Crit Rev Biochem **14**(1): 1-46.

Sieradzki, K. and A. Tomasz (1999). "Gradual alterations in cell wall structure and metabolism in vancomycin-resistant mutants of Staphylococcus aureus." Journal of Bacteriology **181**(24): 7566-7570.

Sivakala, K. K., K. Gutiérrez-García, P. A. Jose, T. Thinesh, R. Anandham, F. Barona-Gómez and N. Sivakumar (2021). "Desert Environments Facilitate Unique Evolution of Biosynthetic Potential in Streptomyces." Molecules **26**(3).

Smith, C. G., A. Dietz, W. T. Sokolski and G. M. Savage (1956). "Streptonivicin, a new antibiotic. I. Discovery and biologic studies." Antibiot Chemother (Northfield) **6**(2): 135-142.

Solomon, D. H., L. Van Houten, R. J. Glynn, L. Baden, K. Curtis, H. Schrager and J. Avorn (2001). "Academic Detailing to Improve Use of Broad-Spectrum Antibiotics at an Academic Medical Center." Archives of Internal Medicine **161**(15): 1897-1902.

Staunton, J. and K. J. Weissman (2001). "Polyketide biosynthesis: a millennium review." Natural Product Reports **18**(4): 380-416.

Stevenson, C. E. M., A. Assaad, G. Chandra, T. B. K. Le, S. J. Greive, M. J. Bibb and D. M. Lawson (2013). "Investigation of DNA sequence recognition by a streptomycete MarR family transcriptional regulator through surface plasmon resonance and X-ray crystallography." Nucleic Acids Research **41**(14): 7009-7022.

Stieger, M., P. Angehrn, B. Wohlgensinger and H. Gmünder (1996). "GyrB mutations in Staphylococcus aureus strains resistant to cyclothialidine, coumermycin, and novobiocin." Antimicrobial agents and chemotherapy **40**(4): 1060-1062.

Stieglmeier, M., A. Klingl, R. J. E. Alves, S. K. R. Rittmann, M. Melcher, N. Leisch and C. Schleper (2014). "Nitrososphaera viennensis gen. nov., sp. nov., an aerobic and mesophilic, ammonia-oxidizing archaeon from soil and a member of the archaeal phylum Thaumarchaeota." Int J Syst Evol Microbiol **64**(Pt 8): 2738-2752.

Sugino, A., N. P. Higgins, P. O. Brown, C. L. Peebles and N. R. Cozzarelli (1978). "Energy coupling in DNA gyrase and the mechanism of action of novobiocin." Proceedings of the National Academy of Sciences **75**(10): 4838-4842.

Travnickova, E., P. Mikula, J. Oprsal, M. Bohacova, L. Kubac, D. Kimmer, J. Soukupova and M. Bittner (2019). "Resazurin assay for assessment of antimicrobial properties of electrospun nanofiber filtration membranes." AMB Express **9**(1): 183.

Vadia, S., J. L. Tse, R. Lucena, Z. Yang, D. R. Kellogg, J. D. Wang and P. A. Levin (2017). "Fatty Acid Availability Sets Cell Envelope Capacity and Dictates Microbial Cell Size." Curr Biol **27**(12): 1757-1767.e1755.

Vanden Broeck, A., C. Lotz, J. Ortiz and V. Lamour (2019). "Cryo-EM structure of the complete E. coli DNA gyrase nucleoprotein complex." Nature Communications **10**(1): 4935.

Ventola, C. L. (2015). "The Antibiotic Resistance Crisis: Part 1: Causes and Threats." Pharmacy and Therapeutics **40**(4): 277-283.

Villanueva, L., F. A. B. von Meijenfeldt, A. B. Westbye, S. Yadav, E. C. Hopmans, B. E. Dutilh and J. S. S. Damsté (2021). "Bridging the membrane lipid divide: bacteria of the FCB group superphylum have the potential to synthesize archaeal ether lipids." The ISME Journal **15**(1): 168-182.

Waksman, S. A., A. Schatz and D. M. Reynolds (1946). "PRODUCTION OF ANTIBIOTIC SUBSTANCES BY ACTINOMYCETES." Annals of the New York Academy of Sciences **48**(2): 73-86.

Walker, B., S. Barrett, S. Polasky, V. Galaz, C. Folke, G. Engström, F. Ackerman, K. Arrow, S. Carpenter, K. Chopra, G. Daily, P. Ehrlich, T. Hughes, N. Kautsky, S. Levin, K.-G. Mäler, J. Shogren, J. Vincent, T. Xepapadeas and A. de Zeeuw (2009). "Looming Global-Scale Failures and Missing Institutions." Science **325**(5946): 1345-1346.

Wang, J., R. Zhang, X. Chen, X. Sun, Y. Yan, X. Shen and Q. Yuan (2020). "Biosynthesis of aromatic polyketides in microorganisms using type II polyketide synthases." Microbial Cell Factories **19**(1): 110.

Weinstein, R. A. and S. K. Fridkin (2001). "Vancomycin-Intermediate and -Resistant Staphylococcus aureus: What the Infectious Disease Specialist Needs to Know." Clinical Infectious Diseases **32**(1): 108-115.

Witte, W. (1998). "Medical Consequences of Antibiotic Use in Agriculture." Science **279**(5353): 996.

Woese, C. R. and G. E. Fox (1977). "Phylogenetic structure of the prokaryotic domain: The primary kingdoms." Proceedings of the National Academy of Sciences **74**(11): 5088-5090.

Wushouer, H., Z.-X. Zhang, J.-H. Wang, P. Ji, Q.-F. Zhu, R. Aishan and L.-W. Shi (2018). "Trends and relationship between antimicrobial resistance and antibiotic use in Xinjiang Uyghur autonomous region, China: based on a 3 year surveillance data, 2014–2016." Journal of Infection and Public Health **11**(3): 339-346.

Xu, M., Y. N. Zhou, B. P. Goldstein and D. J. Jin (2005). "Cross-Resistance of *Escherichia coli* RNA Polymerases Conferring Rifampin Resistance to Different Antibiotics." Journal of Bacteriology **187**(8): 2783-2792.

Yang, F., S. S. Teves, C. J. Kemp and S. Henikoff (2014). "Doxorubicin, DNA torsion, and chromatin dynamics." Biochim Biophys Acta **1845**(1): 84-89.

Yang, L., X. Li, P. Wu, J. Xue, L. Xu, H. Li and X. Wei (2020). "Streptovertimycins A–H, new fasamycin-type antibiotics produced by a soil-derived Streptomyces morookaense strain." The Journal of Antibiotics **73**(5): 283-289.

Yang, W., I. F. Moore, K. P. Koteva, D. C. Bareich, D. W. Hughes and G. D. Wright (2004). "TetX Is a Flavin-dependent Monooxygenase Conferring Resistance to Tetracycline Antibiotics*." Journal of Biological Chemistry **279**(50): 52346-52352.

Yoshida, H., M. Bogaki, M. Nakamura and S. Nakamura (1990). "Quinolone resistance-determining region in the DNA gyrase gyrA gene of Escherichia coli." Antimicrobial agents and chemotherapy **34**(6): 1271-1272.

Yoshida, H., M. Bogaki, M. Nakamura, L. M. Yamanaka and S. Nakamura (1991). "Quinolone resistance-determining region in the DNA gyrase gyrB gene of Escherichia coli." Antimicrobial agents and chemotherapy **35**(8): 1647-1650.

Young, T. P., C. H. Stubblefield and L. A. Isbell (1996). "Ants on swollen-thorn acacias: species coexistence in a simple system." Oecologia **109**(1): 98-107.

Yuan, J., L. Wang, J. Ren, J.-P. Huang, M. Yu, J. Tang, Y. Yan, J. Yang and S.-X. Huang (2020). "Antibacterial Pentacyclic Polyketides from a Soil-Derived Streptomyces." Journal of Natural Products **83**(6): 1919-1924.

Zaffiri, L., J. Gardner and L. H. Toledo-Pereyra (2012). "History of antibiotics. From salvarsan to cephalosporins." J Invest Surg **25**(2): 67-77.